Non-Haem Ligands as Functional Templates for Peptide Attachment

Towards Artificial Peroxidases

Marco van den Heuvel

Cover picture: Marco van den Heuvel

An electronic version of this Ph. D. thesis is available from the University Library at http://www.ub.rug.nl/ (ISBN 90-367-1618-7).

FIRST EDITION

This research project was supported financially by the Dutch Organisation for Scientific Research (NWO/CW)

RIJKSUNIVERSITEIT GRONINGEN

Non-Haem Ligands as Functional Templates for Peptide Attachment

Towards Artificial Peroxidases

Proefschrift

ter verkrijging van het doctoraat in de
Wiskunde en Natuurwetenschappen
aan de Rijksuniversiteit Groningen
op gezag van de
Rector Magnificus, dr. D. F. J. Bosscher,
in het openbaar te verdedigen op
vrijdag 21 juni 2002
om 16.00 uur

door

Marco van den Heuvel

geboren op 5 oktober 1971
te Werkendam

Promotores:	Prof. dr. R. M. Kellogg
	Prof. dr. B. L. Feringa
Referent:	Dr. C. T. Choma
Beoordelingscommissie:	Prof. dr. J. B. F. N. Engberts
	Prof. dr. D. B. Janssen
	Prof. dr. J. G. de Vries

ISBN 90–367–1617–9

Stellingen

1. The implied criticism of Hemmert *et al*. that on use of hydrogen peroxide with N4PyFe as the catalyst "only 36 turnovers per hour" are obtained in the oxidation of cyclohexane to cyclohexanol and cyclohexanone is unjustified in view of the fact that their own tetrapyridinyl iron complex fails to display any turnover at all.

   Hemmert, C.; Maestrin, A. P.; Renz, M.; Gornitzka, H.; Meunier, B. *C. R. Acad. Sci. Paris, Série IIc, Chimie: Chemistry* **2000**, *3*, 735–741.

2. Abbreviations are commonly used to reduce long words or frequently occurring word combinations to a few letters. Therefore, it is pointless to abbreviate *et alia* or *et alii* to *et al*.

3. The merger of different departments within a faculty, or that of separate countries into one union, merely accentuates their internal differences.

4. In order for organic chemists and biochemists to work together more effectively, there should be more clarity and unity in common terminology. For example, a biochemist refers to a metal ion as a ligand when co-ordinated to amino acids in a peptide, whereas for the (in)organic chemist the ligand is the co-ordinating structure around the metal ion.
   N.B. Biochemists sometimes also refer to a substrate for an enzyme as a ligand.

5. The personal findings and experiences gained during a Ph. D. study are to be found in the unwritten chapter of the thesis.

6. It is surprising how unpredictable exact science can be.

7. Nothing in chemistry is straightforward.

8. The positive effect on the motivation of a (young) researcher that stems from good experimental results is often underestimated. But then, the opposite is equally true.

9. The practicality of graduate research is not merely academic.

10. No matter how hard you work, there is always a machine (or machinery) fast enough to slow you down.

11. The validity of the common assumption that all postgraduate studies are equal in the fact that they can be finished within four years should be closely examined.

12. A thesaurus provides a welcomed companion during the lonely process of writing.

13. The ability to reduce many months' work into a few sentences is a disappointing skill.

14. In black & white photography you learn to see things not in black and white, but as different shades of grey.

15. Photography differs from life in that a negative image can directly result in a positive impression.

---

16. Nationalisme gedijt beter in het buitenland.

17. Alhoewel academici en promovendi geacht worden zich te ontwikkelen tot kritische onderzoekers, wordt kritiek leveren niet altijd gewaardeerd.

18. De functie-omschrijving 'Onderzoeker in opleiding' zou beter vervangen kunnen worden door 'Onderzoeker door zelfstudie'.

Preface

Now that this book is complete and another chapter in my life draws to a close, it is time to reflect on the time that has passed by. On a personal level it has been by far the most difficult period and professionally the most challenging. A problem is a challenge that can't be met. If one applies this definition, I have encountered only a few problems during this postgraduate research.

It was painful to experience that hard work is not always rewarded with good results. Although paper is patient and willing, the fumehood often proves otherwise. From that point of view 'paper' or 'black board' chemistry is much easier and more successful than that in the fumehood, simply because it works. Seemingly straightforward approaches on paper often do not reveal the unforeseen and hidden flaws in a synthetic pathway that come to light in the fumehood. And even when a reaction works, defeat during the workup procedure can still rob you of your reward. In that respect, a profession as bricklayer would have been a lot easier: simply by laying one brick onto another a wall can be built. There is even some room for creativity during the assembly process. However, on reflection, this would have been for me far less challenging, and satisfactory, than chemistry could ever be.

It is this challenging nature of organic chemistry that has led me to pursue a profession in this area. And believe me, I have been challenged more than enough over the last few years. This research project for example has been hampered by misfortune on many occasions. If it wasn't yet another futile experiment, it was a machine that failed to function properly. It is often said that no result is still a result. Although this may sometimes be valid for some areas of research, it is not applicable to the synthesis of a compound that continuously fails, and is crucial to the success of the project. But then someone could rightly say that all these learnings and experiences build character. Mine should be fully developed by now.

In all fairness, the reactions and conditions examined may not always have been the right ones, but then this is all part of the learning process. If every Ph. D. student knew at the beginning how to select and perform experiments, then it would actually be possible to complete a Ph. D. study in four years. Unfortunately, reality is quite different, although some institutions fail to acknowledge this fact.

After coming to Groningen from the Randstad, I have often been told: "Je komt hier niet weg." And indeed, I have often had the feeling that I was never going to leave Groningen. But now I am and I would like to take the opportunity to thank several people who have contributed to my research, as well as my time spent in and outside Groningen over the last few years.

Firstly I would like to thank prof. dr. R. M. Kellogg and prof. dr. B. L. Feringa for allowing me to work on this ambitious research project. Despite the difficulties I have experienced and the fact that the goal of the project has not entirely been met, a great deal has been learnt by analysing the problems encountered. There are still plenty of unanswered questions and challenges. I am of the opinion that some of the suggestions presented in this thesis can provide alternative methodologies to bring this project to a successful end. Therefore, I am pleased that dr. C. T. Choma will continue to work on this project. Christin, thanks for introducing me to the intriguing world of *de novo* design and four-helix bundles. Regrettably, I will not be the person who constructs the real four-helix bundle with the N4Py complex incorporated into its structure. Our active communication by email was also greatly appreciated. Good luck with the project and please do not hesitate to contact me regarding any questions you may have. Ben, Dick, and Christin, I am grateful to you all for your prompt and constructive amendments to the draft version of my thesis.

I am also indebted to prof. dr. J. B. F. N. Engberts, prof. dr. D. B. Janssen, and prof. dr. J. G. de Vries who have acted as members of the reading committee. It was interesting to see how different errors and obscurities were spotted by different people. At the same time this also emphasised how crucial it is to have several people review the manuscript in order to spot all of the mistakes.

Special thanks go to Tieme van den Berg who has carried out most of the cross coupling reactions as part of his undergraduate research. Tieme, I have been very fortunate to have you working by my side (literally). You have proved to be a hard working, motivated, and enthusiastic student. Although I have been able only to summarise your work in Chapter 4, your experiments have made a big contribution to this thesis. Your many (test) reactions have also indicated that the newly developed tetrabromo N4Py ligand could be an interesting substrate for further derivatisation by cross coupling reactions. Good luck with your work in the research group of Larry Que Jr. and during your Ph. D. study in the near future. I hope you can find some time to continue working on the tetrabromo N4Py, maybe on a Friday afternoon or so.

To my colleagues in the 'Kellogg College' labroom Tieme, Jan, Hans, and Lorena I would like to say 'bedankt' for the pleasant and refreshing atmosphere in the lab. This also applies to previous colleagues like Bartjan, as well as people from adjacent labrooms. I have also enjoyed the company of Inge who has been my 'neighbour' for some time now. The amusement provided by entertainers like Jan and Tieme has been a sheer delight for me, as well as many others. It made life in front of the fumehood a lot more endurable.

I would also like to thank the current and previous members of our oxidation subgroup for the helpful suggestions and fruitful discussions during our many meetings. Special recognition goes to dr. Ronald Hage and dr. Scott Killeen from Unilever Research, The Netherlands, for performing the cyclic voltammetry measurements on the iron(II) complex of tetrabromo N4Py.

I am also indebted to Margot Jeronimus-Stratingh and Annie van Dam at the Pharmacy Department for performing the electrospray mass analyses, Albert Kiewiet for the chemical ionisation and high resolution mass analyses, and Jan Ebels, Harm Draaier, and Jannes Hommes for the elemental analyses. They are all kindly acknowledged for their contributions to the structural analyses described in this thesis. Thanks also to Wim Kruizinga for performing the

temperature-dependent NMR analysis of the iron(II) complex of tetrabromo N4Py. I am also grateful to Auke Meetsma for solving the crystal structures described in this thesis.

Marc van Gelder I want to thank not only for helping me with the many troublesome purifications of the peptides and N4Py-peptide complexes by reversed-phase HPLC, but also for his company during the many occasions I was in his lab.

I am grateful to prof. dr. R. M. J. Liskamp and dr. ir. J. A. W. Kruijtzer from the Medicinal Chemistry Department of the University Utrecht for their assistance in preparing and purifying a peptide sequence I used during my research.

Niek Buurma I would like to thank for the time he has invested in helping me to analyse the kinetic behaviour of the ABTS oxidation by N4PyFe.

Although conversations with Ebe Schudde are regularly quite long, I would like to thank him for his understanding and sympathy during the personal conversations we have had. Ebe, you take up a special position in our lab that only a few truly know how to appreciate.

I have enjoyed my visit to Washington D.C. and the ICBIC99 in Minneapolis together with Jelle Brinksma. Jelle, that visit with you to the USA has left me with many good memories.

Roos Imbos, thank you for looking after my flat during the many occasions I went to England for a short break. I also enjoyed working together with you and José Nieuwenhuijzen on the organisation of the workweek in 1999. In the busy programme we did not leave much time for relaxation (it is after all a workweek), but I am convinced that it has been a very interesting and enjoyable workweek for our group members and ourselves.

Sports and leisure activities are much more enjoyable in the presence of friends. The regular workouts and ice-skating events with Linda Lucas, Minze Rispens, and Alette Ligtenbarg I have always experienced as a good time that was often combined with excellent dinners. Such a shame that all good things come to an end.

Personally, I have enjoyed assembling the photo board of our research groups and compiling the ChemBase database. It gives me great pleasure to see that I have been able to contribute to a more efficient method of finding chemicals in our labs that is evidently greatly appreciated by all its users. It is therefore only fair to acknowledge Dirk Beetstra, Marco Bouwkamp, and Wouter van Meerendonck who have constructed the actual database. Although I originally composed the photo board in our department to assist our secretary and the new members of our research groups in remembering the many names and faces, I am pleased to see that these photos have also found their way to many other uses and abuses.

Many of these 'faces' have contributed in many ways to an enjoyable period in Groningen, so to all those I have not thanked by name: thank you for the time that has passed by and good luck to you all in the future.

Now that this chapter in my life has come to an end, it is time to start a new one. Firstly, I'll do that by fulfilling a lifelong dream by moving to England. More importantly, I'll be spending that time with Resh who has been my best friend for several years and will be my wife for many years to come. A new home, a new city, a new job, and new friends, unfortunately at the expense of sharing less time with the ones I already have. These will be interesting times indeed.

A special thank you goes to my parents who have supported me in so many different ways throughout my education. I am also grateful to my friends for the interest they have shown in my research as well as my personal well-being. It is a shame that most of you have never been able to understand fully what it was that I was working on. Hopefully this thesis will make things a bit clearer. It is also unfortunate that we haven't been able to see each other as often as I would have liked. Admittedly, by moving to England this will become even rarer.

And finally to Resh I would like to say, thank you for being my 'rock' to rely upon and confide in, and motivating me through the highs and lows. Unfortunately, we both realise that it is far easier to give advice than to follow up on it.

Contents

3 Tetrasubstituted N4Py ligands as templates for peptide attachment

4 Tetrabromo N4Py as a versatile building block for new non-haem metal catalysts

5 Characterisation and application of tetrasubstituted N4Py iron complexes

6 Conclusions and future prospects

"....considering the phrase, 'How do you know it's not possible until you've tried?' And experiments with Hex, the University's thinking engine, had found that, indeed, many things are not impossible *until* they have been tried."

"The last continent"
Terry Pratchett, A Discworld Novel

Chapter 1

An introduction to artificial proteins

1.1 From native to designed proteins

Over the past several decades scientists have been trying to understand, mimic, and enhance the tools provided by mother nature. Although considerable progress has been made to further their understanding, the complexity and sophistication of numerous biological structures remains bewildering. One such enigma is nature's catalyst: the enzyme. A great deal has been discovered about their primary, secondary, and tertiary structures, and many of the working mechanisms have been uncovered together with their substrate ranges and limitations.[1] In addition, genetic methods have been developed to alter the amino acid sequences in enzymes and thereby modify their performance.[2] However, one aspect still remains a mystery: how the primary structure determines the folded conformation of the protein, and thereby influences and governs the function and performance of the enzyme. Although a great deal of work has already been undertaken to unravel this puzzling and intriguing part of biochemistry,[3] there is no doubt that future research shall lead to far deeper insights.

De novo design involves devising a peptide sequence that will give rise to a predicted protein structure.[4–6] This requires a comprehensive understanding of the processes involved in the translation of the amino acid sequence to the tertiary structure of a protein. Many of the reports that have appeared so far in the literature have dealt with the design and synthesis of *de novo* proteins merely as an academic exercise. With an enhanced understanding of the complicated protein folding mechanisms, the design and synthesis of an increasing number of functional artificial proteins has been made possible.[7] These designed structures are in general relatively small, and are more accessible to the study and understanding of complex interactions that are involved in larger native enzymes. Designing large globular or native-like proteins is still a challenge waiting to be accomplished. The development of new artificial proteins will no doubt be boosted by the application of new technology, like combinatorial approaches and high-through-put screening. An effective rationale for the design, however, is still essential to the successful outcome of the overall protein structure.

1.2 From mimic to artificial enzyme

Function can be introduced into a protein scaffold by the incorporation of a new reactive centre. Conversely, a lot of research has been devoted to the design of small molecule catalysts[8] or supramolecular assemblies[9] that can mimic the function of a natural enzyme. In our group we have developed a pentadentate ligand as a model for the glycopeptide bleomycin.[10] This ligand is called N4Py (**1**) and consists of four pyridine rings that are anchored to a central nitrogen atom (Figure 1.1).[11] When its iron(II) complex, $[(N4Py)Fe(MeCN)](ClO_4)_2$ (**2**), reacts with hydrogen peroxide, a transient low-spin iron(III) hydroperoxide species is formed, which is capable of oxidising a wide variety of organic compounds.[12] In addition, it can also function as an effective biomimetic DNA cleaving agent analogous to iron bleomycin.[13] The synthesis and chemistry of N4Py and some of its derivatives will be the subject of Chapter 2.

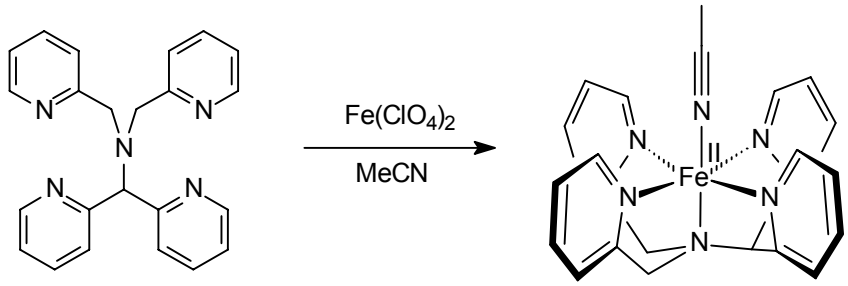

1 **2**

Figure 1.1. N4Py (**1**) and its iron(II) complex $[(N4Py)Fe(MeCN)](ClO_4)_2$ (**2**).

A popular scaffold for the introduction of function into a peptide structure is the four-helix bundle motif, which has been used by many researchers in the field of protein design. The design and construction of these four-helix bundles will be briefly discussed in the following sections, as well as some examples of newly created functional protein mimics based on this architecture.

The work presented in this thesis describes the preliminary studies as part of a larger project, aimed at the design and synthesis of a functional mimic of a water-soluble peroxidase. The design strategy is to embed the N4PyFe catalyst **2** inside a four-helix bundle, where it could function as a synthetic cofactor in the protein environment.

As can be seen in Figure 1.2, the core of the four-helix bundle is well suited to host a small catalyst like the N4PyFe complex. However, the packing of the amino acid side chains can be disrupted by the catalyst and thereby destabilise the four-helix bundle. In the (re)design of the peptide bundle this potential instability can be suppressed by creating a cavity to host the N4PyFe catalyst. At the same time, this cavity can be designed to function as an active site within a synthetic enzyme. With an appropriate selection of proximal amino acids, a local pH can be established to influence the oxidative behaviour of the catalytic centre. The actual binding of the catalyst will not be perturbed by altering the peptide sequences, as these are covalently linked to the ligand. However, the sequence will affect the overall stability of the peptide-N4PyFe structure, and might influence the binding of the substrate and the formation of the reactive intermediate. A successful N4Py ligand modification that enabled the attachment of two peptide chains to the N4PyFe catalyst will be presented in more detail in Chapter 2.

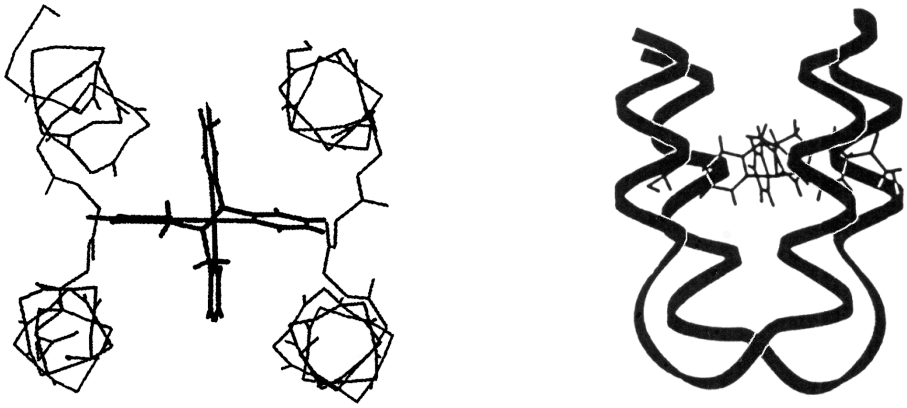

Figure 1.2. The crystal structure of N4PyFe (**2**) superimposed onto the backbone of α_2,[14] a dimeric four-helix bundle (left: top view, right: side view). The amino acid side chains have been omitted for clarity.[15]

The aim of this chapter is neither to present a complete overview of the literature with regard to four-helix bundles and functional peptide structures, nor to provide a full understanding of the underlying fundamental aspects. The examples discussed here have been chosen in the hope that they will provide some understanding of the elegant structures that protein designers have been able to create and the principles involved.

1.3 Four-helix bundles

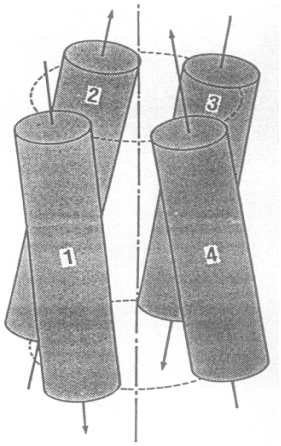

Four-helix bundles (right) are commonly encountered motifs in native enzymes like ferritin, tobacco mosaic virus, myohaemerythrin, haemerythrin, cytochrome *c'*, cytochrome b_{562},[16] as well as in methane mono-oxygenase.[17] These bundles consist of α-helices that are typically fifteen to twenty-six amino acids (residues)[18] long and display a crossing angle of about 20° with a left-handed twist.[19] This is due to the side chain intercalation of adjacent helix' surfaces.[20,21] Depending on the packing restrictions of these side chains, the diameter of the core is about 1 Å and the distance between the axes of the helices in four-helix bundles is generally 10 ± 3 Å.[22]

Although the 3D arrangement of the α-helices in a four-helix bundle motif might be considered aesthetically pleasing, it has not been the main focus of *de novo* protein design because of its architecture. Its relatively simple construction and organisation enables modular (re)design and simulation studies of the factors that determine its shape and stability. A great deal of knowledge has been gathered over the years about four-helix bundles that provides to some extent an understanding of the factors that govern protein folding and stability.[5e,23] Protein designers can now manipulate peptide sequences to introduce function (Section 1.5),[4] and increase the stability of the peptide structure.[6c]

There are many factors that can affect the stability of the α-helix, and consequently the four-helix bundle. Over the past few years it has been suggested that a prerequisite for the formation of an α-helix involved the incorporation of residues with a preference for α-helix formation

(helix propensity).[24] However, Hecht and co-workers demonstrated that a periodic repeat of polar and non-polar residues in the peptide sequence can be sufficient to form an α-helix.[25] The resulting α-helices are amphiphilic, i.e. they have a hydrophilic and a hydrophobic surface (Figure 1.3). In designed four-helix bundles, the carboxyl-termini (*C*-termini) are commonly amidated and the amino-termini (*N*-termini) acylated to prevent these termini from becoming charged, as this would lead to unfavourable interactions with the helix macrodipole.[1,26] This macrodipole is the result of the intramolecular hydrogen bonding that orientates all the carbonyl groups of the peptide amide bonds in the same direction (Figure 1.3). The charge build-up is also pH-dependent due to the different pK_a-values of acidic and basic side chains that might be present in the peptide sequence.

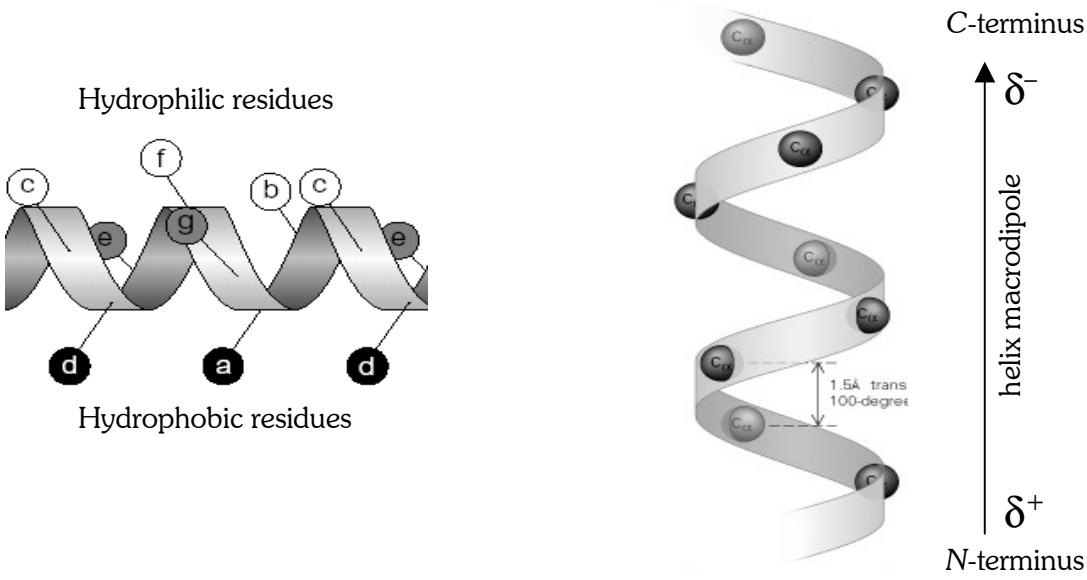

Figure 1.3. The hydrophilic and hydrophobic surface of an amphiphilic α-helix (left)[23c] and the helix macrodipole (right).[27] The letters *a*–*g* denote the positions of the residues in a heptad.

A prerequisite for α-helices to self-assemble into a four-helix bundle in an aqueous solution is that they are amphiphilic. Due to the hydrophobic effect,[28] the hydrophobic side chains will be buried inside the bundle to form a hydrophobic core, whereas the hydrophilic side chains will be exposed to the aqueous medium.[29] The opposite is applicable to membrane proteins and ion channels that span the cell membrane, as the non-polar residues are then exposed to the lipophilic nature of the membrane (Section 1.5.3).

Depending on the design, these four-helix bundles can be tetrameric (A), dimeric (B), or monomeric (C), consisting of four single α-helices, two helix-loop-helix units, or a single peptide chain, respectively, in which the individual helices are connected by loops (Figure 1.4). Furthermore, four-helix bundles are classified as parallel or anti-parallel bundles, depending on the relative orientation of the macrodipoles of the individual helices. In nature four-helix bundles are commonly encountered as anti-parallel dimeric assemblies.[5e]

Figure 1.4. Tetrameric, dimeric, and monomeric four-helix bundles.[30]

Helical bundles are commonly presented as a helical wheel diagram, which illustrates the side chain interactions within a cross-section of the bundle (Figure 1.5). The positions of the residues over two helix turns are referred to by the letters *a* through to *g*, a so-called heptad. The hydrophobic core consists of the residues at positions *a* and *d* of the heptad, whereas the residues at positions *b*, *c* and *f* of the peptide sequence form the hydrophilic exterior. The stability of four-helix bundles can be increased by the formation of interhelical salt bridges between oppositely charged residues,[31] and by optional disulphide bridges between the helices.[32,33] In addition, linking the peptides to a template or directing the assembly by co-ordination to a metal centre will also have a favourable effect on the stability of the protein (Section 1.4).

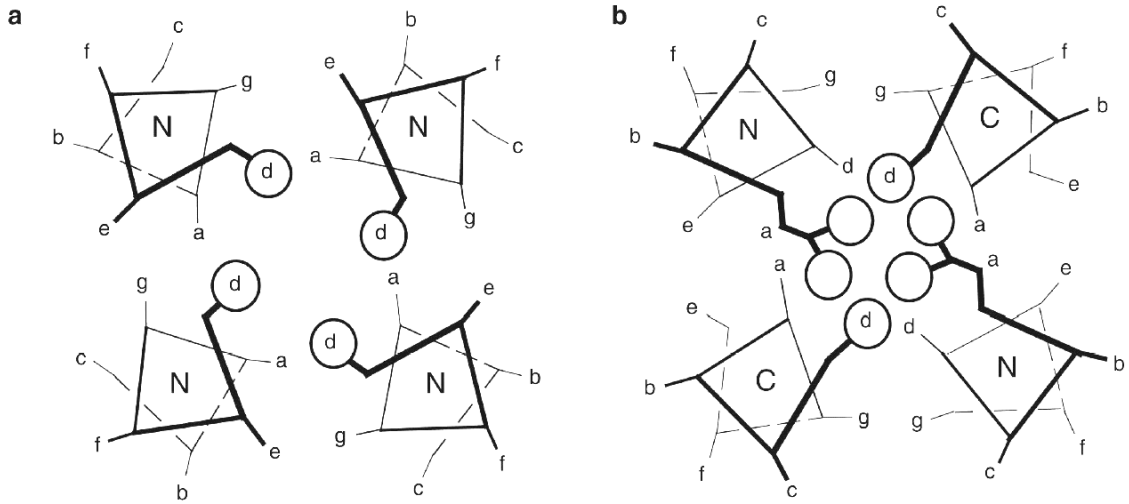

Figure 1.5. Helical wheel diagrams of a parallel (a) and an anti-parallel four-helix bundle (b), viewed from the *N*- or the *C*-terminus (here Leu and Ala are represented at positions *a* and *d*, respectively).[18,23c]

Although a considerable tolerance is accepted for the exact identity and precise packing of the side chains in the secondary structure, these factors are imperative to obtain a well-defined tertiary structure.[5b,34] A general rule applied to protein design in order for the self-assembly of helices to be selective, is that the side chain interactions between individual helices must favour the desired assembly and destabilise competing conformations (i.e. negative design).[6c] For good complementary packing in the hydrophobic core of an anti-parallel four-helix bundle,

alternating small and large residues at positions *a* and *d* are often required (Figure 1.5b).[35] Thus, the association into a parallel four-helix bundle would result in the small side chains occupying the same layer in the hydrophobic core, creating a cavity that is surrounded by layers of the larger side chains (Figure 1.5a). Also, favourable electrostatic interactions between positions *c* and *g*, and *b* and *e* of adjacent helices in anti-parallel bundles will be absent in a parallel orientation, and consequently disfavour the formation of a parallel four-helix bundle.

Although these rules are relatively simple to incorporate into the design, the interactions between positions *a* and *d* one helix turn up and down the bundle also need to be taken into account. To add to the complexity of the design, the amino acid side chains can adopt several spatial orientations. Therefore, tight packing of the hydrophobic core is the most difficult goal to accomplish with regard to the design of native-like *de novo* four-helix bundles. However, this is equally valid for the *de novo* design of proteins in general. Failure to achieve a tight packing most often results in the formation of a molten globule state; a protein folding state with a high degree of secondary structure that lacks well-defined tertiary interactions.[6c,36]

A rational and incremental approach to the *de novo* design of four-helix bundles was pioneered by DeGrado and co-workers.[5e,37] This rational design tested their understanding of the factors involved in the folding processes of the primary structure of a protein into its 3D organisation. In 1987 this research group designed the first α-helices that self-assembled in solution to form α_1, a tetramer of α-helical structures.[14] The degree of α-helicity, however, was found to be concentration dependent, which is often the case for tetrameric assemblies. When the sequence was shortened by four residues, crystals of α_1 could be obtained that consisted of a mixture of tetramers and hexamers.[37b] By connecting two units of α_1 via a short loop these helix-loop-helix units dimerised to form an anti-parallel four-helix bundle, called α_2, to neutralise the overall macrodipole effect.[14] These peptide chains were extended even further by connecting four copies of α_1 via short loops. The resulting 74-residue, single chain peptide folded into a monomeric four-helix bundle, called α_4.[37a] Its construction was the first example of a designed single chain polypeptide that was able to adopt a globular compact structure, which displayed properties that lay in between a native and a molten globule protein.

The design of α_4 resulted in a stability that was not only higher than that of the dimer α_2 and the tetramer α_1, it was also found to be more stable than most natural proteins ($\Delta G = 94.1$ kJ/mol, versus 10–40 kJ/mol for natural proteins, Table 1.1, p. 11).[37a] This stability is considered to originate from the burial and close packing of the hydrophobic leucine residues inside the core of the bundle, thus preventing their contact with water. Other helix and four-helix bundle stabilising factors have also been included into the design.[37a]

Metal-ligand interactions have also been incorporated into the design of helical bundles to furnish more native-like structures. Handel and DeGrado introduced tetrahedral zinc(II) binding sites into the hydrophobic core of four-helix bundles that were based on the sequence of α_2[4,38a] and α_4.[38b] The metal binding site consisted of histidines at three corners of a tetrahedron (H3–α_4), with the fourth position vacant for catalytic activity. The binding of zinc(II) ions did not affect the secondary structure, but it made the overall structure more ordered, causing a change from a molten globule state to a more native-like protein (Table 1.1, p. 11). Introduction of a second

metal binding site (H6–α_4) enhanced the stability of the protein even further, although it still failed to adopt a native-like conformation. Similarly, Regan and Clarke also modified the sequence of α_4 to provide a tetrahedral zinc(II) binding site consisting of histidine and cysteine residues, a chelating environment that is found in several natural metalloproteins.[39]

In contrast to the hierarchical development of four-helix bundles by DeGrado *et al.*, combinatorial libraries have been used by Hecht and co-workers by applying what they call a 'binary code' strategy.[25,40] This code only specifies the locations of polar and non-polar residues in the sequence, and not the exact identity of the amino acids. For this purpose they constructed a family of synthetic genes encoding the intrinsic genetic information that would introduce the (non-)polar residues into the correct sequence positions (binary patterning). They subsequently screened the created library for peptide chains that folded into monomeric four-helix bundles. Without the implementation of a rational design, they obtained a 75-residue protein, called M–60, that displayed native-like behaviour.[41]

Other synthetic tetrameric four-helix bundles have been prepared by redesigning natural proteins, like Rop[5d,34b–d,42] or the GCN4 leucine zipper,[43] or by the self-assembly of individual α-helices.[44] There are multiple examples of helix-loop-helix polypeptides that dimerise spontaneously into anti-parallel four-helix bundles, such as GTD–43,[45] SA–42,[46] or the bimetallic dimer DF1.[47] Single chain, anti-parallel four-helix bundles have been constructed using as many as nineteen of the twenty natural amino acids by Hecht *et al.* in the design of Felix, a 79-residue polypeptide.[48] In contrast, Stroud and co-workers used as few as seven different amino acids in preparation of a 108-residue four-helix bundle.[49] Chymohelizyme is an example of a single chain, parallel four-helix bundle that was designed and synthesised in 1990 by Hahn *et al.* as a mimic for the serine protease chymotrypsin.[50] The four peptide chains were connected through the carboxylic ends by amide bonds via the amino side chain group of lysine or ornithine.[18] Construction of a four-helix bundle by connecting four α-helices via thioether bonds has been demonstrated by Futaki *et al*.[51]

1.4 Template-assembled synthetic proteins

The self-assembly process of individual helices via intermolecular association is concentration dependent. In contrast, a single chain protein will fold through intramolecular interactions to yield a concentration independent folding that is also more stable. In natural proteins, loops and turns are used to link sequences with secondary structure. Therefore, in 1988 Mutter and co-workers introduced the concept of using artificial templates for the attachment of peptides in order to bypass the protein folding problem.[52] Since then extensive work has been published by Mutter and Tuchscherer on the concept of Template-Assembled Synthetic Proteins (TASP).[53]

As mentioned above, the four-helix bundle is a popular motif for the study of protein folding and the design of novel proteins. Therefore, a large number of TASPs with a four-helix bundle topology have been described in the literature.[23d,54] Some frequently applied scaffolds will be briefly discussed in this section. Single α-helices, β-sheets, turns, and loops have also been attached covalently to functionalised templates.[53,54] The reported results illustrate that by using a template the required minimal chain length to form α-helices in four-helix bundles can be reduced to about nine to twelve amino acids, compared to the usually observed fifteen to twenty-six residues (*vide supra*).

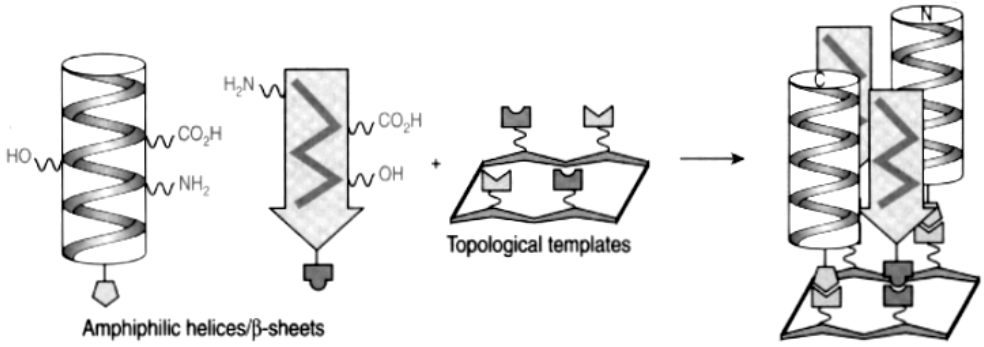

Scheme 1.1. The TASP concept.[55]

When the peptide chains are pre-organised onto a template, the favourable free energy of association will be sufficient to overcome the entropic cost and will direct the peptides to associate into the desired conformation. The template in effect constrains the mobility and orientation of the peptides, and thus can direct the assembly towards the intended peptide structure. The size and shape of the framework is not decisive for the formation of a four-helix bundle on a template.[56] Even though the peptide bundles in principle can be randomly orientated, it is common that these peptide chains come together to form helix bundles. After all, these helix bundles were designed to incorporate a hydrophobic core, and thus the hydrophobic surfaces of each helix will interact with the neighbouring helices due to the hydrophobic effect. When the design of a TASP is directed towards the formation of an anti-parallel four-helix bundle, the inverse orientation is facilitated mainly by the packing interactions of the individual helices, and not by the helix macrodipoles.[53h] Additional linkers on the template can help to form a helix bundle if the template itself is too small. However, the length and structure of the linker can influence the thermodynamic stability of the TASP.[56,57] For instance, the linker might be able to form hydrogen bonds with functional groups on the template.[57]

The TASP concept enables peptide chains to be brought in close proximity in order to study the folding mechanisms of the primary sequences. Similarly to what has been suggested for native proteins, the folding of TASPs commences through the formation of secondary structure, followed by the construction of a compact 3D state, like three- or four-helix bundles (Scheme 1.2).[53a]

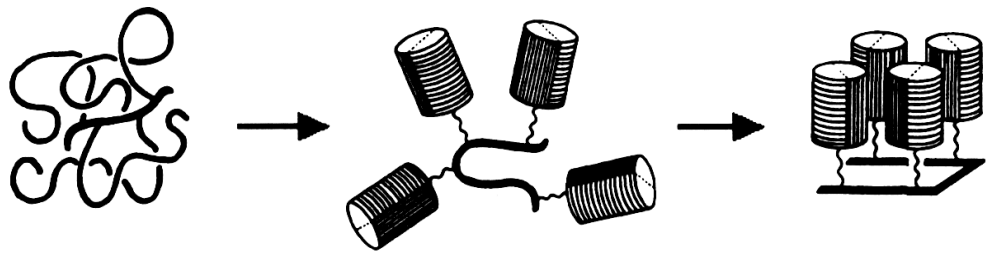

Scheme 1.2. The folding process of a TASP four-helix bundle.[53a]

Numerous molecular structures can be used as a template (Figure 1.7).[58] The only requirements for a template molecule entail stability and the ability to provide functionality (i.e. attachment

sites) at the periphery to obtain the appropriate spatial orientation of peptides. Also, it should be readily accessible and provide the possibility of structural modification of the template or the peptide linkers. Obviously, the number of functional groups defines the number of peptides that can be attached to the template. The distance between the attachment sites can be varied by the frame of choice, and thus makes it possible to optimise the hydrophobic interactions between the amphiphilic peptide chains. The template then serves as a (rigid) scaffold to acquire a maximum stability for the tertiary structure. In addition, the template can contribute to the designed protein function, for instance by providing a cavity for the substrate, or by the use of a metalloporphyrin for oxidative or redox activity (*vide infra*).

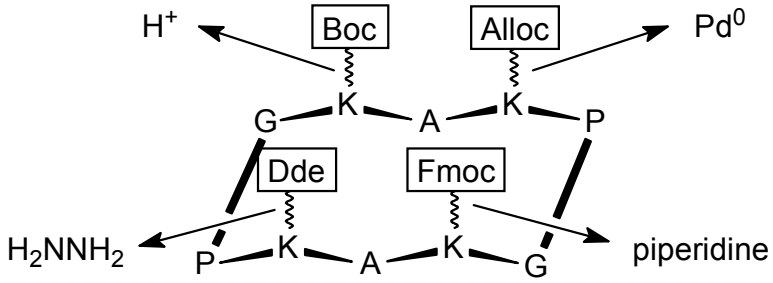

Figure 1.6. Selectively removable protecting groups on a cyclic peptide template (adopted from reference 53g).[18,59]

If the template consists of functional groups that can be selectively addressed, different peptide chains can be attached in a controlled manner (Regioselectively Addressable Functionalised Templates, RAFT).[60] This can be achieved by the use of chemically different attachment sites, or by selectively removable (orthogonal) protecting groups (Figure 1.6). Stepwise attachment of peptide chains is also an option when equimolar amounts relative to a single functional group are being used.[61] The obvious problem, of course, is the formation of side-products from multiple reactions.

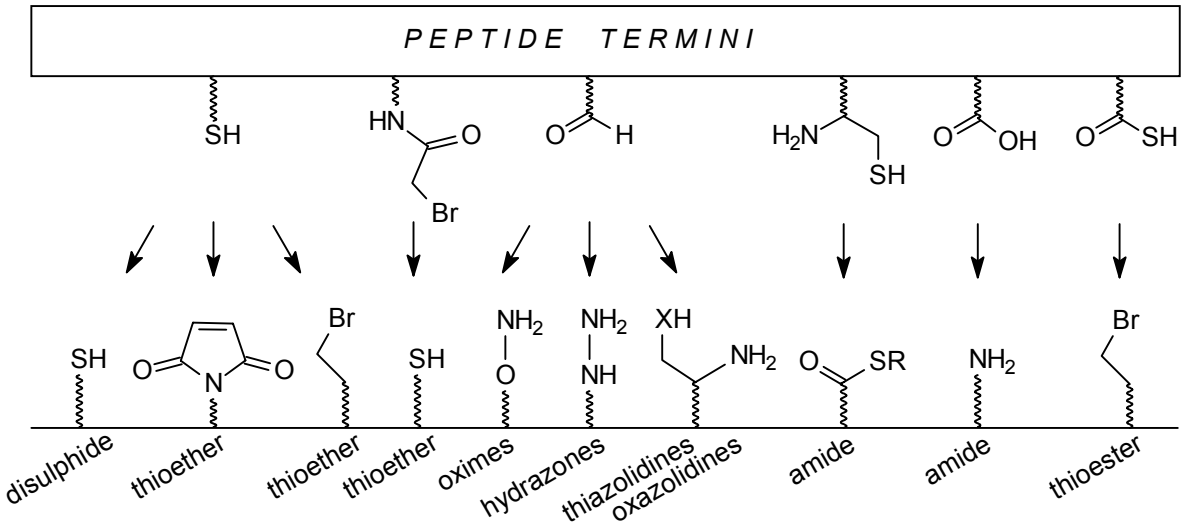

Scheme 1.3. Chemoselective ligation of peptides to functionalised templates.[53d]

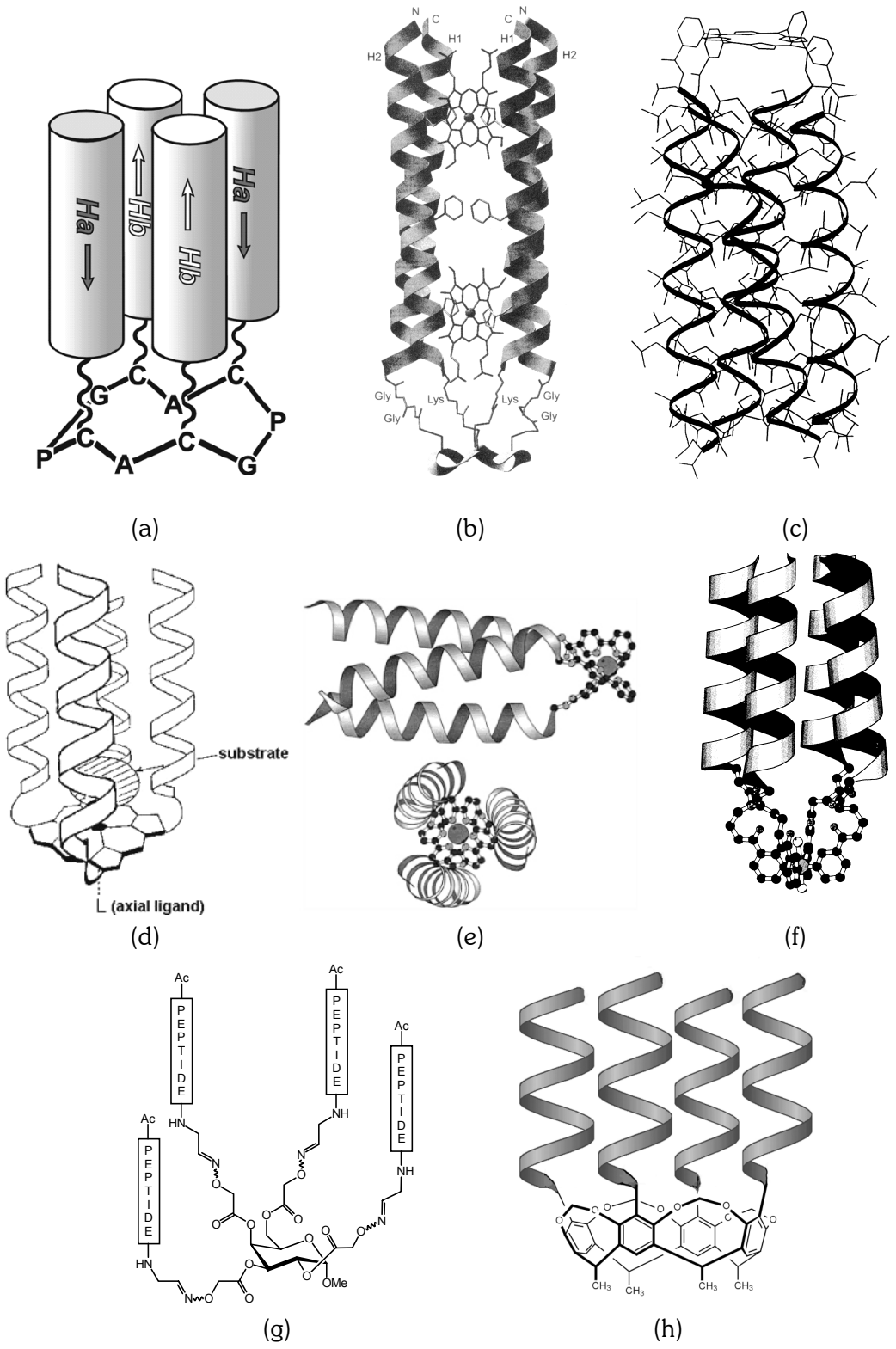

Figure 1.7. Template-Assembled Synthetic Proteins. (a) cyclic peptide as a template;[53d] (b) cyclic peptide as a template with two additional co-ordinated haem groups;[62a] (c) covalently linked tetraphenylporphyrin;[63] (d) covalently linked coproporphyrin I unit;[64] (e) three bipyridine tethers co-ordinated to a Ru(II) ion;[65c] (f) co-ordination of four pyridine tethers to a Ru(II) ion;[66] (g) a D-galacto-pyranoside as a template;[67] (h) a cavitand as a template.[68]

Peptides have been covalently tethered to templates by, for instance, amide,[53a,66,69–72] oxime,[73,74] disulphide,[75–77] and thioester[78] bond formation (Scheme 1.3). Also, peptide chains with bromo- or chloro-acetylated *N*-termini have been linked to thiols[57,79–81] or (thio)phenolic[57,68,82] functionalities to produce a (thio)ether bond. Other methods of chemoselective ligation are a Michael addition[83] and reductive amination.[61] The amino acid sequences themselves can be readily obtained and modified through Solid-Phase Peptide Synthesis (SPPS).[84] In order to prevent unwanted side reactions, protected peptides are usually coupled to the template. However, depending on the chosen ligation method, sometimes good results have also been obtained using unprotected peptides that were attached to the scaffold.[62,73,78,81]

The strength of the TASP approach is that by connecting individual peptides that have a concentration dependent secondary structure, the overall structure has a significantly increased stability that is independent of concentration.[56,71] Another general observation is an increase in α-helicity for template-bound helical bundles. Although the enhanced peptide helicity can also be explained by intermolecular interactions of multiple TASP peptide chains, this effect has been attributed to intramolecular interactions of a single TASP.[56] By tethering peptide chains to

Table 1.1. Protein denaturation and stability parameters.[a]

Protein		$C_{0.5}$ (M)	$-\Delta G^{H_2O}$ (kJ mol^{-1})	Ref.
Native proteins:	Lysozyme	4.2	37	85
	α-Lactalbumin	3.6	18	85
	Apocytochrome b_{562}	n.d.[b]	13	86
	Ferricytochrome b_{562}	n.d.[b]	28	86
	Ribonuclease	3.0	31	85
Designed four-helix bundles:	$(\alpha'-SS-\alpha')_2$ (dimer)	4.8	96.2	87a
	(α–*l*–α–SS–α–*l*–α)	5.2	46.9	87b
	SA–42 (dimer)	~4	53.6	88
	RA–42 (dimer)	~1	36	88
	DF1 (dimer)	n.d.[b]	12.1	47a
	Ac–α_4–$CONH_2$	6.3	64.4	38a
	H6α_4	3.4	10	38b
	Zn^{2+}–H6α_4	5.5	43.1	38b
	M–60	~7	~17	41
TASPs:	Helichrome	5.2	18	64b
	Metal ion-assisted	5.5	23	66
	MOP1	1.3	13.7	62a
	MOP1 bis-haem	2.5	30.4	62a
	Carbohydrate-based	5.1	29	67c
	Cavitein	8.0	95.8	57

[a] The data have been acquired using the equation $\Delta G_{unf} = \Delta G^{H_2O} + mC$,[89] where ΔG^{H_2O} is the free energy of folding in the absence of denaturant, C is the concentration of the denaturant guanidinium hydrochloride, and m is the co-solvation term, which is a measure of the co-operativity of the transition. $C_{0.5}$ is the concentration at which 50% of the protein is denatured. [b] n.d. = not determined.

the template, stronger inter-helical interactions will be induced more than in the absence of a template. Therefore, TASPs are generally found to be thermodynamically more stable than their related helical peptides that are not assembled onto a template. Variations in the design of the protein structure[90] will also contribute to the differences in the reported stabilities given in Table 1.1.

1.4.1 Cyclic peptides

Templates based on cyclic peptides typically consist of ten amino acids. Four residues (usually lysine or cysteine) are then positioned in such a way that their side chains are orientated to provide a well-defined spatial arrangement to accommodate a four-helix bundle.[53,69,71,73] As illustrated in Figure 1.7a, the use of linkers directs the α-helices away from the template. Therefore, the template only facilitates and directs the assembly and folding of the peptide chains without interfering with the stabilising interactions that drive the assembly. Peptide loops are also commonly encountered as a scaffold for TASPs.[53,78,79,91] Although most of the presented work is related to four-helix bundles on one side of the template, some additional work has also led to the construction of TASPs with two bundles; one on either side of the template.[53,91]

The peptides can be grafted onto the template via their *N*- or *C*-terminus using standard peptide coupling reactions as in the case of lysines for attachment sites. Cysteine is also frequently used, which enables peptides to be coupled via the halide displacement of a halo-acylated *N*-terminus, or by disulphide formation (Scheme 1.3). Nowadays, with the availability of a wide range of (un)natural amino acids and a choice of numerous orthogonal protecting groups, these peptidic templates are suited for structural variations and are readily available via SPPS. The strength of utilising templates that contain selectively removable protecting groups is that up to four different peptide sequences can be grafted selectively and modularly onto the template, both in a parallel or anti-parallel orientation.

Due to the ease of a selective modular assembly of peptides onto a peptide template, these templates have been widely used to study the relationships between the protein structure and its stability, and the protein structure and its function.[53d,e] As an example, Rau and Haehnel have designed a modular anti-parallel protein (MOP) that is based on a cyclopeptide as a template (Figure 1.7b).[62] This structure was further stabilised by the incorporation of two haem groups sandwiched between two parallel helices, as observed in cytochrome *b*. These haem groups are axially ligated by histidines in the peptide sequences.

Cyclic peptides have also been applied to TASPs that are immobilised onto a solid phase to facilitate their synthesis and purification.[92] Recently, Haehnel and co-workers assembled a combinatorial library of amphiphilic peptides in an anti-parallel orientation onto a cellulose-bound template (right).[93] This demonstration of the TASP concept resulted in the construction of the first copper binding four-helix bundle by incorporating cysteines and histidines into the peptide sequences.[93b] Similarly, a library of cytochrome *b* mimics was created by incorporating haem-binding sites into the design.[93a]

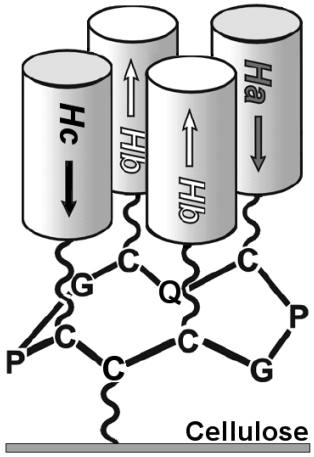

1.4.2 Porphyrins

Construction of novel proteins with functional properties can be achieved, for instance, when a flavin moiety[94–96] or a metal binding site is incorporated.[7c,97] Commonly, haem (iron protoporphyrin IX) or porphyrins are used in the *de novo* design to provide an electron transfer or redox function to the artificial haemoprotein.[97b] Metalloporphyrins in nature are commonly found in haemoglobins, cytochromes, and peroxidases.[98] The different types of porphyrin structures are bound either via co-ordination to histidines residues or by covalent binding to the protein scaffold. Natural haemoproteins can perform dioxygen transport and storage, in addition to oxygen and hydrogen peroxide activation during catalytic oxidation reactions. However, examples of synthetic haemoproteins mimicking these functions are less abundant in the literature.[99–101]

Co-ordination of a haem or a porphyrin unit to a *de novo* designed haemoprotein can be obtained by incorporating binding sites into the sequences (Figure 1.7b).[62,75,97b,102,103] The four-helix bundle motif is flexible and can diverge to accommodate a prosthetic haem group as observed in the natural cytochromes *c*' and b_{562}.[23] In general, the co-ordination of a haem or a porphyrin structure results in an increased stability of the bundle.[38b,75,102] To obtain a tightly packed hydrophobic core, a pocket can be introduced into the design to accommodate the haem more effectively.[95,104] The stabilising effect of porphyrin structures on helical bundles does not solely stem from the axial ligation of co-ordinating histidines. It has been shown that hydrophobic interactions between the (hydrophobic) surfaces of the porphyrin and the hydrophobic face of the helices also stabilise haemoproteins.[105] In contrast to the aforementioned TASPs based on peptidic templates, the metal centre of these metalloproteins can be located anywhere within the protein bundle depending on the position of the chelating residues. The peptides that encapsulate the metal centre can in principle influence the accessibility of a substrate to the embedded active site, and thus might be used to induce substrate specificity.

Choma *et al.* were the first to prepare a four-helix bundle in which a single haem (iron protoporphyrin IX) was sandwiched between α-helices by bis-axial ligation of the imidazole groups of histidine residues (Figure 1.8).[104] The four-helix bundle was constructed by linking two redesigned α_2 units via a disulphide bridge. The introduction of additional histidines into the peptide sequences can result in multi-haem proteins,[62,97,102,106,107] as demonstrated by the designed *maquettes* of Dutton and co-workers (*see* Section 1.5).[32,87,108]

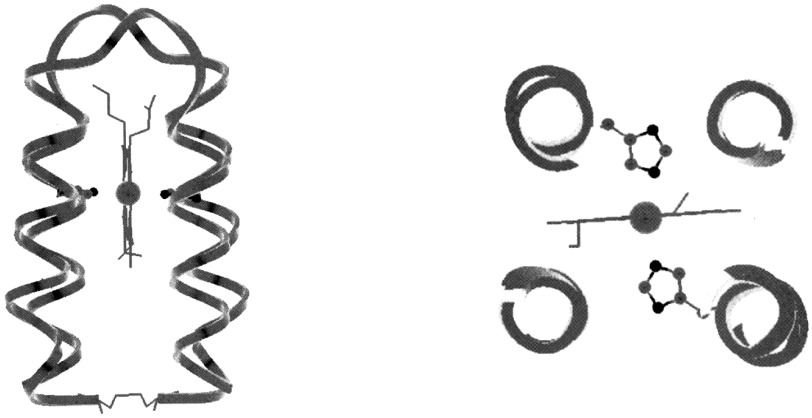

Figure 1.8. A haem-stabilised four-helix bundle; side view (left) and top view (right).[104]

Porphyrins bearing four functional groups can be used as templates for the covalent attachment of peptides at the periphery of the macrocycle (Figure 1.7c,d).[63,64,76,81,96,97b,106,109] These functionalities are commonly located in the *ortho*-positions of tetraphenylporphyrin (TPP) derivatives to facilitate the close proximity of the peptide chains. Only the α,α,α,α-atropisomer of TPP derivatives will uniformly align the attached peptides to establish the formation of the four-helix bundle. When a flexible linker is used, the energy barrier for atropisomerisation can be sufficiently reduced to enable free rotation.[109] The hydrophobic effect will subsequently drive the amphiphilic peptides to assemble into a four-helix bundle. Due to this design strategy, the porphyrin template will be positioned on one side of the bundle. The appending porphyrin ring in Helichrome thereby provides a hydrophobic pocket, which is also active in the catalytic cycle (Figure 1.7d).[64] Similarly, Åkerfeldt *et al*. successfully constructed a membrane ion channel mimic, called Tetraphilin, by coupling unprotected peptides to a TPP scaffold (Figure 1.7c).[63]

1.4.3 Metal ion-assisted self-assembly

Metal-binding sites in proteins can be classified on the basis of either structural or functional roles. In protein design, co-ordination of metal binding sites (ligands) in peptides to a transition metal ion is a means of controlling the assembly process during the formation of helical bundles. Complexation of the α-helices can occur via the covalently bound chelating groups (like pyridine or bipyridine) at the peptide terminus,[65,66,110] or via metal-binding sites inside the hydrophobic core.[47,111] The hydrophobic interactions are the driving force for the formation of the helix bundle, whereas complexation of the ligands to the metal ion controls the number of participating peptide chains. Lieberman and Sasaki have described the use of a 15-residue amphiphilic α-helix with a *N*-terminal bipyridine tether for complexation to an iron(II) ion.[110] Similarly, Ghadiri and co-workers have obtained the resulting parallel three-helix bundle by co-ordination of bipyridine-modified 15-residue peptides around a ruthenium(II) ion (Figure 1.7e).[65] This synthetic metalloprotein was used to measure electron-transfer rates, thus providing a function for the *de novo* designed structure. The assembly resulted in the formation of a three-helix bundle, due to the co-ordination of these bipyridyl moieties to the transition metals. A stable parallel four-helix bundle was assembled by Ghadiri *et al*. by co-ordinating four pyridine-modified 15-residue α-helices around a ruthenium(II) ion with two additional chloride anions as axial ligands (Figure 1.7f).[66]

1.4.4 Carbohydrates

The cyclic structure of carbohydrates has also been applied as a rigid template in the construction of TASPs. Jensen and Barany have outlined a solid-phase preparation of a derivatised D-galactopyranose that enabled the attachment of four identical 16-residue peptides. These peptides are linked to the four available hydroxyl functionalities of the monosaccharide via a short spacer to yield a stable four-helix bundle (Figure 1.7g).[67] The structure, however, lacks function and has only been employed for the design study of a native-like protein.

The rigid cyclic structure of α-, β-, and γ-cyclodextrins makes it possible to assemble six, seven, and eight peptide chains, respectively. Åkerfeldt and DeGrado have been able to prepare a heptameric assembly by coupling 7-residue peptides to a β-cyclodextrin scaffold.[112] Although

the cyclodextrin template can potentially function as a receptor,[113] practical applications for cyclodextrins in the design of artificial enzymes have as yet not been reported by the authors.

1.4.5 Macrocycles

A number of approaches utilising macrocyclic scaffolds have been described in recent years. These more or less rigid organic molecules contain hydrophobic cavities that offer a potential binding site for substrate recognition, although so far no such function has been presented in the literature. Cavitands have been applied as a template for four-helix bundles by Sherman and co-workers (Figure 1.7f).[57,68] These authors proposed the name caviteins for the *de novo* designed proteins, originating from the words *cavit*and and prot*eins*. By varying the length of the spacer between the peptide and the template, they were able to study the influence of the flexibility and rigidity of the scaffold on the overall stability of the structure. Causton and Sherman have also designed and synthesised a three-helix bundle by attaching the peptide chains to a rigid cyclotribenzylene (CTB) macrocycle (Figure 1.9).[76] The three thiol groups on the periphery of CTB were used to covalently link unprotected peptides with *N*-terminal cysteines via disulphide bonds. Similarly, van Wageningen and Liskamp have used a cyclotriveratrylene-based scaffold (CTV) that enabled the covalent attachment of three amino acid sequences via amide bonds.[72] The calix[4]arene has been used by Hamilton and co-workers as a scaffold for the attachment of four peptide loops to mimic an antibody recognition site.[114]

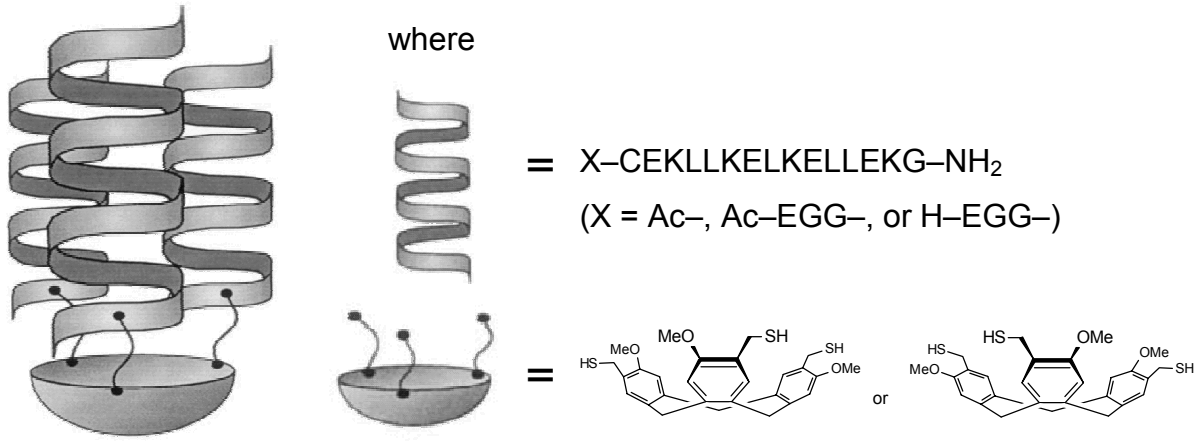

Figure 1.9. Schematic representation of CTB as a template for three-helix bundles.[18,76]

1.5 Artificial proteins: Function by design

Until recently, the major focus of protein design has been the understanding of the protein folding processes and the construction of small tertiary polypeptide structures with a pre-defined conformation. Without such an understanding of folding principles and structure-stability relationships, the introduction of useful function into the design of artificial proteins will be unsuccessful. It has already been mentioned that many designed protein structures behave as molten globules. The fluctuating conformations will therefore have a negative effect on the spatial organisation of the artificial protein, and hence its active site.

With regard to the designed functional proteins in this section, the focus will be directed towards helical bundles. The active centre of the functionalised structures is usually located inside the hydrophobic core of the four-helix bundle. Their relatively small size and ease of modification has made four-helix bundles the most commonly studied motif for the design of synthetic proteins. Furthermore, they have high solubilities in water and are in general relatively stable over a wide pH-range.

Natural haemoproteins are capable of catalysing redox reactions, binding small molecules (e.g. CO, NO, CN), and performing electron transfer reactions. These enzyme functions have all been established by *de novo* designed haemoproteins.[101]

1.5.1 Artificial enzymes

Artificial enzymes are, almost by definition, inspired by natural enzymes.[8,115] The residues used to form the active site often resemble the substrate binding pockets of the native protein. The substrate specificity of enzymes is determined by the arrangement of amino acid residues in the active site that bind to the functional groups of the substrate molecules, and in the case of metalloproteins also by the positioning of the metal ion. Therefore, in order for a designed peptide to act truly as an enzyme mimic, these characteristics will need to be incorporated and expressed by the artificial protein. The use of templates in the *de novo* design of functional four-helix bundles not only offers the opportunity to construct more native-like proteins; the size and shape of the template can in principle allow for selectivity during the reaction, based on the size and nature of the substrate.

The main disadvantage of porphyrin-based (per)oxidases is their sensitivity towards oxidative degradation, either by the oxidant or by the reactive metal-oxo intermediate. However, it has been found that the stability of a peroxidase can be increased by the nature of the peptide surrounding.[116] The peptides are thought to act as radical scavengers or as an alternative source for hydrogen abstraction, which would otherwise take place on the porphyrin ring.

Substrate recognition[30,117,118] and rate enhancements of more than three orders of magnitude over background reactions[117a,118,119] have been reported for reactions catalysed by designed helical bundles (*vide infra*). So far, artificial proteins capable of stereospecific reduction and oxidation have yet to be constructed, but taking into consideration the progress made over the last few decades, even this function might become reality in the near future.

Mihara *et al*. have constructed an artificial flavin protein that is capable of *oxidising* dihydronicotinamides.[95,96] Their design consisted of a 53-residue single chain four-helix bundle,[95] or four appending α-helices on a Mn–TPP moiety[96] in which all helices were identical except for one helix with a flavin-modified cysteine in the centre of the hydrophobic core. The oxidation of 1-benzyl-1,4-dihydronicotinamide, with a rate constant of 290 $M^{-1}s^{-1}$, was 1.35 times faster than the reaction catalysed by the unbound 7-acetylflavin moiety.[95] This rate was more than doubled (k 660 $M^{-1}s^{-1}$) when a second flavin group was introduced into the helix bundle. By electron transfer via the flavin unit the liberated electrons in this oxidation process were also capable of reducing the manganese(III) in the porphyrin ring to Mn^{II}–TPP.[96]

By employing a combinatorial approach to the design of single chain four-helix bundles, Hecht and colleagues have been able to obtain some haem-binding peptides that displayed *peroxidase* activity.[103] Although a haem-binding site had not been incorporated into the design itself, one protein in particular, protein 86, was capable of oxidising ABTS with a maximum turnover frequency of 17,000 min^{-1}. Even though this is over forty times faster than any other artificial porphyrin-based peroxidase, it is still much slower than the native horseradish peroxidase (HRP) (~60,000 min^{-1}).[103b] Peroxidase activity has also been achieved with a disulphide linked three-helix bundle to which a haem is covalently attached,[76] and a disulphide linked dimeric four-helix bundle that contained a co-ordinated haem group.[75b] The potential oxidation of the disulphide bonds by the terminal oxidant hydrogen peroxide was not addressed by the authors.

Mono-oxygenation of styrene and its derivatives to their epoxides has been achieved by a peptide-modified manganese(III)TPP, using iodosylbenzene as the oxidant.[80] Substrate discrimination could be established depending on the solvent. The authors did not mention any oxidation of the thioether linkage that had been used to span the peptide across the porphyrin.

Benson *et al*. have designed novel proteins that displayed *superoxide dismutase* (SOD) activity of about 1% of the wild-type SOD.[120]

A *de novo* designed peptide *ligase*, consisting of a dimeric 33-residue amphiphilic helical sequence, catalysed the ligation of hydrophobic peptides (Scheme 1.4) with rate enhancements of up to five orders of magnitude over that of the uncatalysed reaction.[117b]

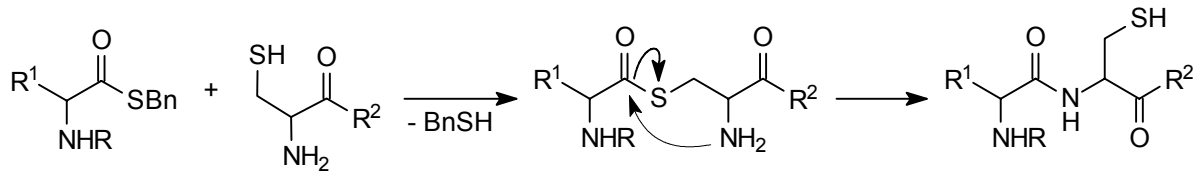

Scheme 1.4. The peptide ligation reaction.

Broo and co-workers have constructed a symmetric 42-residue helix-loop-helix homo-dimer (KO–42) with a reactive site consisting of twelve histidine residues.[30,117] This artificial enzyme is capable of substrate specific *transesterification* reactions, as well as nucleophilic and general acid *hydrolysis* of *p*-nitrophenyl esters. The pH-dependent reaction rate is up to three orders of magnitude faster than compared to the 4-methylimidazole catalysed reaction.

Hahn *et al.* have reduced the sequence of the *protease* chymotrysin, a single chain peptide with 245 residues, to a 73-residue protein, called Chymohelizyme.[50] Although the substrate specificity was of a similar nature and the catalyst achieved over a hundred catalytic turnovers, the rate of hydrolysis was about one hundred times less effective than that of the natural enzyme.

In an effort to construct a synthetic *decarboxylase*, Benner and co-workers have designed a *de novo* enzyme, called oxaldie, that self-assembles in solution to form helical structures.[119] The rate of decarboxylation of oxaloacetate is about five orders slower than that of the natural enzyme. However, this is still about nine hundred times faster than the uncatalysed decarboxylation and three to four orders of magnitude faster than the reaction catalysed by simple amines. Remarkably, oxaldie does not require any metal ions, as opposed to the natural

oxaloacetate decarboxylases, which require magnesium or manganese ions as a cofactor. Even less effective is the dimeric four-helix bundle NP–42, designed by Baltzer and co-workers, that decarboxylates oxaloacetate only ten times faster than butylamine.[121]

The coproporphyrin-based four-helix bundle Helichrome, which was designed by Sasaki and Kaiser to function as an *aniline hydroxylase*, produces *p*-aminophenol in the presence of NADH and oxygen with a rate comparable to that of the natural haemoprotein haemoglobin.[64]

The examples presented here of functional four-helix bundles are capable of catalysing a variety of enzymatic reactions, although most of them are often inferior to their natural equivalents. Even though the reports in the literature only describe the successful attempts, the fact that protein designers are now capable of designing and constructing functional synthetic proteins, it is still seen as a quite remarkable achievement. With an increased understanding of the processes involved, the implementation of the required adjustments into the design will no doubt facilitate the construction of more native-like performances by artificial enzymes.

1.5.2 Redox activity

Many approaches to redox active four-helix bundles have been followed in recent years.[4,7e] For the design of redox proteins the co-ordination environment for the metal can be provided by correctly positioning two to four amino acids with chelating side chains, commonly histidine or cysteine. These residues can be co-ordinated to a transition metal or a prosthetic group (haem or porphyrin) with a vacant or loosely bound site for its function, such as carbon monoxide binding.[101] Metallo- and haemoproteins can display a pH-dependence for the binding of metal ions or haem groups, as protonation of histidine will result in the dissociation of the cofactor. With precise design, site-selective binding of different metals,[122] or iron(III) and zinc(II) protoporphyrin IX can be accomplished.[108e]

The work carried out by Dutton and co-workers serves as an illustrative example of the *de novo* design of novel *redox proteins* based on the four-helix bundle topology.[32,87,108] The initially designed assembly consisted of a parallel dimer of two identical, disulphide-linked α-helices, each containing thirty-one residues.[32] The authors refer to these $(\alpha\text{–SS–}\alpha)_2$ motifs as '*maquettes*'; simplified synthetic protein scaffolds that still retain some of the functions of the native enzyme. Structural variations enabled them to incorporate up to four iron haem units inside the hydrophobic core (right)[108a] without significantly affecting the helical content of the four-helix bundle.[87b] The nature of the prosthetic groups was found to be able to control the parallel or anti-parallel orientation of the protein bundle through steric interactions.[108g] By connecting two helix-loop-helix (α–*l*–α) units via a disulphide bridge a single chain four-helix bundle (α–*l*–α–SS–α–*l*–α) was obtained that was somewhat more resistant to denaturation than the dimer (Table 1.1).[87b]

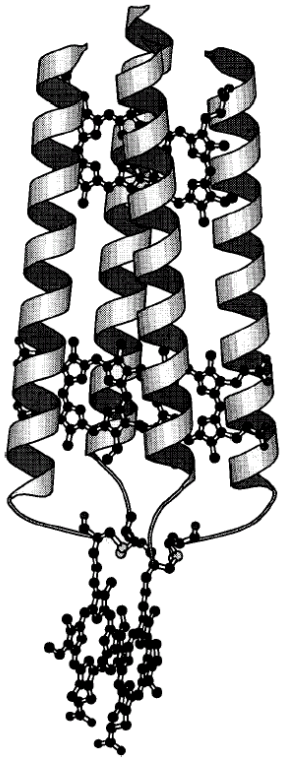

The use of *de novo* designed *maquettes* allowed Dutton and colleagues to selectively introduce different haem groups,[108g] and construct a protein with an affinity for halothane,[123] a volatile anaesthetic guest molecule.[108c] In addition, they succeeded in constructing proteins with a pH-controlled redox potential.[108d] Conversely, major pK_a shifts were observed for the acidic and basic groups upon reduction or oxidation of the haem group, as oxidation of the cofactor increased its positive charge and, thereby, reduced its proton affinity. The multi-haem *maquettes* display a co-operative redox behaviour, which is thought to arise from the electronic interactions between the individual haems. As a result, they were able to acquire significant diversity in the haem reduction midpoint potential (−350 to +175 mV at neutral pH compared to −400 to +400 mV for natural haem proteins).[108h,i] A photosynthetic reaction centre was introduced by integrating two appending coproporphyrin I moieties. However, this approach resulted in a disappointing quantum yield of <0.01.[108a]

In view of the number of possible structural variations in the amino acid sequence, *de novo* design of artificial (metallo)proteins lends itself to combinatorial design strategies. As an example of a library approach, McLendon and co-workers have mutated cytochrome b_{562}, a haem-binding four-helix bundle peptide, at two positions in the sequence near the site for haem binding while maintaining the original structural motif.[124] The resulting structures displayed redox potential variations of over 1000 mV.

A great deal of research has been devoted to the study of (light-induced)[62b] *electron transfer* for *de novo* designed redox proteins.[65,108a,124] Willner *et al.* have presented an elegant example by incorporating two iron(III) protoporphyrin IX (Fe−PP) units into a four-helix bundle that was assembled as a monolayer onto a gold electrode.[106] Electron transfer was made possible by a difference in the redox potential of the Fe−PPs due to a difference in the distance to the gold surface. The helix bundle has also been connected covalently to a cytochrome b_1-dependent nitrate reductase, establishing a bioelectrocatalysed *reduction* of NO_3^- in 80% yield (Figure 1.10).[107] Alternatively, cross-linking the helix bundle to Co−PP−reconstituted myoglobin enabled the electrocatalysed *hydrogenation* of acetylene dicarboxylic acid to maleic acid possible in 85% yield.[107b]

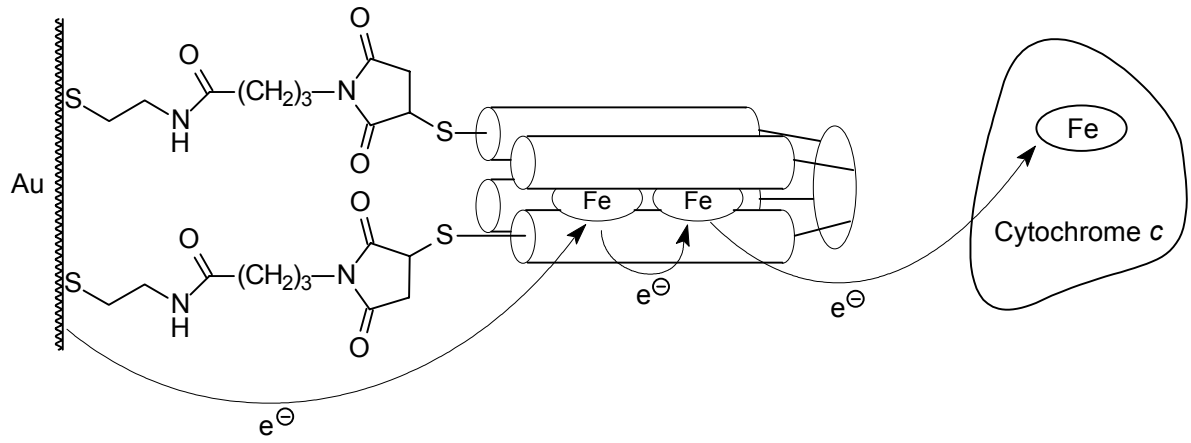

Figure 1.10. Electrochemical reduction of cytochrome *c*.[107b]

1.5.3 Membrane proteins and ion channels

Helical bundles have also been designed to function as ion channels that can distinguish between small ions, like H^+, Li^+, K^+, Na^+, and Cs^+. In order to act as a pore, these bundles need to span the cell membrane. Incorporation into the lipophilic membrane requires a hydrophobic exterior, which is contrary to the helical bundles that have been discussed so far. A representative example by DeGrado and colleagues utilises amphiphilic helices consisting of only leucines and serines that self-assembled into a four-helix bundle.[125] The exact sequence composition affected the packing of the protein core, which as a result directed the cation-selectivity of the ion channel. The membrane protein in turn could be 'coated' by amphiphilic helices to change the hydrophobic nature of its exterior, making the protein soluble in water.[126] As observed for other TASPs, covalent attachment of the sequences to a (cyclic) peptide[69,79b,127] or TPP[63] template (Figure 1.7c) enhanced the stability of the synthetic pore.

1.5.4 Antibody recognition

Template-assembled synthetic proteins have also been described as functional mimics in antibody recognition.[60,114] The template is often a cyclic peptide, but also self-assembled tetrameric and dimeric four-helix bundles have been described as an antigenic determinant.[44a] By duplicating only the functional part of a protein (Figure 1.11), the properties of the large natural enzyme can be effectively replicated. Normally, small antigen mimics are rapidly degraded *in vivo*, unless the sequences are assembled as loops onto a scaffold or protein.[128]

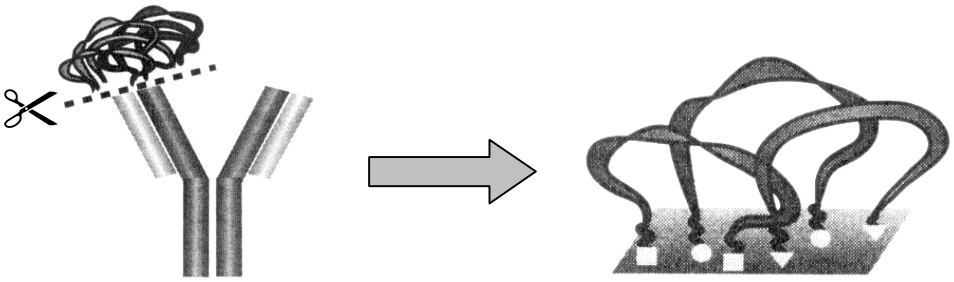

Figure 1.11. Receptor mimetics using regioselectively addressable templates.[53f]

These small designed, synthetic peptides are capable of liberating antibodies that can for instance recognise the natural HLA–A2 antigen.[128] It is also worthwhile mentioning that self-assembled monolayers of TASP molecules on a gold surface have been examined as potential *biosensors*.[53e]

1.6 Research objectives and outline of this thesis

The presented examples of functional enzyme mimics based on the four-helix bundle motif clearly demonstrate that these small peptide bundles can be provided with a function that resembles that of a larger protein structure. Although a great deal of progress has been made in the last decade towards the design of small peptide structures, designing architectures that have function as well as a defined construction still remains an extremely difficult task to master and should not be underestimated.

Despite all the examples of functional four-helix bundles presented in the literature, so far no examples have been published for the design of a synthetic peroxidase or oxygenase-based on a non-haem catalytic centre. The small oxidising catalyst N4PyFe that was developed in our group opens up an opportunity to create such a functional enzyme mimic. The design strategy is to embed the catalyst inside a four-helix bundle by attaching four helical peptides via a cysteine residue to a tetrafunctionalised N4Py ligand. Suffice it to say that the position of the cysteine in the peptide sequence will enable a site-specific introduction of the catalyst into the core of the bundle. In Scheme 1.5 a schematic representation of this concept is depicted where the four-helix bundle is tethered to the catalyst via a terminal cysteine residue. Alternatively, if the cysteine residues are positioned centrally in the peptide sequence, the N4PyFe catalyst will be situated in the middle of the bundle (Figure 1.2). The relative orientation of the individual helices is then an issue, which could be controlled by directed interactions that will favour the designed helix bundle. First, we need to evaluate the feasibility of this ambitious project.

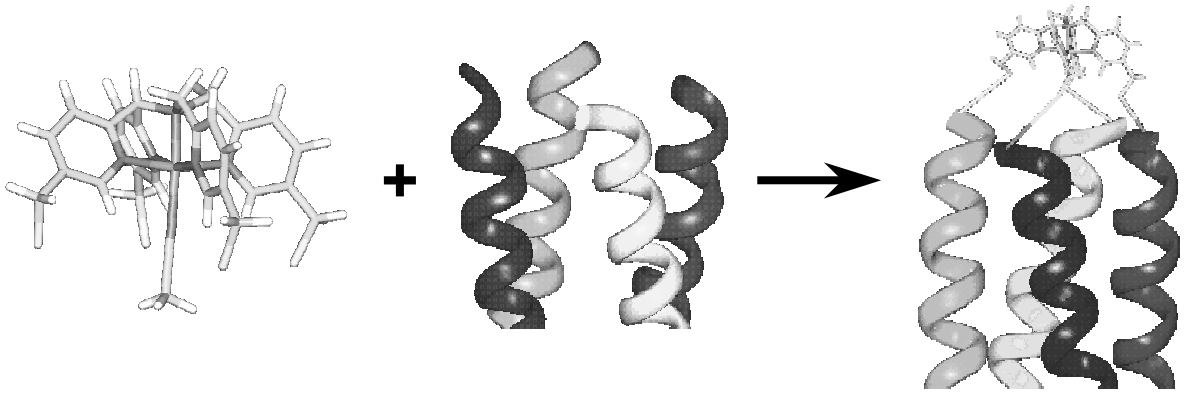

Scheme 1.5. Schematic representation of tethering a four-helix bundle to the N4PyFe catalyst.

The aim of the research presented in this thesis is to develop modified N4Py ligands that will enable the covalent attachment of four peptide chains. Once that has been accomplished successfully, peptide sequences can be selected, which have been designed to fold into a four-helix bundle. However, before the catalyst is incorporated into a bundle protein, it needs to be ascertained whether or not the attached peptides can withstand the oxidising conditions, as well as the highly reactive iron-oxo intermediate, and thereby do not diminish the catalyst activity.

We first tested this concept by attaching two peptide chains to a disubstituted N4Py ligand (Chapter 2).[15] The iron(II) complex retained its catalytic oxidation activity with hydrogen peroxide in water. Subsequently, the N4Py ligand was successfully modified into a template by the introduction of functional groups. This enabled the application of the TASP methodology to the N4Py ligand and established the incorporation of the N4PyFe catalyst in a peptide environment by the covalent attachment of four peptides (Chapter 3).

The presented synthetic route follows a convergent strategy for the construction of tetrafunctionalised N4Py ligands. An alternative, a divergent synthesis has also been developed that facilitated the construction of the N4Py skeleton prior to its functionalisation (Chapter 4). The potential strength of this latter method is that it will also enable structural variations using for instance cross coupling reactions to prepare a small library of functionalised N4Py ligands.

And finally, the application of several tetrasubstituted N4PyFe catalysts in oxidation reactions will be discussed in Chapter 5, as well as the peroxidase activity of an assembled N4PyFe-peptide complex. As is commonly found for oxidising haemoproteins, the N4PyFe catalyst and the peptide-bound equivalents are also susceptible to oxidative degradation. Optimisation of the peptide surrounding could eventually result in a prolonged lifetime of the future non-haem peroxidase.

1.7 References and notes

1. (a) Creighton, T. E., In *Protein Structure: a Practical Approach*; IRL Press, Oxford Press: UK, 1989; pp. 169–224. (b) Creighton, T. E., In *Protein Function*; W. H. Freeman and Co.: USA, 1992. (c) Creighton, T. E., In *Proteins; Structures and Molecular Properties*; W. H. Freeman and Co.: USA, 1993. (d) Darby, N. J.; Creighton, T. E., In *Protein Structure*; IRL Press, Oxford Press: UK, 1993. (e) Creighton, T. E., In *Protein Function*; IRL Press, Oxford Press: UK, 1997; pp. 57–100. (f) Fersht, A., In *Structure and Mechanism in Protein Science: a Guide to Enzyme Catalysis and Protein Folding*; W. H. Freeman and Co.: USA, 1999.
2. (a) Jaeger, K.-E.; Reetz, M. T. *Curr. Opin. Chem. Biol*. **2000**, *4*, 68–73. (b) Penning, T. M.; Jez, J. M. *Chem. Rev*. **2001**, *101*, 3027–3046. (c) Lu,Y.; Berry, S. M.; Pfister, T. D. *Chem. Rev*. **2001**, *101*, 3047–3080. (d) Qi, D.; Tann, C.-M.; Haring, D.; Distefano, M. D. *Chem. Rev.* **2001**, *101*, 3081–3111. (e) Brakmann, S. *CHEMBIOCHEM* **2001**, *2*, 865–871.
3. Serrano, L. *Adv. Prot. Chem.* **2000**, *53*, 50–85.
4. DeGrado, W. F.; Summa, C. M.; Pavone, V.; Nastri, F.; Lombardi, A. *Annu. Rev. Biochem.* **1999**, *68*, 779–819.
5. (a) DeGrado, W. F.; Raleigh, D. P.; Handel, T. M. *Curr. Opin. Struct. Biol.* **1991**, *1*, 984–993. (b) Betz, S. F.; Raleigh, D. P.; DeGrado, W. F. *Curr. Opin. Struct. Biol.* **1993**, *3*, 601–610. (c) Bryson, J. W.; Betz, S. F.; Lu, H. S.; Suich, D. J.; Zhou, H. X.; ONeil, K. T.; DeGrado, W. F. *Science* **1995**, *270*, 935–941. (d) Betz, S. F.; Liebman, P. A.; DeGrado, W. F. *Biochemistry* **1997**, *36*, 2450–2458. (e) Hill, R. B.; Raleigh, D. P.; Lombardi, A.; DeGrado, W. F. *Acc. Chem. Res.* **2000**, *33*, 745–754.
6. (a) Sander, C. *Curr. Opin. Struct. Biol.* **1991**, *1*, 630–637. (b) Beasley, J. R.; Hecht, M. H. *J. Biol. Chem.* **1997**, *272*, 2031–2034. (c) Baltzer, L.; Nilsson, H.; Nilsson, J. *Chem. Rev.* **2001**, *101*, 3153–3163.
7. (a) Baltzer, L.; Nilsson, J. *Curr. Opin. Biotechnol*. **2001**, *12*, 355–360. (b) Bornscheuer, U. T.; Pohl, M. *Curr. Opin. Chem. Biol*. **2001**, *5*, 137–143. (c) Xing, G.; DeRose, V. J. *Curr. Opin. Chem. Biol.* **2001**, *5*, 196–200. (d) Woolfson, D. N. *Curr. Opin. Struct. Biol*. **2001**, *11*, 464–471. (e) Kennedy, M. L.; Gibney, B. R. *Curr. Opin. Struct. Biol*. **2001**, *11*, 485–490.
8. Motherwell, W. B.; Bingham, M. J.; Six, Y. *Tetrahedron* **2001**, *57*, 4663–4686 and references cited therein.
9. Feiters, M.C., Rowan, A.E., Nolte, R. J. M. *Chem. Soc. Rev*. **2000**, *29*, 375–384.
10. (a) Lubben, M., In *Model Systems for Iron and Copper Containing Oxygenases*, Ph. D. thesis, Groningen, 1994; pp. 43–71. (b) Lubben, M.; Meetsma, A.; Wilkinson, E. C.; Que, Jr., L; Feringa, B. L. *Angew. Chem. Int. Ed. Engl.* **1995**, *34*, 1512–1514. (c) Roelfes, J.

G., In *Models for Non-Heme Iron Containing Oxidation Enzymes*, Ph. D. thesis, Groningen, 2000.

11. For an explanation of the abbreviations used, see Appendix 1 (p. 149).
12. (a) Roelfes, G.; Lubben, M.; Leppard, S. W.; Schudde, E. P.; Hermant, R. M.; Hage, R.; Wilkinson, E. C.; Que, L., Jr.; Feringa, B. L. *J. Mol. Catal. A: Chem.* **1997**, *117*, 223–227. (b) Roelfes, G.; Lubben, M.; Hage, R.; Que, L., Jr.; Feringa, B.L. *Chem. Eur. J.* **2000**, *6*, 2152–2159.
13. Roelfes, J. G.; Branum, M. E.; Wang, L.; Que, L., Jr.; Feringa, B. L. *J. Am. Chem. Soc.*, **2000**, *122*, 11517–11518.
14. Ho, S. P.; DeGrado, W. F. *J. Am. Chem. Soc.* **1987**, *109*, 6751–6758.
15. Choma, C. T.; Schudde, E. P.; Kellogg, R. M.; Robillard, G. T.; Feringa, B. L. *J. Chem. Soc.*, *Perkin Trans. 1* **1998**, 769–773.
16. (a) Weber, P. C.; Salemme, F. R. *Nature* **1980**, *287*, 82–82 and references cited therein. (b) Richardson, J. S. *Adv. Protein Chem.* **1981**, *34*, 167–339.
17. Merkx, M.; Kopp, D. A.; Sazinsky, M. H.; Blazyk, J. L.; Müller, J.; Lippard, S. J. *Angew. Chem. Int. Ed.* **2001**, *40*, 2782–2807.
18. See Appendix 2 (p. 151) for the α-amino acid structures and abbreviations.
19. Image adapted from Chou, K.-C.; Maggiora, G. M.; Némethy, G.; Scheraga, H. A. *Proc. Natl. Acad. Sci. USA* **1988**, *85*, 4295–4299.
20. Taylor, K. S.; Lou, M.-Z.; Chin, T.-M.; Yang, N. C.; Garavito, R. M. *Protein Sci.* **1996**, *5*, 414–421.
21. (a) Chotia, C. *Annu. Rev. Biochem.* **1984**, *53*, 537–572. (b) DeGrado, W. F.; Wasserman, Z. R.; Lear, J. D. *Science* **1989**, *243*, 622–628.
22. Reddy, B. V. B.; Blundell, T. L. *J. Mol. Biol.* **1993**, *233*, 464–479.
23. (a) Cohen, C.; Parry, D. A. D. *Proteins Struct. Funct. Genet.* **1990**, *7*, 1–15. (b) Betz, S. F.; Bryson, J. W.; DeGrado, W. F. *Curr. Opin. Struct. Biol.* **1995**, *5*, 457–463. (c) Kohn, W. D.; Hodges, R. S. *Trends Biotechnol.* **1998**, *16*, 379–389. (d) Venkatraman, J.; Shankaramma, S. C.; Balaram, P. *Chem. Rev.* **2001**, *101*, 3131–3152.
24. Myers, J. K.; Pace, C. N.; Scholtz, J. M. *Proc. Natl. Acad. Sci. USA* **1997**, *94*, 2833–2837.
25. Kamtekar, S.; Schiffer, J. M.; Xiong, H.; Babik, J. M.; Hecht, M. H. *Science* **1993**, *262*, 1680–1685.
26. (a) Chakrabartty, A.; Baldwin, R. L. *Adv. Prot. Chem.* **1995**, *46*, 141–176. (b) Andrews, M. J. I.; Tabor, A. B. *Tetrahedron* **1999**, *55*, 11711–11743.
27. Stryer, L. In *Biochemistry*; W. H. Freeman and Co.: USA, 1995.
28. Blokzijl, W.; Engberts, J. B. F. N. *Angew. Chem. Int. Ed. Engl.* **1993**, *32*, 1545–1579.
29. Dill, K. A. *Biochemistry* **1990**, *29*, 7133–7155.
30. Baltzer, L.; Broo, K. S. *Biopolymers (Peptide Sci.)* **1998**, *47*, 31–40.
31. Schneider, J. P.; Lear, J. D.; DeGrado, W. F. *J. Am. Chem. Soc.* **1997**, *119*, 5742–5743.
32. Robertson, D. E.; Farid, R. S.; Moser, C. C.; Urbauer, J. L.; Mulholland, S. E.; Pidikiti, R.; Lear, J. D.; Wand, A. J.; DeGrado, W. F.; Dutton, P. L. *Nature* **1994**, *368*, 425–432.
33. Zhou, N. E.; Kay, C. M.; Hodges, R. S. *Biochemistry* **1992**, *31*, 5739–5746.

34. (a) Sandberg, W. S.; Terwilliger, T. C. *Science* **1989**, *245*, 54–56. (b) Munson, M.; O'Brien, R.; Sturtevant, J. M.; Regan, L. *Protein Sci.* **1994**, *3*, 2015–2022. (c) Munson, M.; Balasubramanian, S.; Fleming, K. G.; Nagi, A. D.; O'Brien, R.; Sturtevant, J. M.; Regan, L. *Protein Sci.* **1996**, *5*, 1584–1593. (d) Vlassi, M.; Cesareni, G.; Kokkinidis, M. *J. Mol. Biol.* **1998**, *285*, 817–827.
35. Betz, S. F.; DeGrado, W. F. *Biochemistry* **1996**, *35*, 6955–6962.
36. (a) Kuwajima, K. *Proteins Struct. Funct. Genet.* **1989**, *6*, 87–103. (b) Ptitsyn, O. B. *Adv. Prot. Chem.* **1995**, *47*, 83–229. (c) Arai, M.; Kuwajima, K. *Adv. Prot. Chem.* **2000**, *53*, 209–282.
37. (a) Regan, L.; DeGrado, W. F. *Science* **1988**, *241*, 976–978. (b) Hill, C. P.; Anderson, D. H.; Wesson, L.; DeGrado, W. F.; Eisenberg, D. *Science* **1990**, *249*, 543–546. (c) Raleigh, D. P.; DeGrado, W. F. *J. Am. Chem. Soc.* **1992**, *114*, 10079–10081. (d) Raleigh, D. P.; Betz, S. F.; DeGrado, W. F. *J. Am. Chem. Soc.* **1995**, *117*, 7558–7559. (e) Hill, R. B.; DeGrado, W. F. *J. Am. Chem. Soc.* **1998**, *120*, 1138–1145.
38. (a) Handel, T. M.; DeGrado, W. F. *J. Am. Chem. Soc.* **1990**, *112*, 6710–6711. (b) Handel, T. M.; Williams, S. A.; DeGrado, W. F. *Science* **1993**, *261*, 879–885.
39. Regan, L.; Clarke, N. D. *Biochemistry* **1990**, *29*, 10878–10883.
40. (a) Xiong, H.; Buckwalter, B. L.; Shieh, H. M.; Hecht, M. H. *Proc. Natl. Acad. Sci., USA* **1995**, *92*, 6349–6353. (b) Moffet, D. A.; Hecht, M. H. *Chem. Rev.* **2001**, *101*, 3191–3203.
41. Roy, S.; Ratnaswamy, G.; Boice, J. A.; Fairman, R. McLendon, G.; Hecht, M. H. *J. Am. Chem. Soc.* **1997**, *119*, 5302–5306.
42. (a) Predki, P. F.; Regan, L. *Biochemistry* **1995**, *34*, 9834–9839. (b) Lassalle, M. W.; Hinz, H. J.; Wenzel, H.; Vlassi, M.; Kokkinidis, M.; Cesareni, G. *J. Mol. Biol.* **1998**, *279*, 987–1000. (c) Ceruso, M. A.; Grottesi, A.; Di Nola, A. *Proteins Struct. Funct. Genet.* **1999**, *36*, 436–446.
43. (a) Harbury, P. B.; Zhang, T.; Kim, P. S.; Alber, T. *Science* **1993**, *262*, 1401–1407. (b) DeLano, W. L.; Brünger, A. T. *Proteins Struct. Funct. Genet.* **1994**, *20*, 105–123. (c) Gonzalez, Jr. L.; Woolfson, D. N.; Alber, T. *Nature Struct. Biol.* **1996**, *3*, 1011–1018.
44. Kaumaya, P. T. P.; Berndt, K. D.; Heidorn, D. B.; Trewhella, J.; Kezdy, F. J.; Goldberg, E. *Biochemistry* **1990**, *29*, 13–23.
45. (a) Dolphin, G. T.; Brive, L.; Johansson, G.; Baltzer, L. *J. Am. Chem. Soc.* **1996**, *118*, 11297–11298. (b) Brive, L.; Dolphin, G. T.; Baltzer, L. *J. Am. Chem. Soc.* **1997**, *119*, 8598–8607. (c) Dolphin, G. T.; Baltzer, L. *Fold. Design* **1997**, *2*, 319–330.
46. Olofsson, S.; Johansson, G.; Baltzer, L. *J. Chem. Soc., Perkin Trans. 2* **1995**, 2047–2056.
47. (a) Lombardi, A.; Summa, C. M.; Geremia, S.; Randaccio, L.; Pavone, V.; DeGrado, W. F. *Proc. Natl. Acad. Sci. USA* **2000**, *97*, 6298–6305. (b) Di Costanzo, L.; Wade, H.; Geremia, S.; Randaccio, L.; Pavone, V.; DeGrado, W. F.; Lombardi, A. *J. Am. Chem. Soc.* **2001**, *123*, 12749–12757.
48. Hecht, M. H.; Richardson, J. S.; Richardson, D. C.; Ogden, R. C. *Science*, **1990**, *249*, 884–891.
49. Schafmeister, C. E.; LaPorte, S. L.; Miercke, L. J. W.; Stroud, R. M. *Nature Struct. Biol.* **1997**, *4*, 1039–1046.

50. Hahn. K. W.; Kliss, W. A.; Stewart, J. M. *Science* **1990**, *248*, 1544–1547.
51. Futaki, S.; Ishikawa, T.; Niwa, M.; Kitagawa, K.; Yagami, T. *Bioorg. Med. Chem.* **1997**, *5*, 1883–1891.
52. (a) Mutter, M.; Tuchscherer, G. *Makromol. Chem.*, *Rapid Commun*. **1988**, *9*, 437–443. (b) Mutter, M.; Altmann, E.; Altmann, K.-H.; Hersperger, R.; Koziej, P.; Nebel, K.; Tuchscherer, G.; Vuilleumier, S.; Gramlich, H.-U.; Müller, K. *Helv. Chim. Acta* **1988**, *71*, 835–847.
53. (a) Mutter, M.; Vuilleumier, S. *Angew. Chem. Int. Ed. Engl.* **1989**, *28*, 535–554. (b) Tuchscherer, G.; Dumy, D.; Mutter, M. *Chimia* **1996**, *50*, 644–648. (c) Eggleston, I. M.; Mutter, M. *Macromol. Symp.* **1996**, *101*, 397–404. (d) Mutter, M.; Tuchscherer, G. *Cell. Mol. Life. Sci.* **1997**, *53*, 851–863. (e) Tuchscherer, G.; Scheibler, L.; Dumy, P.; Mutter, M. *Biopolymers (Peptide Sci.)* **1998**, *47*, 63–73. (f) Tuchscherer, G.; Grell, D.; Mathieu, M.; Mutter, M. *J. Peptide Res.* **1999**, *54*, 185–194. (g) Mutter, M.; Tuchscherer, G. *Chimia* **2000**, *54*, 552–557. (h) Grell, D.; Richardson, J. S.; Mutter, M. *J. Peptide Sci.* **2001**, *7*, 146–151.
54. Fernandez-Carneado, J.; Grell, D.; Durieux, P.; Hauert, J.; Kovacsovics, T.; Tuchscherer, G. *Biopolymers (Peptide Sci.)* **2000**, *55*, 451–458.
55. Tuchscherer, G.; Mutter, M. *Chem.Ind*. **1997**, 597–601.
56. Wong, A. K.; Jacobsen, M. P.; Winzor, D. J.; Fairlie, D. P. *J. Am. Chem. Soc.* **1998**, *120*, 3836–3841.
57. Mezo, A. R.; Sherman, J. C. *J. Am. Chem. Soc.* **1999**, *121*, 8983–8994.
58. (a) Schneider, J. P.; Kelly, J. W. *Chem. Rev.* **1995**, *95*, 2169–2187. (b) Tuchscherer, G.; Mutter, M. *J. Biotechnol.* **1995**, *41*, 197–210.
59. For an explanation of the abbreviations used, see Appendix 1 (p. 149).
60. Mutter, M.; Dumy, P.; Garrouste, P.; Lehmann, C.; Mathieu, M.; Peggion, C.; Peluso, S.; Razaname, A.; Tuchscherer, G. *Angew. Chem. Int. Ed. Engl.* **1996**, *35*, 1482–1485.
61. Tahmassebi, D. C.; Sasaki, T. *J. Org. Chem.* **1998**, *63*, 728–731.
62. (a) Rau, H. K.; Haehnel, W. *J. Am. Chem. Soc.* **1998**, *120*, 468–476. (b) Rau, H. K.; DeJonge, N.; Haehnel, W. *Proc. Natl. Acad. Sci.*, *USA* **1998**, *95*, 11526–11531. (c) Fahnenschmidt, M.; Rau, H. K.; Bittle, R.; Haehnel, W.; Lubitz, W. *Chem. Eur. J.* **1999**, *5*, 2327–2334. (d) Fahnenschmidt, M.; Bittle, R.; Schlodder, E.; Haehnel, W.; Lubitz, W. *Phys. Chem. Chem. Phys.* **2001**, *3*, 4082–4090.
63. (a) Åkerfeldt, K. S.; Kim, R. M.; Camac, D.; Groves, J. T.; Lear, J. D.; DeGrado, W. F. *J. Am. Chem. Soc.* **1992**, *114*, 9656–9657. (b) Åkerfeldt, K. S.; Lear, J. D.; Wasserman, Z. R.; Chung, L. A.; DeGrado, W. F. *Acc. Chem. Res.* **1993**, *26*, 191–197.
64. (a) Sasaki, T.; Kaiser, E. T. *J. Am. Chem. Soc.* **1989**, *111*, 380–381. (b) Sasaki, T.; Kaiser, E. T. *Biopolymers* **1990**, *29*, 79–88.
65. (a) Ghadiri, M. R.; Soares, C.; Choi, C. *J. Am. Chem. Soc.* **1992**, *114*, 825–831. (b) Mutz, M. W.; Case, M. A.; Wishart, J. F.; Ghadiri, M. R.; McLendon, G. L. *J. Am. Chem. Soc.* **1999**, *121*, 858–859. (c) Case, M. A.; Ghadiri, M. R.; Mutz, M. W.; McLendon, G. L. *Chirality*, **1998**, *10*, 35–40.
66. Ghadiri, M. R.; Soares, C.; Choi, C. *J. Am. Chem. Soc.* **1992**, *114*, 4000–4002.

67. (a) Jensen, K. J.; Barany, G. *J. Peptide Res.* **2000**, *56*, 3–11. (b) Brask, J.; Jensen, K. J. *J. Peptide Sci.* ***2000***, *6*, 290–299. (c) Brask, J.; Jensen, K. J. *Bioorg. Med. Chem. Lett.* **2001**, *11*, 697–700.
68. Gibb, B. C.; Mezo, A. R.; Sherman, J. C. *Tetrahedron Lett.* **1995**, *36*, 7587–7590.
69. Pawlak, M.; Meseth, U.; Dhanapal, B.; Mutter, M.; Vogel, H. *Protein Sci.* **1994**, *3*, 1788–1805.
70. Bambino, F.; Brownlee, R. T. C.; Chiu, F. C. K. *Tetrahedron Lett.* **1994**, *35*, 4619–4622.
71. Mutter, M.; Tuchscherer, G.; Miller, C.; Altmann, K.-H.; Carey, R. I.; Wyss, D. F.; Labhardt, A. M.; Rivier, J. E. *J. Am. Chem. Soc.* **1992**, *114*, 1463–1470.
72. Van Wageningen, A. M. A.; Liskamp, R. M. J. *Tetrahedron Lett.* **1999**, *40*, 9347–9351.
73. Tuchscherer, G. *Tetrahedron Lett.* **1993**, *34*, 8419–8422.
74. Rose, K. *J. Am. Chem. Soc.* **1994**, 116, 30–33.
75. (a) Sakamoto, S.; Ueno, A.; Mihara, H. *Chem. Commun.* **1998**, 1073–1074. (b) Sakamoto, S.; Obataya, I.; Ueno, A.; Mihara, H. *J. Chem. Soc.*, *Perkin Trans. 2* **1999**, 2059–2069.
76. Obataya, I.; Kotaki,T.; Sakamoto,S.; Ueno, A.; Mihara, H. *Bioorg. Med. Chem. Lett.* **2000**, *10*, 2719–2722.
77. Causton, A. S.; Sherman, J. C. *Bioorg. Med. Chem.* **1999**, *7*, 23–27.
78. Dawson, P. E.; Kent, S. B. *J. Am. Chem. Soc.* **1993**, *115*, 7263–7266.
79. (a) Futaki, S.; Sogawa, K.; Maruyama, J.; Asahara, T.; Niwa, M. *Tetrahedron Lett.* **1997**, *38*, 6237–6240. (b) Futaki, S.; Aoki, M.; Fukada, M.; Kondo, F.; Niwa, M.; Kitagawa, K.; Nakaya, Y. *Tetrahedron Lett.* **1997**, *38*, 7071–7074.
80. Geier, G. R.; Sasaki, T. *Tetrahedron* **1999**, *55*, 1859–1870.
81. Choma, C. T.; Kaestle, K.; Åkerfeldt, K. S.; Kim, R. M.; Groves, J. T.; DeGrado, W. F. *Tetrahedron Lett.* **1994**, *35*, 6191–6194.
82. Gibb, B. C.; Mezo, A. R.; Causton, A. S.; Fraser, J. R.; Tsai, F. C. S.; Sherman, J. C. *Tetrahedron* **1995**, *51*, 8719–8732.
83. Nefzi, A., Sun, X., Mutter, M. *Tetrahedron Lett.* **1995**, *36*, 229–230.
84. (a) Atherton, E.; Sheppard, R. C., In *Solid Phase Peptide Synthesis: a Practical Approach*; IRL Press, Oxford Press: UK, 1989. (b) Fields, G. B., In *Methods in Enzymology*, *Solid-Phase Peptide Synthesis*; Academic Press, Inc.: USA, 1997; Vol. 289.
85. Ahmad, F.; Bigelow, C. C. *Biopolymers* **1986**, *25*, 1623–1633.
86. Feng, Y.; Sligar, S. G. *Biochemistry* **1991**, *30*, 10150–10155.
87. (a) Gibney, B. R.; Rabanal, F.; Skalicky, J. J.; Wand, A. J.; Dutton, P. L. *J. Am. Chem. Soc.* **1997**, *119*, 2323–2324. (b) Gibney, B. R.; Rabanal, F.; Reddy, K. S.; Dutton, P. L. *Biochemistry* **1998**, *37*, 4635–4643.
88. Lundhl, A.-C.; Broo, K.; Baltzer, L. *J. Chem. Soc.*, *Perkin Trans. 2* **1997**, 209–212.
89. Santoro, M. M.; Bolen, D. W. *Biochemistry* **1988**, *27*, 8063–8068.
90. E.g. by difference in side chain packing due to the newly created substrate pocket, or by unfavourable macrodipole interaction due to parallel vs. antiparallel orientation of the helices.

91. Mutter, M.; Hersperger, R.; Gubernator, K.; Müller, K. *Proteins Struct. Funct. Genet.* **1989**, *5*, 13–21.
92. Peluso, S.; Dumy, P.; Nkubana, C.; Yokokawa, Y.; Mutter, M. *J. Org. Chem.* **1999**, *64*, 7114–7120.
93. (a) Rau, H. K.; DeJonge, N.; Haehnel, W. *Angew. Chem. Int. Ed.* **2000**, *39*, 250–253. (b) Schnepf, R.; Hörth, P.; Bill, E.; Wieghardt, K.; Hildebrandt, P.; Haehnel, W. *J. Am. Chem. Soc.* **2001**, *123*, 2186–2195.
94. (a) Sharp, R. E.; Moser, C. C.; Rabanal, F.; Dutton, P. L. *Proc. Natl. Acad. Sci. USA* **1998**, *95*, 10465–10470. (b) Tomizaki, K.-Y.; Tsunekawa, Y.; Akisada, H.; Mihara, H.; Nishino, N. *J. Chem. Soc., Perkin Trans. 2* **2000**, 813–822.
95. Mihara, H.; Tomizake, K.; Nishino, N.; Fujimoto, T. *Chem. Lett.* **1993**, 1533–1536.
96. Mihara, H.; Tomizake, K.; Fujimoto, T.; Sakamoto, S.; Aoyagi, H.; Nishino, N. *Chem. Lett.* **1996**, 187–188.
97. Lombardi, A.; Nastri, F.; Pavone, V. *Chem. Rev.* **2001**, *101*, 3165–3189.
98. Ballou, D. P. (Ed.), In *Essays in Biochemistry: Metalloproteins*; Portland Press: UK, 1999; Vol. 34, pp. 51–100.
99. For the catalytic oxidation of alkenes, see (a) reference 80. (b) Geier, G. R.; Sasaki, T. *Tetrahedron* **1999**, *55*, 1871–1880.
100. For aryl- and alkyl-substituted iron porphyrins as functional models for oxygen binding and activation, see (a) Collman, J. P.; Eberspacher, T.; Fu, L.; Herrmann, P. C. *J. Mol. Catal. A: Chem.* **1997**, *117*, 9–20. (b) Nastri, F.; Lombardi, A.; D'Andrea, L. D.; Sanseverino, M.; Maglio, O.; Pavone, V. *Biopolymers* **1998**, *47*, 5–22, and references cited therein.
101. For carbon monoxide binding, see Moffet, D. A.; Case, M. A.; House, J. C.; Vogel, K.; Williams, R. D.; Spiro, T. G.; McLendon, G. L.; Hecht, M. H. *J. Am. Chem. Soc.* **2001**, *123*, 2109–2115.
102. Xu, Z.; Farid, R. S. *Protein Sci.* **2001**, *10*, 236–249.
103. (a) Rojas, N. R. L.; Kamtekar, S.; Simons, C. T.; McLean, J. E.; Vogel, K. M.; Spiro, T. G.; Farid, R. S.; Hecht, M. H. *Protein Sci.* **1997**, *6*, 2512–2524. (b) Moffet, D. A.; Certain, L. K.; Smith, A. J.; Kessel, A. J.; Beckwith, K. A.; Hecht, M. H. *J. Am. Chem. Soc.* **2000**, *122*, 7612–7613.
104. Choma, C. T.; Lear, J. D.; Nelson, M. J.; Dutton, P. L.; Robertson, D. E.; DeGrado, W. F. *J. Am. Chem. Soc.* **1994**, *116*, 856–865.
105. Huffman, D. L.; Suslick, K. S. *Inorg. Chem.* **2000**, *39*, 5418–5419.
106. (a) Ushiyama, M.; Arisaka, F.; Yamamura, T. *Chem. Lett.* **1999**, 127–128. (b) Ushiyama, M.; Yoshino, A.; Yamamura, T.; Shida, Y.; Arisaka, F. *Bull. Chem. Soc. Jpn.* **1999**, *72*, 1351–1364.
107. (a) Katz, E.; Heleg-Shabtai, V.; Willner, I.; Rau, H. K.; Haehnel, W. *Angew. Chem. Int. Ed.* **1998**, *37*, 3253–3256. (b) Willner, I.; Heleg-Shabtai, V.; Katz, E.; Rau, H. K.; Haehnel, W. *J. Am. Chem. Soc.* **1999**, *121*, 6455–6468.
108. (a) Rabanal, F.; DeGrado, W. F.; Dutton, P. L. *J. Am. Chem. Soc.* **1996**, *118*, 473–474. (b) Gibney, B. R.; Johansson, J. S.; Rabanal, F.; Skalicky, J. J.; Wand, A. J.; Dutton, P. L.

Biochemistry **1997**, *36*, 2798–2806. (c) Johansson, J. S.; Gibney, B. R.; Rabanal, F.; Reddy, K. S.; Dutton, P. L. *Biochemistry* **1998**, *37*, 1421–1429. (d) Shifman, J. M.; Moser, C. C.; Kalsbeck, W. A.; Bocian, D. F.; Dutton, P. L. *Biochemistry* **1998**, *37*, 16815–16827. (e) Sharp, R. E.; Diers, J. R.; Bocian, D. F.; Dutton, P. L. *J. Am. Chem. Soc.* **1998**, *120*, 7103–7104. (f) Tommos, C.; Skalicky, J. J.; Pilloud, D. L. Wand, A. J.; Dutton, P. L. *Biochemistry* **1999**, *38*, 9495–9507. (g) Gibney, B. R.; Isogai, Y.; Rabanal, F.; Reddy, K. S.; Grosset, A. M.; Moser, C. C.; Dutton, P. L. *Biochemistry* **2000**, *39*, 11041–11049. (h) Shifman, J. M.; Gibney, B. R.; Sharp, R. E.; Dutton, P. L. *Biochemistry* **2000**, *39*, 14813–14821. (i) Gibney, B. R.; Huang, S. S.; Skalicky, J. J.; Fuentes, E. J.; Wand, A. J.; Dutton, P. L. *Biochemistry* **2001**, *40*, 10550–10561.

109. Arai, T.; Kobata, K.; Mihara, H.; Fujimoto, T.; Nishino, N. *Bull. Chem. Soc. Jpn.* **1995**, *68*, 1989–1998.
110. (a) Lieberman, M.; Sasaki, T. *J. Am. Chem. Soc.* **1991**, *113*, 1470–1471. (b) Sasaki, T.; Lieberman, M. Tetrahedron 1993, 49, 3677–3689.
111. For 3-helix bundle, see (a) Suzuki, K.; Hiroaki, H.; Kohda, D.; Nakamura, H.; Tanaka, T. *J. Am. Chem. Soc.* **1998**, *120*, 13008–13015. (b) Li, X.; Suzuki, K.; Kanaori, K.; Tajima, K.; Kashiwada, A.; Hiroaki, H.; Kohda, D.; Tanaka, T. *Protein Sci.* **2000**, *9*, 1327–1333.
112. Åkerfeldt, K. S.; DeGrado, W. F. *Tetrahedron Lett.* **1994**, *35*, 4489–4492.
113. (a) Breslow, R.; Dong, S. D. *Chem. Rev*. **1998**, *98*, 1997–2011. (b) Uekama, K.; Hirayama, F.; Irie, T. *Chem. Rev*. **1998**, *98*, 2045–2076.
114. Hamuro, Y.; Calama, M. C.; Park, H. S.; Hamilton, A. D. *Angew. Chem. Int. Ed. Engl.* **1997**, *36*, 2680–2683.
115. Ishida, H.; Inoue, Y. *Biopolymers* (*Peptide Sci.*) **2000**, *55*, 469–478.
116. Spee, J. H.; Boersma, M. G.; Veeger, C.; Samyn, B.; Van Beeumen, J.; Warmerdam, G.; Canters, G. W.; Van Dongen, W. M. A. M.; Rietjens, I. M. C. M. *Eur. J. Biochem.* **1996**, *241*, 215–220.
117. (a) Broo, K. S.; Brive, L.; Ahlberg, P.; Baltzer, L. *J. Am. Chem. Soc.* **1997**, *119*, 11362–11372. (b) Broo, K. S.; Nilsson, H.; Nilsson, J.; Flodberg, A.; Baltzer, L. *J. Am. Chem. Soc.* **1998**, *120*, 4063–4068. (c) Broo, K. S.; Nilsson, H.; Nilsson, J.; Baltzer, L. *J. Am. Chem. Soc.* **1998**, *120*, 10287–10295. (d) Baltzer, L.; Broo, K. S.; Nilsson, H.; Nilsson, J. *Bioorg. Med. Chem.* **1999**, *7*, 83–91. (e) Nilsson, J.; Baltzer, L. *Chem. Eur. J*. **2000**, *6*, 2214–2220.
118. (a) Severin, K.; Lee, D. H.; Kennan, A. J.; Ghadiri, M. R. *Nature* **1997**, *389*, 706–709. (b) Kennan, A. J.; Haridas, V.; Severin, K.; Lee, D. H.; Ghadiri, M. R. *J. Am. Chem. Soc.* **2001**, *123*, 1797–1803.
119. Johnsson, K.; Allemann, R. K.; Widmer, H.; Benner, S. A. *Nature* **1993**, *365*, 530–532.
120. Benson, D. E.; Wisz, M. S.; Hellinga, H. W. *Proc. Natl. Acad. Sci. USA* **2000**, *97*, 6292–6297.
121. Allert, M.; Kjellstrand, M.; Broo, K.; Nilsson, Å.; Baltzer, L. *J. Chem. Soc.*, *Perkin Trans. 2* **1998**, 2271–2274.
122. Ghadiri, M. R.; Case, M. A. *Angew. Chem. Int. Ed. Engl.* **1993**, *32*, 1594–1597.
123. Halothane: 2-bromo-2-chloro-1,1,1-trifluoroethane.

124. Springs, S. L.; Bass, S. E.; McLendon, G. L. *Biochemistry* **2000**, *39*, 6075–6082.
125. (a) Lear, J. D.; Wasserman, Z. R.; DeGrado, W. F. *Science* **1988**, *240*, 1177–1181. (b) DeGrado, W. F.; Lear, J. D. *Biopolymers* **1990**, *29*, 205–213. (c) Lovejoy, B.; Åkerfeldt, K. S.; DeGrado, W. F.; Eisenberg, D. *Protein Sci.* **1992**, *1*, 1073–1077.
126. Schafmeister, C. E.; Miercke, L. J. W.; Stroud, R. M. *Science* **1993**, *262*, 734–738.
127. (a) Montal, M. *FASEB J.* **1990**, *4*, 2623–2635. (b) Montal, M.; Montal, M. S.; Tomich, J. M. *Proc. Natl. Acad. Sci. USA* **1990**, *87*, 6929–6933. (c) Oiki, S.; Madison, V.; Montal, M. *Proteins Struct. Funct. Genet.* **1990**, *8*, 226–236. (d) Grove, A.; Tomich, J. M.; Montal, M. *Proc. Natl. Acad. Sci. USA* **1991**, *88*, 6418–6422. (e) Grove, A.; Mutter, M.; Rivier, J. E.; Montal, M. *J. Am. Chem. Soc.* **1993**, *115*, 5919–5924.
128. Tuchscherer, G.; Servis, C.; Corradin, G.; Blum, U.; Rivier, J.; Mutter, M. *Protein Sci.* **1992**, *1*, 1377–1386.

Chapter 2

Models for non-haem iron-containing oxygenases

2.1 Introduction

Several micro-organisms facilitate the metabolism of various hydrocarbons and aromatic compounds via the activation of molecular oxygen by metalloproteins to provide a vital source of energy for the organism.[1] Many of these enzymes contain a transition-metal ion at the reactive site of the protein. The rate of aerobic degradation of these substrates is in general relatively slow. Metalloenzymes, one class of nature's catalysts, provide a low energy pathway for oxidation by either enhancing the susceptibility of the substrate towards molecular oxygen, or by increasing the reactivity of dioxygen. A great deal of research has been dedicated to the development of small synthetic catalysts that are also capable of activating molecular oxygen or oxidising hydrocarbons.[2,3]

Oxidases form a category of enzymes that employ dioxygen as an electron acceptor.[1,4] The reduction products are either water or hydrogen peroxide, depending on the number of electrons involved. The oxygenases are a distinct class of enzymes that are able to incorporate dioxygen into (in)organic substrates.[1,3,4] This conversion is crucial to their aerobic degradation, which is accompanied by, for example, the oxygenation or cleavage of the aromatic ring. These oxidising enzymes can be divided into mono-oxygenases or dioxygenases, depending on the

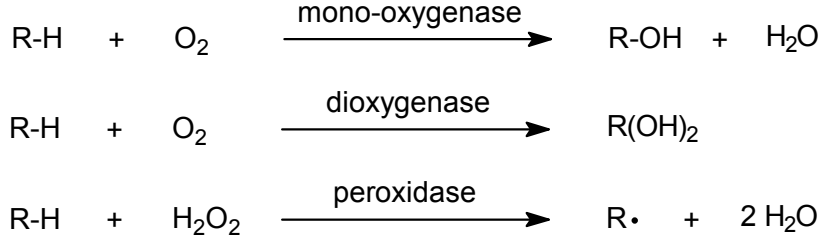

Figure 2.1. Classification of oxidising enzymes (R–H = substrate).

number of oxygen atoms that are introduced into the substrate. For mono-oxygenases the remaining oxygen atom is reduced to water. Another class of oxidising enzymes are the peroxidases, like horseradish peroxidase.[5] These natural antioxidants are able to facilitate the oxidation of a variety of (in)organic compounds with the concomitant reduction of hydrogen peroxide or alkyl peroxides to water or alcohols, respectively.[6]

In a number of metalloproteins the transition metal can be positioned in a prosthetic haem group where it is able to activate dioxygen.[4,7] In other enzymes a mononuclear or dinuclear metal centre is present that functions as a cofactor in a non-haem environment.[1,8] This leads to a distinction between haem and non-haem enzymes, although this subdivision is not restricted exclusively to oxidising enzymes.[1,5,9]

Metalloporphyrins and haem systems in nature can be found in haemoglobin, cytochromes, oxidases and peroxidases.[4,5,9] A well-studied family of haem-containing mono-oxygenases includes the cytochromes P-450, which can catalyse the epoxidation of olefins, and the hydroxylation of aromatic or saturated hydrocarbons by molecular oxygen in the presence of the reducing agent NADH or NADPH.[4,5,10] These haemoproteins are also capable of oxidising inactive hydrocarbons to functionalised compounds by using oxidants like hydrogen peroxide, iodosylbenzene, and peracids.[11] Therefore, a number of approaches to haem mimics have been presented in recent years.[12]

Rieske oxygenases are able to *cis*-dihydroxylate inactivated benzene rings. These non-haem mononuclear iron(II) dioxygenases require NADH as a source of electrons to perform the oxidation reaction.[1,3a] The diol products are then converted into catechols, which are subsequently degradated by catechol dioxygenases. These non-haem mononuclear iron(II) enzymes accept the required electrons from the substrate molecules after binding dioxygen.[3a]

2.2 Bleomycin

Although bleomycin (BLM) is not formally considered to be a protein, this natural glycopeptide is often referred to as a non-haem oxidising enzyme.[13] It has been administered as an antitumour antibiotic for the treatment of different types of cancers,[14,15] and is most active as the corresponding mononuclear iron(II) complex, Fe–BLM. Its structure, depicted in Figure 2.2,

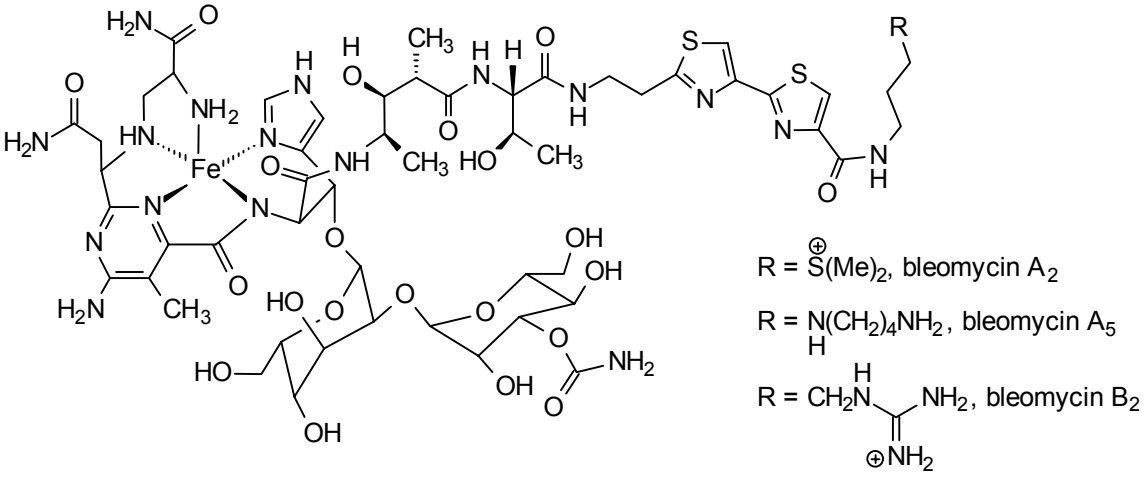

Figure 2.2. Structure of iron bleomycin (Fe–BLM).[25b]

was deduced from the spectroscopic and NMR investigations of several metallo-BLMs.[16] Recently, X-ray structures of Cu-BLM complexed with a bleomycin-binding protein have also been reported.[17]

An activated species is formed by reacting Fe–BLM with molecular oxygen,[8,15,18] and this "activated BLM" is the last detectable intermediate in the catalytic cycle of BLM that leads to an oxidative cleavage of DNA.[15,19] This reactive intermediate of Fe–BLM is a low-spin iron(III) hydroperoxo ($Fe^{III}OOH$, **1**) species.

The reaction of Fe–BLM towards DNA proceeds through one of three possible pathways (Scheme 2.1): (a) a heterolytic cleavage of the O–O bond in (BLM)$Fe^{III}OOH$ furnishing the high-valent Fe^{V}=O species **2**; (b) an O–O bond dissociation to produce the Fe^{IV}=O species **3** and a hydroxyl radical; or (c) (BLM)$Fe^{III}OOH$ reacts directly with DNA (R–H) to generate the Fe^{IV}=O moiety **3**, a DNA radical, and water without invoking a high-valent intermediate or free hydroxyl radicals. Qualitative investigations on metallo-BLMs tend to favour option (c) as the undiscriminating behaviour of free hydroxyl radicals is inconsistent with the highly specific DNA degradation by Fe–BLM.[16] However, results with non-haem iron oxidation catalysts have been interpreted to indicate that the end-on hydroperoxo ligand in the $Fe^{III}OOH$ intermediate **1** functions as a precursor for the highly oxidative hydroxyl radical and the Fe^{IV}=O species via a homolytic cleavage of the O–O bond.[20,21]

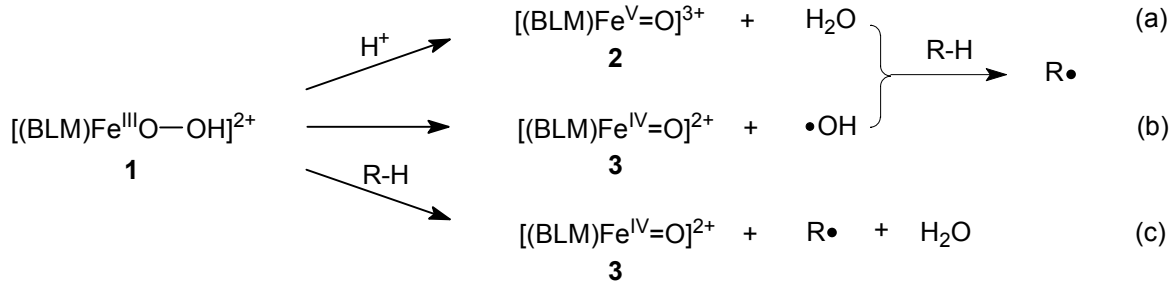

Scheme 2.1. Possible pathways for DNA (R–H) degradation mediated by (BLM)$Fe^{III}OOH$ (**1**) after heterolytic (a) or homolytic (b) O–O bond cleavage, or directly by **1** (c).

The chemistry of (BLM)$Fe^{III}OOH$ is also utilised in reactions other than those involving DNA. Organic substrates can also be oxidised, examples include the epoxidation of styrene,[22] the oxidation of stilbene to the corresponding epoxide with the additional formation of benzaldehyde,[23] and the hydroxylation of aromatic compounds like naphthalene and anisole.[24] In recent years several BLM analogues have been synthesised in order to gain a better understanding of the mechanism, and to study the effect of structural changes on the activity and selectivity of metallo-BLMs.[15,22,25]

2.3 N4Py synthesis and chemistry

Many research groups have invested a great deal of effort into unravelling the intricate mechanisms of various natural enzymes.[8a] Due to their complex composition and immense size, these enzymes and their active species are often studied by investigating the mechanisms of smaller catalytic structures that resemble their behaviour. The data gathered from these

functional mimics can then be compared to that obtained with the native enzyme.[26] For instance, a mononuclear non-haem iron(II) complex has been developed as a functional model for Rieske oxygenases.[27] Non-haem diiron oxygenase mimics have also been designed,[28] as well as metalloporphyrins as versatile oxidation catalysts.[29]

A model has been developed in our group to study the oxidation mechanism of Fe–BLM, as well as to provide an approach to new iron-based oxidation catalysts. The model for the apo-enzyme BLM is a pentadentate ligand, called N4Py.[30] This neutral ligand consists of four pyridine rings that are anchored to a central nitrogen atom (Scheme 2.2).[13] N4Py (**6a**) and its disubstituted derivatives **6b–d** are obtained by dialkylating bis(2-pyridinyl)methylamine (**2**) with the picolyl chlorides **5a–d**, respectively, in the presence of a base. The amine **4** can be obtained from the commercially available 2,2'-dipyridyl ketone by conversion to the corresponding ketoxime, and subsequent reduction to afford **4**. The synthesis of the picolyl chlorides **5b–d** has previously been described.[20,31]

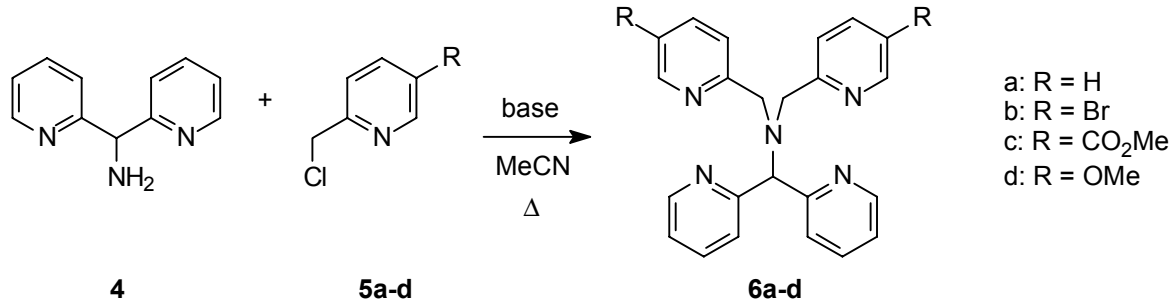

Scheme 2.2. Synthesis of N4Py (**6a**) and disubstituted derivatives (**6b–d**).

The monosubstituted N4Py derivatives **9** have previously been prepared in a similar fashion.[20] Prior to the alkylation step using a functionalised picolyl chloride, the amine **4** is converted to the secondary amine N3Py (**8**) via a reductive amination using 2-pyridinecarboxaldehyde (**7**) (Scheme 2.3).

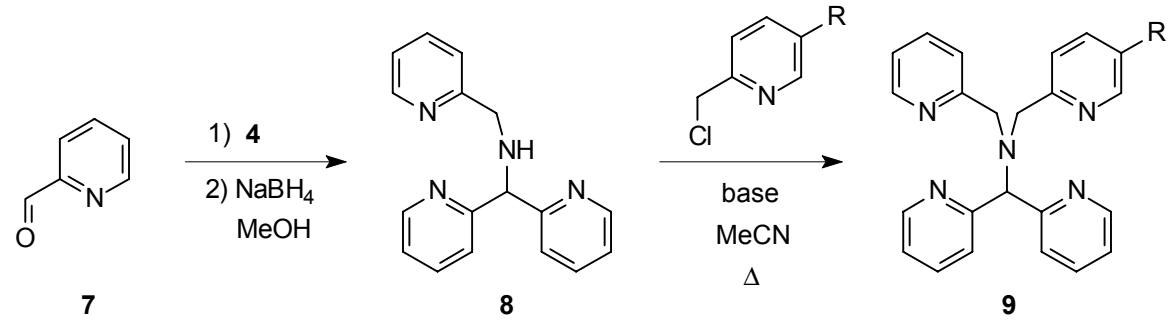

Scheme 2.3. Synthesis of monosubstituted N4Py ligands.

To encapsulate an iron metal ion, five co-ordination sites are occupied by the ligand **6a**, resulting in the iron(II) complex $[(N4Py)Fe(MeCN)](ClO_4)_2$ (**10**) (Scheme 2.4). Consequently, the metal ion is positioned in the centre of the generated cavity at 0.2071(5) Å above the mean plane that is formed by the four iron-bound pyridine nitrogen atoms.[30c] The sixth co-ordination site is therefore accessible to axial ligands like the solvent-derived acetonitrile molecule in **10**.

Although N4Py was developed as a model for bleomycin, the co-ordination environment around the iron metal centre is quite different from that of Fe–BLM (Figure 2.2). The $[(N4Py)Fe(MeCN)](ClO_4)_2$ complex **10** has been characterised by ^1H NMR and EPR as a low-spin iron(II) complex with a high redox potential ($E_{½}$ = 1010 mV vs. SCE) for the Fe^{III}/Fe^{II} couple.[30c] The effect of ligand modification on the electron density of the iron metal was determined by measuring the Fe^{III}/Fe^{II} couples of the low-spin iron(II) complexes of disubstituted N4Py derivatives **6b–d**. It was established that substituents at the 5-position of the pyridine ring only have a minor effect on the redox potential of these iron complexes ($E_{½}$ = 996–1100 mV vs. SCE).[20] The UV-Vis spectrum of **10** displays an absorption band at 458 nm in acetone (ε 4000 $M^{-1}cm^{-1}$). EPR and NMR studies revealed that the spin state of the iron atom is dependent on the temperature and the charge of the axial ligand.[30c] Thus, the replacement of the neutral acetonitrile molecule by a chloride anion leads to a high-spin iron(II) complex. Similarly, a methoxy anion as an axial ligand gives rise to a high-spin iron(III) at room temperature.

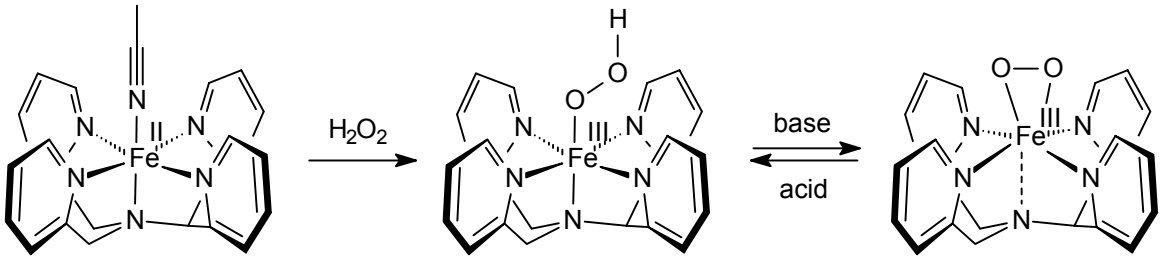

10 **11** **12**

Scheme 2.4. Proposed reaction intermediates **11** and **12** that originate from N4PyFe (**10**) and hydrogen peroxide.

When N4PyFe (**10**) is allowed to react with one equivalent of hydrogen peroxide, **10** is converted to an iron(III) complex. A large excess of hydrogen peroxide is required to produce the iron(III) hydroperoxide intermediate **11**. This purple species has been characterised by UV-Vis spectroscopy, EPR, ESI-MS, and resonance Raman spectroscopy[32] as a low-spin iron(III) hydroperoxide in which the hydroperoxo ligand is co-ordinated to the iron centre in an end-on η^1-binding mode (Scheme 2.4).[30] Only in acetone and methanol is the formation of this transient $Fe^{III}OOH$ species quantitative.[33] The slow and incomplete formation of **11** in acetonitrile is substantiated by the unfavourable equilibrium for the displacement of the axial ligand in **10**. The purple intermediate **11** has a characteristic absorption band at 530 nm in acetone (ε 1100 $M^{-1}cm^{-1}$) and 548 nm in methanol (ε 1100 $M^{-1}cm^{-1}$). The observed EPR signals at g = 2.17, 2.12, 1.98 resemble those of the low-spin iron(III) species of activated BLM.[18] This $Fe^{III}OOH$ intermediate is capable of catalytically reducing hydrogen peroxide in the concomitant oxidation of a wide variety of organic compounds.[20,34] Similar reactivity has been observed with non-haem dinuclear[35] and mononuclear[20,36] iron complexes of N3Py derivatives, the iron complex of the pentadentate ligand 5Py,[37] as well as many other non-haem iron catalysts.[2,38]

Furthermore, N4PyFe is able to cleave DNA in the absence of hydrogen peroxide.[20] The efficiency of this oxidation reaction was substantially enhanced by attaching a DNA-intercalating

acridine moiety to the N4Py ligand. The resulting iron complex was found to cleave DNA using molecular oxygen without requiring any additional reducing agents.[39] These findings established that this modified N4PyFe catalyst functioned as an effective mimic for Fe–BLM.

These mechanistic studies have led to a proposed catalytic cycle in which $[(N4Py)Fe(MeCN)](ClO_4)_2$ (**10**) is initially converted into the mononuclear species $[(N4Py)Fe^{III}OH]^{2+}$ **14** and the dinuclear species $[\{(N4Py)Fe^{III}\}_2(\mu\text{–}O)]^{4+}$ **15** (Scheme 2.5).[20,30c] In methanol as the solvent, these aforementioned intermediates are also in equilibrium with the $Fe^{III}OMe$ species **16**.[30c] However, upon addition of excess hydrogen peroxide these species are converted into the transient intermediate **11**.

Mechanistic studies have provided evidence that the $Fe^{III}OOH$ intermediate **11** is in fact not the active species, but merely serves as a precursor in the catalysed oxidation of alkanes. Although an oxoferryl (Fe^{IV}=O) species with a porphyrin π-radical cation is often observed during the reduction of molecular oxygen by haem peroxidases[4,29] and other mononuclear iron centres,[8] a heterolytic cleavage of the O–O bond in **11** to a high-valent, formally iron(V)-oxo intermediate is considered energetically too unfavourable to occur (Scheme 2.1).[16,34]

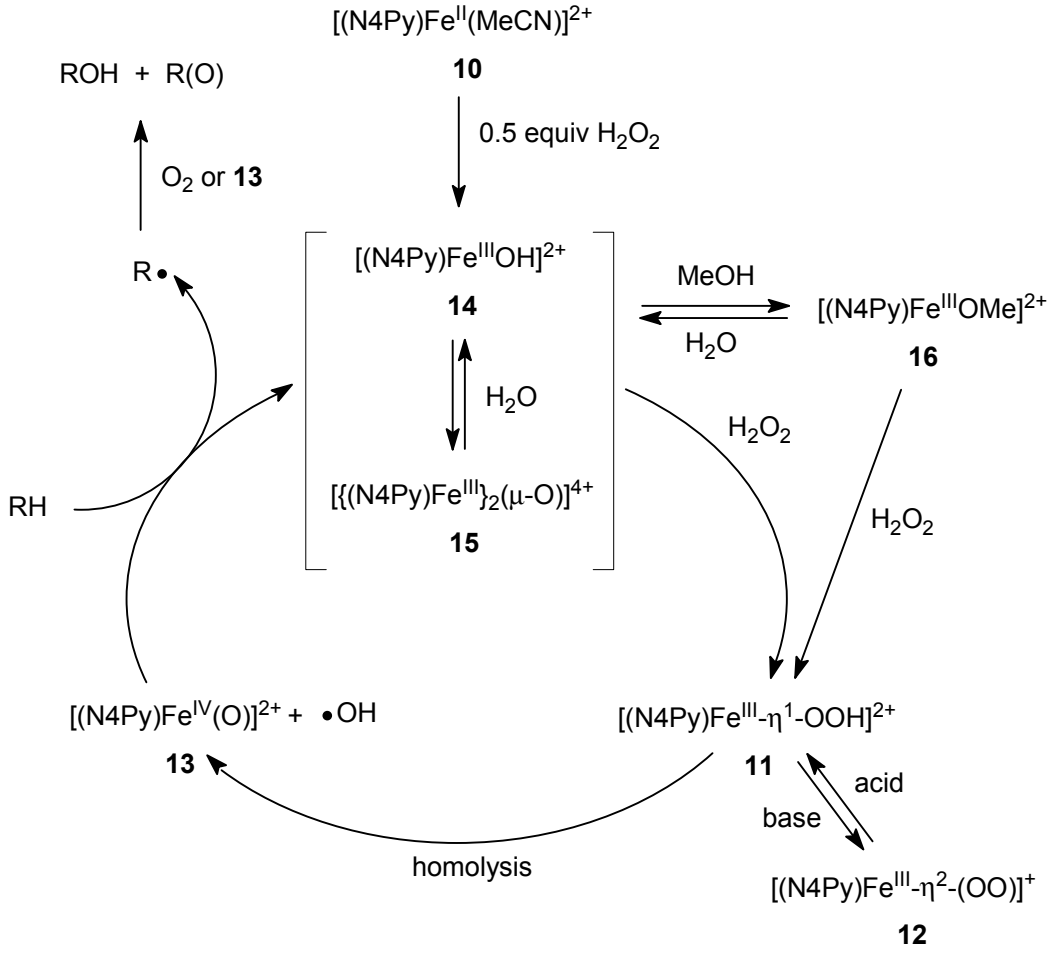

Scheme 2.5. Proposed catalytic cycle for the oxidation of alkanes by N4PyFe (**10**) and hydrogen peroxide.

A homolytic scission of the O–O bond in **11** would produce two one-electron oxidants, $[(N4Py)Fe^{IV}O]^{2+}$ (**13**) and a hydroxyl radical (•OH). The involvement of hydroxyl radicals in the

catalytic cycle of [(N4Py)Fe(MeCN)]$(ClO_4)_2$ (**10**) was established by employing radical traps such as acetone,[40] benzene,[41] and dibromomethane[11c] during the oxidation reaction. The rationale for these observations is that the neutral pentadentate ligand N4Py is not capable of stabilising the high valent iron in the formally iron(V) oxidation state, and therefore leads to a homolytic rather than a heterolytic scission of the O–O bond.[34] In addition, resonance Raman spectroscopy demonstrated that the O–O bond in the $Fe^{III}OOH$ intermediate **11** is unusually weak.

In the oxidation of alkanes catalysed by N4PyFe the hydroxyl radical produced reacts with a substrate molecule to give rise to a substrate radical after hydrogen abstraction (Scheme 2.5). This intermediate subsequently reacts with dioxygen or **13** to propagate a radical chain auto-oxidation pathway to furnish the oxidation products and the intermediates **14** and **15**.[42] The proposed catalytic cycle has been elucidated by employing radical scavengers and mechanistic probes to determine the kinetic isotope effects, the ratio of oxidation at the tertiary over secondary carbon centres in adamantane, and the stereoselectivity in the hydroxylation of *trans*-1,2-dimethylcyclohexane.[20,34] However, these mechanistic studies have indicated that another, more selective oxidising intermediate is also involved in the hydrogen abstraction of alkanes catalysed by **10**, which is most probably the $[(N4Py)Fe^{IV}O]^{2+}$ species **13**.[20,34]

When the reactivities of the iron(II) complexes of **6b–d** towards the oxidation of alkanes were investigated, the results were comparable to those of N4PyFe.[20] This suggests that a similar mechanism must be involved, irrespective of the electronic properties of the ligand. This is not surprising when taking into account the good correlation between the analytical data of these iron(II) complexes and the corresponding $Fe^{III}OOH$ species. However, the number of free co-ordination sites at the iron centre in the complex has been found to determine the type of chemistry observed during the catalysed oxidation reactions. This is clearly demonstrated by the difference in oxidation behaviour and the proposed mechanism for N3Py derivatives with respect to N4Py ligands (Scheme 2.6).[20,36] The effect of the co-ordination mode of non-haem ligands, as well as their electronic and steric factors on the oxidation chemistry of the $Fe^{III}OOH$ intermediate has recently been described by Que and co-workers.[43]

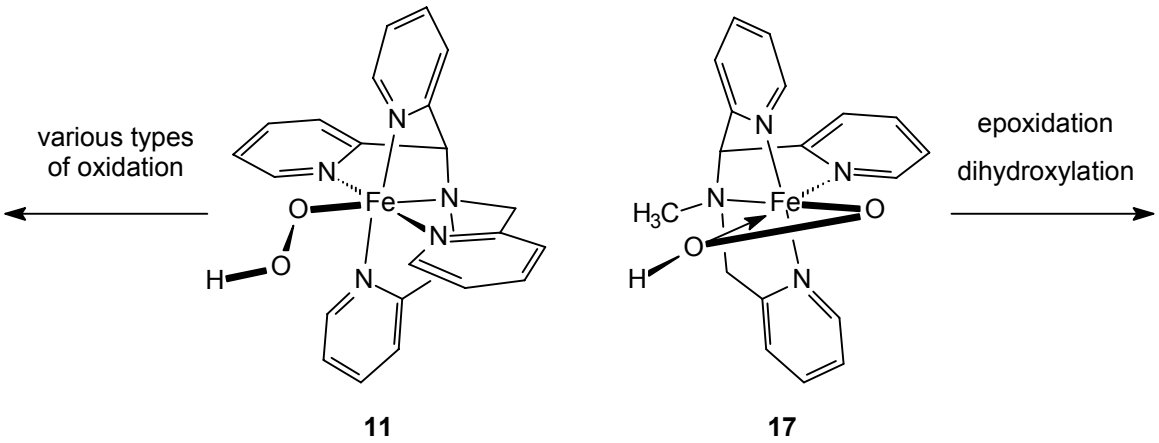

11 **17**

Scheme 2.6. The effect of the co-ordination mode of the hydroperoxo ligand on the type of oxidation chemistry in reactions catalysed by the iron complexes of N4Py (left) and N3Py (right).

The fact that acetone effectively traps hydroxyl radicals can result in different catalytic activities (or turnover number, TON) for the catalyst upon changing the solvent from acetonitrile to acetone. As a result, the selectivity in the oxidation of cyclohexane has been found to be noticeably solvent-dependent. For instance, the ratio of cyclohexanol over cyclohexanone (A/K) changed from 1.4 to 2.6 in acetonitrile and acetone, respectively. When only free radical intermediates are involved in the catalytic cycle, oxidation generally results in A/K ~ 1.[42a] By the slow addition of hydrogen peroxide to the reaction mixture the A/K ratio could be increased even further to 5.2, which indicates that oxidation by the non-selective hydroxyl radicals is suppressed in favour of a more selective oxidising species, presumably **13**.[34]

When the axial ligand of the $[(N4Py)Fe(MeCN)](ClO_4)_2$ complex is a chloride anion, the purple intermediate **11** cannot be formed. This is presumably due to the strong binding of the anion to the metal, which prevents the displacement of the ligand.[30c] The catalyst is deactivated to a certain extent during the catalytic cycle, which is probably due to the oxidative degradation of the ligand by the hydroxyl radicals that are formed.

The purple $Fe^{III}OOH$ intermediate **11** can be converted reversibly into its conjugate base **12** upon the addition of aqueous ammonia in methanol at −45°C. The resulting blue species has been characterised by UV-Vis (λ_{max} 685 nm, ε 520 $M^{-1}cm^{-1}$), ESI-MS, and resonance Raman spectroscopy as a high-spin $[Fe^{III}O_2]^+$ species.[44] In the proposed structure the peroxo ligand is co-ordinated to the iron metal via a side-on binding mode,[33b,c,45] whereby the weakly bound tertiary nitrogen is detached from the metal centre (Scheme 2.4).[44]

Related $[Fe^{III}-\eta^2-O_2]^+$ intermediates have also been proposed as the source of nucleophilic peroxides in the oxidation mechanism of haem enzymes (Figure 2.3).[46] This $[Fe^{III}O_2]^+$ species is completely unreactive towards the oxidation of alkanes until the $Fe^{III}OOH$ intermediate **11** is regenerated by the addition of acid.[44] This observation seems to support the hypothesis that protonation of the peroxo species is a prerequisite for catalytic activity.[47]

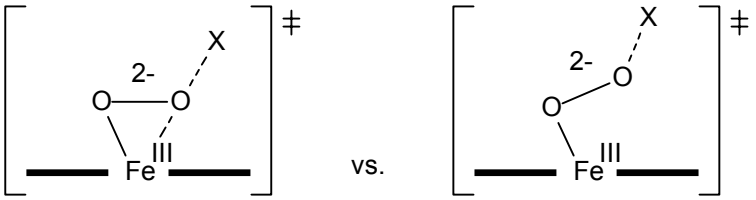

Figure 2.3. Possible transition states for oxygen transfer of peroxo ferric haem complexes: closed (left) and open (right) peroxo complexes (X = substrate).[46b]

2.4 An initial step towards artificial peroxidases

The mechanistic studies of $[(N4Py)Fe(MeCN)](ClO_4)_2$ (**10**) and its oxidation chemistry correlate very well with the reactivity and spectroscopic data of Fe−BLM, suggesting that a comparable mechanistic pathway is plausible for both catalysts. Therefore, the iron complex **10** poses as a good functional mimic for Fe−BLM. It will be interesting to ascertain whether or not the incorporation of this model catalyst in a peptide environment will facilitate the construction of a synthetic peroxidase. The outline of this project has already been discussed briefly in Chapter 1.

The four-helix bundle motif has been selected as a potential scaffold to embed the N4PyFe catalyst, where it will hopefully function as a synthetic co-factor. It was illustrated in Chapter 1 that the four-helix bundle appears to be able to accommodate the N4PyFe catalyst. The peptide chains will be attached to a modified N4Py ligand via a cysteine residue in the peptide sequence. Halide displacement on the ligand by the cysteine thiolate is the key to a site-specific attachment of the peptides. This concept has been tested in a preliminary study whereby two unprotected peptides were coupled to the difunctionalised N4Py ligand **18**.[48]

It had already been shown that substituents at the 5-position of the pyridine rings have no major effect on the electron density of the iron centre (*vide supra*).[20] Therefore, it is unlikely that substituents at this position will interfere with the redox potential of the catalyst. Furthermore, these attachment sites will direct the peptides away from the iron centre (Scheme 2.7), which allows the formation of the $Fe^{III}OOH$ intermediate without affecting its oxidation chemistry. Steric properties in the ligand too close to the iron centre could result in a change in oxidation behaviour, as was described by Que and co-workers for 5- and 6-methyl-substituted tris(2-pyridinylmethyl)amine (TPA) iron catalysts.[43]

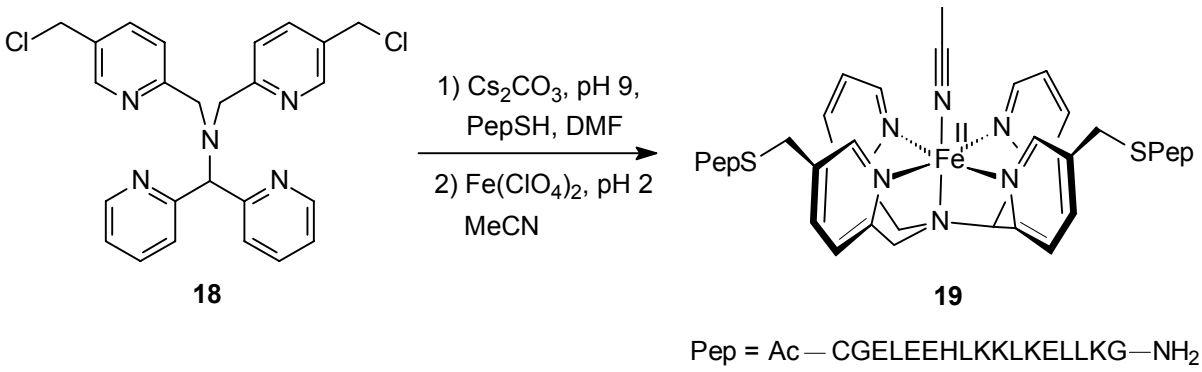

18 **19**

Pep = Ac—CGELEEHLKKLKELLKG—NH_2

Scheme 2.7. Synthesis of the N4PyFe-dipeptide complex **19**.[49]

The dichloride N4Py derivative **18** was prepared from **6c** by initially reducing the ester groups and subsequently converting the alcohol functionalities to the chlorides.[48] The reported low yield of only 8% was due to the decomposition of **18** during purification by column chromatography. This can probably be attributed to the benzylic nature of the two chlorides.

The methodology of coupling peptides via a cysteine thioether linkage has several advantages. Firstly, the position of the cysteine residue in the peptide sequence can facilitate a site-specific attachment of the ligand and thereby control the location of the catalyst in the prospective four-helix bundle structure. Secondly, the cysteine thiolate is an efficient nucleophile that can enable the successful coupling of unprotected peptides.[50] The presence of other nucleophilic side chains in the sequence (from histidine, lysine, and glutamic acid for instance) can interfere with the chloride displacement in **18**. The selected peptide sequence for this experiment consisted of a representative number of residues with nucleophilic side chains (Scheme 2.7). However, the use of caesium carbonate as a base and an excess of peptide afforded a selective and clean conversion to the dipeptide complex **19** after chelation to iron.[48] The use of excess peptide was required, as oxidation to the corresponding disulphide occurs readily. UV-Vis, electrospray ionisation mass spectrometry, and protolytic digestion by a

protease verified the incorporation of iron in **19** and the presence of covalently linked peptide chains.[48]

The retained catalytic activity of **19** was successfully demonstrated by its ability to oxidise the peroxidase activity probes ABTS[51] and 1,2,4,5-tetramethoxybenzene (**20**)[52] in water with a performance that was comparable to N4PyFe under identical conditions. In addition, the oxidation of **20** by catalyst **10** gave rise to a benzene radical cation that was also detected by EPR when horseradish peroxidase (HRP) was employed as the catalyst (Scheme 2.8).[48]

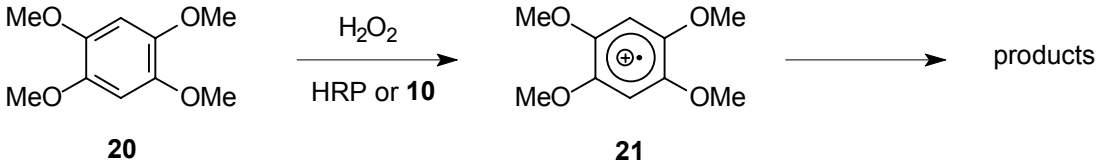

Scheme 2.8. Formation of the radical cation **21** in the oxidation of methoxybenzene **20** catalysed by horseradish peroxidase (HRP).

The pH-dependence of the catalytic system was optimal at pH 4 or lower. At higher pH ranges the activity of the catalyst rapidly diminished. Examination of the reactions over time revealed that after five minutes the oxidation had essentially terminated for both [(N4Py)Fe(MeCN)](ClO$_4$)$_2$ (**10**) and **19**, presumably due to an oxidative degradation. The similar oxidation behaviour of **10** and **19** clearly demonstrated that the attachment of two peptide chains to the catalyst had no significant effect on its performance.

2.5 Conclusions

Earlier work by Gerard Roelfes lead to the formulation of a mechanism for the oxidation catalyst [(N4Py)Fe(MeCN)](ClO$_4$)$_2$ (**10**). The good correlation between the oxidation chemistry and the spectroscopic data of the reactive intermediates proved that **10** functions as an effective mimic for Fe–BLM.

The oxidation behaviour and performance of the N4PyFe catalyst remains unaffected by the attachment of two peptide chains in close proximity to the iron complex. These findings suggest that the catalyst can be embedded into a peptide environment without substantial loss of activity. This paves the way for the design of water-soluble peroxidase mimetics. At the same time this sets the stage for the challenging task to modify the N4Py ligand in order to host four peptide chains. This will hopefully facilitate the incorporation of the catalyst into a four-helix bundle. The synthesis of such a tetrafunctionalised N4Py derivative will be presented in Chapter 3.

2.6 References and notes

1. Coulter, E. D.; Ballou, D. P., In *Essays in Biochemistry*: *Metalloproteins*; Ballou, D. P. (Ed.); Portland Press: UK, 1999; Vol. 34, pp. 31–49.
2. (a) Selke, M.; Sisemore, M. F.; Ho, R. Y. N.; Wertz, D. L.; Valentine, J. S. *J. Mol. Catal. A: Chem.* **1997**, *117*, 71–82. (b) Moro-oka, Y. *Catalysis Today* **1998**, *45*, 3–12.

3. (a) Que, L., Jr.; Ho, R. Y. N. *Chem. Rev.* **1996**, *96*, 2607–2624. (b) Wallar, B. J.; Lipscomb, J. D. *Chem. Rev.* **1996**, *96*, 2625–2657.
4. Sono, M.; Roach, M. P.; Coulter, E. D.; Dawson, J. H. *Chem. Rev.* **1996**, *96*, 2841–2887.
5. Isaac, I. S.; Dawson, J. H., In *Essays in Biochemistry*: *Metalloproteins*; Ballou, D. P. (Ed.); Portland Press: UK, 1999; Vol. 34, pp. 51–69.
6. Everse, J., Everse, K. E., Grisham, M. B., In *Peroxidases in Chemistry and Biology*; CRC Press: Boca Raton, USA, 1991; Vol. 2, pp. 1–24.
7. Ortiz de Montellano, P. R. *Acc. Chem. Res.* **1998**, *31*, 543–549.
8. (a) Feig, A. L.; Lippard, S. J. *Chem. Rev.* **1994**, *94*, 759–805. (b) Solomon, E. I.; Brunold, T. C.; Davis, M. I.; Kemsley, J. N.; Lee, S.-K.; Lehnert, N.; Neese, F.; Skulan, A. J.; Yang, Y.-S.; Zhou, J. *Chem. Rev.* **2000**, *100*, 235–349.
9. Stryer, L. In *Biochemistry*; W. H. Freeman: USA, 1995.
10. (a) Groves, J. T.; Nemo, T. E.; Meyers, R. S. *J. Am. Chem. Soc.* **1979**, *101*, 1032–1033. (b) Groves, J. T.; Watanabe, Y. *J. Am. Chem. Soc.* **1988**, *110*, 8443–8452.
11. (a) Groves, J. T.; Kruper, W. J. *J. Am. Chem. Soc.* **1979**, *101*, 7613–7615. (b) Hill, C. L.; Schardt, B. C. *J. Am. Chem. Soc.* **1980**, *102*, 6374–6375. (c) Groves, J. T.; Kruper, W. J., Jr.; Hauschalter, R. C. *J. Am. Chem. Soc.* **1980**, *102*, 6375–6377. (d) Groves, J. T.; Quinn, R. *J. Am. Chem. Soc.* **1985**, *107*, 5790–5792. (e) Che, C. M.; Chung, W. C. *J. Chem. Soc., Chem. Commun.* **1986**, 386–388.
12. (a) Rocha Gonsalves, A. M. d'A.; Pereira, M. M. *J. Mol. Catal. A: Chem.* **1996**, *113*, 209–211. (b) Collman, J. P.; Eberspacher, T.; Fu, L.; Herrmann, P. C. *J. Mol. Catal. A: Chem.* **1997**, *117*, 9–20. (c) Nastri, F.; Lombardi, A.; D'Andrea, L. D.; Sanseverino, M.; Maglio, O.; Pavone, V. *Biopolymers* **1998**, *47*, 5–22, and references cited therein.
13. For an explanation of the abbreviations used, see Appendix 1 (p. 149).
14. Sikic, B. I., Rosencweig, M., Carter, S. K., In *Bleomycin Chemotherapy*; Academic Press: Orlando, USA, 1985.
15. Hecht, S. M. *J. Nat. Prod.* **2000**, *63*, 158–168.
16. (a) Wu, W.; Vanderwall, D. E.; Turner, C. J.; Kozarich, J. W.; Stubbe, J. *J. Am. Chem. Soc.* **1996**, *118*, 1281–1294. (b) Lehman, T. E.; Ming, L.-J.; Rosen, M. E.; Que, L., Jr. *Biochemistry* **1997**, *36*, 2807–2816. (c) Lehmann, T. E.; Serrano, M. L.; Que, L., Jr. *Biochemistry* **2000**, *39*, 3886–3898. (d) Neese, F.; Zaleski, J. M.; Zaleski, K. L.; Solomon, E. I. *J. Am. Chem. Soc.* **2000**, *122*, 11703–11724.
17. Sugiyama, M.; Kumagai, T.; Hayashida, M.; Maruyama, M.; Matoba, Y. *J. Biol. Chem.* **2002**, *277*, 2311–2320.
18. (a) Burger, R. M.; Peisach, J.; Horwitz, S. B. *J. Biol. Chem.* **1981**, *256*, 11636–11644. (b) Sam, J. W.; Tang, X.-J.; Peisach, J. *J. Am. Chem. Soc.* **1994**, *116*, 5250–5256. (c) Marusak, R. A.; Meares, C. F., In *Active Oxygen in Biochemistry*; Valentine, J. S., Foote, C. S., Greenberg, A. and Liebman, J. F., Eds.; Blackie Academic and Professional, Chapman and Hall: Glasgow, UK, 1995; pp. 342–349.
19. (a) Hecht, S. M. *Acc. Chem. Res.* **1986**, *19*, 383–391. (b) Stubbe, J.; Kozarich, J. W. *Chem. Rev.* **1987**, *87*, 1107–1136. (c) Stubbe, J.; Kozarich, J. W.; Wu, W.; Vanderwall,

D. E. *Acc. Chem. Res.* **1996**, *29*, 322–330. (d) Burger, R. M. *Chem. Rev.* **1998**, *98*, 1153–1169.

20. Roelfes, J. G., In *Models for Non-Heme Iron Containing Oxidation Enzymes*, Ph. D. thesis, Groningen, 2000.
21. (a) Mekmouche, Y.; Ménage, S.; Toia-Duboc, C.; Fontecave, M.; Galey, J.-B.; Lebrun, C.; Pécaut, J. *Angew. Chem. Int. Ed.* **2001**, *40*, 949–952. (b) Lehnert, N.; Ho, R. Y. N.; Que, L., Jr.; Solomon, E. I. *J. Am. Chem. Soc.* **2001**, *123*, 8271–8290. (c) Lehnert, N.; Ho, R. Y. N.; Que, L., Jr.; Solomon, E. I. *J. Am. Chem. Soc.* **2001**, *123*, 12802–12816.
22. Boger, D. L.; Ramsey, T. M.; Cai, H.; Hoehn, S. T.; Stubbe, J. *J. Am. Chem. Soc.* **1998**, *120*, 9139–9148.
23. Heimbrook, D. C.; Carr, S. A.; Mentzer, M. A.; Long, E. C.; Hecht, S. M. *Inorg. Chem.* **1987**, *26*, 3835–3836.
24. Murugesan, N.; Hecht, S. M. *J. Am. Chem. Soc.* **1985**, *107*, 493–500.
25. (a) Leitheiser, C. J.; Rishel, M. J.; Wu, X.; Hecht, S. M. *Org. Lett.* **2000**, *2*, 3397–3399. (b) Abraham, A. T.; Zhou, X.; Hecht, S. M. *J. Am. Chem. Soc.* **2001**, *123*, 5167–5175.
26. For bleoycin-like DNA cleavage by a non-haem iron(II) catalyst, see also Mialane, P.; Nivorojkine, A.; Pratviel, G.; Azéma, L.; Slany, M.; Godde, F.; Simaan, A.; Banse, F.; Kargar-Grisel, T.; Bouchoux, G.; Sainton, J.; Horner, O.; Guilhem, J.; Tchertanova, L.; Meunier, B.; Girerd, J.-J. *Inorg. Chem.* **1999**, *38*, 1085–1092.
27. (a) Chen, K.; Que, L., Jr. *Angew. Chem. Int. Ed.* **1999**, *38*, 2227–2229. (b) Costas, M.; Tipton, A. K.; Chen, K.; Jo, D.-H.; Que, L., Jr. *J. Am. Chem. Soc.* **2001**, *123*, 6722–6723.
28. (a) Que, L., Jr.; Dong, Y. *Acc. Chem. Res.* **1996**, *29*, 190–196. (b) Fontecave, M.; Ménage, S.; Duboc-Toia, C. *Coor. Chem. Rev.* **1998**, *178–180*, 1555–1572.
29. Meunier, B. *Chem. Rev.* **1992**, *92*, 1411–1456.
30. (a) Lubben, M., In *Model Systems for Iron and Copper Containing Oxygenases*, Ph. D. thesis, Groningen, 1994, pp. 43–71. (b) Lubben, M.; Meetsma, A.; Wilkinson, E. C.; Que, L., Jr.; Feringa, B. L. *Angew. Chem. Int. Ed. Engl.* **1995**, *34*, 1512–1514. (c) Roelfes, G.; Lubben, M.; Chen, K.; Ho, R. Y. N.; Meetsma, A.; Genseberger, S.; Hermant, R. M.; Hage, R.; Mandal, S. K.; Young, V. G., Jr.; Zang, Y.; Kooijman, H.; Spek, A. L.; Que, L., Jr.; Feringa, B. L. *Inorg. Chem.* **1999**, *38*, 1929–1936.
31. See also Chapter 3 (p. 47) for an overview of synthetic pathways to picolyl chlorides **5b–d**.
32. Ho, R. Y. N.; Roelfes, G.; Feringa, B. L.; Que, L., Jr. *J. Am. Chem. Soc.* **1999**, *121*, 264–265.
33. End-on iron(III) hydroperoxo and side-on iron(III) peroxo intermediates have also been reported by (a) reference 26. (b) Simaan, A. J.; Banse, F.; Mialane, P.; Boussac, A.; Un, S.; Kargar-Grisel, T.; Bouchoux, G.; Girerd, J.-J. *Eur. J. Inorg. Chem.* **1999**, 993–996. (c) Simaan, A. J.; Döpner, S.; Banse, F.; Bourcier, S.; Bouchoux, G.; Boussac, A.; Hildebrandt, P.; Girerd, J.-J. *Eur. J. Inorg. Chem.* **2000**, 1627–1633.
34. (a) Roelfes, G.; Lubben, M.; Leppard, S. W.; Schudde, E. P.; Hermant, R. M.; Hage, R.; Wilkinson, E. C.; Que, L., Jr.; Feringa, B. L. *J. Mol. Catal. A: Chem.* **1997**, *117*, 223–227. (b) Roelfes, G.; Lubben, M.; Hage, R.; Que, L., Jr.; Feringa, B.L. *Chem. Eur. J.* **2000**, *6*, 2152–2159.

35. Ligtenbarg, A. G. J.; Oosting, P.; Roelfes, G.; La Crois, R. M.; Lutz, M.; Spek, A. L.; Feringa, B. L. *Chem. Commun.* **2001**, 385–386.
36. M. Klopstra, *forthcoming Ph. D. thesis*.
37. (a) De Vries, M. E.; La Crois, R. M.; Roelfes, G.; Kooijman, H.; Spek, A. L.; Hage, R.; Feringa, B. L. *Chem. Commun.* **1997**, 1549–1550. (b) Goldsmith, C. R.; Jonas, R. T.; Stack, T. D. P. *J. Am. Chem. Soc.* **2002**, *124*, 83–96.
38. (a) Ménage, S.; Galey, J.-B.; Dumats, J.; Hussler, G.; Seité, M.; Luneau, I. G.; Chottard, G.; Fontecave, M. *J. Am. Chem. Soc.* **1998**, *120*, 13370–13382. (b) Chen, K.; Que, L., Jr. *Chem. Commun*. **1999**, 1375–1376. (c) Chen, K.; Que, L., Jr. *J. Am. Chem. Soc.* **2001**, *123*, 6327–6337. (d) Sams, C. K.; Somoza, F.; Bernal, I.; Toftlund, H. *Inorg. Chim. Acta* **2001**, *318*, 45–52.
39. Roelfes, J. G.; Branum, M. E.; Wang, L.; Que, L., Jr.; Feringa, B. L. *J. Am. Chem. Soc.* **2000**, *122*, 11517–11518.
40. Walling, C.; Goosen A. *J. Am. Chem. Soc.* **1973**, *95*, 2987–2991.
41. (a) Walling, C.; Johnson, R. A. *J. Am. Chem. Soc.* **1975**, *97*, 363–367. (b) Brook, M. A.; Castle, L.; Lindsay Smith, J. R.; Higgins, R.; Morris, K. P. *J. Chem. Soc.*, *Perkin Trans 2* **1982**, 687–692. (c) Ito, S.; Ueno, K.; Mitarai, A.; Sasaki, K. *J. Chem. Soc.*, *Perkin Trans. 2* **1993**, 255–259.
42. (a) Arends, I. W. C. E.; Ingold, K. U.; Wayner, D. D. M. *J. Am. Chem. Soc.* **1995**, *117*, 4710–4711 (b) MacFaul, P. A.; Arends, I. W. C. E.; Ingold, K. U.; Wayner, D. D. M. *J. Chem. Soc.*, *Perkin Trans. 2* **1997**, 135–145. (c) MacFaul, P. A.; Ingold, K. U.; Wayner, D. D. M.; Que, L., Jr. *J. Am. Chem. Soc.* **1997**, *119*, 10594–10598.
43. Chen, K.; Costas, M.; Kim, J.; Tipton, A. K.; Que, L., Jr. *J. Am. Chem. Soc.* **2002**, *124*, 3026–3035.
44. Ho, R. Y. N.; Roelfes, G.; Hermant, R.; Hage, R.; Feringa, B. L.; Que, L., Jr. *Chem. Commun.* **1999**, 2161–2162.
45. (a) Simaan, A. J.; Banse, F.; Girerd, J.-J.; Wieghardt, K.; Bill, E. *Inorg. Chem.* **2001**, *40*, 6538–6540. (b) Hazell, A.; McKenzie, C.J.; Nielsen, L. P.; Schindler, S.; Weitzer, M. *J. Chem. Soc.*, *Dalton Trans.* **2002**, 310–317.
46. (a) Coon, M. J.; Vaz, A. D. N.; Bestervelt, L. L. *FASEB J.* **1996**, *10*, 428–434. (b) Selke, M.; Sisemore, M. F.; Valentine, J. S. *J. Am. Chem. Soc.* **1996**, *118*, 2008–2012. (c) Selke, M.; Valentine, J. S. *J. Am. Chem. Soc.* **1998**, *120*, 2652–2653.
47. (a) Harris, D. L.; Loew, G. H. *J. Am. Chem. Soc.* **1998**, *120*, 8941–8948. (b) Neese, F.; Solomon, E. I. *J. Am. Chem. Soc.* **1998**, *120*, 12829–12848. (c) Davydov, R.; Macdonald, I. D. G.; Makris, T. M.; Sligar, S. G.; Hoffman, B. M. *J. Am. Chem. Soc.* **1999**, *121*, 10654–10655.
48. Choma, C. T.; Schudde, E. P.; Kellogg, R. M.; Robillard, G. T.; Feringa, B. L. *J. Chem. Soc.*, *Perkin Trans. 1* **1998**, 769–773.
49. See Appendix 2 (p. 151) for the α-amino acid structures and one-letter abbreviations.
50. Choma, C. T.; Kaestle, K.; Åkerfeldt, K. S.; Kim, R. M.; Groves, J. T.; DeGrado, W. F. *Tetrahedron Lett.* **1994**, *35*, 6191–6194.

51. (a) Childs, R. E.; Bardsley, W. G. *Biochem. J.* **1975**, *145*, 93–103. (b) Adams, P. A.; Goold, R. D. *J. Chem. Soc., Chem. Commun.* **1990**, 97–98. (c) Adams, P. A. *J. Chem. Soc., Perkin Trans. 2* **1990**, 1407–1414.
52. Kersten, P. J.; Kalyanaraman, B.; Hammel, K. E.; Reinhammar, B.; Kirk, T. K. *Biochem. J.* **1990**, *268*, 475–480.

Chapter 3

Tetrasubstituted N4Py ligands as templates for peptide attachment

3.1 Introduction

Over the past few years a number of different approaches to modified enzymes and artificial functional proteins have been developed. However, despite the synthetic or modified oxidases and peroxidases reported so far, artificial proteins based upon a non-haem reaction centre in a four-helix bundle have not yet been described (See Chapter 1). In an attempt to initiate the construction of such a functional artificial enzyme an ambitious strategy was formulated in which the N4PyFe catalytic unit is embedded inside a four-helix bundle.[1] This concept was initially tested by the construction of the dipeptide system described in Chapter 2.[2] The positive results of the oxidation reactions implied that the oxidising capability of the N4PyFe catalyst was not affected by the peptide surrounding. More importantly, these results indicated that the concept of embedding the N4PyFe catalyst into a more organised peptide environment might in fact be feasible. The work described in this chapter outlines the exploratory preparation of a tetrafunctionalised N4Py derivative with four appending peptide chains as a basis for the design and synthesis of an artificial peroxidase in the future.

The methodology that had been applied successfully to make the dipeptide N4PyFe complex involved the use of chloromethylene ($-CH_2Cl$) groups as sites for peptide attachment.[2] These peptides were coupled to the ligand by a nucleophilic substitution reaction of cysteine thiolates with the halide leaving groups of the ligand. The key feature of this procedure infers that the position of the cysteine in the peptide sequence will facilitate the site-specific attachment of the ligand to the peptide chains. In a four-helix bundle this methodology will in turn determine the position of the catalyst inside the hydrophobic core of the bundle. The same approach will now be employed to prepare the corresponding tetrasubstituted N4Py ligand in order to tether four peptides to the N4PyFe catalyst. Ultimately, by selecting a peptide sequence that will fold into an α-helix, the catalyst can be incorporated inside a four-helix bundle.

In the following sections compounds and ligands with a one carbon linker ($-CH_2-$) at the periphery will be referred to as comprising of a C1-spaced functionality. From modelling studies

it was deduced that these groups should be positioned at the 5-position of the pyridine ring, so that the 2-positions can be used to construct the N4Py ligand core. For reasons that will become more apparent later in this chapter, N4Py derivatives with four propyl linkers ($-CH_2CH_2CH_2-$) have also been prepared, which will be referred to as C3-spaced moieties.

Disubstituted N4Py ligands are readily available from the dialkylation of di(2-pyridinyl)methylamine with an appropriate picolyl chloride derivative as described in chapter 2.[3] Construction of a tetrafunctionalised N4Py ligand therefore requires the introduction of functionalities in the bis(2-pyridinyl)methylamine moiety for which a new synthetic route had to be developed. As a result, the desired functionalities in the final N4Py derivative need to be carefully selected, as these must be introduced in the initial steps of the synthetic pathway. The choice of these functionalities, however, might be limited due to its incompatibility towards the required synthetic procedures.

The retrosynthesis of the target tetrasubstituted N4Py derivatives **1** and **2** involves two main disconnection paths (Scheme 3.1). Following path A, bis(2-pyridinyl)methylamines **3** and **4** are dialkylated with picolyl chlorides **5** and **6**, respectively. All of these 2,5-disubstituted pyridine compounds can be obtained from the corresponding bromopyridines **7** and **8**, making these important, and versatile building blocks for the synthesis of tetrasubstituted N4Py ligands **1** and **2**. Finally, bromopyridines **7** and **8** can be prepared from the commercially available 2,5-dibromopyridine (**9**).

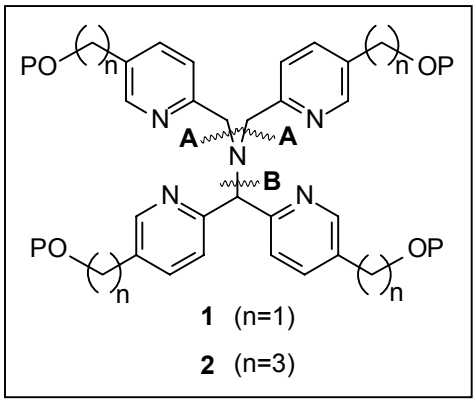

1 (n=1)
2 (n=3)

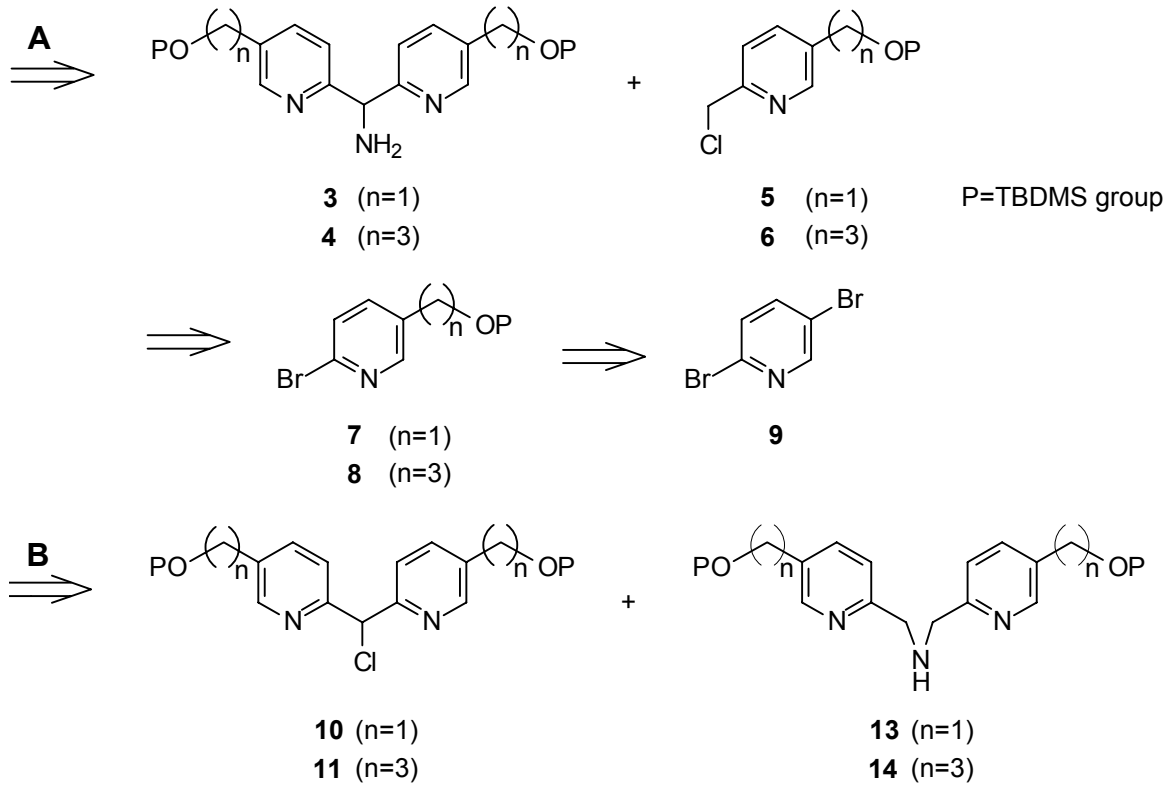

3 (n=1)
4 (n=3)

5 (n=1)
6 (n=3)

7 (n=1)
8 (n=3)

9

10 (n=1)
11 (n=3)

13 (n=1)
14 (n=3)

Scheme 3.1. Retrosynthesis of tetrasubstituted N4Py ligands **1** and **2**.[1]

Alternatively, **1** and **2** can be obtained from the alkylation of the secondary amines **12** and **13** with the bis(2-pyridinyl)methylene chlorides **10** and **11**, respectively (Scheme 3.1, path B). These in turn can be prepared from the corresponding aforementioned bromopyridines **7** and **8**.

From hands-on experience with N4Py chemistry within our research group, a decision was taken to follow path A for the synthesis of tetrasubstituted N4Py derivatives **1** and **2**. The synthesis of the required building blocks will be elaborated upon in subsequent chapters. After completing the synthesis of **1** and **2** the protecting groups, like silyl ether groups, can be removed. The corresponding hydroxyl moieties can then be converted into leaving groups to enable these ligands to act as templates for the covalent attachment of peptides via a cysteine residue in the sequence.

3.2 2,5-Disubstituted pyridines as synthons

As briefly mentioned above, the resulting functionality at the periphery of the ligand has to be introduced at the start of the synthetic route. The developed synthetic route, therefore, needed to be carefully selected to minimise the conflict that might arise between the functionalities and the applied reaction conditions throughout the synthetic pathway. Fortunately, a number of procedures are available for acquiring various 2,5-disubstituted pyridines that can be used as synthons for the construction of tetrafunctionalised N4Py ligands. Outlined in Scheme 3.2 are some typical synthetic approaches to picolyl chloride derivatives that have previously been used to synthesise N4Py derivatives.[3]

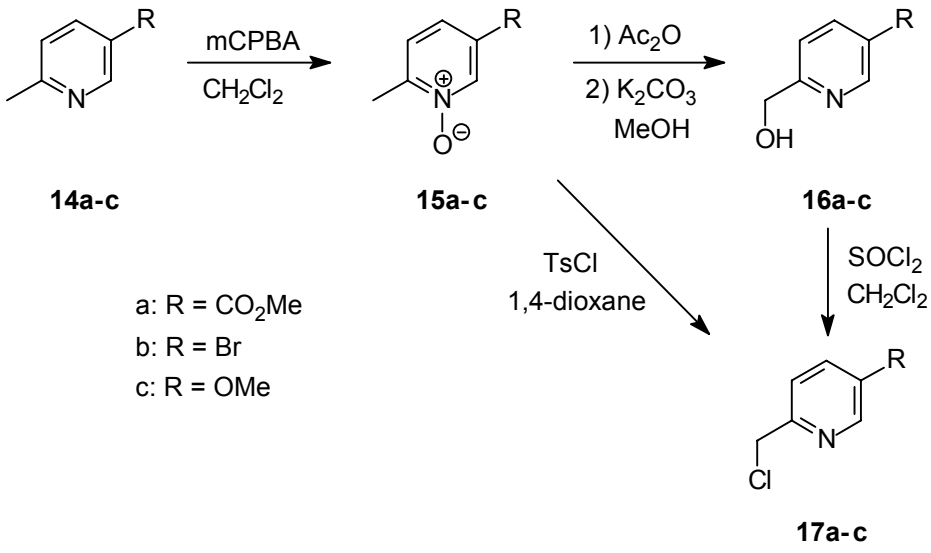

Scheme 3.2. Synthesis of 5-substituted 2-picolyl chlorides **17a–c**.

Although **14a** is commercially available, it is more expensive than **14b**[4] and **14c**,[3] which can be obtained from cheaper starting materials. These pyridine derivatives are readily oxidised to the corresponding *N*-oxides, and after acylation by acetic anhydride the intermediate acetates can be hydrolysed to produce the alcohols **16a–c**.[5] It is also possible to obtain picolyl alcohol **16a** from the reduction of dimethyl 2,5-pyridinedicarboxylate with sodium borohydride in the presence of calcium chloride (Scheme 3.3).[6] However, due to the poorly described experimental conditions, it was not possible to reproduce the high yield reported by the authors. The

subsequent reaction of picolyl alcohols **16a–c** with thionyl chloride furnished the corresponding picolyl chlorides **17a–c**. A synthetic shortcut to **17a** was established by the reaction of *N*-oxide **15a** with *p*-toluenesulphonyl chloride (TsCl), which is probably also applicable to **17b–c**.[3]

Using the developed synthetic route to tetrasubstituted N4Py ligands as depicted in Scheme 3.1, the starting materials **14a–c** do not permit the synthesis of the required corresponding bis(2-pyridinyl)methylamines. The preparation of the latter compounds utilises the lithiation of 2-bromopyridine derivatives to couple two pyridine moieties together. This will be dealt with in more detail in Section 3.3.3. Although a small number of 5-substituted 2-bromopyridines are commercially available, their functionalities limit the structure variations possible for tetrasubstituted N4Py ligands onto which peptides can be assembled. Examples of synthetic pathways to the required 5-substituted 2-bromopyridines for the C1-spaced N4Py ligand are depicted in Scheme 3.3.

Dimethyl 2,5-pyridinedicarboxylate (**18**) was converted to the monoester *N*-oxide **19** by a reaction with hydrogen peroxide in boiling acetic acid.[7] The diacid from which **18** was obtained, could not be converted directly into the *N*-oxide due to its zwitterionic nature,[7] although some success has been reported utilising tungsten catalysts.[8] After alkaline hydrolysis of **19** and subsequent acidification the diacid was obtained. Unfortunately, the described experimental conditions proved to be difficult to reproduce. Using a patented procedure the diacid was converted conveniently to 6-bromo-nicotinic acid (**20**).[9] Alternatively, **20** could also be obtained from 2,5-dibromopyridine (**9**) by lithiation with *n*-butyllithium (*n*-BuLi), followed by quenching the 2-bromo-5-lithiopyridine with carbon dioxide. The latter procedure is more efficient, and provides **20** in a single step in 82% yield from the commercially available 2,5-dibromopyridine (**9**).

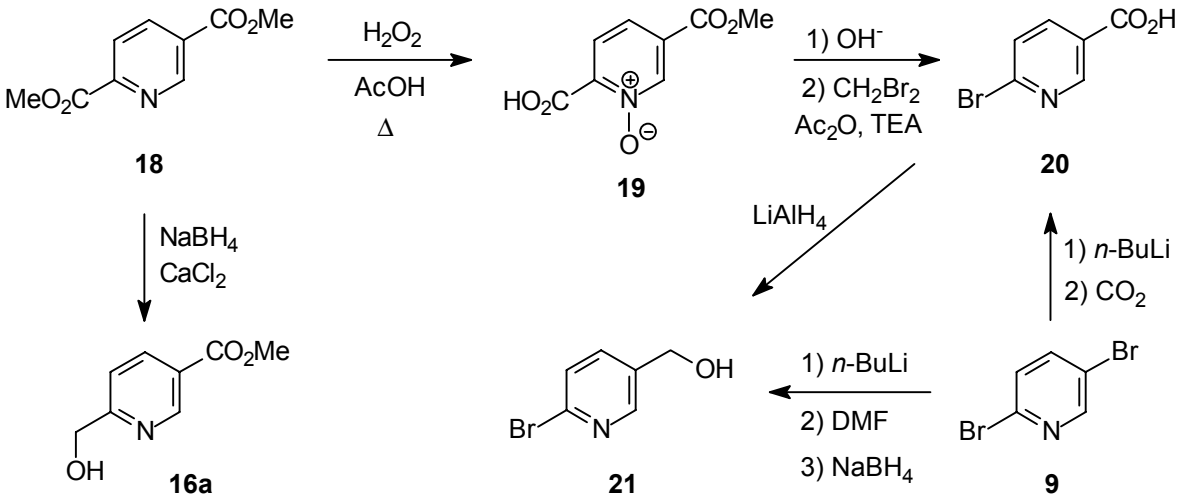

Scheme 3.3. Examples of synthetic pathways to 2,5-disubstituted pyridines.

The method in which two pyridine units will be coupled together for the preparation of bis(2-pyridinyl)methylamines **3** and **4** involves a lithiation reaction (*vide infra*), and thereby limits the use of an ester or acid functionality. Despite this problem, it is of interest to note that procedures have recently been described utilising halogen-magnesium exchange reactions that tolerate ester and nitrile functionalities.[10] However, by reducing carboxylic acid **20** to alcohol **21**, and subsequent protection of the hydroxyl group, the compound can be subjected to a lithiation

reaction. Alternatively, **21** can also be obtained directly from dibromopyridine **9** by reducing the intermediate aldehyde *in situ* using sodium borohydride.

For practical reasons a decision was taken to construct tetrasubstituted N4Py ligands **1** and **2** starting from **9**. This facilitates the versatile and controlled introduction of the desired functionalities at the correct position on the pyridine ring. In principle, by employing various electrophiles to quench the lithiated species derived from **9**, a wide range of tetrafunctionalised N4Py derivatives should be accessible.

3.3 Synthesis of tetrasubstituted N4Py ligands

As indicated in the retrosynthesis outlined in Scheme 3.1, bromopyridine **7** is a particularly important building block for the synthesis of the C1-spaced N4Py derivative **1**. All other pyridine units that are required to obtain the ligand structure can be prepared from **7**. Similarly, the building block **8** has been used to construct the corresponding C3-spaced N4Py ligand **2**. The developed synthetic route makes it imperative that the essential functionalities for the targeted ligand are incorporated into these building blocks before the core of the ligand is constructed. This approach of building the functionalised N4Py framework entails the convergent synthesis of the ligand.[11]

3.3.1 Preparation of the building blocks

The C1-spacer in building block **7** has been introduced by preparing 2-bromo-5-pyridinecarboxaldehyde (**22**). This aldehyde is commonly obtained from the oxidation of 2-bromo-5-methylpyridine to the acid, followed by reduction to the aldehyde.[12] However, as the starting material is expensive and the reaction proceeds in a low yield, a preferred method involves the use of the commercially available 2,5-dibromopyridine (**9**). Subsequent lithiation with *n*-BuLi at −80°C afforded 2-bromo-5-lithiopyridine,[13] which was quenched with *N*,*N*-dimethyl-formamide (DMF) to furnish the aldehyde **22** in 96% yield (Scheme 3.4).

When tetrahydrofuran (THF) was selected as the solvent, the monolithiation of **9** was found to be less selective than the results described in the literature.[14] The intermediate lithiated species is commonly quenched with electrophiles such as aldehydes,[14b] nitriles,[14a] and secondary amides[14a] to provide the corresponding alcohols and ketones, respectively. When DMF was used to quench 2-bromo-5-lithiopyridine in diethyl ether as the solvent, aldehyde **22** was obtained in a near quantitative yield and in high purity.[15] Similar results were obtained via a bromine-magnesium exchange of **9** using isopropylmagnesium chloride in THF at room temperature.[16] For the synthesis of the C1-spaced N4Py ligand **1** the aldehyde **22** was reduced with $NaBH_4$ in methanol to furnish the alcohol **21**. When **21** was subsequently allowed to react with *tert*-butyldimethylsilyl chloride (TBDMSCl)[17] in DMF in the presence of triethylamine (TEA) the C1-spaced building block **7** was obtained in 85% yield after purification.[18]

In order to obtain the building block **8** for the construction of the C3-spaced N4Py ligand **2**, aldehyde **22** was converted to the α,β-unsaturated ester **24** by a Horner-Emmens reaction using triethyl phosphonoacetate (**23**). Only the *E*-isomer of **24** was observed by ^{1}H NMR. Subsequent reduction by $LiAlH_4$ to the saturated alcohol **25** was followed by a silylation to afford the silyl ether **8** in 81% yield after purification. Normally, $LiAlH_4$ is not known to reduce the carbon–

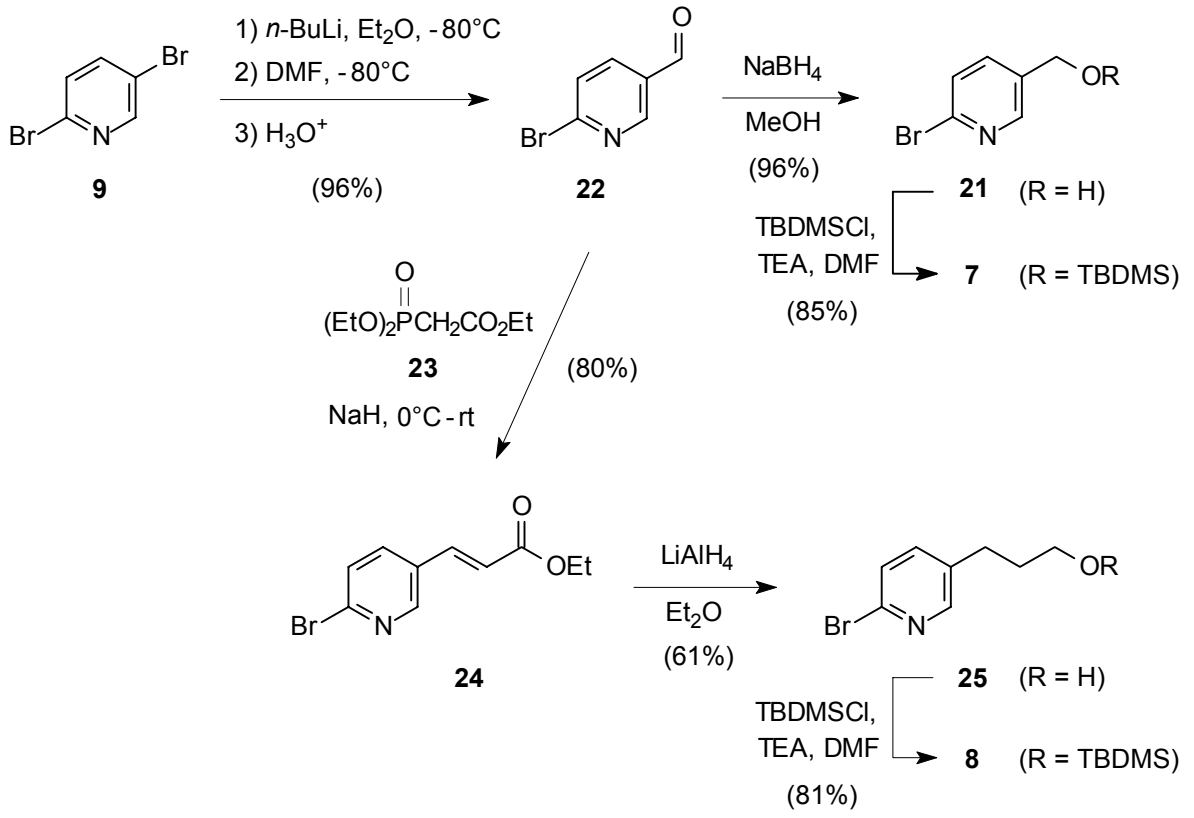

Scheme 3.4. Synthesis of building blocks **7** and **8**.

carbon double bond of α,β-unsaturated esters, unless it is conjugated with a phenyl group, like for example in cinnamic esters.[19] Under the applied conditions full reduction of **24** was observed, although the saturated alcohol **25** could only be isolated in a moderate yield of 61%.

Therefore as an alternative, hydrogenation using palladium on carbon was attempted to reduce the double bond, followed by the reduction of the remaining ester functionality in **26** (Figure 3.1) using $LiAlH_4$. However, under these hydrogenation conditions reductive debromination occurred to furnish **27**.[20] Using Adam's catalyst (platinum oxide) under similar conditions also resulted mainly in reductive debromination. In both cases the saturated ester **26** was only observed in small quantities.[21] Furthermore, the complete reduction of the pyridine ring to yield the corresponding piperidine derivative **28** was observed under these conditions.[22]

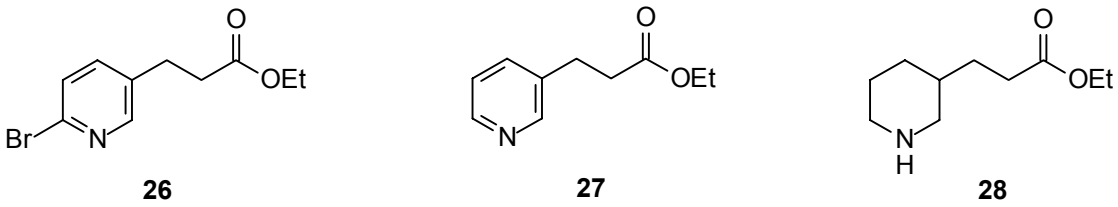

Figure 3.1. Observed products from the metal-catalysed hydrogenation.

In conclusion, building blocks **7** and **8** have been prepared in good to excellent yields. It is of interest to note that, due to the high purity of the isolated intermediates, the crude end products of each step can be used without any deleterious effects in subsequent reactions.

3.3.2 Preparation of 5-substituted 2-picolyl chlorides

Depending on the desired spacer length in the final ligand, the required 2-picolyl chlorides **5** and **6** can be obtained from building blocks **7** and **8**, respectively (Scheme 3.5). These building blocks were lithiated with *n*-butyllithium in THF at −80°C and subsequently quenched with DMF to provide the aldehydes **29** and **30**. In contrast to the lithiation of 2,5-dibromopyridine, employing THF instead of diethyl ether as a solvent led to superior results. An aqueous workup was sufficient enough to hydrolyse the intermediate DMF adduct to the aldehyde, as an acidic workup would have led to the hydrolysis of the silyl ethers. These aldehydes can in principle be reduced *in situ* to the picolyl alcohols **31** and **32**. However, since both aldehydes are also required for the synthesis of di(2-pyridinyl)methylamine **3** and **4** (Scheme 3.6), the reduction was carried out separately. Finally, the reaction of alcohols **31** and **32** with thionyl chloride in the presence of triethylamine cleanly and quantitatively afforded the 2-picolyl chlorides **5** and **6**. Flash column chromatography proved to be crucial to minimise decomposition during the purification of the product on the column. The synthesised 2-picolyl chlorides **5** and **6** were fully characterised by ^{1}H and ^{13}C NMR, and mass analysis.

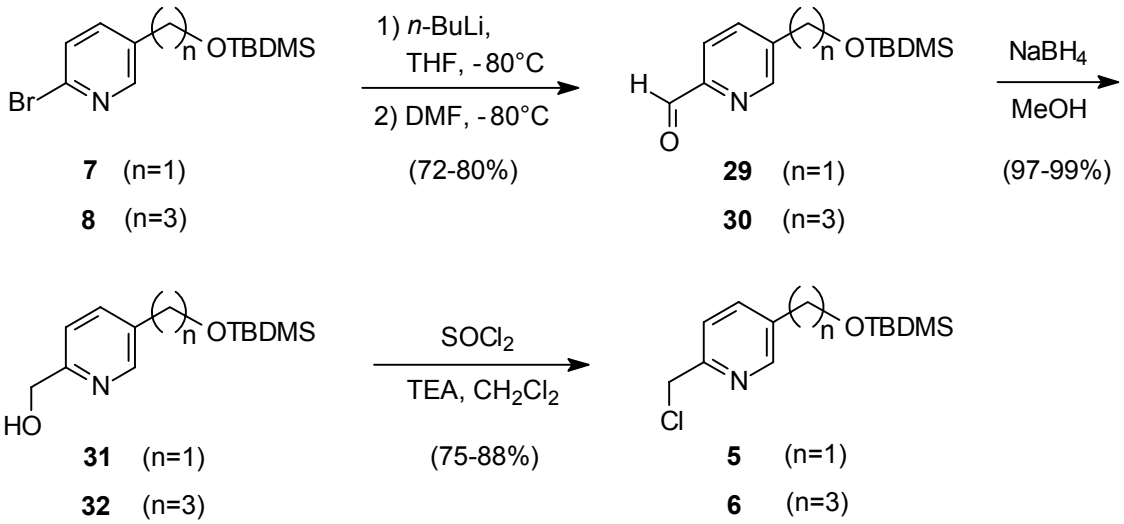

7 (n=1) **8** (n=3) (72-80%) **29** (n=1) **30** (n=3) (97-99%)

31 (n=1) **32** (n=3) (75-88%) **5** (n=1) **6** (n=3)

Scheme 3.5. Synthesis of picolyl chloride derivatives **5** and **6**.

Again as before, all of the reaction steps proceeded smoothly, thereby eliminating the need to purify the intermediate products, with one exception: when the aldehydes **29** and **30** were employed for the synthesis of bis(2-pyridinyl)methylamines **3** and **4**, respectively (Scheme 3.6).

3.3.3 Preparation of disubstituted dipyridinyl methylamines

The key step in the synthesis of tetrasubstituted N4Py ligands is the coupling of two functionalised pyridine rings via a methylene bridge, preceding the formation of the required bis(2-pyridinyl)methylamines **3** and **4**. This coupling reaction was carried out by reacting the lithiated **7** or **8** with the 2-formylpyridine derivatives **29** or **30**, respectively, under the same conditions that were applied to prepare these aldehydes (Scheme 3.6). The intermediate bis(2-pyridinyl)methanols were subsequently oxidised by manganese dioxide to produce bis(2-pyridinyl) ketones **33** and **34** in good overall yields. In contrast to the commercially

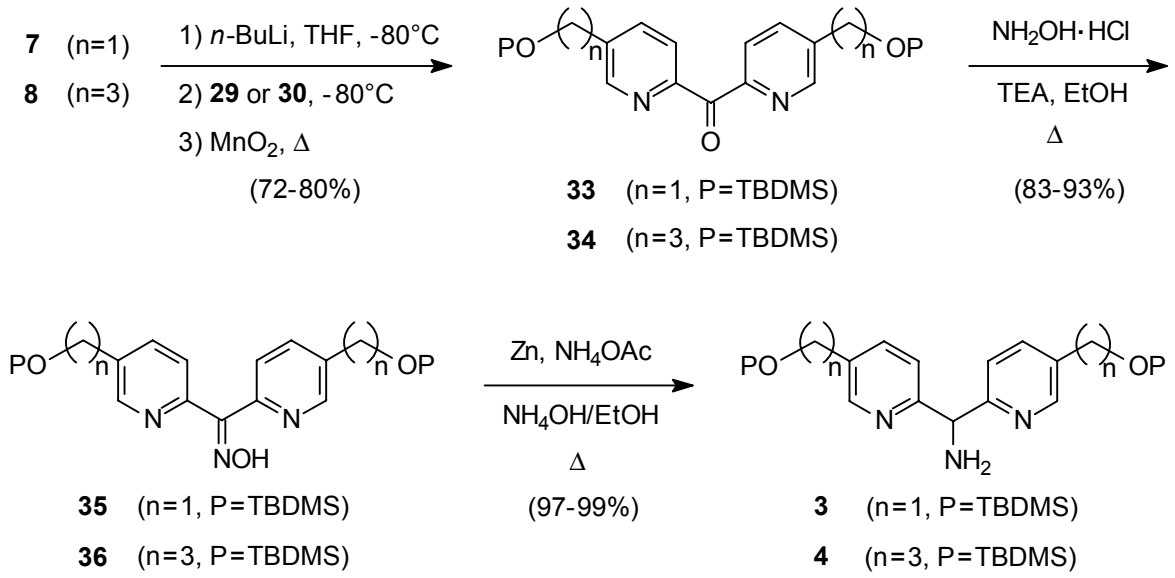

Scheme 3.6. Synthesis of bis(2-pyridinyl)methylamine derivatives **3** and **4**.

available 2,2'-dipyridinyl ketone that is used for the synthesis of N4Py itself, five or six reaction steps had to be performed to obtain the related ketones for the C1- and C3-spaced N4Py ligands, respectively.

Subsequently, **33** and **34** were converted to the bis(2-pyridinyl) ketoximes **35** and **36** by reacting with hydroxylammonium chloride in the presence of a base. The purification of the preceding intermediates was deemed unnecessary due to the ease with which these ketoximes were crystallised from ethanol and water. Finally, the bis(2-pyridinyl) ketoximes **35** and **36** were converted to bis(2-pyridinyl)methylamines **3** and **4** by a mild and quantitative reduction using zinc powder under basic conditions.[23] Hydrogenation of **35** and **36** utilising palladium on carbon as an alternative reduction procedure failed: even after prolonged reaction times and elevated temperatures, only the starting material could be isolated. It is assumed that the amine products poisoned the catalyst, thus preventing further hydrogenation.

The prepared bis(2-pyridinyl)methylamines **5** and **6** were characterised by ^{1}H and ^{13}C NMR, and mass analysis. The doubly benzylic hydrogen atoms of these amines give rise to a distinctive signal in the ^{1}H NMR with a chemical shift at δ 5.3 ppm. Furthermore, a dramatic shift of the ^{1}H NMR signals in the aromatic region was observed due to the reduction of the oxime double bond.

3.3.4 Construction of the N4Py scaffold

Analogous to other N4Py derivatives that have been made in the past,[3] tetrasubstituted N4Py ligands can be prepared by the dialkylation of bis(2-pyridinyl)methylamines **3** and **4** with 2-picolyl chloride derivatives **5** and **6** in the presence of base. The first alkylation step to the secondary amines **37** and **38** (Figure 3.2) proceeded quickly. In contrast, the reaction of these so-called N3Py derivatives with a second equivalent of 2-picolyl chloride proved to be more difficult. Nevertheless, the tertiary amines **1** and **2** were eventually isolated in moderate yields after purification.

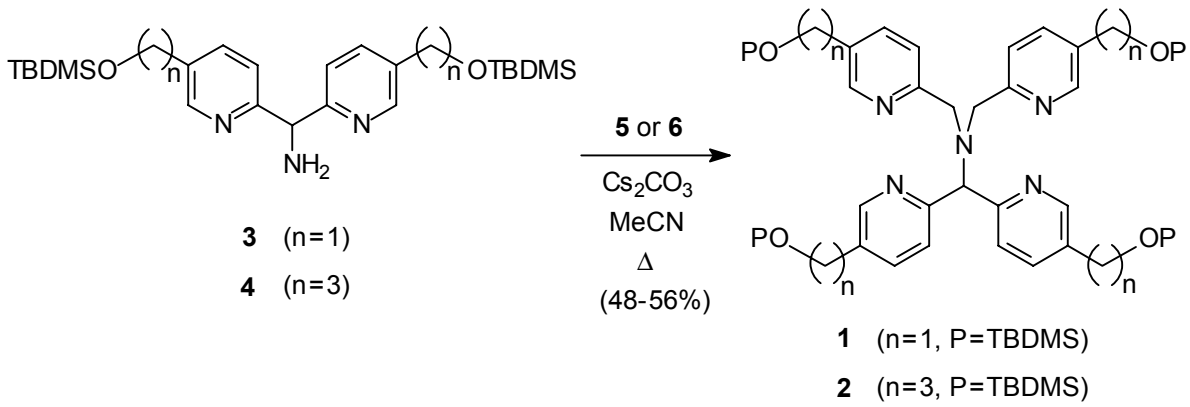

Scheme 3.7. Synthesis of tetrasubstituted N4Py derivatives **1** and **2**.

A variety of bases and solvents have been tested to find the optimal conditions to obtain **1** and **2**. Decomposition of the starting materials was observed when *N*,*N*-diisopropylethylamine (DIEA) was employed as a base in boiling chloroform. Potassium carbonate in refluxing acetonitrile is commonly applied to the synthesis of various N4Py ligands.[3] However, when these conditions were used to prepare **1** and **2**, decomposition of the starting materials was also observed. Attempts to improve the reaction by adding catalytic amounts of 18-crown-6 or sodium iodide proved to be unfruitful. A clean but slow conversion was observed when a two-phase system of dichloromethane and aqueous sodium hydroxide was used at room temperature or under reflux conditions. The addition of tetrabutylammonium iodide to the reaction mixture as a phase-transfer catalyst did not enhance the reaction rate. Other methods that were attempted with little success involved the use of sodium hydride, potassium carbonate, or DIEA in DMF as the solvent. Fortunately, successful conversion to **1** and **2** was accomplished by utilising DIEA or caesium carbonate as a base in refluxing acetonitrile. The advantage of using caesium carbonate over DIEA is that it resulted in a cleaner conversion to the desired product.

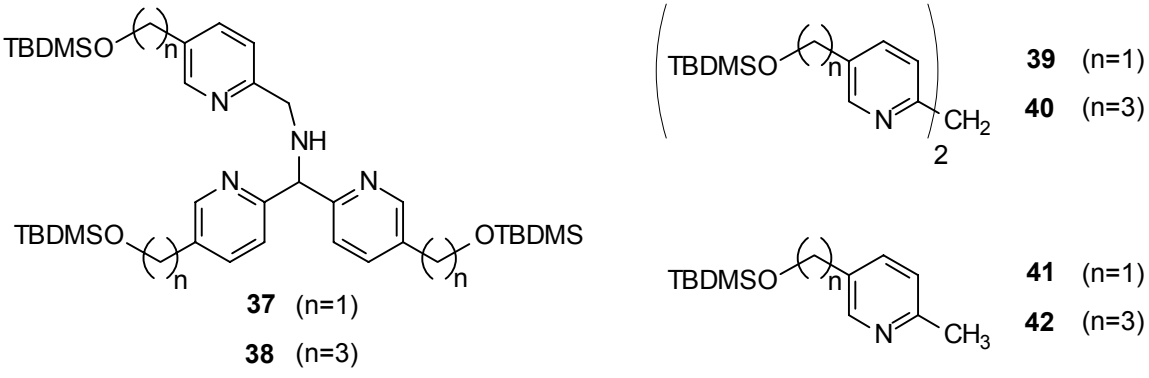

Figure 3.2. Observed side-products in the preparation of tetrasubstituted N4Py ligands **1** and **2**.

The moderate yields of **1** and **2** are partly attributed to the formation of side-products **39**–**42**,[24] a problem that became more pronounced as the reaction time was extended. Furthermore, the conversion of N3Py derivatives **37** and **38** to the products **1** and **2** did not proceed to

completion, despite the presence of excess picolyl chloride derivatives. Additional loss of product occurred during purification by flash column chromatography, which was further hampered by the poor separation of the N3Py compounds from the N4Py products. It is crucial that the obtained tetrasubstituted N4Py derivatives are free of N3Py structures, as subsequent reactions with peptide sequences will also be susceptible to the N3Py analogues. As a result, separation of these peptide-coupled N4Py ligands will then be hampered by their structural similarities.

Once the construction of tetrasubstituted N4Py ligands had been accomplished, all that remained was removal of the silyl protecting groups, followed by the conversion of the hydroxyl functionalities into suitable leaving groups for the covalent attachment of peptides.

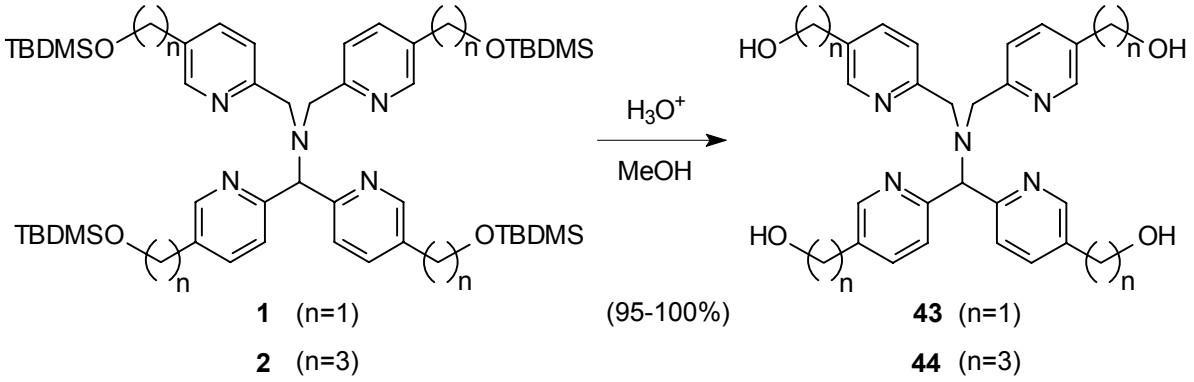

Scheme 3.8. Deprotection of the silyl ethers **1** and **2**.

A variety of standard conditions were employed to remove the silyl protecting groups. The first method involved tetrabutylammonium fluoride, which resulted in a fast and complete conversion. Unfortunately, removal of the resulting silyl products proved to be troublesome due to the high polarity and water solubility of **43**. The use of $Zn(BF_4)_2$ as an alternative method was successful, although this did not afford the desired free ligand **43** but its zinc complex instead. The best results obtained so far involved using dilute hydrochloric acid in methanol or ethanol. However, the removal of residual solvent was complicated by hydrogen bond formation to the four hydroxyl groups of the N4Py derivatives **43** and **44**. After prolonged high-vacuum conditions the pure product was obtained, as verified by ^{1}H and ^{13}C NMR, and mass analysis.

3.4 Chlorination attempts

Many attempts have been undertaken to convert **43** to the tetrachloride N4Py derivative **45**, either to be isolated as such or converted *in situ* to a sulphide. As indicated in Scheme 3.9, all attempts so far have proven to be unsuccessful. It appears that replacing the four hydroxyl groups for (chloride) leaving groups leads to the formation of an intrinsically unstable structure. The exact origin of this intrinsic instability can only be speculated upon, although the probable source is attributed to the doubly benzylic, tertiary hydrogen in **45** (Scheme 3.9).

In the dichloride N4Py ligand that was discussed in Chapter 2, the benzylic chlorides were positioned within the upper half of the ligand structure. This structural feature did not prevent its formation. In the tetrachloride N4Py derivative **45**, however, the doubly benzylic proton is now flanked by two pyridine groups that each contain a benzylic chloride moiety. Such benzylic

positions are often reactive sites, especially in pyridine compounds as they can be susceptible to *N*-alkylation. This significant difference can be sufficient enough to lead to the observed decomposition of **45**, presumably initiated by an elimination of the doubly benzylic proton.

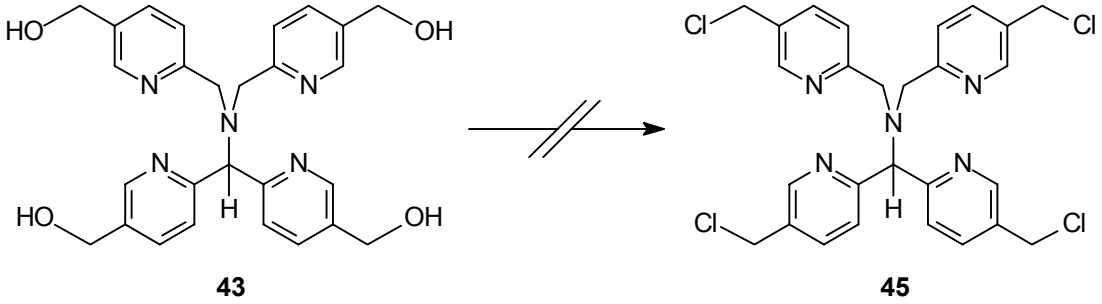

43 **45**

Scheme 3.9. The unsuccessful attempt to prepare **45** from **43**

The anticipated instability and disappointing initial results suggested that mild reaction conditions needed to be employed to convert **43** to **45**. These experiments involved the use of methanesulphonyl chloride, collidine, and lithium chloride in DMF at 0°C to room temperature.[25] Other attempts involved the use of thionyl chloride in the presence of TEA or pyridine in dichloromethane and/or DMF, or triphenylphosphine and tetrachloromethane[26] in acetonitrile and/or pyridine. Solvent mixtures were often required due to the poor solubility of **43** in common solvents like chloroform, dichloromethane, and acetonitrile due to its four hydroxyl groups. Nevertheless, **45** (or any other related N4Py structure) could not be isolated, even at low temperatures.

Tetrachloride **45** could only be detected by electrospray mass analysis (ESI-MS) as its hydrochloride salt from the reaction using thionyl chloride in DMF.[27] Unfortunately, as soon as water or base was added, the product decomposed immediately upon contact. After further attempts, it quickly became apparent that **45** could not be isolated nor prepared due to its instability. It was also impossible to convert **45**·HCl *in situ* into a N4Py ligand with four appending sulphide groups via the addition of a thiol like benzyl mercaptan or *p*-methylthiophenol. The required basic conditions resulted in the decomposition of the intermediate at a rate that was apparently faster than its conversion to the sulphide. Although the advanced intermediate **43** had been synthesised successfully, the sensitivity to decomposition of the tetrachloride **45** precluded its application as a template for peptide attachment.

In order to establish that the doubly benzylic proton in **45** is the origin of its intrinsic instability, attempts have been made to replace the proton by a methyl group. This had already been accomplished successfully for N4Py (**46**) by Gerard Roelfes during his postgraduate research.[3] However, lithiation of **1** in the presence of *N*,*N*,*N*',*N*'-tetramethylethylenediamine (TMEDA), followed by quenching with methyl iodide resulted repeatedly only in the recovery of starting material, and not to the desired product **48**. The unsuccessful methylation might be due to the steric hindrance of the four bulky TBDMS groups at the periphery of the ligand. Another explanation implies that the lithiated species is stabilised by the co-ordination of the silyl ether groups, thereby preventing alkylation.

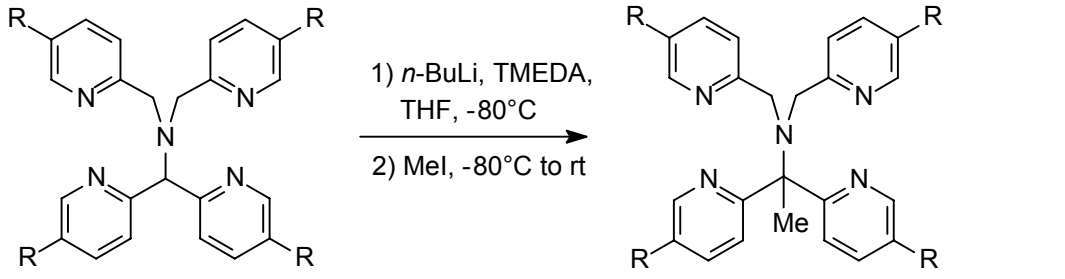

46 (R=H)
1 (R=CH_2OTBDMS)

47 (R=H)
48 (R=CH_2OTBDMS)

Scheme 3.10. Methylation of the doubly benzylic position in N4Py structures.

Another speculated approach to introduce the N4PyFe catalyst inside a four-helix bundle involved connecting two helix-loop-helix units via two chloromethylene linkers on the ligand (See Section 1.2). To obtain an anti-parallel orientation of the helix macrodipoles in the four-helix bundle, these linkers will have to be positioned on opposite sides of the ligand. To meet this prerequisite the synthesis of the dissymmetric ligand **51** was initiated, but due to the unsuccessful attempts to prepare tetrachloride **45** this synthetic route has not been examined any further (Scheme 3.11).

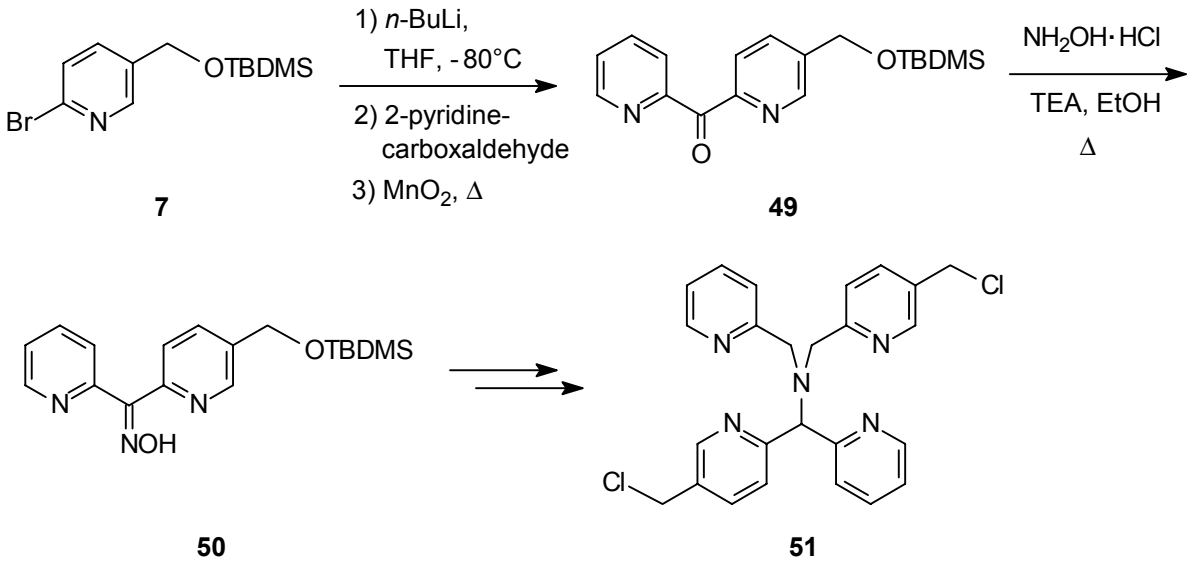

7 **49** **50** **51**

Scheme 3.11. Discontinued synthesis of the N4Py derivative **51**.

3.5 Model reactions

A number of reactions have been performed to understand the origin of the decomposition of tetrachloride **45** when prepared from the tetrahydroxyalkyl N4Py derivative **43**. The attempt to replace the doubly benzylic proton by a methyl group was unfortunately unsuccessful (*vide supra*). Some of the model reactions on 3-(hydroxymethyl)pyridine (**52**) discussed here could also provide alternative means of functionalising the N4Py structure **43**.

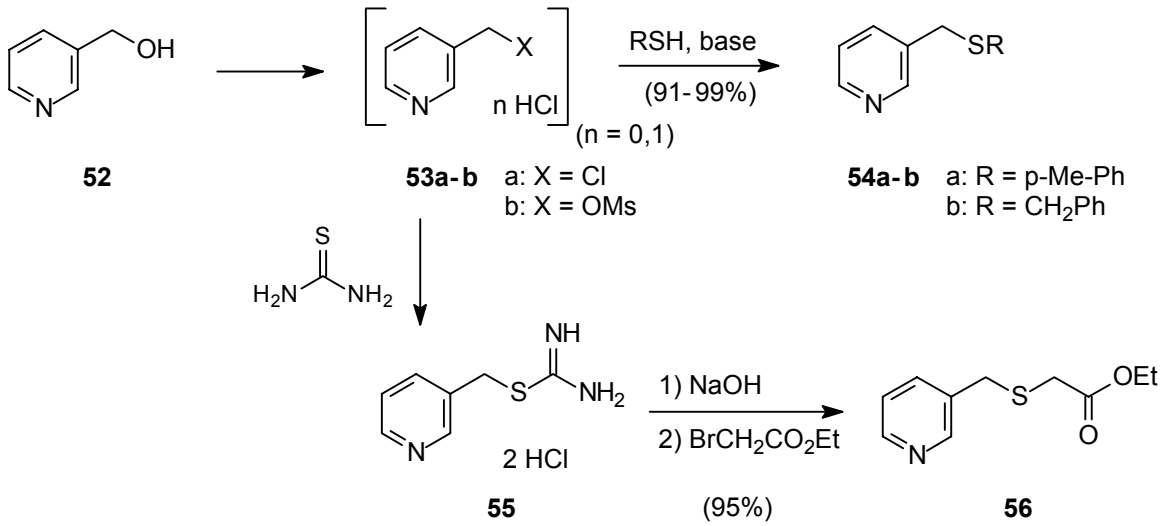

Scheme 3.12. Thioether functionalisation of **52** via an electrophilic leaving group.

The hydroxyl group of **52** was converted into a leaving group using thionyl chloride to yield **53a**, which was only stable when isolated as its hydrochloride salt (Scheme 3.12). A rapid decomposition was observed when attempts were made to isolate the free pyridines **53a–b** (n = 0). Despite this fact, these unprotonated pyridines could be converted *in situ* to the sulphides **54a–b** in excellent yields. In contrast to these successful conversions of the benzylic hydroxyl group in **52**, the experimental conditions applied to the tetrahydroxy N4Py derivative **43** as mentioned earlier were fruitless. Similarly, the Mitsunobu reaction[28] of **52**, utilising triphenylphosphine and diethyl azodicarboxylate, and the subsequent reaction with ethanol, ethyl glycolate, or methyl *N*-acetylcysteine (**57**) also proved to be unsuccessful. The presence of triphenylphosphine oxide was established by ^{31}P NMR, but mass analysis and ^{1}H NMR clearly indicated that the desired (thio)ether products had not been formed. One reason for the unsuccessful outcome might lie with the intermediate of this reaction, which again converts the benzylic hydroxyl function in **52** into a leaving group.

These findings appear to support the assumption that the benzylic chloride segments in **45** might be the source of its instability. Replacement of the chlorides by different leaving groups, therefore, does not offer any further hope. This instability of **45** presented a problem for the proposed methodology in which peptides can be attached to **45** via a nucleophilic substitution using a cysteine thiolate.

A thioether linkage can also be achieved by converting the hydroxyl groups of **43** into thiols, which can then react with a *N*-chloroacetylated peptide chain. To test this concept, **52** was initially converted into the thiourea adduct **55**, followed by hydrolysis to furnish the free thiol,[29] and then alkylated by reacting with ethyl bromoacetate to produce **56** in an excellent yield of 93% (Scheme 3.12). In spite of this successful model reaction, employing this methodology with the tetrahydroxy N4Py **43** would mean that peptide sequences could only be linked via an amide bond. This in turn would obstruct the coupling of unprotected peptides to the N4PyFe catalyst, as the side chains of certain residues will interfere with the reaction of interest. The use of protected peptides would make it possible to bypass these unwanted side reactions, but then the peptide chains can be only be tethered to the ligand through their *N*-terminus, unless selectively removable protecting groups are employed.

Circumventing the instability problem associated with **45** could involve converting the benzylic hydroxyl groups in **43** into nucleophiles rather than electrophilic groups. By simply deprotonating the hydroxyl group and quenching the oxy anion with an alkyl halide, a variety of ether products can be envisaged. Model reactions that made use of **52** have proven to be successful in the formation of the ethers **58a–b** by utilising ethyl bromoacetate and *p*-methoxybenzyl bromide, respectively (Scheme 3.13). However, attempts to alkylate **52** with *p*-nitrobenzyl chloride failed.

In sugar chemistry ether bonds are commonly formed by converting the targeted hydroxyl group into a trichloroacetimidate, followed by a (Lewis) acid-catalysed reaction with a second alcohol.[30] Accordingly, trichloroacetimidate **59** was prepared from alcohol **52** by a base catalysed reaction with trichloroacetonitrile. Unfortunately, the subsequent conversion into an ether was unsuccessful, despite the addition of more than one equivalent of a (Lewis) acid (LA).

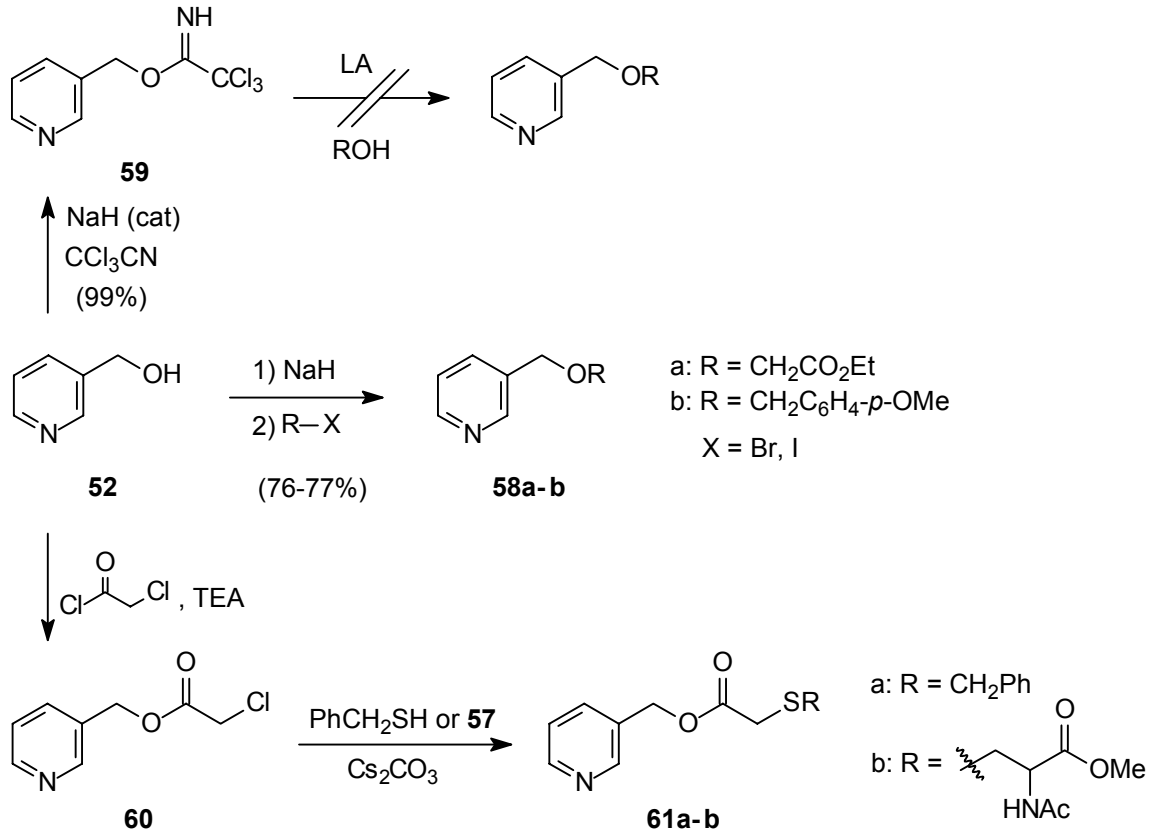

Scheme 3.13. Other examples of converting the benzylic hydroxyl group in **52**.

If the instability of the N4Py structure **45** is attributed to the benzylic chlorides, this complication can be resolved by modifying the spacer by re-positioning the leaving group into a non-benzylic site. To test this approach, **52** was acylated by chloroacetyl chloride to furnish **60**, followed by the reaction with benzyl mercaptan or methyl *N*-acetylcysteine (**57**) in the presence of caesium carbonate as a base to yield **61a** and **61b**, respectively (Scheme 3.13). However, if this methodology was to be used for the preparation of a peptide-bound N4PyFe catalyst, the introduced ester linkage might be prone to hydrolysis. A more stable linker, therefore, can be acquired via an ether bond (Scheme 3.14). For this reason, the sodium salt of **52** was allowed to react with 1-bromo-2-chloroethane (**62a**) to yield **63a**. Unfortunately, the reaction failed as

only the starting material was recovered. Similar results were obtained using ethoxy ethyl (EE) protected 2-iodoethanol (**62b**). The use of *N*-protected bromoalkylamines **62c–e**[31] would not only increase the length, but also modify the nature of the linker. When applied to the N4Py derivative **43** and after deprotection of the amine functionality, protected peptides can in principle be coupled through their *C*-termini. Many procedures are known in peptide chemistry for such an amide bond formation. The observed reaction in the preparation of **63c–e**, however, led to the elimination of hydrogen bromide to yield alkenes **64c–d**.[32] In the case of **62e** decomposition of the starting materials was observed, rather than the formation of **63e** or **64e**. Changing the order of addition of the sodium salt of **52** and the reagents **62c–e** had no effect on the outcome of the reaction.

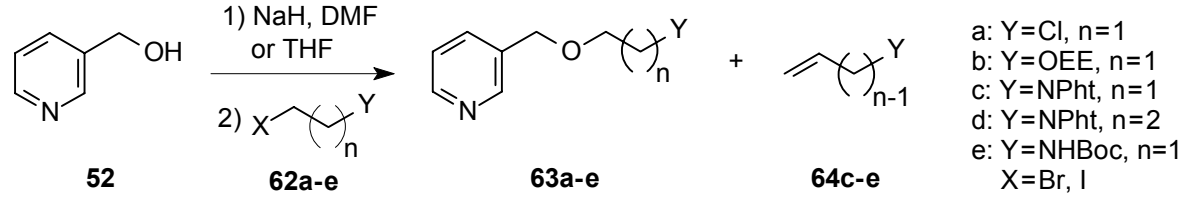

52 **62a-e** **63a-e** **64c-e**

Scheme 3.14. Unsuccessful alkylations to increase both the length and the nature of the spacer.[1]

Another strategy to attach peptides to the N4Py ligand **43** is through their *N*-termini via a carbamate linkage (Scheme 3.15). This approach was tested by the preparation of carbamate **66** via a two step procedure starting with **52** and *p*-nitrophenyl chloroformate (**65**). The intermediate carbonate was allowed to react with methyl L-valine hydrochloride in boiling chloroform and in the presence of TEA to furnish **66** in 54% isolated yield in two steps. This successful coupling of an amino acid to a pyridinyl methanol group illustrates the potential application of this methodology to couple peptides to **43**.

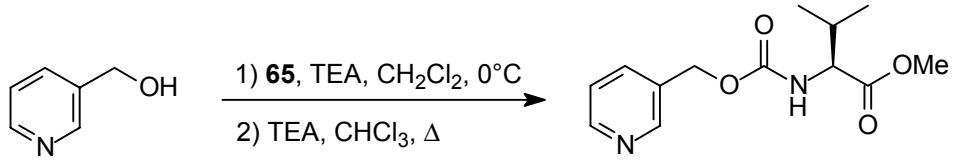

52 (54%) **66**

Scheme 3.15. Carbamate group as a potential linker for peptide attachment.

In relation to any of these functionalisation reactions of **52** it is imperative that the conversion is accompanied by a high yield, as an incomplete conversion of the four hydroxyl groups in **43** will result in product mixtures, and thereby reduce the yield of the targeted ligand structure. In Scheme 3.13 a method is presented to enable the attachment of cysteines to **43** via an ester linker. In this reaction in particular it is even more important that the reactions proceed to completion as two consecutive transformations are required. When applied to **43**, indeed only the tetracysteine derivatised ligand **72** was observed (Scheme 3.16). Mass analysis of the reaction mixture established that both the esterification and the alkylation step were successful, as side-products resulting from incomplete reactions were not observed. It is therefore apparent

that this methodology can be used successfully to attach four peptide chains to the N4Py ligand **43**. However, as mentioned earlier, the ester linkage might present a complication with regard to the stability when the structure forms part of an iron complex that is applied to catalytic oxidation reactions in an aqueous medium.

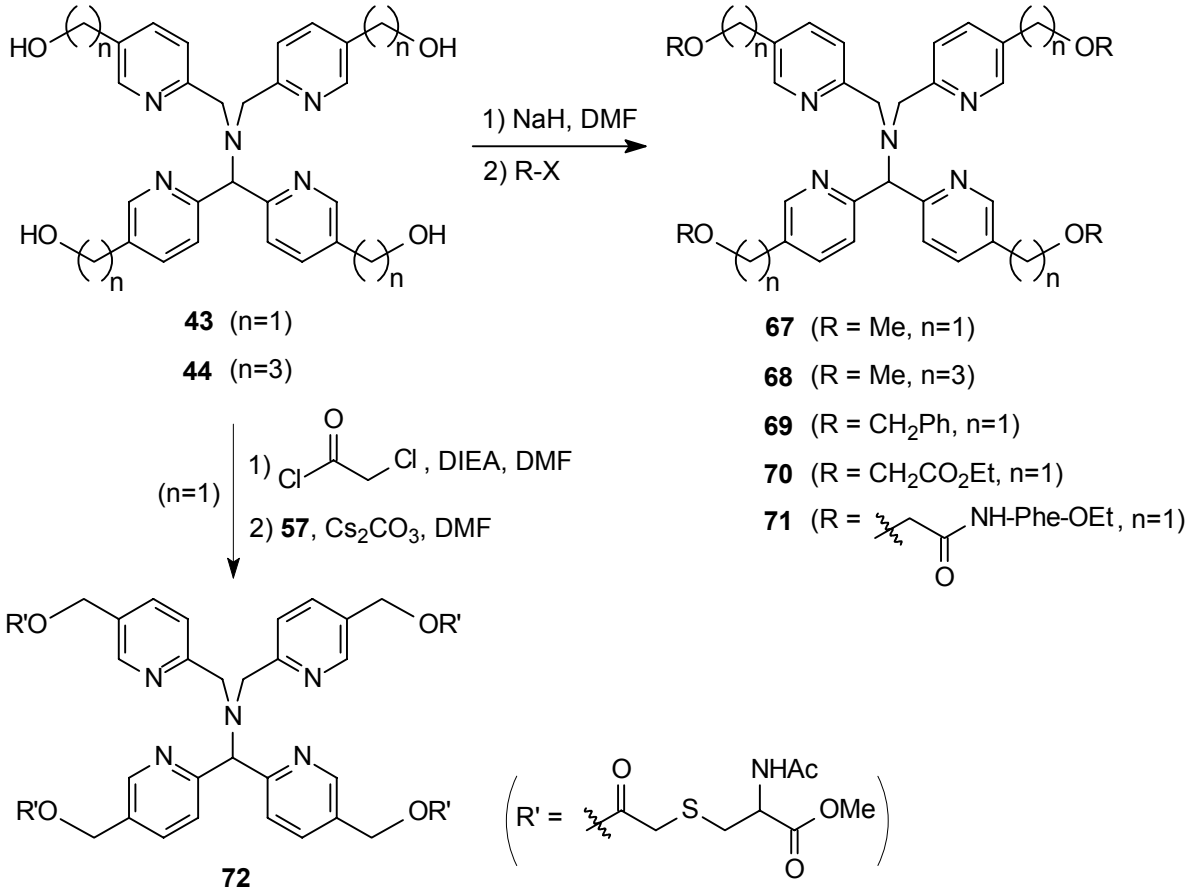

Scheme 3.16. Alkylation of tetrahydroxy derivatised N4Py ligands **43** and **44** and attachment of cysteine residues to **43** via ester linkages.

The hydroxyl groups of **43** and **44** were successfully alkylated with methyl iodide or benzyl bromide after deprotonation by sodium hydride (Scheme 3.16). Although the resulting N4Py derivatives **67–69**[33] do not present an alternative means of attaching peptides to the ligand, these tetrafunctionalised N4Py ligands might provide interesting iron(II) complexes for the catalytic oxidation of organic substrates (See Chapter 5). Although *p*-methoxybenzyl bromide has been used successfully for the alkylation of **52**, similar conditions did not yield satisfactory results when applied to **43**.

When ethyl bromoacetate is used for the alkylation of **43**, the introduced ester groups can in principle create the possibility to couple peptides via an amide bond through their *N*-termini. Unfortunately, under the experimental conditions that were employed full substitution of **43** to furnish **70** was not observed. Instead, a mixture of di-, tri-, and tetra-alkylated products was identified by mass analysis.[34] In an attempt to introduce four amino acids into **43**, the tetra-alcohol was deprotonated and subjected to *N*-bromoacetyl L-phenylalanine ethyl ester to prepare **71**. Using this methodology, *N*-bromoacetylated peptides can in principle be coupled to

the ligand. Unfortunately, no conversion of deprotonated **43** to **71** was observed under these conditions either. As the reaction conditions have not yet been optimised for compounds **69–72**, no yields are shown in Scheme 3.16.

3.6 Increasing the spacer length

The decomposition of the tetrachloride **45** is probably inherent to its structure and might be triggered by hydrogen chloride elimination. The mechanism is, unfortunately, still insufficiently understood. As suggested above, one option to circumvent the instability induced by benzylic chlorides is to extend the linkers between the pyridine moieties and the leaving groups. These linkers should be short, stable, and readily introduced. Although the model studies presented in Section 3.5 provide some alternatives for a successful functionalisation of the C1-spacer in **43**, the application and the effect on the stabilisation are not by any means straightforward. For example, the unsuccessful formation of the ether **63a** (Scheme 3.14) illustrated that modification of **43** in a similar fashion is unlikely to be fruitful. A chloroacetyl linker can be readily introduced (see **72** in Scheme 3.13), although the resulting ester linkage is not very stable. This instability was exposed when the iron(II) complex of **72** was found to decompose during crystallisation.

An all-carbon linker at the periphery of the ligand presents another alternative to place the leaving groups further away from the benzylic position. However, using the currently developed methodology this approach implies that these linkers will have to be introduced at the start of the synthetic pathway. A C2-spacer can be created by quenching 2-bromo-5-lithio-pyridine with ethylene oxide, analogous to the synthesis of the aldehyde **22** (Scheme 3.4). The resulting C2-spaced hydroxyl group can also be obtained via the Wittig reaction of **22** with methoxymethylenephosphorane, followed by the reduction of the extended aldehyde functionality. The synthetic pathway would lead to the corresponding N4Py derivative with C2-spaced hydroxyl functionalities that will have to be converted into chloride groups. However, if hydrogen chloride elimination triggered the decomposition of **45**, then this might also be applicable to the C2-spaced analogue. The elimination of hydrogen chloride can be anticipated due to the energetically favourable conjugation between the ethylene groups with the pyridine rings of the ligand.

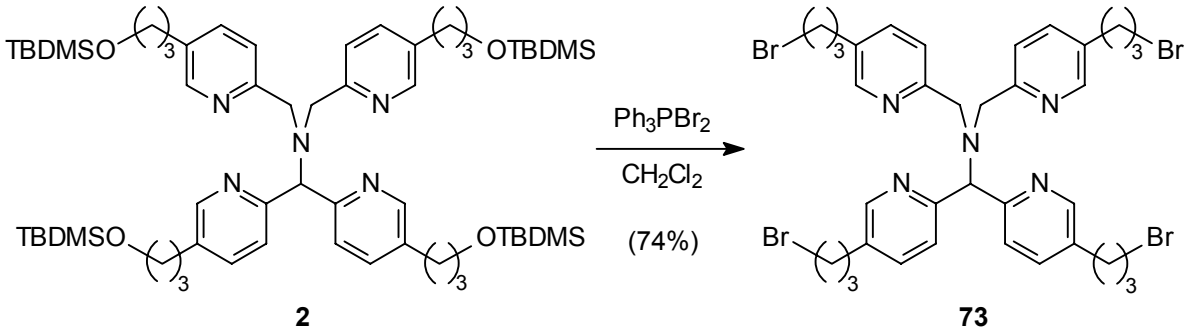

2 **73**

Scheme 3.17. Synthesis of the tetrabromide N4Py ligand **73**.

The decision was taken to prepare the C3-spaced N4Py derivative **2**, as the preparation of the C2-spaced ligand would involve an extensive synthesis of a structure that could potentially

decompose. The synthesis of **2** is outlined in Scheme 3.4 to Scheme 3.7 for n = 3. In order to enhance the leaving group ability of the non-benzylic leaving group, a bromide was introduced by converting the silyl ether groups directly into bromides by reacting with triphenylphosphine dibromide (Scheme 3.17).[30,35]

Intra- or intermolecular alkylation of the pyridine or tertiary amine nitrogens in **73** is a potential problem, but from our past experience it is known that this does not occur even for hexyl chains (n = 6).[36] The long synthetic route to prepare **73** was rewarded by the observed enhanced stability of the ligand, enough to bear more reactive bromides as terminal leaving groups. Electrospray mass analysis of **73** ($[M+H]^+$ at *m/z* 848.0) corresponded to the calculated isotope distribution pattern (top and bottom right, respectively).

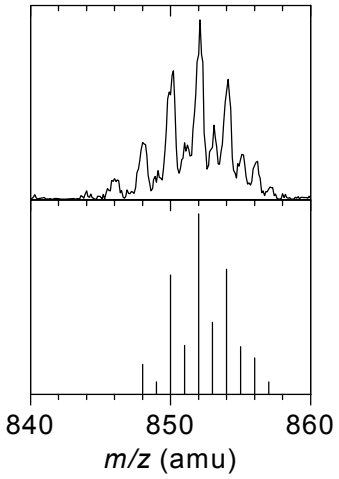

It is of interest to note, that 3'-(3-bromopropyl)-pyridine[37] as a model compound for **73** decomposed rapidly upon isolation, whereas **71** was found to be stable at room temperature for at least a day. Therefore, it is quite surprising, and satisfying, that the introduction of the labile terminal bromide functionalities did not lead to the formation of a more unstable compound.

3.7 Cysteine substitution and peptide coupling

In order to tether four peptides to N4Py (**46**) the ligand had to be modified. For this purpose the synthesis of the tetrachloride **45** was attempted as it would enable the attachment of peptides via a cysteine residue in the sequence. Although this C1-spaced template was found to be too unstable, the C3-spaced tetrabromide **73** was obtained successfully. The peptide coupling to this ligand can formally be considered an alkylation reaction of cysteine. With regard to the ligand, it is imperative that the nucleophilic substitution reaction goes to completion, as an incomplete reaction with the peptides would result in a mixture of mono-, di-, tri-, and tetrasubstituted template-assembled peptide complexes. To force the substitution reaction to go to completion, an excess of peptide must be used.

Another hurdle to overcome relates to the peptides that will be used in the absence of side chain protecting groups. Various reactive functionalities in the amino acid side chains in, for instance, histidine and lysine might interfere in the alkylation reaction.[38] It is therefore important to elucidate the optimal conditions for the alkylation of the cysteine thiolate substitution reaction. Some of the methods that have been described in the literature for cysteine alkylation involve (a) ammonia in methanol,[39] (b) DIEA or TEA in polar non-protic solvents, like DMSO, DMF, or acetonitrile,[40] (c) sodium ethoxide in refluxing ethanol,[41] or (d) caesium carbonate in aqueous DMF at pH 9.[2,42] Previously in the preparation of the N4PyFe-dipeptide complex (Chapter 2),[2] caesium carbonate was applied with great success. Deprotonation of the cysteine under these conditions converts the thiol group into an excellent nucleophile ('caesium effect'), which is well suited for S_N2 substitution of primary and secondary halides.[43] Under these conditions the peptides are coupled to the ligand solely via the cysteine residue, even in the presence of other nucleophilic side chains.[2] To test the potential use of **73** as a template for the

attachment of peptides, the nucleophilic substitution reaction was first tested by a cysteine thiolate displacement of the bromides (Scheme 3.18). Compound **74** was obtained in a 12% isolated yield after purification by preparative reversed-phase high-performance liquid chromatography (RP-HPLC). Its structure was verified by ^{1}H NMR and mass analysis.

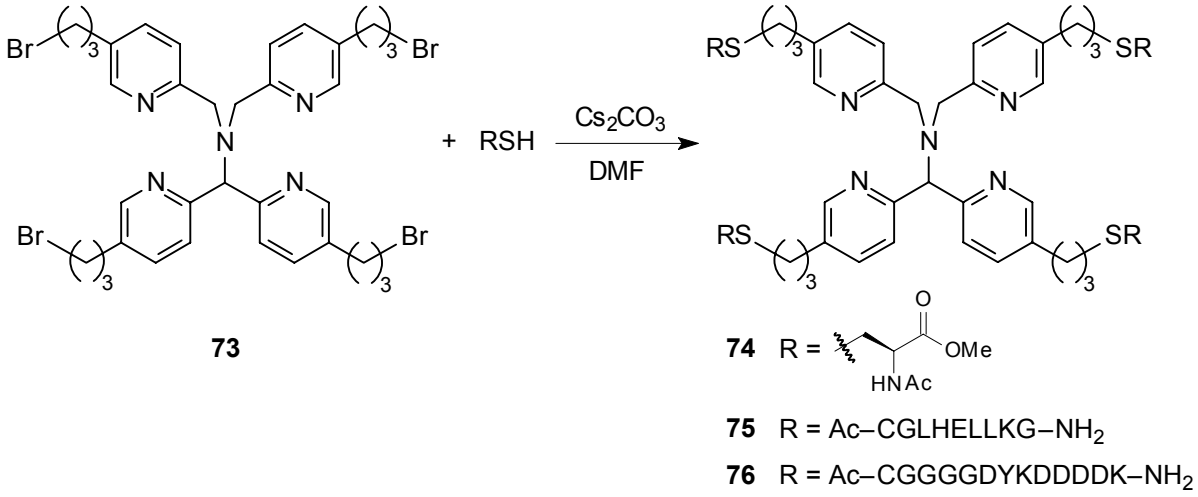

73

74 R =

75 R = Ac–CGLHELLKG–NH_2

76 R = Ac–CGGGGDYKDDDDK–NH_2

Scheme 3.18. Cysteine and peptide coupling to tetrabromide **73**.[38]

After establishing the successful coupling of four protected cysteines to **73** to furnish **74**, the peptide coupled products **75** and **76** were obtained after using the corresponding unprotected peptides in excess (*vide infra*). These peptides have been selected only on the basis of their representative amino acid content and length that might lead to complications during the coupling reactions. Furthermore, it is imperative to note that these peptide sequences have not been designed to fold into a four-helix bundle.

Upon complexation of the ligands **74–76** with iron(II) perchlorate, the corresponding iron(II) complexes were obtained with four appending cysteines or peptides, respectively (Scheme 3.19). The iron(II) complexes **78–79** were prepared *in situ* after coupling the peptides to the ligand. The tetracysteine adduct **74** was purified by preparative RP-HPLC prior to complexation with iron(II) perchlorate (Figure 3.3).

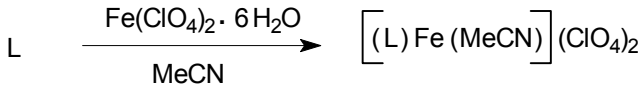

77: L = **74**
78: L = **75**
79: L = **76**

Scheme 3.19. Complexation of ligands **74–76** with iron(II) perchlorate.

The ESI-MS spectrum of purified **74** exhibited two peaks at *m/z* 1236.7 and 619.1, corresponding to $[M+H]^+$ and $[M+2H]^{2+}$, respectively. Its iron(II) complex **77** displayed an UV-VIS spectrum that is characteristic for iron(II) complexes of N4Py ligands (Figure 3.4, left).[3] Electrospray mass analysis of **77** revealed the masses of $[M-(ClO_4)^--(MeCN)]^+$ (*m/z* 1390.4), and the doubly-charged particle of $[M-2(ClO_4)^--(MeCN)]^{2+}$ (*m/z* 646.0) (Figure 3.4, right). The singly-charged peak observed at *m/z* 1326.5 was assigned as [(**74**)Fe(MeCN)](Cl), because

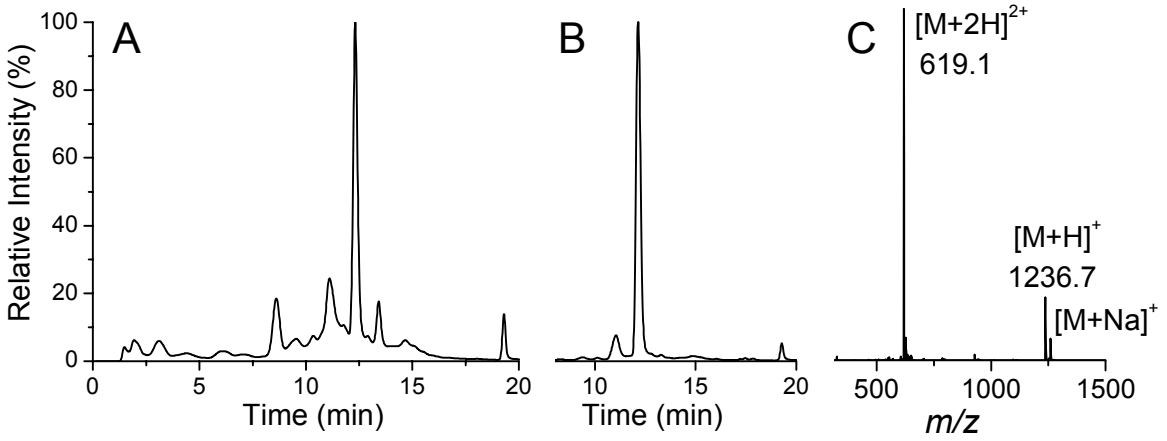

Figure 3.3. HPLC profile of the crude (A) and purified (B) **74** with ESI-MS analysis of the purified sample (C).

the observed and calculated isotope patterns were identical. Its formation could stem from the reaction of **77** with traces of chloride salts present during the sample preparation. The peak at *m/z* 707.5 was attributed to an unknown contaminant.

The uniformity of the peptide coupling was confirmed by MALDI mass analysis of the crude template-assembled peptide complexes **78** and **79**. It is important to note that side-products from incomplete substitution reactions were not detected. The peptide complexes **78** and **79** were purified by preparative RP-HPLC. The absorption band around 450 nm, which is characteristic for N4PyFe complexes (see Figure 3.4, left), makes it possible to distinguish readily between the single peptide chains and the N4PyFe-peptide complexes. This point is illustrated in Figure 3.5, which shows the same HPLC run that was used for the purification of **79**, monitored at all wavelengths (TIC) and at 450 nm.

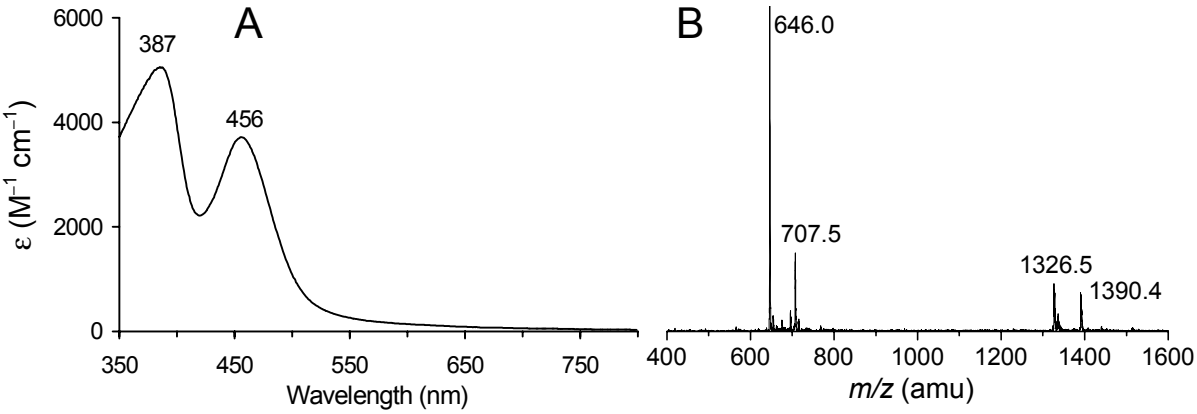

Figure 3.4. UV-Vis spectrum of **77** in acetone (A) and its ESI-MS spectrum (B).

The chemical integrity and the inclusion of iron in the peptide complexes was verified by MALDI mass analysis of the collected homogeneous fractions. The calculated mass for **78** corresponded to the detected mass (Figure 3.6A) (calcd for [**78**– $2(ClO_4)^-$ – (MeCN)]$^{2+}$ *m/z* 4620.38 amu (monoisotopic), 4623.43 amu (average isotope composition), found 4619.2 amu). This is equally valid for **79** (Figure 3.6B) (calcd for [**79**– $2(ClO_4)^-$ – (MeCN)]$^{2+}$ *m/z* 6121.3 amu (monoisotopic), 6125.1 amu (average isotope composition), found 6124.0 amu). Remarkably,

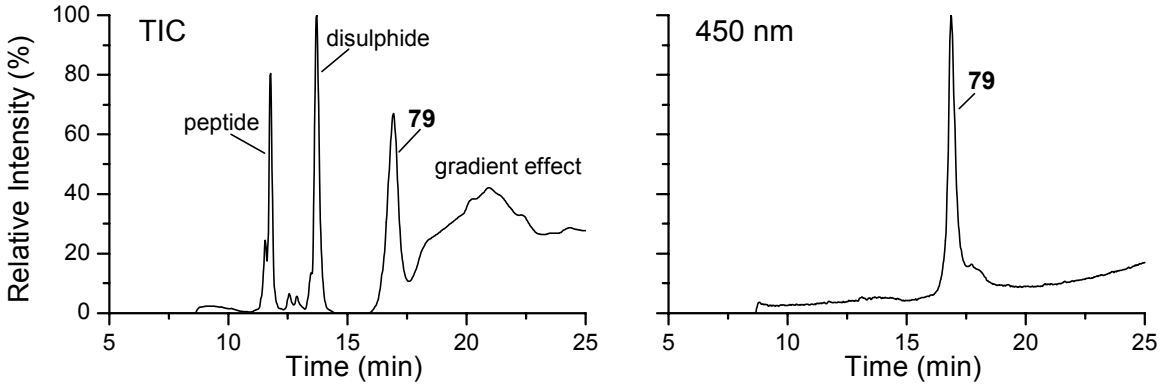

Figure 3.5. RP-HPLC plot of crude **79** monitored at all wavelengths (TIC, left) and 450 nm (right).

these doubly-charged species for **78** and **79** are not observed at *m/2z*, but at *m/z*. For both peptide complexes higher charged species have also been detected. The *m/2z* species (2309.6 for **78**, 3063.5 for **79**) were always observed as a set of four signals. In the lower regions, two masses were detected that were assigned to the *m/4z* species, which did not match exactly the calculated values (calcd for **78** *m/4z* 1154.8, found 1158.0; calcd for **79** *m/4z* 1531.2, found 1536.0). The patterns observed for multiply-charged species were similar for both **78** and **79**, although an appropriate explanation for these observations is not available at the present time.

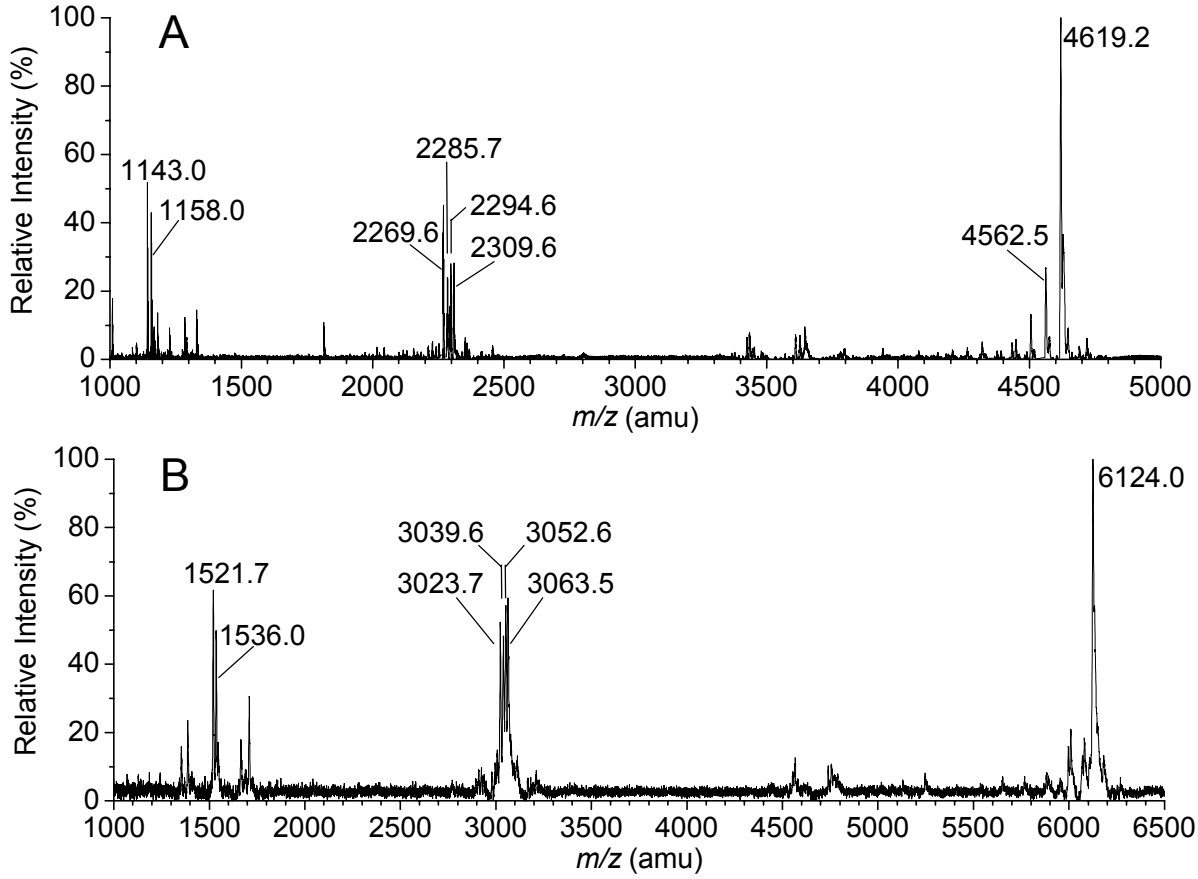

Figure 3.6. MALDI mass analyses of the purified **78** (A) and **79** (B).

The examination of the catalytic oxidative activity of the peptide complexes **77–79** will be elaborated upon in Chapter 5, where the results for other tetrasubstituted N4Py derivatives will also be described with regard to their ability to act as oxidation catalysts.

3.8 Discussion and conclusions

Chapter 2 described the work previously carried out on the modification of the non-functionalised N4PyFe catalyst to enable the covalent attachment of two peptide chains.[2] For this purpose, two chloromethylene groups had been introduced at the periphery of the N4Py ligand. The intention to use the same methodology for the introduction of four equivalent attachment sites for the coupling of four peptides, was clearly over-estimated. So far, all attempts to synthesise and convert tetrachloride **45** have been unproductive. The intrinsic instability of this compound makes it unlikely that this ligand can be used to incorporate the N4PyFe complex inside a four-helix bundle. Alternative coupling strategies will have to be employed to tether peptides to the C1-spaced N4Py template, some of which have been presented by the model reactions in Section 3.5. However, a satisfactory solution for coupling peptide chains to the C1-spaced ligand **43** has yet to be found.

To overcome the instability of the tetrachloride **45**, structural changes had to be incorporated into the N4Py ligand. Although extended spacers enabled the synthesis of the tetrabromide **73**, this approach at the same time illustrated the flaw in the developed synthetic route. Even though in principle various spacers can be tethered to the N4Py framework, these modifications entail the reconstruction of the ligand from scratch. It would therefore be more practical to synthesise a N4Py ligand that can be modified after it has been constructed, which also allows a variety of spacers to be introduced (a divergent synthesis). At the same time, such a ligand will also enable a range of structural variations to be created at the periphery of the N4Py ligand. These ligands in turn can be screened for their catalytic activity towards the oxidation of organic substrates. The synthesis of such a ligand will be discussed further in Chapter 4.

In spite of the encountered synthetic problems, the developed convergent synthesis has led to the preparation of a tetrasubstituted N4Py ligand to which four peptides can be attached. This was demonstrated by MALDI mass analysis of the peptide complexes **78** and **79**. The pentadentate nature of the N4Py ligand makes it possible to use tetrabromide **73** as a functional template for the covalent attachment of peptide chains. The oxidation behaviour of the iron(II) peptide complexes **78** and **79**, and their resistance towards oxidative degradation will be presented in Chapter 5.

3.9 Experimentals

Instrumentation

The NMR spectra were recorded on a Varian Gemini-200 (^{1}H NMR at 200 MHz, ^{13}C NMR at 50.3 MHz), a Varian VXR-300 (^{1}H NMR at 300 MHz, ^{13}C NMR at 75.5 MHz), or on a Varian Unity Plus (^{1}H NMR at 500 MHz). Chemical shifts (δ) are denoted in ppm and referenced to the residual proton resonance in $CDCl_3$ (^{1}H: δ 7.25 ppm, ^{13}C: δ 77.0 ppm), CD_3OD (^{1}H: δ 3.30 ppm, ^{13}C: δ 49.0 ppm), DMSO–d_6 (^{1}H: δ 2.49 ppm, ^{13}C: δ 39.5 ppm), or CD_3CN (^{1}H: δ 1.93 ppm). The splitting patterns are designated as follows: s (singlet), d (doublet), dd (double

doublet), t (triplet), q (quartet), m (multiplet), br (broad), and for ^{13}C NMR determined with the ATP pulse sequence. The mass spectra were recorded by Albert Kiewiet on a JEOL JMS-600H for electron impact (MS EI), chemical ionisation (MS CI), and exact mass determination (HRMS). Matrix-assisted laser desorption ionisation time-of-flight mass spectrometry (MALDI) analyses were carried out on a Micromass TofSpec E, equipped with a N_2 UV-laser ($\lambda = 337$ nm, 4 ns pulse, $E_{pulse} = 180$ mJ). Samples were prepared in an α-cyano matrix (1:1, dissolved in MeCN and 0.1% TFA (7:3), 20 mg/mL). Electrospray ionisation mass spectrometry (ESI-MS) was performed by Margot Jeronimus-Stratingh on a Nermag mass spectrometer. Elemental analysis was carried out in the microanalytical department of the University of Groningen by Harm Draaier, Jan Ebels, and Jannus Hommes on an EuroVector CHNS-O Elemental Analyzer Euro EA 3000. Melting points were determined on a Mettler FP-2 melting point apparatus, equipped with a Mettler FP-21 microscope, and are uncorrected. UV-Vis spectra were recorded on a Hewlett-Packard 8453 single-beam spectrophotometer. Data acquisition was performed using the UV-Visible ChemStation software package by Agilent Technologies. Reversed-phase high-performance liquid chromatography (RP-HPLC) was conducted on a Waters 2690 Separations Module equipped with a Waters 996 Photodiode Array Detector (set at TIC and 450 nm) and a Micromass ZMD Quadrupole mass spectrometer with the co-operation of Marc van Gelder. The Alltech Econosil C18 analytical column (150 x 2.1 mm, 5μ) was run at a flow of 0.3 mL/min, and the semi-preparative column (250 x 4.5 mm, 5μ) at a flow of 1.5 mL/min. The peptide complexes were purified using linear gradients of mixtures of solvent A (10% acetonitrile in water with 0.1% TFA) and solvent B (95% acetonitrile in water with 0.1% TFA). The crude products were dissolved in mixtures of solvents A and B. Ligand **74** was purified using a linear gradient of MeCN in 0.05 M ammonium acetate. The homogeneous fractions were collected, lyophilised, and analysed by ESI-MS or MALDI.

Methods and chemicals

Glassware used for the reactions performed under dry conditions were first flame-dried under vacuum. For lithiation reactions THF and diethyl ether were freshly distilled from sodium/benzophenone, and toluene from sodium under a nitrogen atmosphere. For other purposes, dichloromethane, diethyl ether, and hexane were distilled from P_2O_5 and stored over 4Å molecular sieves. DMF and acetonitrile were distilled from calcium hydride, and TEA from potassium hydride, and were stored over 4Å molecular sieves under nitrogen. Sodium hydride (60% in mineral oil) was washed three times with dry hexane prior to use. Commercially available reagents were purchased from Acros, Aldrich, Fluka, or Merck, and employed as received. Butyllithium (*n*-BuLi) was used as a 1.6 M solution in hexane. Flash column chromatography was performed on aluminium oxide 90 (neutral, act. III) from Merck or silica gel 60 (230–400 mesh) from Aldrich. The peptide sequences have been synthesised using conventional solid-phase Fmoc-chemistry.[44] The IUPAC names of novel compounds were generated using the software package ACD/IUPAC Name Pro, version 3.50.

5-Bromonicotinic acid (20)

To a suspension of **9** (0.47 g, 2.0 mmol) in dry diethyl ether (50 mL) at –80°C was added *n*-BuLi (1.4 mL, 2.2 mmol, 1.1 equiv) under a nitrogen atmosphere. After 60 min at –80°C the reaction mixture was poured onto a solution of CO_2 in diethyl ether, and allowed to warm to

room temperature. The organic layer was washed with water (3x10 mL). The aqueous layer was acidified and extracted with diethyl ether (3x10 mL). After washing with brine (10 mL), drying over Na_2SO_4, and evaporation of the solvent, a white solid was obtained (0.33 g, 82%).
mp 191.7–192.8°C (lit.[12] 195°C). ^{1}H NMR (DMSO–d_6, 300 MHz) δ 7.80 (d, J = 8.2 Hz, 1H), 8.16 (dd, J = 8.2, 2.2 Hz, 1H), 8.85 (d, J = 2.2 Hz, 1H), 13.65 (br.s, 1H). ^{13}C NMR (DMSO–d_6, 75.5 MHz) δ 126.2 (s), 128.1 (d), 139.7 (d), 145.4 (s), 150.9 (d), 165.3 (s). HRMS calcd for $C_5H_4BrNO_2$ 200.942, found 200.944.

2-Bromo-5-pyridinecarbaldehyde (22)[45]
n-BuLi (62 mL, 99 mmol, 1.05 equiv) was added to a suspension of **9** (22.7 g, 94.1 mmol) in dry diethyl ether (1 L) at –80°C under a nitrogen atmosphere. Dry DMF (8.0 mL, 103 mmol, 1.1 equiv) was added after stirring the suspension at –80°C for 1 h. After an additional hour at –80°C the reaction mixture was allowed to warm to room temperature. Dilute HCl (1 M, 200 mL) was added and the mixture was stirred for 15 min. After separation the aqueous layer was extracted with diethyl ether (3x100 mL). The organic layer was washed with water (2x100 mL), brine (100 mL), and dried over Na_2SO_4. Concentration by rotary evaporation yielded **22** as a light brown solid (16.8 g, 96%). R_f = 0.49 (SiO_2, hexane/ethyl acetate = 3:1).
mp 100.7–102.2°C (lit.[12] 100°C). ^{1}H NMR ($CDCl_3$, 300 MHz) δ 7.67 (d, J = 8.4 Hz, 1H), 8.01 (dd, J = 8.4, 2.2 Hz, 1H), 8.82 (d, J = 2.2 Hz, 1H), 10.08 (s, 1H). ^{13}C NMR ($CDCl_3$, 75.5 MHz) δ 129.0 (d), 130.5 (s), 137.5 (d), 148.2 (s), 152.4 (d), 189.4 (d). HRMS calcd for C_6H_4NOBr 184.948, found 184.949.

(6-Bromo-3-pyridinyl)methanol (21)
$NaBH_4$ (2.28 g, 60.3 mmol, 0.5 equiv) was added to a solution of **22** (22.4 g, 120 mmol) in methanol (400 mL) at 0°C. After 15 min concentrated HCl was added until pH 2 was reached. Then saturated aqueous Na_2CO_3 solution was added until pH 10 was observed. The solution was concentrated and extracted with ethyl acetate (4x100 mL). The organic layer was washed with brine (75 mL) and dried over Na_2SO_4. When the solvent was evaporated, the product was obtained as a yellow/brown oil that solidified upon standing (21.8 g, 96%). R_f = 0.12 (SiO_2, hexane/ethyl acetate = 3:1).
mp 42.5–45.0°C (lit.[18] 49–51°C). ^{1}H NMR ($CDCl_3$, 300 MHz) δ 2.82 (br.s, 1H), 4.68 (s, 2H), 7.45 (d, J = 8.1 Hz, 1H), 7.57 (dd, J = 8.1, 2.2 Hz, 1H), 8.29 (s, 1H). ^{13}C NMR ($CDCl_3$, 75.5 MHz) δ 61.6 (t), 128.0 (d), 135.8 (s), 137.5 (d), 140.8 (s), 148.5 (d). HRMS calcd for C_6H_6BrNO 186.963, found 186.964.

2-Bromo-5-({[*tert*-butyl(dimethyl)silyl]oxy}methyl)pyridine (7)[18]
To a stirred solution of **21** (21.8 g, 116 mmol) and TEA (25.0 mL, 179 mmol, 1.5 equiv) in dry DMF (50 mL) was added *tert*-butyldimethylsilyl chloride (18.8 g, 125 mmol, 1.05 equiv). After stirring for 15 min, protected from moisture, the mixture was diluted with diethyl ether (200 mL) and washed with water (4x150 mL) and brine (150 mL). The organic phase was dried over Na_2SO_4 and concentrated by rotary evaporation to yield a yellow/brown oil (35.0 g, quant.). Purification by flash column chromatography over silica using a gradient of hexane/diethyl ether (19:1 to 9:1) yielded **7** as colourless oil (29.8 g, 85%). R_f=0.43 (SiO_2, hexane/diethyl ether = 9:1).

^{1}H NMR ($CDCl_3$, 300 MHz) δ 0.09 (s, 6H), 0.92 (s, 9H), 4.69 (s, 2H), 7.43 (d, J = 8.1 Hz, 1H), 7.52 (dd, J = 8.1, 2.2 Hz, 1H), 8.30 (d, J = 2.2 Hz, 1H). ^{13}C NMR ($CDCl_3$, 75.5 MHz) δ –5.4 (q), 18.2 (s), 25.7 (q), 61.9 (t), 127.5 (d), 136.0 (s), 136.5 (d), 140.4 (s), 148.0 (d). HRMS calcd for $C_{12}H_{20}BrNOSi$ 303.048, found 303.048.

Ethyl (*E*)-3-(6-bromo-3-pyridinyl)-2-propenoate (24)

A solution of triethyl phosphonatoacetate (12.0 g, 53.6 mmol) in dry diethyl ether (50 mL) was added over 10 min to a suspension of NaH (2.35 g, 58.8 mmol) in dry diethyl ether (130 mL) at 5°C. The icebath was removed and after 10 min a solution of **22** (9.97 g, 53.6 mmol) in dry THF/diethyl ether (250 mL, 1:1) was added over 10 min. After 15 min water (150 mL) was added and the phases were separated. The aqueous layer was extracted with diethyl ether (50 mL). The combined organic layer was washed with brine (100 mL) and dried over Na_2SO_4. Evaporation of the solvent produced **24** as a brown solid. Recrystallisation from hexane yielded analytically pure product as white needles (9.96 g pure *E*-isomer, 75%). From the concentrated filtrate a further 1.24 g of **24** (85% combined yield) was obtained after flash column chromatography over silica using hexane/diethyl ether (9:1) as the eluent. R_f = 0.53 (SiO_2, hexane/ethyl acetate = 3:1).

mp 83.6–84.1°C. ^{1}H NMR ($CDCl_3$, 300 MHz) δ 1.33 (t, J = 7.3 Hz, 3H), 4.26 (q, J = 7.3 Hz, 2H), 6.48 (d, J = 16.1 Hz, 1H), 7.50 (d, J = 8.4 Hz, 1H), 7.59 (d, J = 16.1 Hz, 1H), 7.67 (dd, J = 8.4, 2.2 Hz, 1H), 8.47 (d, J = 2.2 Hz, 1H). ^{13}C NMR ($CDCl_3$, 50.3 MHz) δ 14.2 (q), 60.9 (t), 121.2 (d), 128.3 (d), 129.5 (s), 136.2 (d), 139.3 (d), 143.4 (s), 149.8 (d), 166.0 (s). HRMS calcd for $C_{10}H_{10}NO_2Br$ 254.989, found 254.990. Anal. calcd for $C_{10}H_{10}BrNO_2$: C 46.90; H 3.90; N 5.50; Br 31.20. Found: C 46.96; H 3.97; N 5.43; Br 31.18.

3-(6-Bromo-3-pyridinyl)-1-propanol (25)

To a stirred suspension of $LiAlH_4$ (1.90 g, 50.1 mmol) in dry diethyl ether (75 mL) at 0°C was added a solution of **24** (6.40 g, 25.0 mmol) in dry diethyl ether (75 mL) over 20 min. After 10 min at 0°C the reaction mixture was allowed to warm to room temperature and stirred for 45 min. The reaction was quenched by carefully adding $Na_2SO_4{\cdot}10H_2O$ and stirring the mixture for 1 h. The solids were removed by filtration and washed with diethyl ether. Evaporation of the solvent yielded **25** as a light brown oil (3.27 g, 61%), which was used without any further purification. R_f = 0.29 (SiO_2, hexane/ethyl acetate = 1:1).

^{1}H NMR ($CDCl_3$, 300 MHz) δ 1.84 (m, 2H), 2.68 (t, J = 7.9 Hz, 2H), 3.66 (t, J = 6.0 Hz, 2H), 7.38 (s, 1H), 7.39 (s, 1H), 8.19 (s, 1H). ^{13}C NMR ($CDCl_3$, 75.5 MHz) δ 28.2 (t), 33.3 (t), 60.9 (t), 127.6 (d), 136.7 (s), 138.8 (d), 139.0 (s), 149.8 (d). HRMS calcd for $C_8H_{10}NOBr$ 214.995, found 214.996.

2-Bromo-5-(3-{[*tert*-butyl(dimethyl)silyl]oxy}propyl)pyridine (8)

The same procedure was used as described for **7**. Starting from **25** (12.7 g, 58.7 mmol) the product was obtained as a brown oil (18.6 g, 96%). Purification by flash column chromatography over silica using a gradient of hexane/diethyl ether (19:1 to 9:1) yielded **8** as a light brown oil (15.7 g, 81%). R_f = 0.43 (Al_2O_3, hexane/diethyl ether = 19:1).

^{1}H NMR ($CDCl_3$, 300 MHz) δ 0.03 (s, 6H), 0.89 (s, 9H), 1.79 (m, 2H), 2.64 (t, J = 7.9 Hz, 2H),

3.60 (t, J = 6.0 Hz, 2H), 7.36 (s, 1H), 7.37 (s, 1H), 8.20 (s, 1H). ^{13}C NMR ($CDCl_3$, 75.5 MHz) δ –5.4 (q), 18.2 (s), 25.8 (q), 28.3 (t), 33.6 (t), 61.4 (t), 127.5 (d), 136.7 (s), 138.6 (d), 139.2 (s), 150.2 (d). MS CI $[M+H]^+$ calcd for $C_{14}H_{25}BrNOSi$ m/z 330.1, found 330.2.[46]

5-({[*tert*-Butyl(dimethyl)silyl]oxy}methyl)-2-pyridinecarbaldehyde (29)[45]

Method A: To a solution of **7** (10.4 g, 34.3 mmol) in dry THF (450 mL) at –80°C under a nitrogen atmosphere was slowly added *n*-BuLi (24.0 mL, 38.4 mmol, 1.1 equiv). After 40 min at –80°C dry DMF (3.0 mL, 39 mmol, 1.1 equiv) was added to the red solution. The reaction mixture was allowed to warm to room temperature after 1 h at –80°C. Brine (100mL) and diethyl ether (50 mL) were added and the layers were separated. The aqueous layer was extracted with diethyl ether (50 mL). The combined organic layers were washed with brine (50 mL) and dried over Na_2SO_4. Concentration by rotary evaporation afforded a light brown oil (8.98 g).[47] Purification by flash column chromatography over silica using hexane/ethyl acetate (9:1) as the eluent yielded 6.88 g (80%) of **29** as a light brown oil. R_f = 0.54 (SiO_2, hexane/ethyl acetate = 3:1).

Method B: To a solution of isopropylmagnesium bromide (11 mL, 22 mmol, 2 M in THF) in dry THF (10 mL) was added **7** (6.02 g, 19.9 mmol). Heat was evolved during the reaction and after 1 h dry DMF (1.7 mL, 22 mmol) was added. The reaction was quenched after an additional hour by the addition of a saturated aqueous NH_4Cl solution (20 mL). Diethyl ether was added and the layers separated. The aqueous layer was extracted with diethyl ether (2x5 mL). The combined organic layers were washed with water (3x5 mL), brine (5mL), and dried over Na_2SO_4. Evaporation of the solvent furnished an orange/brown oil (5.12 g).[48]

^{1}H NMR ($CDCl_3$, 300 MHz) δ 0.12 (s, 6H), 0.94 (s, 9H), 4.84 (s, 2H), 7.82 (d, J = 8.1 Hz, 1H), 7.94 (d, J = 8.1 Hz, 1H), 8.72 (s, 1H), 10.06 (s, 1H). ^{13}C NMR ($CDCl_3$, 75.5 MHz) δ –5.4 (q), 18.2 (s), 25.8 (q), 62.4 (t), 121,9 (d), 134.4 (d), 141.7 (s), 148.0 (d), 151.8 (s), 193.1 (d). HRMS calcd for $C_{13}H_{21}NO_2Si$ 251.134, found 251.133.

5-(3-{[*tert*-Butyl(dimethyl)silyl]oxy}propyl)-2-pyridinecarbaldehyde (30)

Starting from **8** (9.90 g, 30.0 mmol) and following Method A as described for **29**, the product was obtained as a light brown oil (6.03 g, 72%) after purification by flash column chromatography over silica using a gradient of hexane/diethyl ether (9:1 to 3:1).[49] R_f = 0.25 (SiO_2, hexane/diethyl ether = 9:1).

^{1}H NMR ($CDCl_3$, 300 MHz) δ 0.04 (s, 6H), 0.89 (s, 9H), 1.85 (m, 2H), 2.79 (t, J = 7.9 Hz, 2H), 3.62 (t, J = 6.0 Hz, 2H), 7.68 (dd, J = 7.7, 1.5 Hz, 1H), 7.88 (d, J = 7.7 Hz, 1H), 8.61 (d, J = 1.5 Hz, 1H), 10.04 (s, 1H). ^{13}C NMR ($CDCl_3$, 75.5 MHz) δ –5.5 (q), 18.2 (s), 25.8 (q), 29.4 (t), 33.5 (t), 61.5 (t), 121.4 (d), 136.7 (d), 142.8 (s), 150.5 (d), 150.9 (s), 193.0 (d). MS CI $[M+H]^+$ calcd for $C_{15}H_{26}NO_2Si$ m/z 280.2, found 280.3.[46]

[5-({[*tert*-butyl(dimethyl)silyl]oxy}methyl)-2-pyridinyl]methanol (31)

To a solution of **29** (5.87 g, 23.3 mmol) in methanol (90 mL) at 0°C was slowly added $NaBH_4$ (0.44 g, 12 mmol, 0.5 equiv). The reaction mixture was allowed to warm to room temperature and after 30 min dilute HCl (2 M) was added until pH 7, followed by a saturated aqueous Na_2CO_3 solution (20 mL). The solvent was evaporated and the residue was extracted with

diethyl ether (3x30 mL). The organic layer was washed with brine (40 mL), dried over Na_2SO_4, and concentrated by rotary evaporation to yield **31** as a light yellow oil (5.73 g, 97%). The crude product was used without any further purification.
^{1}H NMR ($CDCl_3$, 300 MHz) δ 0.09 (s, 6H), 0.92 (s, 9H), 3.93 (br.s, 1H), 4.74 (s, 4H), 7.21 (d, J = 8.1 Hz, 1H), 7.64 (d, J = 8.1 Hz, 1Hz), 8.48 (s, 1H). ^{13}C NMR ($CDCl_3$, 75.5 MHz) δ –5.3 (q), 18.3 (s), 25.8 (q), 62.5 (t), 64.1 (t), 120.2 (d), 134.9 (s), 135.3 (d), 146.5 (d), 158.1 (s). HRMS calcd for $C_{13}H_{23}NO_2Si$ 253.150, found 253.149.

[5-(3-{[*tert*-Butyl(dimethyl)silyl]oxy}propyl)-2-pyridinyl]methanol (32)
The same procedure was used as described for **31**. Starting from **30** (3.91 g, 14.0 mmol) the product was obtained as a light brown oil (3.91 g, 99%). R_f = 0.20 (SiO_2, hexane/ethyl acetate = 3:1).
^{1}H NMR ($CDCl_3$, 300 MHz) δ 0.04 (s, 6H), 0.89 (s, 9H), 1.80 (m, 2H), 2.68 (t, J = 7.9 Hz, 2H), 3.47 (br.s, 1H), 3.61 (t, J = 6.0 Hz, 2H), 4.71 (s, 2H), 7.15 (d, J = 8.1 Hz, 1H), 7.50 (dd, J = 8.1, 1.8 Hz, 1H), 8.37 (s, 1H). ^{13}C NMR ($CDCl_3$, 75.5 MHz) δ –5.4 (q), 18.2 (s), 25.9 (q), 28.8 (t), 34.0 (t), 61.8 (t), 64.1 (t), 120.3 (d), 136.1 (s), 136.8 (d), 148.5 (d), 156.8 (s). MS CI $[M+H]^+$ calcd for $C_{15}H_{28}NO_2Si$ m/z 282.2, found 282.3.[46]

5-({[*tert*-Butyl(dimethyl)silyl]oxy}methyl)-2-(chloromethyl)pyridine (5)
To a solution of **31** (5.98 g, 23.6 mmol) and TEA (6.6 mL, 47 mmol, 2 equiv) in dry CH_2Cl_2 (100 mL) at 0°C under a nitrogen atmosphere was slowly added $SOCl_2$ (2.6 mL, 35 mmol, 1.5 equiv). The reaction mixture was allowed to warm to room temperature and stirred overnight. Saturated aqueous $NaHCO_3$ solution (100 mL) was added. After separation the aqueous layer was extracted with CH_2Cl_2 (3x40 mL). The combined organic layers were washed with brine (40 mL), dried over Na_2SO_4, and the solvent was evaporated by rotary evaporation. The product was obtained as a dark red/brown oil (6.08 g, 95%). The crude product was purified over alumina using hexane/ethyl acetate/TEA (200:9:1) as the eluent to provide pure **5** (4.24 g, 66%). R_f = 0.32 (Al_2O_3, hexane/diethyl ether = 9:1).
^{1}H NMR ($CDCl_3$, 300 MHz) δ 0.10 (s, 6H), 0.93 (s, 9H), 4.66 (s, 2H), 4.75 (s, 2H), 7.43 (d, J = 8.1 Hz, 1H), 7.69 (dd, J = 8.1, 2.2 Hz, 1H), 8.51 (d, J = 2.2 Hz, 1H). ^{13}C NMR ($CDCl_3$, 75.5 MHz) δ –5.4 (q), 18.2 (s), 25.8 (q), 47.5 (t), 62.5 (t), 120.7 (d), 134.5 (s), 134.6 (d), 147.3 (d), 160.5 (s). HRMS calcd for $C_{13}H_{22}ClNOSi$ 271.116, found 271.118.

5-(3-{[*tert*-Butyl(dimethyl)silyl]oxy}propyl)-2-(chloromethyl)pyridine (6)
The same procedure was used as described for **5**. Starting from **32** (3.91 g, 14.0 mmol) flash column chromatography over alumina using a gradient of hexane/diethyl ether (9:1 to 5:1) afforded **6** as a light brown oil (3.14 g, 75%). R_f = 0.31 (SiO_2, hexane/diethyl ether = 9:1).
^{1}H NMR ($CDCl_3$, 300 MHz) δ 0.04 (s, 6H), 0.89 (s, 9H), 1.81 (m, 2H), 2.69 (t, J = 7.9 Hz, 2H), 3.62 (t, J = 6.0 Hz, 2H), 4.64 (s, 2H), 7.36 (d, J = 7.9 Hz, 1H), 7.53 (dd, J = 7.9, 2.0 Hz, 1H), 8.41 (d, J = 2.0 Hz, 1H). ^{13}C NMR ($CDCl_3$, 75.5 MHz) δ –5.4 (q), 18.2 (s), 25.8 (q), 28.8 (t), 33.8 (t), 46.6 (t), 61.7 (t), 122.3 (d), 136.9 (d), 136.9 (s), 149.6 (d), 153.9 (s). MS CI $[M+H]^+$ calcd for $C_{15}H_{27}ClNOSi$ m/z 300.2, found 300.5.

Bis[5-({[*tert*-butyl(dimethyl)silyl]oxy}methyl)-2-pyridinyl]methanone (33)[45]

To a solution of **7** (6.36 g, 21.0 mmol) in dry THF (250 mL) at –80°C was added *n*-BuLi (36.0 mL, 22.5 mmol, 1.07 equiv) under a nitrogen atmosphere. After 40 min at –80°C a solution of **29** (5.29 g, 21.0 mmol) in dry THF (50 mL) was added to the red reaction mixture. The blue/purple reaction mixture was stirred at –70°C for 1 h, and then allowed to warm to room temperature. Brine (100mL) and diethyl ether (50 mL) were added and the layers were separated. The aqueous layer was extracted with diethyl ether (2x50 mL). The combined organic layers were washed with brine (50 mL), dried over Na_2SO_4, and concentrated by rotary evaporation to yield an orange/brown oil. This residue was then dissolved in chloroform (130 mL). Activated MnO_2 (4.4 g, 43 mmol) was added and the suspension was heated under reflux. At 1 h intervals 13.2 g MnO_2 was added in portions of 4.4 g. The reaction mixture was refluxed overnight. After evaporation of the solvent the residue was filtered through Celite and washed with diethyl ether. The filtrate was dried over Na_2SO_4 and concentrated by rotary evaporation to yield a brown solid (8.97 g, 90%).[47] The crude product was purified over silica using hexane/ethyl acetate (5:1) as the eluent (7.76 g, 78%). R_f = 0.40 (SiO_2, hexane/ethyl acetate = 3:1).

^{1}H NMR ($CDCl_3$, 300 MHz) δ 0.12 (s, 12H), 0.94 (s, 18H), 4.84 (s, 4H), 7.84 (d, J = 8.1 Hz, 2H), 8.08 (d, J = 8.1 Hz, 2H), 8.69 (s, 2H). ^{13}C NMR ($CDCl_3$, 75.5 MHz) δ –5.4 (q), 18.2 (s), 25.8 (q), 62.4 (t), 124.9 (d), 134.0 (d), 139.8 (s), 147.0 (d), 153.2 (s), 192.5 (s). HRMS calcd for $C_{25}H_{40}N_2O_3Si_2$ 472.258, found 472.258.

Bis[5-(3-{[*tert*-butyl(dimethyl)silyl]oxy}propyl)-2-pyridinyl]methanone (34)

The same procedure was used as described for **33**. Starting from **8** (5.11 g, 15.4 mmol) and **30** (4.47 g, 16.0 mmol) ketone **34** was obtained as a light brown solid (6.49 g, 80%) after flash column chromatography over silica using hexane/ethyl acetate (6:1) as the eluent. R_f = 0.42 (SiO_2, hexane/ethyl acetate = 3:1).

^{1}H NMR ($CDCl_3$, 300 MHz) δ 0.05 (s, 12H), 0.90 (s, 18H), 1.85 (m, 4H), 2.78 (t, J = 7.9 Hz, 4H), 3.65 (t, J = 6.0 Hz, 4H), 7.68 (dd, J = 8.1, 1.5 Hz, 2H), 8.02 (d, J = 8.1 Hz, 2H), 8.58 (d, J = 1.5 Hz, 2H). ^{13}C NMR ($CDCl_3$, 50.3 MHz) δ –5.4 (q), 18.2 (s), 25.8 (q), 29.2 (t), 33.6 (t), 61.7 (t), 125.1 (d), 136.4 (d), 140.9 (s), 149.4 (d), 152.2 (s), 192.5 (s). HRMS calcd for $C_{29}H_{48}N_2O_3Si_2$ 528.320, found 528.321.

Bis[5-({[*tert*-butyl(dimethyl)silyl]oxy}methyl)-2-pyridinyl]methanone oxime (35)

A mixture of hydroxylammonium chloride (2.60 g, 37.4 mmol, 2 equiv) and TEA (7.8 mL, 56 mmol, 3 equiv) in ethanol (50 mL) was stirred at room temperature for 0.5 h. The salts were removed by filtration and the filtrate was added to **33** (8.84 g, 18.7 mmol). After heating under reflux for 1 h the solvent was removed by rotary evaporation, and the residue was extracted with ethyl acetate (2x50 mL). The organic layer was washed with brine (25 mL), dried over Na_2SO_4, and concentrated to give a brown oil that solidified on standing (7.51 g, 83%). The crude product was recrystallised from ethanol/water to yield analytically pure **35** as white plates.

mp 106.3–107.4°C. ^{1}H NMR ($CDCl_3$, 300 MHz) δ 0.11 (s, 6H), 0.12 (s, 6H), 0.93 (s, 9H), 0.94 (s, 9H), 4.81 (s, 4H), 7.64 (d, J = 8.4 Hz, 1H), 7.75 (dd, J = 8.1, 2.0 Hz, 1H), 7.80 (dd, J = 8.4, 2.0 Hz, 2H), 8.55 (s, 1H), 8.59 (s, 1H). ^{13}C NMR ($CDCl_3$, 75.5 MHz) δ –5.4 (q), 5.3 (q),

18.3 (s), 25.8 (q), 25.9 (q), 62.3 (t), 62.6 (t), 123.8 (d), 124.7 (d), 134.9 (d), 135.2 (d), 136.6 (s), 138.4 (s), 143.6 (d), 146.5 (d), 150.0 (s), 150.1 (s), 153.5 (s). HRMS calcd for $C_{25}H_{41}N_3O_3Si_2$ 487.269, found 487.268. Anal. calcd for $C_{25}H_{41}N_3O_3Si_2$: C 61.56; H 8.47; N 8.61. Found: C 61.48; H 8.58; N 8.50.

Bis[5-(3-{[*tert*-butyl(dimethyl)silyl]oxy}propyl)-2-pyridinyl]methanone oxime (36)

The same procedure was used as described for **35**. Starting from **34** (1.12 g, 2.06 mmol) the product was obtained as a brown oil that solidified on standing (1.06 g, 93%). The crude product was recrystallised from ethanol/water to yield analytically pure **36** as white plates.

mp 110.1–110.4°C. ^{1}H NMR ($CDCl_3$, 300 MHz) δ 0.05 (s, 12H), 0.90 (s, 18H), 1.85 (m, 4H), 2.76 (m, 4H), 3.64 (m, 4H), 7.57 (d, J = 8.1 Hz, 1H), 7.62 (dd, J = 8.1, 2.0 Hz, 1H), 7.67 (dd, J = 8.1, 2.0 Hz, 1H), 7.74 (d, J = 8.1 Hz, 1H), 8.44 (d, J = 2.0 Hz, 1H), 8.47 (d, J = 2.0 Hz, 1H). ^{13}C NMR ($CDCl_3$, 50.3 MHz) δ –5.3 (q), 18.2 (s), 25.9 (q), 29.0 (t), 29.2 (t), 33.7 (t), 33.9 (t), 61.5 (t), 61.8 (t), 123.9 (d), 124.8 (d), 137.1 (d), 137.5 (s), 137.6 (d), 139.4 (s), 145.7 (d), 148.6 (d), 150.1 (s), 152.2 (s). HRMS calcd for $C_{29}H_{49}N_3O_3Si_2$ 543.331, found 543.333. Anal. calcd for $C_{29}H_{49}N_3O_3Si_2$: C 64.04; H 9.08; N 7.73. Found: C 63.97; H 9.03; N 7.70.

Bis[5-({[*tert*-butyl(dimethyl)silyl]oxy}methyl)-2-pyridinyl]methylamine (3)

A mixture of **35** (2.00 g, 4.10 mmol) and NH_4OAc (0.42 g, 5.5 mmol, 1.3 equiv) in ethanol (25 mL) and NH_4OH (15 mL, 25% v/v) was heated under reflux. Zinc powder (1.34 g, 20.5 mmol, 5 equiv) was added in portions through the condenser at 15 min intervals over 2 h. After refluxing for an additional hour the reaction mixture was cooled to room temperature and concentrated NaOH was added until pH~12 was reached. After filtration through Celite and washing with diethyl ether the layers were separated. The aqueous layer was extracted with diethyl ether (2x15 mL). The organic phase was washed with brine (15 mL), dried over Na_2SO_4, and concentrated *in vacuo* to yield a green/brown viscous oil (1.91 g, 99%).

^{1}H NMR ($CDCl_3$, 300 MHz) δ 0.06 (s, 12H), 0.90 (s, 18H), 2.34 (br.s, 2H), 4.70 (s, 4H), 5.31 (s, 1H), 7.33 (d, J = 8.1 Hz, 2H), 7.58 (dd, J = 8.1, 2.2 Hz, 2H), 8.48 (d, J = 2.2 Hz, 2H). ^{13}C NMR ($CDCl_3$, 75.5 MHz) δ –5.4 (q), 18.3 (s), 25.8 (q), 61.8 (d), 62.5 (t), 121.3 (d), 134.7 (d), 135.0 (s), 147.2 (d), 161.5 (s). MS CI $[M+H]^+$ calcd for $C_{25}H_{44}N_3O_2Si_2$ m/z 474.3, found 474.0.[46]

Bis[5-(3-{[*tert*-butyl(dimethyl)silyl]oxy}propyl)-2-pyridinyl]methylamine (4)

Prepared following the procedure as described for **3**, starting from **36** (1.42 g, 2.61 mmol) amine **4** was obtained as a green/brown viscous oil (1.34 g, 97%).

^{1}H NMR ($CDCl_3$, 300 MHz) δ 0.02 (s, 12H), 0.87 (s, 18H), 1.77 (m, 4H), 2.73 (br.s, 2H), 2.63 (t, J = 7.7 Hz, 4H), 3.60 (t, J = 6.2 Hz, 4H), 5.26 (s, 1H), 7.26 (d, J = 7.9 Hz, 2H), 7.43 (dd, J = 7.9, 2.0 Hz, 2H), 8.38 (d, J = 2.0 Hz, 2H). ^{13}C NMR ($CDCl_3$, 50.3 MHz) δ –5.5 (q), 18.0 (s), 25.7 (q), 28.6 (t), 33.8 (t), 61.4 (d), 61.6 (t), 121.1 (d), 135.5 (s), 136.5 (d), 149.0 (d), 160.0 (s). HRMS calcd for $C_{29}H_{51}N_3O_2Si_2$ 529.352, found 529.350.

***N*-{Bis[5-({[*tert*-butyl(dimethyl)silyl]oxy}methyl)-2-pyridinyl]methyl}-*N*,*N*-bis{[5-({[*tert*-butyl(dimethyl)silyl]oxy}methyl)-2-pyridinyl]methyl}amine (1)**

A mixture of **3** (0.21 g, 0.44 mmol), **5** (0.36 g, 1.3 mmol, 3 equiv), and Cs_2CO_3 (0.44 g, 1.4 mmol, 3 equiv) in dry acetonitrile (30 mL) was heated under reflux under a nitrogen atmosphere for 60 h. The reaction mixture was filtered through Celite, washed with diethyl ether, and concentrated *in vacuo*. Purification by flash chromatography over alumina using a gradient of hexane/ethyl acetate/TEA (20:9:1 to 0:9:1) afforded **1** as a brown viscous oil (0.23 g, 56%).

^{1}H NMR ($CDCl_3$, 300 MHz) δ 0.08 (s, 24H), 0.91 (s, 36H), 3.92 (s, 4H), 4.69 (s, 4H), 4.70 (s, 4H), 5.30 (2, 1H), 7.61 (m, 8H), 8.43 (s, 2H), 8.49 (s, 2H). ^{13}C NMR ($CDCl_3$, 75.5 MHz) δ –5.4 (q), –5.4 (q), 18.2 (s), 25.8 (q), 56.6 (t), 62.6 (t), 62.6 (t), 71.0 (d), 122.3 (d), 123.4 (d), 134.1 (d), 134.4 (d), 134.5 (s), 134.7 (s), 147.0 (d), 147.2 (d), 158.6 (s), 158.7 (s). ESI-MS $[M+H]^+$ calcd for $C_{51}H_{86}N_5O_4Si_4$ *m/z* 944.8, found 944.6.

***N*-{Bis[5-(3-{[*tert*-butyl(dimethyl)silyl]oxy}propyl)-2-pyridinyl]methyl}-*N*,*N*-bis{[5-(3-{[*tert*-butyl(dimethyl)silyl]oxy}propyl)-2-pyridinyl]methyl}amine (2)**

Following the procedure for **1**, starting from **4** (0.58 g, 1.1 mmol) and **6** (0.98 g, 3.3 mmol, 3 equiv) the product was obtained as a brown viscous oil (0.55 g, 48%).

^{1}H NMR ($CDCl_3$, 300 MHz) δ 0.02 (s, 24H), 0.87 (s, 36H), 1.77 (m, 8H), 2.61 (m, 8H), 3.60 (m, 8H), 3.87 (s, 4H), 5.24 (s, 1H), 7.41 (dd, J = 7.9, 2.0 Hz, 2H), 7.46 (dd, J = 7.9, 2.0 Hz, 2H), 7.51 (d, J = 7.9 Hz, 2H), 7.59 (d, J = 7.9 Hz, 2H), 8.30 (d, J = 2.0 Hz, 2H), 8.37 (d, J = 2.0 Hz, 2H). ^{13}C NMR ($CDCl_3$, 75.5 MHz) δ –5.5 (q), 18.0 (s), 25.7 (q), 28.6 (t), 28.7 (t), 33.7 (t), 33.9 (t), 56.7 (t), 61.7 (t), 61.8 (t), 71.2 (d), 122.3 (d), 123.3 (d), 135.0 (s), 135.2 (s), 135.9 (d), 136.0 (d), 148.8 (d), 149.1 (d), 157.2 (s), 157.5 (s). ESI-MS $[M+H]^+$ calcd for $C_{59}H_{102}N_5O_4Si_4$ *m/z* 1056.7, found 1056.9.

{6-[({Bis[5-(hydroxymethyl)-2-pyridinyl]methyl}{[5-(hydroxymethyl)-2-pyridinyl]methyl}amino)methyl]-3-pyridinyl}methanol (43)

Dilute HCl (2 mL, 1 M) was added to a solution of **1** (0.22 g, 0.23 mmol) in ethanol (10 mL). After 0.5 h the reaction mixture was extracted with diethyl ether (3x5 mL). The aqueous layer was neutralised with solid Na_2CO_3 and lyophilised or azeotropically removed with ethanol. The residue was taken up in dry ethanol, and after filtration and evaporation of the solvent **43** was obtained as a viscous brown, hygroscopic oil (0.12 g, 100%).

^{1}H NMR (CD_3OD, 300 MHz) δ 3.86 (s, 4H), 4.58 (s, 4H), 4.91 (s, 4H), 5.32 (s, 1H), 7.39 (d, J = 8.1 Hz, 2H), 7.63 (d, J = 8.1 Hz, 4H), 7.73 (d, J = 8.1 Hz, 1H), 7.74 (d, J = 8.1 Hz, 1H), 8.38 (s, 2H), 8.49 (s, 2H). ^{13}C NMR (CD_3OD, 75.5 MHz) δ 58.3 (t), 62.3 (t), 62.4 (t), 74.3 (d), 124.6 (d), 125.3 (d), 137.0 (d), 137.0 (d), 137.1 (s), 137.7 (s), 148.7 (d), 149.3 (d), 158.8 (s), 159.4 (s). ESI-MS $[M+H]^+$ calcd for $C_{27}H_{30}N_5O_4$ *m/z* 488.2, found 488.0.

3-(6-{(Bis{[5-(3-hydroxypropyl)-2-pyridinyl]methyl}amino)[5-(3-hydroxypropyl)-2-pyridinyl]methyl}-3-pyridinyl)-1-propanol (44)

The same procedure was used as described for **43**. Starting from **2** (0.30 g, 0.28 mmol) **44** was obtained as a viscous brown, hygroscopic oil (0.16 g, 95%).

^{1}H NMR (CD_3OD, 300 MHz) δ 1.78 (m, 8H), 2.65 (m, 8H), 3.55 (m, 8H), 3.85 (s, 4H), 5.24 (s, 1H), 7.44 (d, J = 8.1 Hz, 2H), 7.54 (dd, J = 8.1, 1.8 Hz, 2H), 7.61 (s, 2H), 7.62 (s, 2H), 8.22 (d, J = 1.8 Hz, 2H), 8.33 (s, 2H). ^{13}C NMR (CD_3OD, 50.3 MHz) δ 29.7 (t), 34.9 (t), 35.0 (t), 58.4 (t), 61.8 (t), 74.2 (d), 124.4 (d), 125.3 (d), 137.6 (s), 138.2 (s), 138.3 (d), 149.5 (d), 150.1 (d), 157.7 (s), 158.3 (s). MS CI $[M+H]^+$ calcd for $C_{35}H_{46}N_5O_4$ m/z 600.3, found 600.6.

Attempted methylation at the doubly benzylic position in 1 to furnish 48

To **1** (160 mg, 0.17 mmol) in dry THF (2 mL) at –80°C was added *n*-BuLi (120 µL, 0.19 mmol, 1.1 equiv). The solution changed from brown to red. After 15 min at –80°C TMEDA (30 µL, 0.20 mmol, 1.2 equiv) was added, followed by MeI (16 µL, 0.26 mmol, 1.5 equiv) after stirring at this temperature for 15 min. After 1 h at –80°C the reaction mixture was allowed to warm to –40°C over 30 min. A sample was taken, quenched with MeOH/water and analysed by ESI-MS to reveal only $[M+H]^+$, $[M+Li]^+$, and a trace of $[M+Na]^+$ of the starting material. No product (**48**) was present. The reaction mixture was cooled again to –80°C, MeI (20 µL) was added, and the mixture was allowed to warm to room temperature overnight. Again, **48** could not be detected by mass analysis, not even after stirring at room temperature for another 24 h. After workup pure starting material (160 mg) was recovered.

[5-({[*tert*-Butyl(dimethyl)silyl]oxy}methyl)-2-pyridinyl](2-pyridinyl)methanone (49)

To isopropylmagnesium chloride (11 mL, 22 mmol, 2 M in THF) was added **7** (6.04 g, 20 mmol). When no more heat was evolved, THF (15 mL) was added and the solution stirred at room temperature for 1 h. A solution of 2-cyanopyridine (2.10 g, 20 mmol) in THF (20mL) was added and after 1 h the reaction mixture was poured into a saturated aqueous NH_4Cl solution. Diethyl ether was added and after phase separation the aqueous layer was extracted with diethyl ether (3x10 mL). The organic layer was washed with brine (15 mL), dried over Na_2SO_4, and concentrated in vacuo to yield a brown oil (6.83 g).[50] The crude product was purified by flash chromatography over silica using a gradient of hexane/diethyl ether (1:1 to 1:4) to afford **49** as a yellow viscous oil (3.46 g, 63%).

^{1}H NMR ($CDCl_3$, 300 MHz) δ 0.11 (s, 6H), 0.93 (s, 9H), 4.84 (s, 2H), 7.46 (m, 1H), 7.87 (m, 2H), 8.08 (m, 2H), 8.69 (s, 1H), 8.74 (d, J = 4.8 Hz, 1H). ^{13}C NMR ($CDCl_3$, 75.5 MHz) δ –5.5 (q), 18.1 (s), 25.7 (q), 62.4 (t), 124.9 (d), 125.1 (d), 126.2 (d), 134.0 (d), 136.6 (d), 139.9 (s), 147.0 (d), 149.0 (d), 152.8 (s), 154.4 (s) 192.7 (s). HRMS calcd for $C_{18}H_{24}N_2O_2Si$ 328.161, found 328.158.

[5-({[*tert*-Butyl(dimethyl)silyl]oxy}methyl)-2-pyridinyl](2-pyridinyl)methanone oxime (50)

The same procedure was used as described for **35**. Starting from **49** (0.54 g, 1.6 mmol) the product was obtained as a light brown oil (0.55 g, 100%). The crude product was purified by flash chromatography over silica using diethyl ether as the eluent to yield **50** as a viscous colourless oil (0.45 g, 82%).

^{1}H NMR ($CDCl_3$, 300 MHz) δ 0.12 (s, 6H), 0.94 (s, 9H), 4.76 (s, 2H), 7.30 (m, 1H), 7.56 (d, J = 8.1 Hz, 1H), 7.75 (m, 3H), 8.55 (m, 2H). ^{13}C NMR ($CDCl_3$, 75.5 MHz) δ –5.5 (q), 18.2 (s), 25.7 (q), 62.3 (t), 123.8 (d), 124.7 (d), 126.2 (d), 134.9 (d), 136.6 (d), 139.5 (s), 147.0 (d), 149.0 (d), 150.1 (s), 151.4 (s) 153.9 (s). HRMS calcd for $C_{18}H_{25}N_3O_2Si$ 343.172, found 343.172.

Benzyl 3-pyridinylmethyl sulphide (54a)

$SOCl_2$ (0.16 mL, 2.2 mmol) was slowly added to **52** (0.22 g, 2.0 mmol) in dry CH_2Cl_2 (5 mL) at 0°C. To the formed **53a**·HCl was added a solution of benzyl mercaptan (0.24 mL, 2.0 mmol) in dilute NaOH (8 mL, 1M). The yellow reaction mixture was allowed to warm to room temperature and stirred for 4 h. The phases were separated and the aqueous layer was extracted with CH_2Cl_2 (2x5 mL). The organic layer was washed with brine (10 mL), dried over Na_2SO_4, and concentrated *in vacuo* to yield a yellow liquid (0.42 g, 99%). R_f = 0.50 (Al_2O_3, hexane/ethyl acetate = 3:1).

^{1}H NMR ($CDCl_3$, 300 MHz) δ 3.56 (s, 2H), 3.60 (s, 2H), 7.28 (m, 6H), 7.62 (dd, J = 5.9, 1.8 Hz, 1H), 8.48 (m, 2H). MS CI $[M+H]^+$ calcd for $C_{13}H_{14}NS$ m/z 216.1, found 216.2.

4-Methylphenyl 3-pyridinylmethyl sulphide (54b)

The same procedure was used as described for **54a**, using *p*-thiocresol (0.25 g, 2.0 mmol) to afford **54b** as a light brown oil (0.38 g, 90%).

^{1}H NMR ($CDCl_3$, 200 MHz) δ 2.30 (s, 3H), 4.01 (s, 2H), 7.13 (m, 5H), 7.55 (m, 1H), 8.39 (d, J = 1.9 Hz, 1H), 8.45 (m, 1H). MS CI $[M+H]^+$ calcd for $C_{13}H_{14}NSO_2$ m/z 216.1, found 216.1.

Ethyl 2-[(3-pyridinylmethyl)sulphanyl]acetate (56)[51]

3-(Chloromethyl)pyridine hydrochloride (**53a**) was prepared as described for **54a**, and then isolated by filtration. A warm solution of **53a** (0.33 g, 2.0 mmol) in absolute ethanol (10 mL) was added to a refluxing solution of thiourea (0.17 g, 2.2 mmol) in absolute ethanol (10 mL). After heating for 2.5 h the reaction mixture was allowed to cool to room temperature. The product was precipitated by the addition of dry diethyl ether to give **55** as white solid (0.41 g, 86%).

^{1}H NMR (D_2O, 300 MHz) δ 4.52 (s, 2H), 7.96 (m, 1H), 8.56 (d, J = 8.1 Hz, 1H), 8.65 (d, J = 5.9 Hz, 1H), 8.77 (s, 1H). ^{13}C NMR (D_2O, 50.3 MHz) δ 29.9 (t), 126.0 (d), 134.4 (s), 139.3 (d), 139.5 (d), 145.6 (d). MS EI $[M]^{+\cdot}$ calcd for $C_7H_9N_3S$ m/z 167.1, found 167.2.

Under a nitrogen atmosphere concentrated NaOH (0.31 mL) was added dropwise to a solution of **55** (0.23 g, 0.95 mmol) in water (1 mL). After heating at 50°C for 15 min ethyl bromoacetate (0.11 mL, 0.95 mmol) in CH_2Cl_2 (3 mL) and a catalytic amount of tetrabutylammonium bromide were added. After 18 h the phases were separated and the aqueous layer was extracted with CH_2Cl_2 (3x3 mL). The organic layer was washed with brine and dried over Na_2SO_4. Evaporation of the solvent afforded **56** as a brown oil (0.19 g, 95%).

^{1}H NMR ($CDCl_3$, 200 MHz) δ 1.28 (t, J = 7.2, 3H), 3.04 (s, 2H), 3.82 (s, 2H), 4.16 (q, J = 7.2 Hz, 2H), 7.25 (m, 1H), 7.69 (m, 1H), 8.52 (s, 1H), 8.56 (s, 1H). ^{13}C NMR ($CDCl_3$, 75.5 MHz) δ 13.9 (q), 32.0 (t), 33.1 (t), 61.2 (t), 123.3 (d), 132.9 (s), 136.4 (d), 148.4 (d), 150.0 (d), 169.8 (s). MS CI $[M+H]^+$ calcd for $C_{10}H_{14}NSO_2$ m/z 212.1, found 212.1.

Methyl *N*-acetylcysteine (57)

$SOCl_2$ (1.0 mL, 14 mmol) was slowly added to absolute methanol (40 mL) at –20°C. After 15 min a solution of *N*-acetylcysteine (2.01 g, 12.3 mmol) in absolute methanol (10 mL) was added dropwise. When the addition was complete, the reaction mixture was allowed to warm to room temperature. After 2.5 h the solvent was evaporated and the residue triturated with ethyl acetate. After removal of the solvent the product was obtained as a white solid (1.33 g, 61%).

^{1}H NMR ($CDCl_3$, 300 MHz) δ 1.33 (t, J = 9.0 Hz, 1H), 2.06 (s, 3H), 3.00 (m, 2H), 3.78 (s, 3H),

4.88 (m, 1H), 6.40 (br.s, 1H). ^{13}C NMR ($CDCl_3$, 75.5 MHz) δ 23.1 (q), 26.8 (t), 52.8 (q), 53.5 (d), 169.9 (s), 170.6 (s). HRMS calcd for $C_6H_{11}NO_3S$ 177.046, found 177.045.

Ethyl 2-(3-pyridinylmethoxy)acetate (58a)

To a stirred suspension of NaH (2.25 g, 56 mmol) in dry DMF (35 mL) was slowly added **52** (5.46 g, 50 mmol). After stirring at room temperature for 40 min the reaction mixture was cooled to 0°C. Ethyl bromoacetate (5.9 mL, 53 mmol) was added neat and the mixture was stirred for 18 h at room temperature. Ethyl acetate was added and the solution was washed with water (5x20 mL), brine (20 mL), and dried over Na_2SO_4. Evaporation of the solvent yielded the product as a brown oil (7.45 g, 76%).

^{1}H NMR ($CDCl_3$, 300 MHz) δ 1.28 (t, J = 7.0 Hz, 3H), 4.11 (s, 2H), 4.23 (t, J = 7.0 Hz, 2H), 4.64 (s, 2H), 7.29 (m, 1H), 7.74 (d, J = 7.7 Hz, 1H), 8.55 (d, J = 1.5 Hz, 1H), 8.59 (s, 1H). ^{13}C NMR ($CDCl_3$, 50.3 MHz) δ 13.9 (q), 60.9 (t), 67.4 (t), 70.7 (t), 124.6 (d), 135.7 (d), 138.8 (s), 148.4 (d), 148.5 (d), 169.8 (s). MS CI $[M+H]^+$ calcd for $C_{10}H_{14}NO_3$ *m/z* 196.1, found 196.2.

4-Methoxybenzyl 3-pyridinylmethyl ether (58b)

The same procedure was used as described for **58a**, using *p*-methoxybenzyl bromide[52] to afford **58b** as a light brown oil (77%).

^{1}H NMR ($CDCl_3$, 200 MHz) δ 3.81 (s, 3H), 4.51 (s, 2H), 4.53 (s, 2H), 6.89 (d, J = 8.4 Hz, 2H), 7.27 (m, 1H), 7.29 (d, J = 8.4 Hz, 2H), 7.69 (m, 1H), 8.54 (d, J = 1.3 Hz, 1H), 8.56 (s, 1H). MS CI $[M+H]^+$ calcd for $C_{14}H_{16}NO_2$ *m/z* 230.1, found 230.2.

3-Pyridinylmethyl 2,2,2-trichloroethanimidoate (59)

To a stirred mixture of **52** (1.11 g, 10 mmol) and a catalytic amount of NaH in dry diethyl ether (25 mL) was slowly added trichloroacetonitrile (1.05 mL, 10 mmol). After 0.5 h a small amount of MeOH was added, the mixture was filtered through Celite and concentrated to dryness to provide **59** as a light brown liquid (2.35 g, 93%).

^{1}H NMR ($CDCl_3$, 300 MHz) δ 5.35 (s, 2H), 7.31 (dd, J = 7.7, 4.8 Hz, 1H), 7.76 (d, J = 7.7 Hz, 1H), 8.45 (s, 1H), 8.58 (dd, J = 4.8, 1.6 Hz, 1H), 8.68 (d, J = 1.6 Hz, 1H). MS CI $[M+H]^+$ calcd for $C_8H_8Cl_3N_2O$ *m/z* 253.0, found 253.1.

3-Pyridinylmethyl 2-(benzylsulphanyl)acetate (61a)

To a solution of **52** (0.55 g, 5.0 mmol) and TEA (0.77 mL, 5.5 mmol) in dry CH_2Cl_2 (10 mL) at 0°C was added dropwise a solution of chloroacetyl chloride (0.50 mL, 6.3 mmol) in dry CH_2Cl_2 (10 mL). After 1.5 h at room temperature the reaction mixture was washed with water (3x5 mL), brine (5 mL), and dried over Na_2SO_4. Evaporation of the solvent furnished the intermediate chloroacetic ester **60** as a brown oil.

^{1}H NMR ($CDCl_3$, 300 MHz) δ 4.09 (s, 2H), 5.22 (s, 2H), 7.31 (dd, J = 7.7, 4.8 Hz, 1H), 7.70 (d, J = 7.7 Hz, 1H), 8.61 (s, 1H), 8.63 (s, 1H).

To a solution of **60** in dry CH_2Cl_2 was added K_2CO_3 (0.75 g, 5.4 mmol) and benzyl mercaptan (0.64 mL, 5.4 mmol). After stirring overnight at room temperature the reaction mixture was washed with water (3x5 mL), brine (5 mL), and dried over Na_2SO_4. Evaporation of the solvent

yielded **61a** as a brown oil[53] that was purified by flash column chromatography over alumina using hexane/ethyl acetate (3:1) as the eluent (0.22 g, 16%).
^{1}H NMR ($CDCl_3$, 300 MHz) δ 3.09 (s, 2H), 3.77 (s, 2H), 5.14 (s, 2H), 7.27 (m, 7H), 7.69 (d, J = 7.7 Hz, 1H), 8.58 (d, J = 1.5 Hz, 1H), 8.62 (s, 1H). MS CI $[M+H]^+$ calcd for $C_{15}H_{16}NO_2S$ m/z 274.1, found 274.2.

Cysteine derivative 61b
Similar procedure as is described for **61a**, using methyl *N*-acetylcysteine (**57**) to afford **61b** as a light brown oil.
^{1}H NMR ($CDCl_3$, 300 MHz) δ 2.03 (s, 3H), 3.04 (m, 2H), 3.72 (s, 3H), 4.10 (s, 2H), 4.81 (m, 1H), 5.18 (s, 2H), 6.64 (br.d, 1H), 7.31 (m, 1H), 7.69 (m, 1H), 8.61 (m, 2H). MS CI $[M+H]^+$ calcd for $C_{14}H_{19}N_2O_5S$ m/z 327.1, found 327.3.

***N*-[(3-Pyridinemethoxy)carbonyl]valine methyl ester (66)**[54]
A solution of **52** (0.55 g, 5.0 mmol) and TEA (0.77 mL, 5.5 mmol) in dry CH_2Cl_2 (20 mL) was cooled to 0°C, and treated with *p*-nitrophenyl chloroformate (1.05 g, 5.0 mmol). The reaction mixture was stirred at 0°C for 1 h and then allowed to warm to room temperature for 2 h. Washing with saturated aqueous $NaHCO_3$ solution (2x20 mL) and brine (20 mL), drying over Na_2SO_4 and evaporation of the solvent yielded the carbonate as a yellow solid (1.36 g, 99%).
^{1}H NMR ($CDCl_3$, 300 MHz) δ 5.31 (s, 2H), 7.33 (m, 3H), 7.79 (m, 1H), 8.27 (m, 2H), 8.65 (dd, J = 4.8, 1.5 Hz, 1H), 8.71 (d, J = 1.5 Hz, 1H).
A mixture of the carbonate (1.08 g, 3.9 mmol), L-valine methyl ester (0.66 g, 3.9 mmol), and TEA (1.1 mL, 7.8 mmol, 2 equiv) was heated under reflux in $CHCl_3$ (25 mL) overnight. The reaction mixture was washed with saturated aqueous $NaHCO_3$ solution (3x10 mL), brine (10 mL), and dried over Na_2SO_4. Evaporation of the solvent yielded **66** as a yellow oil that solidified on standing. Flash column chromatography over alumina using a gradient of hexane/ethyl acetate (3:1 to 1:1) provided the product as a yellow solid (0.57 g, 54%).
^{1}H NMR ($CDCl_3$, 300 MHz) δ 0.86 (d, J = 7.0 Hz, 3H), 0.93 (d, J = 7.0 Hz, 3H), 2.14 (m, 1H), 3.71 (s, 3H), 4.26 (m, 1H), 5.10 (s, 2H), 5.40 (d, J = 8.8 Hz, 1H), 7.28 (dd, J = 7.7, 4.8 Hz, 1H), 7.68 (d, J = 7.7 Hz, 1H), 8.54 (d, J = 4.8 Hz, 1H), 8.59 (s, 1H). ^{13}C NMR ($CDCl_3$, 75.5 MHz) δ 17.3 (q), 18.7 (q), 30.9 (d), 51.8 (q), 59.0 (d), 64.0 (t), 123.2 (d), 131.9 (s), 135.7 (d), 149.0 (d), 155.8 (s), 172.3 (s). MS CI $[M+H]^+$ calcd for $C_{13}H_{19}N_2O_4$ m/z 267.1, found 267.4.

***N*-{Bis[5-(methoxymethyl)-2-pyridinyl]methyl}-*N*,*N*-bis{[5-(methoxymethyl)-2-pyridinyl]methyl}amine (67)**
To a stirred suspension of NaH (55 mg, 1.4 mmol, 8 equiv) in dry DMF (1 mL) at 0°C was added a solution of **43** (83 mg, 0.17 mmol) in dry DMF (1 mL). After 30 min MeI (85 µL, 1.4 mmol, 8 equiv) was added at 0°C. The reaction mixture was allowed to warm to room temperature and stirred for 2 h. Water was added and the mixture extracted with CH_2Cl_2 (5x3 mL). The organic layer was washed with water (2x2 mL) and brine (2 mL). After drying over Na_2SO_4 and evaporation of the solvent, the product was obtained as a red/brown oil (83 mg, 89%). Purification by flash column chromatography over alumina using hexane/ethyl acetate/TEA (10:18:2) yielded **67** as a light brown oil (37 mg, 40%).

^{1}H NMR ($CDCl_3$, 300 MHz) δ 3.33 (s, 12 H), 3.91 (s, 4H), 4.83 (s, 8H), 5.30 (s, 1H), 7.60 (s, 4H), 7.62 (s, 4H), 8.40 (s, 2H), 8.46 (s, 2H). ^{13}C NMR ($CDCl_3$, 75.5 MHz) δ 56.8 (t), 58.1 (q), 58.2 (q), 71.4 (d), 71.9 (t), 122.5 (d), 123.5 (d), 131.4 (s), 131.7 (s), 135.7 (d), 135.8 (d), 148.4 (d), 148.6 (d), 159.3 (s), 159.4 (s). ESI-MS $[M+H]^+$ calcd for $C_{31}H_{38}N_5O_4$ *m/z* 544.3, found 544.4.

_N_-{Bis[5-(3-methoxypropyl)-2-pyridinyl]methyl}-_N_,_N_-bis{[5-(3-methoxypropyl)-2-pyridinyl]methyl}amine (68)

The same procedure was used as described for **67**. Starting from **44** (0.30 g, 0.28 mmol) **68** was obtained as a brown oil (0.14 g, 85%). Purification by flash column chromatography over alumina using hexane/ethyl acetate/TEA (10:18:2) yielded the product as a light brown oil (80 mg, 49%).

^{1}H NMR ($CDCl_3$, 300 MHz) δ 1.82 (m, 8H), 2.61 (t, J = 7.0 Hz, 8H), 3.30 (s, 12H), 3.35 (m, 8H), 3.87 (s, 4H), 5.24 (s, 1H), 7.40 (dd, J = 8.0, 1.8 Hz, 2H), 7.45 (dd, J = 8.0, 1.8 Hz, 2H), 7.51 (d, J = 8.0 Hz, 2H), 7.59 (d, J = 8.0 Hz, 2H), 8.29 (d, J = 1.1 Hz, 2H), 8.36 (d, J = 1.5 Hz, 2H). ^{13}C NMR ($CDCl_3$, 75.5 MHz) δ 29.0 (t), 29.1 (t), 30.8 (t), 30.9 (t), 56.8 (t), 58.6 (q), 71.3 (d), 71.5 (t), 71.6 (t), 122.5 (d), 123.5 (d), 135.0 (s), 135.3 (s), 136.2 (d), 136.3 (d), 149.0 (d), 149.3 (d), 157.4 (s), 157.6 (s). ESI-MS $[M+H]^+$calcd for $C_{39}H_{54}N_5O_4$ *m/z* 656.4, found 656.3.

_N_-{Bis[5-(3-bromopropyl)-2-pyridinyl]methyl}-_N_,_N_-bis{[5-(3-bromopropyl)-2-pyridinyl]methyl}amine (73)

PPh_3Br_2 was freshly prepared by the addition of Br_2 (75 µL, 1.4 mmol, 4.7 equiv) to a stirred solution of Ph_3P (395 mg, 1.51 mmol, 5. equiv) in dry CH_2Cl_2 (1 mL) under a nitrogen atmosphere. To the resulting yellow suspension was added a solution of **2** (321 mg, 0.304 mmol) in dry CH_2Cl_2 (1 mL). The reaction mixture was stirred at room temperature until all the solids had disappeared (2 d), and extracted with 1 M HCl (5x2 mL). The aqueous layer was neutralised with solid $NaHCO_3$, and extracted with CH_2Cl_2 (6x2 mL). The organic layer was washed with brine (2 mL) and dried over Na_2SO_4. Evaporation of the solvent afforded **73** as a red oil (190 mg, 74%).

^{1}H NMR ($CDCl_3$, 300 MHz) δ 2.07 (t, J = 6.6 Hz, 8H), 2.67 (t, J = 6.6 Hz, 8H), 3.32 (m, 8H), 3.84 (s, 4H), 5.22 (s, 1H), 7.34–7.58 (m, 8H), 8.28 (s, 2H), 8.34 (s, 2H). ^{13}C NMR ($CDCl_3$, 75.5 MHz) δ 30.5 (s), 30.6 (s), 32.5 (s), 32.6 (s), 33.3 (s), 33.4 (s), 56.6 (s), 71.1 (d), 122.3 (d), 123.4 (d), 133.6 (s), 133.8 (s), 136.1 (d), 136.2 (d), 148.8 (d), 149.1 (d), 157.5 (s), 157.7 (s). ESI-MS $[M+H]^+$ calcd for $C_{35}H_{42}N_5Br_4$ *m/z* 848.0, found 848.0.

Tetracysteine N4Py derivative 74

Methyl *N*-acetylcysteine (114 mg, 0.64 mmol) was dissolved in nitrogen-purged DMF (1 mL) and titrated with a Cs_2CO_3 solution (~100 mg/mL) to pH 9 under a nitrogen atmosphere. A solution of **73** (53 mg, 0.062 mmol) in DMF (1 mL) was added and the reaction mixture was stirred at room temperature overnight. The solution was diluted with water (5 mL) and lyophilised. The brown residue was purified by preparative RP-HPLC with a gradient of 0.05 M ammonium acetate/MeCN (50:50) to 100% MeCN over 10 min. The product eluted at t_R = 7.2

min, was collected and lyophilised to yield a brown oil (9.5 mg, 12%).
^{1}H NMR ($CDCl_3$, 500 MHz) δ 1.88 (m, 8H), 2.04 (s, 12H), 2.55 (m, 8H), 2.68 (m, 8H), 3.00 (m, 8H), 3.78 (m, 12H), 3.90 (s, 4H), 4.83 (m, 4H), 5.28 (s, 1H), 6.39 (br.d, 4H), 7.47 (m, 8H), 8.35 (s, 2H), 8.41 (s, 2H). ESI-MS $[M+H]^+$ calcd for $C_{59}H_{82}N_9O_{12}S_4$ *m/z* 1236.5, found 1236.1.

Peptide complex 78
The procedure for **74** using the peptide sequence Ac–Cys–Gly–Leu–His–Glu–Leu–Leu–Lys–Gly–NH_2 was employed.[55] After stirring overnight the solution was diluted with 0.1% TFA in water and $Fe(ClO_4)_2$ (1.1 equiv) was added as a solution in MeCN. The orange/red solution was purified by semi-preparative RP-HPLC using a linear gradient of 20–40% solvent B over 10 min. The product eluted at $t_R = 8.6$ min, was collected, and lyophilised to yield a yellow/orange solid (2.1 mg, 18%).
MALDI calcd for $[\mathbf{78}-2(ClO_4)^- - (MeCN)]^{2+}$ *m/z* 4620.38 (monoisotopic), 4623.43 (average isotope composition), found 4619.2.

Peptide complex 79
The same procedure was used as described for **78**, employing the peptide sequence Ac–Cys–Gly–Gly–Gly–Gly–Asp–Tyr–Lys–Asp–Asp–Asp–Asp–Lys–NH_2.[56] The orange/red solution was purified by semi-preparative RP-HPLC using a linear gradient of 20–40% solvent B over 4 min, followed by 40–100% in 1 min. The product eluted at $t_R = 4.6$ min, was collected, and lyophilised to yield a yellow/orange solid.[57] For analytical RP-HPLC a linear gradient of 0–100% solvent B in solvent A was applied over 30 min. The product eluted at $t_R = 16.9$ min.
MALDI calcd for $[\mathbf{79}-2(ClO_4)^- - (MeCN)]^{2+}$ *m/z* 6121.3 (monoisotopic), 6125.1 (average isotope composition), found 6124.0.

3.10 References and notes

1. For an explanation of the abbreviations used, see Appendix 1 (p. 149).
2. Choma, C. T.; Schudde, E. P.; Kellogg, R. M.; Robillard, G. T.; Feringa, B. L. *J. Chem. Soc., Perkin Trans. 1* **1998**, 769–773.
3. Roelfes, J. G., In *Models for Non-Heme Iron Containing Oxidation Enzymes*, Ph. D. thesis, Groningen, 2000.
4. Ablard, J.; Decoret, C.; Cronenberger, L.; Pacheyo, H. *Bull. Soc. Chim. France* **1972**, 2466–2481.
5. (a) Boekelheide, V.; Linn, W. J. *J. Am. Chem. Soc.* **1954**, *76*, 1286–1291. (b) Hardegger, E.; Nikles, E. *Helv. Chim. Acta* **1957**, *249*, 2428–2433.
6. Langlois, Y.; Potier, P. *Tetrahedron* **1975**, *31*, 419–422.
7. Peterson, M. L. *J. Org. Chem.* **1960**, *25*, 565–569.
8. (a) Bailey, A. J.; Griffith, W. P.; Parkin, B. C. *J. Chem. Soc., Dalton Trans.* **1995**, 1833–1838. (b) Gresley, N. M.; Griffith, W. P.; Parkin, B. C.; White, A. J. P.; Williams, D. J. *J. Chem. Soc., Dalton Trans.* **1996**, 2039–2046.
9. Patent, Lonza AG, Gampel/Wallis (CH), EP 0084118 B1, **1982**.

10. (a) Lee, J.-K.; Velarde-Ortiz, R.; Guijarro, A.; Wurst, J. R.; Rieke, R. D. *J. Org. Chem.* **2000**, *65*, 5428–5430. (b) Rottländer, M.; Boymond, L.; Bérillon, L.; Leprêtre, A.; Varchi, G.; Avolio, S.; Laaziri, H.; Quéguiner, G.; Ricci, A.; Cahiez, G.; Knochel, P. *Chem. Eur. J.* **2000**, *6*, 767–770. (c) Boudier, A.; Bromm, L. O.; Lotz, M.; Knochel, P. *Angew. Chem. Int. Ed.* **2000**, *39*, 4414–4435. (d) Abarbri, M.; Thibonnet, J.; Bérillon, L.; Dehmel, F.; Rottländer, M.; Knochel, P. *J. Org. Chem.* **2000**, *65*, 4618–4634. (e) Dohle, W.; Kopp, F.; Cahiez, G.; Knochel, P. *Synlett* **2001**, 1901–1904. (f) Inoue, A.; Kitagawa, K.; Shinokubo, H.; Oshima, K. *J. Org. Chem.* **2001**, *66*, 4333–4339. (g) Jensen, A. E.; Dohle, W.; Sapountzis, I.; Lindsay, D. M.; Vu, V. A.; Knochel, P. *Synthesis* **2002**, 565–569.
11. See Chapter 4 for the divergent synthesis of a tetrafunctionalised N4Py derivative.
12. Windscheif, P.-M.; Vögtle, F. *Synthesis* **1994**, 87–92.
13. See Section 4.2 (p. 86) for more information on the regioselective lithiation of 2,5-dibromopyridine.
14. (a) Parham, W. E.; Piccirilli, R. M. *J. Org. Chem.* **1977**, *42*, 257–260. (b) Kondo, Y.; Shilai, M.; Uchiyama, M.; Sakamoto, T. *J. Chem. Soc., Perkin Trans.1* **1996**, 1781–1782.
15. (a) Bolm, C.; Ewald, M.; Felder, M.; Schlingloff, G. *Chem. Ber.* **1992**, *125*, 1169–1190. (b) Wang, X.; Rabbat, P.; O'Shea, P.; Tillyer, R.; Grabowski, E. J. J.; Reider, P. J. *Tetrahedron Lett.* **2000**, *41*, 4335–4338.
16. Adopted procedure from (a) Trécourt, F.; Breton, G.; Bonnet, V.; Mongin, F.; Marsais, F.; Quéguiner, G. *Tetrahedron Lett.* **1999**, *40*, 4339–4342. (b) Trécourt, F.; Breton, G.; Bonnet, V.; Mongin, F.; Marsais, F.; Quéguiner, G. *Tetrahedron* **2000**, *56*, 1349–1360.
17. Corey, E. J.; Venkateswarlu, A. *J. Am. Chem. Soc.* **1972**, *94*, 6190–6191.
18. Procedure adapted from Ellingboe, J. W.; Antane, M.; Nguyen, T. T.; Collini, M. D.; Antane, S.; Bender, R.; Hartupee, D.; White, V.; McCallum, J.; Park, C. H.; Russo, A.; Osler, M. B.; Wojdan, A.; Dinish, J.; Ho, D. M.; Bagli, J. F. *J. Med. Chem.* **1994**, *37*, 542–550.
19. Gaylord, N. G., In *Reduction with Complex Metal Hydrides*; Interscience: New York, 1956; pp. 90, 446.
20. Ethyl 3-(3-pyridinyl)propionate (**27**): MS CI $[M+H]^+$ calcd for $C_{10}H_{14}NO_2$ *m/z* 180.1, found 180.0.
21. Ethyl 3-(6-bromo-3-pyridinyl)propionate (**26**): ^{1}H NMR ($CDCl_3$, 300 MHz) δ 1.21 (t, J = 7.3 Hz, 3H), 2.60 (t, J = 7.3 Hz, 2H), 2.89 (t, J = 7.3 Hz, 2H), 4.10 (q, J = 7.3 Hz, 2H), 7.39 (s, 1H), 7.40 (s, 1H), 8.22 (s, 1H). ^{13}C NMR ($CDCl_3$, 75.5 MHz) δ 14.0 (q), 27.1 (t), 34.9 (t), 60.5 (t), 127.6 (d), 135.2 (s), 138.6 (d), 139.7 (s), 150.0 (d), 171.8 (s). HRMS calcd for $C_{10}H_{12}NO_2Br$ 257.005, found 257.007.
22. Ethyl 3-(3-piperidinyl)propionate (**28**): MS CI $[M+H]^+$ calcd for $C_{10}H_{20}NO_2$ *m/z* 186.1, found 186.0.
23. Niemers, E.; Hiltmann, R. *Synthesis* **1976**, 593–595.
24. **39**: ^{1}H NMR ($CDCl_3$, 300 MHz) δ 0.07 (s, 12H), 0.90 (s, 18H), 4.30 (s, 2H), 4.69 (s, 4H), 7.20 (d, J = 7.9 Hz, 2H), 7.54 (dd, J = 7.9, 1.8 Hz, 2H), 8.47 (d, J = 1.8 Hz, 2H). MS CI $[M+H]^+$ calcd for $C_{25}H_{45}N_2O_2Si_2$ *m/z* 459.3, found 459.1. **40**: MS CI $[M+H]^+$ calcd for $C_{29}H_{51}N_2O_2Si_2$ *m/z* 515.3, found 515.5. **41**: ^{1}H NMR ($CDCl_3$, 300 MHz) δ 0.07 (s, 6H),

0.90 (s, 9H), 2.56 (s, 3H), 4.70 (s, 2H), 7.11 (d, J = 8.1 Hz, 1H), 7.52 (d, J = 1.8 Hz, 1H), 8.42 (s, 1H). MS CI $[M+H]^+$ calcd for $C_{13}H_{24}NOSi$ m/z 238.2, found 238.1. **42**: MS CI $[M+H]^+$ calcd for $C_{15}H_{28}NOSi$ m/z 266.2, found 266.3.

25. Collington, E. W.; Meyers, A. I. *J. Org. Chem.* **1971**, *36*, 3044–3045.
26. (a) Appel, R. *Angew. Chem. Int. Ed. Engl.* **1975**, *14*, 801–811. (b) Anisuzzaman, A. K. M.; Whistler, R. L. *Carbohydr. Res.* **1978**, *61*, 511–518. (c) Slagle, J. D.; Huang, T. T. S.; Franzus, B. *J. Org. Chem.* **1981**, *46*, 3526–3530. (d) Falorni, M.; Lardicci, L. *J. Org. Chem.* **1986**, *51*, 5291–5294.
27. The molecular ion was observed at m/z 560.1 $[M+H]^+$ for the main isotope peak, which corresponded to the expected mass of 559.1 $[M]^+$, and the detected isotope distribution pattern matched the calculated arrangement.
28. (a) Mitsunobu, O.; Wada, M.; Sano, T. *J. Am. Chem. Soc.* **1972**, *94*, 679–680. (b) Mitsunobu, O. *Synthesis* **1981**, 1–28. (c) Hughes, D. L., In *Organic Reactions*; Paquette, L. A. *et al.*, Eds.; John Wiley: USA, 1992; Vol. 42. (d) For diphenyl 2-pyridinylphosphine in Mitsunobu reactions, see Kiankarimi, M.; Lowe, R.; McCarthy, J. R.; Whitten, J. P. *Tetrahedron Lett.* **1999**, *40*, 4497–4500. (e) For alkylthioether synthesis, see Falck, J. R.; Lai, J.-Y.; Cho, S.-D.; Yu, J. *Tetrahedron Lett.* **1999**, *40*, 2903–2906.
29. Brown, T. J.; Chapman, R. F.; Cook, D. C.; Hart, T. W.; McLay, I. M.; Jordan, R.; Mason, J. S.; Palfrey, M. N.; Walsh, R. J. A.; Withnall, N. T.; Aloup, J.-C.; Cavero, I.; Farge, D.; James, C.; Mondot, S. *J. Med. Chem.* **1992**, *35*, 3613–3624.
30. Paquette, L. A., In *Encyclopedia of Reagents for Organic Synthesis*; John Wiley: UK, 1995; Vol. 7, and references cited therein.
31. Compounds **59a** and **59c–d** are commercially available. Compound **59b** was prepared analogous to a procedure by Suginome, H.; Yamada, S. *Tetrahedron* **1987**, *43*, 3371–3386. For **59e**, see Ehrenstorfer-Schaefers, E.-M.; Steiner, N.; Altman, J. *Z. Naturforsch. B* **1990**, *45*, 817–827.
32. **61c**: ^{1}H NMR ($CDCl_3$, 200 MHz) δ 5.04 (d, J = 9.9 Hz, 1H), 6.08 (d, J = 16.6 Hz, 1H), 6.87 (dd, J = 16.6, 9.9 Hz, 1H), 7.75 (m, 2H), 7.87 (m, 2H). ^{13}C NMR ($CDCl_3$, 50.3 MHz) δ 104.4 (t), 123.6 (d), 123.7 (d), 131.5 (s), 134.4 (d), 166.4 (s). MS EI $[M]^{+\cdot}$ calcd for $C_{10}H_7NO_2$ m/z 173.0, found 173.1. **61d**: ^{1}H NMR ($CDCl_3$, 300 MHz) δ 4.28 (d, J = 5.5 Hz, 2H), 5.21 (m, 2H), 5.89 (m, 1H), 7.72 (m, 2H), 7.85 (m, 2H). ^{13}C NMR ($CDCl_3$, 75.5 MHz) δ 40.0 (t), 117.7 (t), 123.3 (d), 131.5 (d), 132.1 (s), 133.9 (d), 167.9 (s). HRMS calcd for $C_{11}H_9NO_2$ 187.063, found 187.062.
33. The synthesis of **67** was also attempted analogous to **65**. ESI-MS $[M+H]^+$ calcd for $C_{55}H_{58}N_5O_4$ m/z 848.4, found 848.3. No further experimental data was obtained due to an incomplete reaction: m/z 651.3 (trialkylation), m/z 440.2 (dialkylation).
34. Experimental conditions according to the synthesis of the tetramethoxy N4Py derivative **65**, and then quenched with ethyl bromoacetate. ESI-MS $[M+H]^+$ calcd for $C_{43}H_{54}N_5O_{12}$ m/z 832.4, found 832.4. No further experimental data was obtained due to an incomplete reaction: m/z 746.3 (trialkylation), 666.3 (dialkylation).
35. Aizpurua, J. M.; Cossio, F. P.; Palomo, C. *J. Org. Chem.* **1986**, *51*, 4941–4943.
36. J. G. Roelfes, unpublished results.

37. For the preparation of the hydrobromide, see Van der Made, A. W.; Nolte, R. J. M.; Drenth, W. *Recl. Trav. Chim. Pays-Bas* **1990**, *109*, 537–551.
38. See Appendix 2 (p. 151) for the structures and one-letter abbreviations of the α-amino acids.
39. (a) Or, Y. S.; Clark, R. F.; Luly, J. R. *J. Org. Chem.* **1991**, *56*, 3146–3149. (b) Brown, M. J.; Milano, P. D.; Lever, D. C.; Epstein, W. W.; Poulter, C. D. *J. Am. Chem. Soc.* **1991**, *113*, 3176–3177.
40. (a) Henkel, J. G.; Amato, G. S. *J. Med. Chem.* **1988**, *31*, 1279–1282. (b) Yang, C.-C.; Marlowe, C. K.; Kania, R. *J. Am. Chem. Soc.* **1991**, *113*, 3177–3178.
41. Perrey, D. A.; Uckun, F. M. *Tetrahedron Lett.* **2001**, *42*, 1859–1861.
42. Choma, C. T.; Kaestle, K.; Åkerfeldt, K. S.; Kim, R. M.; Groves, J. T.; DeGrado, W. F. *Tetrahedron Lett.* **1994**, *35*, 6191–6194.
43. Dijkstra, G.; Kruizinga, W. H.; Kellogg, R. M. *J. Org. Chem.* **1987**, *52*, 4230–4234.
44. (a) Atherton, E.; Sheppard, R. C., In *Solid Phase Peptide Synthesis: A Practical Approach*; IRL Press, Oxford Press: UK, 1989. (b) Fields, G. B., In *Methods in Enzymology*, *Solid-Phase Peptide Synthesis*; Academic Press: USA, 1997; Vol. 289. (c) Aimoto, S. *Curr. Org. Chem*. **2001**, *5*, 45–87.
45. Isopropylmagnesium chloride in THF at room temperature can be used as an alternative procedure to obtain similar yields. The conditions were adopted from ref. 16.
46. Exact mass (HRMS) was not possible.
47. The crude product contained about 10–15% of the quenched 2-lithio starting material, 3-({[*tert*-butyl(dimethyl)silyl]oxy}methyl)pyridine: ^{1}H NMR ($CDCl_3$, 200 MHz) δ 0.09 (s, 6H), 0.92 (s, 9H), 4.69 (s, 2H), 7.28 (m, 1H), 7.72 (d, J = 7.7 Hz, 1H), 8.55 (d, J = 1.5 Hz, 1H), 8.58 (s, 1H).
48. The 'quenched' side-product observed when using Method A was not present according to ^{1}H NMR. A small excess of Grignard reagent is required to drive the bromine-magnesium exchange to completion. A distinct difference between the product obtained from the lithiation- or magnesium-bromine exchange reaction is its colour and smell, even after purification by column chromatography.
49. The crude product contained about 10–15% of the quenched 2-lithio starting material, 3-(3-{[*tert*-butyl(dimethyl)silyl]oxy}propyl)pyridine: ^{1}H NMR ($CDCl_3$, 300 MHz) δ 0.03 (s, 6H), 0.89 (s, 9H), 1.81 (m, 2H), 2.67 (t, J = 7.9 Hz, 2H), 3.61 (t, J = 6.0 Hz, 2H), 7.18 (dd, J = 7.7, 4.8 Hz, 1H), 7.49 (d, J = 7.7 Hz, 1H), 8.41 (d, J = 4.8 Hz, 1H), 8.44 (s, 1H). ^{13}C NMR ($CDCl_3$, 75.5 MHz) δ –5.5 (q), 18.2 (s), 25.8 (q), 29.0 (t), 33.8 (t), 61.7 (t), 123.1 (d), 135.7 (d), 137.3 (s), 147.0 (d), 149.8 (d). MS CI $[M+H]^+$ calcd for $C_{14}H_{26}NOSi$ *m/z* 252.2, found 252.3.
50. About 17% of the starting material **7** was still present due to an incomplete reaction.
51. Procedure adapted from Brown, T. J.; Chapman, R. F.; Cook, D. C.; Hart, T. W.; McLay, I. M. *J. Med. Chem.* **1992**, *35*, 3612–3624.
52. (a) Wang, X.; Cui, Y.; Pan, X.; Chen, Y. *Bull. Soc. Chim. Belg.* **1995**, *104*, 563–565. (b) Hung, D. T.; Nerenberg, J. B.; Schreiber, S. L. *J. Am. Chem. Soc.* **1996**, *118*, 11054–11080.

53. The crude product contained a substantial amount of the intermediate chloride compound according to ^{1}H NMR.
54. Procedure adapted from Kempf *et al. J. Med. Chem.* **1998**, *41*, 602–617.
55. Peptide was synthesised by dr. ir. J. A. W. Kruijtzer, Medicinal Chemistry, University Utrecht, The Netherlands.
56. Peptide was synthesised by dr. C. T. Choma, Rensselaer Polytechnic Institute, Troy, U.S.A.
57. No yield is reported due to a considerable loss of product during HPLC optimisation.

Chapter 4

Tetrabromo N4Py as a versatile building block for new non-haem metal catalysts

4.1 Convergent versus divergent ligand synthesis

In the previous chapter the synthesis of a tetrasubstituted N4Py ligand was described to which four peptide chains could be coupled via spacers at the periphery of the N4Py template.[1] The synthetic pathway that was designed required these spacers to be introduced into the building blocks at the very beginning. This stipulation will be a major drawback if at the end of the synthesis the prepared structure does not meet the requirements that were envisaged at the outset. The introduction of new alternative spacers can result in different problems that are encountered during the construction of the new target ligand. Also, once the ligand has been prepared to all intents and purposes, its function still needs to be established. This, however, is applicable to any chosen synthetic pathway. Therefore, flexibility in the developed synthetic route is a prerequisite for an efficient access to a range of derivatives.

The synthesis of the functional template for the construction of a peptide-tethered N4PyFe catalyst was therefore initiated using the 2,5-disubstituted pyridine compound **1** (Chapter 3). The spacer, which provided the functionality to which the peptides would be attached in the final ligand system, was subsequently introduced at the 5-position of the pyridine ring to furnish compounds of the general structure **2** (Scheme 4.1). Depending on the electrophile used for the introduction of the spacer, a variety of linkers can thereby in principle be obtained. The bromide at the 2-position was used as a reactive site to construct the core of N4Py ligand **4**. Such a long and convergent synthesis is not ideally suited for a convenient modification of the attached linkers in **4**.

From a practical point of view it would be more beneficial to initially construct the ligand scaffold, and subsequently introduce the required functionalities. If these functionalities were then found to be unsatisfactory, modifications can be made to the ligand without having to start from the initial building blocks. Such a divergent synthetic pathway would thus facilitate the versatile preparation of alternative ligand systems. This accessibility and flexibility to a new

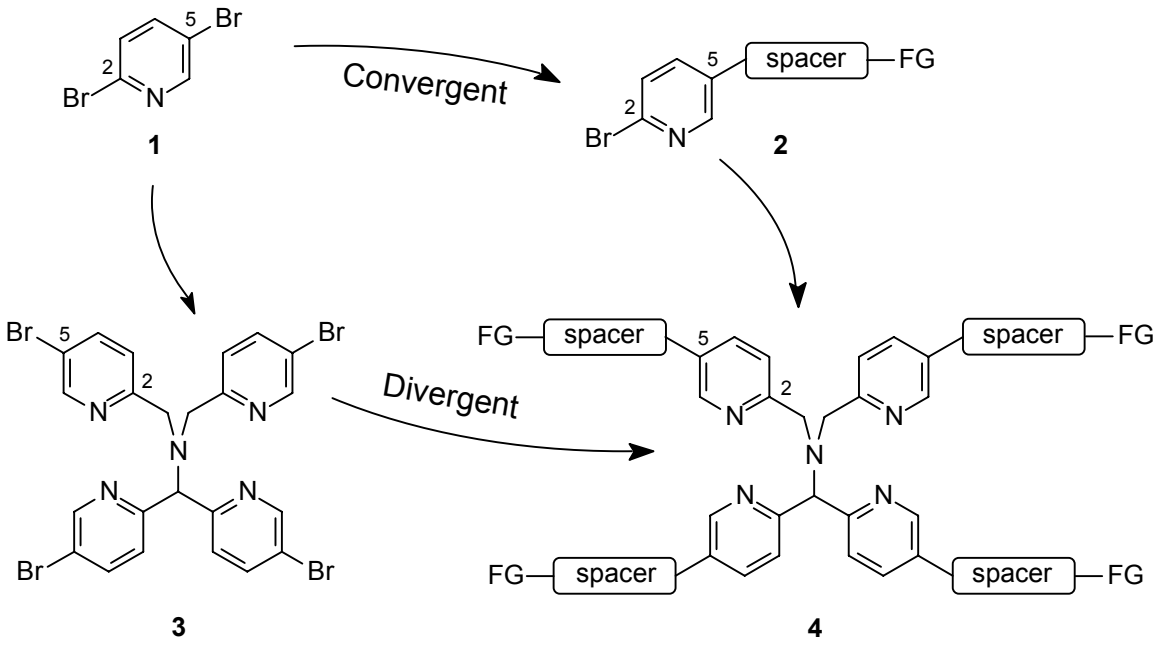

Scheme 4.1. Convergent vs. divergent synthesis of tetrasubstituted N4Py ligands starting from **1** (FG = functional group).

range of N4Py templates could prove to be essential if the ligand needed to be redesigned or improved to enable the incorporation of the N4PyFe catalyst into a four-helix bundle (see Chapter 1). In addition, the possibility of simultaneously introducing a range of functionalities creates an opportunity to potentially tune the oxidation behaviour of the corresponding iron(II) complexes.

A potential N4Py framework that could enable a variety of derivatives to be generated via a divergent synthesis is presented in Scheme 4.1 and Scheme 4.2 as the tetrabromide N4Py derivative **3**. Again starting from 2,5-dibromopyridine (**1**), tetrabromo N4Py (**3**) can be prepared by initially using the bromide at the 2-position of the pyridine ring to construct the core of the N4Py scaffold. This in turn leaves the remaining bromide at the 5-position of **1** in **3** available for further functionalisation. However, in order to establish the construction of **3** a regioselective lithiation at the 2-position of **1** is an absolute prerequisite (*vide infra*). The bromide functionalities in **3** can, in principle, be employed as sites for metal-catalysed cross coupling methodologies or bromide-metal exchange reactions. A variety of substituents can be introduced into the N4Py scaffold depending on the reagents employed, which in addition could provide interesting features for novel oxidising catalysts, either directly or through subsequent functional group interconversions (Scheme 4.2).

4.2 Selective lithiation of dibromopyridines

Several procedures have been reported for a regioselective bromine-metal exchange reaction with 2,5-dibromopyridine (**1**). Although the 2-position in **1** is more electron-deficient than the 5-position, the mono-metalation occurs preferentially at the 5-position upon lithiation with *n*-butyllithium (*n*-BuLi) at –100°C in THF (Scheme 4.3).[2,3] A more selective bromine-lithium exchange,[4,5] however, is obtained using diethyl ether as the solvent at –80°C.[6] The low

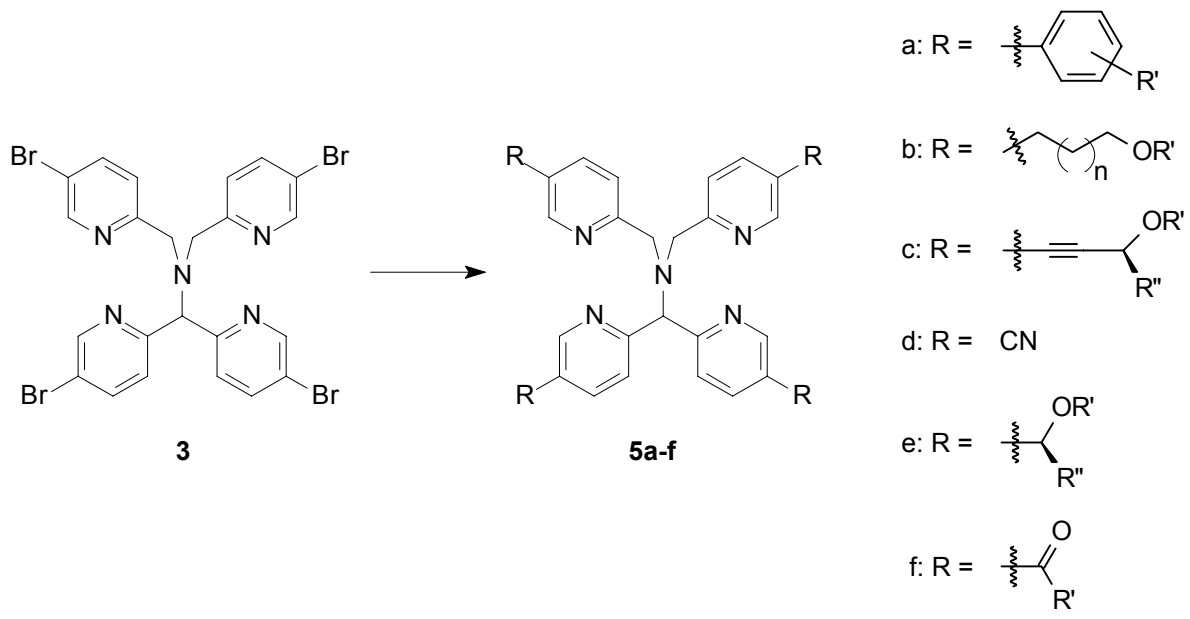

Scheme 4.2. A selection of potential N4Py ligands that can be envisaged from tetrabromo N4Py (**3**) by, for instance, cross coupling (**5a–d**) or lithiation reactions (**5e–f**).

temperature is not only required to achieve a high regioselectivity, but it also helps to prevent alkylation of the lithiopyridine by the *n*-butyl bromide that is formed during the reaction.[2]

This halogen-metal exchange, which is a rapid and complete process, is controlled by thermodynamic rather than kinetic factors.[2] This has been demonstrated by the resistance of 3-lithiopyridine towards a lithium exchange with 2-bromopyridine.[2] In contrast, 2-lithiopyridine undergoes a rapid exchange with 3-bromopyridine to produce 2-bromopyridine and 3-lithiopyridine.

The selective mono-lithiation has also been described for 2,6-dibromopyridine at –78°C in THF[7] or in dichloromethane.[8] Although *n*-BuLi can react with dichloromethane, it is stable in this solvent in the absence of ethereal solvents.[8] In addition, the potential dilithiation of 2,6-dibromopyridine is reduced substantially in dichloromethane compared to diethyl ether or THF as a solvent under identical conditions.[8]

Surprisingly, when dichloromethane is used as the solvent for the mono-lithiation of **1**, the regioselectivity is completely reversed (Scheme 4.3). Wang *et al.* found that in non-co-ordinating solvents like toluene and dichloromethane at low concentrations, lithiation occurred preferentially at the 2-position rather than the 5-position of **1** (approximately in an 85 : 15 ratio).[4] A small excess of *n*-BuLi (1.2 equiv) was required to accomplish a complete mono-lithiation of **1**. Via the preparation of a 2-pyridinyltellurium derivative of **1**, Sakamoto and co-workers were also able to lithiate selectively at the 2-position.[3] This procedure is inferior to that of Wang *et al.*, as a separate reaction step is involved that proceeds only in a moderate yield of 55%.

A bromine-magnesium exchange on dibromopyridines can also be carried out regioselectively. Although a direct oxidative addition of magnesium to a halopyridine is known to be problematic,[9] a pyridine Grignard reagent can be obtained via a halogen-metal exchange with an alkylmagnesium halide in THF.[10,11] In contrast to the cryogenic conditions for the

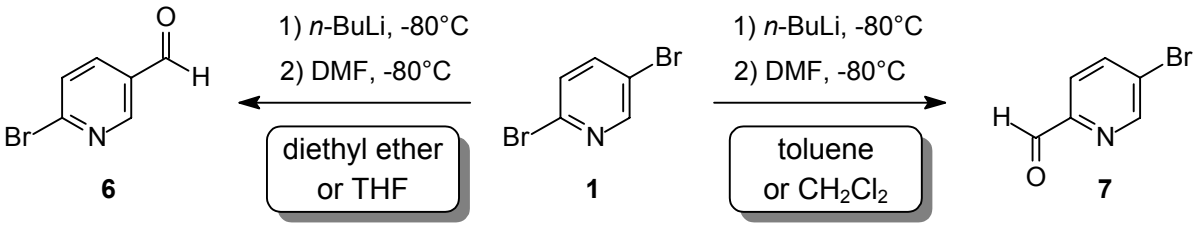

Scheme 4.3. Solvent-dependent regioselective lithiation of **1**.

halogen-lithium exchange, this Grignard interconversion can often be performed at room temperature. Queguiner and co-workers have exploited this procedure to prepare various functionalised pyridines from mono- and dibromopyridines using isopropylmagnesium chloride.[10] The regioselectivity and yields were found to be comparable to the related bromine-lithium exchange reactions. Triethylamine (TEA) was sometimes added to the reaction mixture prior to the addition of the electrophile in order to increase the reactivity of the Grignard reagent, and thereby enhance the reaction. It was found that a slight excess of isopropylmagnesium chloride is required to achieve a complete bromine-magnesium exchange with bromopyridines,[12] an observation also reported by other researchers.[3]

An interesting alternative is the lithium tributyl magnesate complex that mediates a highly selective mono-metalation of aryl and heteroaryl dibromides, even in the presence of excess metalation reagent.[13] This *n*-Bu_3MgLi complex, which can be readily prepared from *n*-BuMgCl and *n*-BuLi, enabled Iida *et al*. to perform the mono-formylation of 2,6-dibromopyridine on a twenty-five kilogram scale at only −10°C in toluene in an excellent yield of 91%. In a similar way the authors could obtain aldehyde **6** in a toluene/THF (1:1) mixture in 71% yield from **1**. Under these conditions, however, a lower regioselectivity was observed for the mono-lithiation of **1**.

In conclusion, the regioselectivity of the bromo-metal exchange in 2,5-dibromopyridine (**1**) can be directed by the choice of solvent. The reversed regioselectivity, reported by Wang *et al*.,[4] for the lithiation of **1** was a prerequisite to facilitate the synthesis of tetrabromo N4Py (**3**) and at the same time creates the opportunity to prepare tetrasubstituted N4Py derivative by functionalising the remaining bromides in **3**.

4.3 Synthesis of tetrabromo N4Py

The synthesis of tetrasubstituted N4Py derivatives is channelled through the preparation of the desired disubstituted bispyridinyl ketones. The corresponding bispyridinyl ketoximes and bispyridinyl amines are readily accessible and the required functionalised picolyl chlorides can be prepared from a wide range of starting materials.[14] The difficulty with the synthetic pathway outlined in the previous chapter is that two functionalised pyridines are linked via a carbon bridge that is put in place by a lithiation reaction. Under these conditions some functionalities of interest might not be stable, which would require the development of new synthetic procedures to accomplish this pyridine linkage. This might limit the general application of the established methodology.

With the realisation of a selective lithiation at the 2-position of 2,5-dibromopyridine (**1**) by Wang *et al*.,[4] a key transformation was accomplished that would enable the synthesis of bispyridinyl ketone **8** (Scheme 4.4). The remaining two bromine atoms in **8** will thus provide

sites for further functionalisation in the final N4Py derivative **3**. As depicted in Scheme 4.4, **1** was lithiated at the 2-position by *n*-BuLi in toluene at –80°C and quenched with *N*,*N*-dimethylformamide (DMF) to furnish 5-bromo-2-pyridinecarboxaldehyde (**7**) in 73% yield. The aldehyde **7** was found to be contaminated with its regio-isomer **6** (approximately 18% from **1**, 91% combined yield) due to an incomplete regioselectivity under these conditions. Unfortunately, aldehyde **7** could not be purified due to its instability.[15]

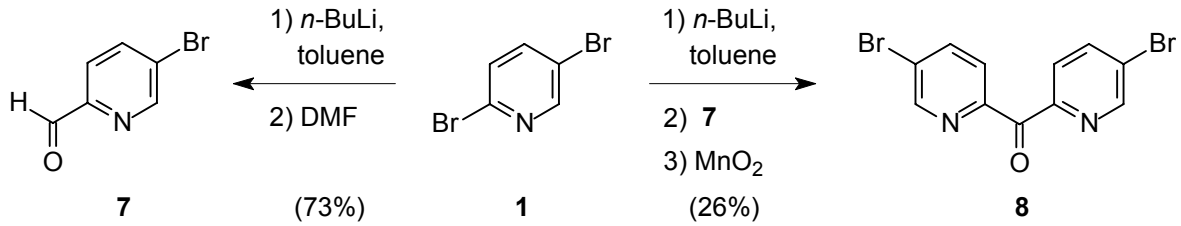

Scheme 4.4. Synthesis of aldehyde **7** from **1**, and its subsequent application in the preparation of ketone **8**.

In a subsequent step 2,5-dibromopyridine (**1**) was lithiated once more at the 2-position, as in the preparation of **7**, and now quenched with aldehyde **7** instead of DMF. The small amount of aldehyde **6** present in crude **7** and the incomplete regioselectivity of the lithiation reaction resulted in a mixture of products. However, after the oxidation of the bispyridinyl alcohol product by manganese dioxide, precipitation of the crude product from diethyl ether furnished pure bispyridinyl ketone **8**. An excess of *n*-BuLi was used to ensure a complete bromide-lithium exchange of **1**,[4] the unreacted lithiating reagent, therefore, must also have reacted with the aldehyde added, leading to a further reduction in the yield for the reaction. Therefore, the low yield of 26% cannot solely be attributed to the 'contaminated' aldehyde **7**.

The formation of ketone **8** was most effectively achieved by quenching *in situ* the prepared 5-bromo-2-lithiopyridine in toluene at –80°C with 0.5 equivalents of diethyl carbonate (Scheme 4.5).[16] Although the reaction conditions have not yet been optimised, bispyridinyl ketone **8** was isolated in a higher yield of 37%. Reducing the number of reaction steps was not only practical,

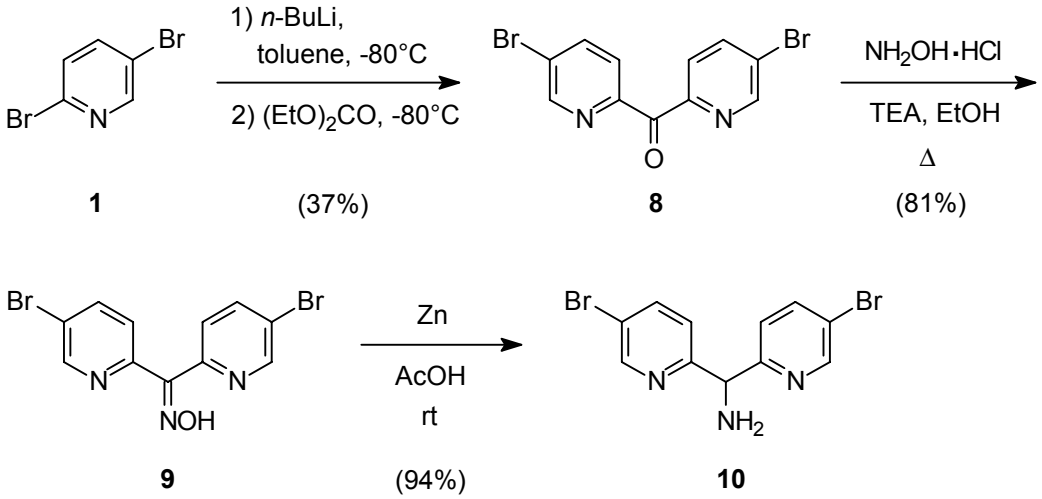

Scheme 4.5. Synthesis of bis(5-bromo-2-pyridinyl)methylamine (**10**).

but it also resulted in an increase in the yield of **8**. In order to optimise this reaction, the regioselectivity of the bromide-lithium exchange will have to be enhanced. As the efficiency of a halogen-lithium exchange is higher for an iodide than for a bromide, superior results can be expected by initially converting **1** into 5-bromo-2-iodopyridine.[17,18] Recent work from Sauvage and co-workers has indeed demonstrated that this preceding interconversion is accompanied by a complete regioselectivity in the lithiation step.[19]

Subsequent conversion of the ketone **8** into the bispyridinyl ketoxime proceeded smoothly in 81% yield in a reaction using hydroxylamine as its hydrochloride salt. The synthesis of bispyridinyl methylamine **10** was achieved by the highly efficient reduction of the ketoxime **9** using zinc in acetic acid at room temperature.

With the amine **10** in hand, the preparation of tetrabromo N4Py (**3**) was now within reach, as the synthesis of the required corresponding picolyl chloride **13** had already previously been achieved (Scheme 4.6).[20] Starting from 5-bromo-2-picoline[21] (**11**) the *N*-oxide **12** was obtained in 98% yield after oxidation by *meta*-chloroperoxybenzoic acid (mCPBA). Subsequent reaction of the *N*-oxide **12** with trifluoroacetic acid anhydride (TFAA), followed by the hydrolysis of the resulting acetate furnished 5-bromo-2-(hydroxymethyl)pyridine in 81% yield.[21b] Next, this picolyl alcohol was allowed to react with thionyl chloride to furnish **13** in 97% yield (overall yield of these two steps was 79%). The picolyl chloride **13** with its electron-withdrawing bromide was unexpectedly found to be remarkably stable,[22] as 2-picolyl chlorides are generally prone to self *N*-alkylation.

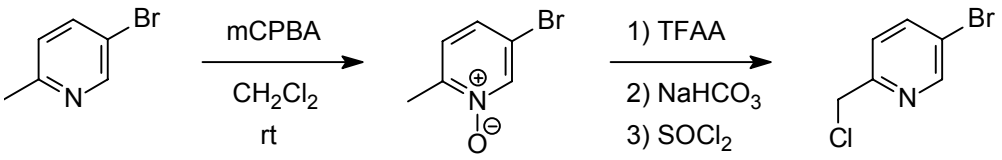

11 (98%) **12** (79%) **13**

Scheme 4.6. Synthesis of 5-bromo-2-picolyl chloride (**13**).

In an alternative procedure, picolyl chloride **12** can also be obtained from aldehyde **7** via the lithiation of 2,5-dibromopyridine (**1**) in toluene (Scheme 4.4), followed by a reduction of the aldehyde to the picolyl alcohol, which can then be converted into **12**. However, the incomplete regioselectivity under these conditions in the lithiation of **1** results in a mixture of aldehydes **6** and **7** (*vide supra*). These could not be separated by column chromatography, and continuation with this mixture would afford regio-isomers of picolyl chloride **12**, and thus lead to complications during the preparation of the N4Py ligand **3**. Therefore, the procedure outlined in Scheme 4.6 was undertaken, which allows full control over the position of the substituents.

Analogous to the previously described preparation of N4Py derivatives,[20,23] the dialkylation of amine **10** with two equivalents of picolyl chloride **13** in the presence of a base enabled the construction of tetrabromo N4Py (**3**) (Scheme 4.7). The first alkylation step proceeded rapidly in the presence of *N*,*N*-diisopropylethylamine (DIEA) or caesium carbonate, as is observed in the preparation of other N4Py derivatives as well. However, the rate of the second alkylation step was retarded substantially by the electron-withdrawing nature of the bromides in the reactants. This was generally observed for other picolyl chlorides with electron-withdrawing substituents.[24]

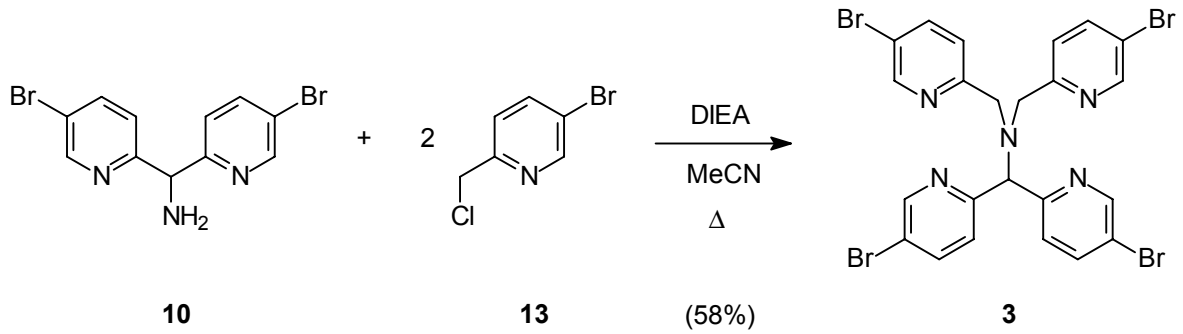

10 **13** (58%) **3**

Scheme 4.7. Synthesis of tetrabromo N4Py (**3**).

The best results were obtained by using a large excess of DIEA and a minimal amount of acetonitrile to dissolve the reactants. Under these conditions the required reaction time was reduced from a week to two days at reflux. Traces of mono-alkylated product could be removed simply by precipitation of **3** in diethyl ether after the removal of other minor contaminants by flash column chromatography. With a 58% yield in this final step the synthesis of tetrabromide N4Py (**3**) was now finally completed as verified by ^{1}H NMR, ^{13}C NMR, mass analysis, and elemental analysis.

4.4 Cross couplings reactions

It is not the purpose of this section to provide a complete overview of all available cross coupling methodologies. Instead, the discussion will be focussed on cross coupling reactions on halopyridine compounds, as the examined model reactions should serve as a possible means by which the tetrabromo N4Py (**3**) can be functionalised. The selected test reactions will hopefully provide a set of reaction conditions that will facilitate a flexible derivatisation of **3** by a number of cross coupling methodologies.

In recent years the Suzuki[25] and the Stille[26] cross coupling reactions have developed into commonly applied synthetic methodologies for the metal-catalysed C–C bond formation of biaryl compounds as an alternative to the Ullmann reaction.[27] Since the initial reports approximately two decades ago, many excellent examples of these cross coupling reactions have been presented that can tolerate a wide variety of functional groups.[28–30] Recently, the use of alkylboronic acids has been added to the long list of possible applications of the Suzuki reaction,[31] as well as the reaction of alkylboranes[32] with alkyl bromides in the formation of an alkyl-alkyl bond.[33] Other cross coupling methodologies have also been developed over the past few decades. The Sonogashira[34] reaction involves the palladium-catalysed reaction of, for instance, an aryl halide with a terminal acetylene in the formation of aryl acetylenes.[35] The Heck reaction[36] is the palladium-catalysed arylation of olefins by aryl halides.[37] Within this still developing field, the cross coupling methodology has established itself as one of the most actively studied topics in synthetic organic chemistry.[38]

The many variables in these cross coupling reactions need to be tuned in order to find an effective catalytic system. The combinations that can be varied involve the choice of the catalyst (or precursor), the catalyst loading, the solvent, and the addition of a supplementary base or ligand. The multitude of structural variations that can be introduced is enormous, bolstered by a continuously growing number of commercially available functionalised reagents. Also, many

newly developed synthetic procedures have been reported in the literature that, for instance, enable the use of the less reactive aryl chlorides[39] or alkylboronic acids[31] in Suzuki reactions, and a palladium-catalysed borylation of aryl halides and triflates.[40] Recently, the iridium-catalysed activation of an aromatic C–H bond was described, which allows the direct introduction of a boron moiety onto an arene, even in the presence of bromide or chloride functionalities.[41]

The metal-catalysed carbonylation,[18,42] allylation,[43] or arylation with arylzinc halides[43] of 2,5-dibromopyridine (**1**) occurs exclusively at the 2-position, indicating that this position in the pyridine ring is more reactive in metal-mediated coupling reactions.[43–45] The bromine atom at the 5-position, however, is quite capable of undergoing cross coupling reactions in the absence of other functional groups that are susceptible to oxidative addition.[43,46–48] Minor changes in the substrate and the palladium source can result in dramatic changes in the efficiency of the cross coupling reaction,[42b,49] as exemplified by a more efficient palladium-catalysed arylation of 3-bromopyridine with respect to 2-bromopyridine.[46b,e]

As already depicted in Scheme 4.2, the four bromides in the N4Py derivative **3** can in principle be functionalised by a number of coupling reagents. However, because these bromides are presented within a single molecule, a highly efficient coupling reaction at each site is a prerequisite for acquiring the product in a high overall yield. If the four reactions on **3** each proceed in a yield of 90%, the overall yield will only be 66%, and a yield of 80% per bromide site will result in a final yield of only 41%! More importantly, complete substitution at all four sites is imperative in order to reduce the amount of incompletely substituted N4Py structures. Furthermore, as the side-products from these incomplete reactions will be structurally similar compounds, these will be difficult to separate from the desired molecule.

4.4.1 The Suzuki reaction

The Suzuki, or Suzuki-Miyaura, reaction involves the palladium- or nickel-catalysed[50] cross coupling of an aryl, alkenyl, or *n*-alkylboronic acid or ester and an aryl halide or triflate (Scheme 4.8).[25,28] The ever growing list of applicable and commercially available organoboronic reagents, and its tolerance towards many functional groups, make the Suzuki reaction an effective and flexible procedure for creating aryl-aryl C–C bonds. Recently, palladium-catalysed methods have been reported by which pinacol arylboronates can be prepared from the corresponding aryl chlorides,[51] or even by activation of an aromatic C–H bond,[41] thus broadening the range of applicable substrates.

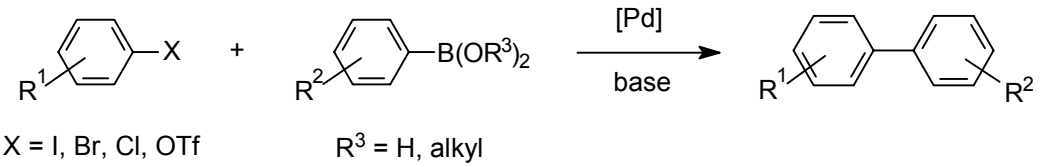

Scheme 4.8. The Suzuki reaction in the formation of biaryl compounds.

The most commonly employed palladium source is $Pd(PPh_3)_4$, a palladium(0) species that can be used directly for the catalytic cycle (Scheme 4.9). Other palladium(II) catalysts like $PdCl_2(PPh_3)_2$ or $Pd(OAc)_2$ are readily reduced to the active palladium(0) species by the addition

of base or phosphine ligands to form *in situ* the effective transient intermediate. Nowadays, even palladium[52] or nickel[53] on carbon can affect the formation of biaryl compounds from aryl chlorides.

According to the generally accepted mechanism of the Suzuki reaction,[28] the Pd^0 species is inserted into the aryl C–X bond via an oxidative addition step to generate the Pd^{II} intermediate I (Scheme 4.9). In this rate determining step the electronic effects of the aryl halide play an important role, as the relative reactivity of the halide and triflate substrates decreases in the order of I > OTf > Br > > Cl.[28] Furthermore, substrates bearing electron-withdrawing substituents are more reactive towards the oxidative addition than those with electron-donating groups.[48] In a subsequent 'transmetalation' step species I reacts with the organoboronic substrate to form the *trans*–σ–Pd^{II} complex II. Generally, a base is added to the reaction mixture to activate the boronic acid, presumably by creating an anionic boronic species. As the product of the cross coupling reaction can only be released via the cis-complex, intermediate II has to undergo an isomerisation step. The following reductive elimination of the *cis*-isomer III then affords the product and simultaneously regenerates the Pd^0 catalyst.

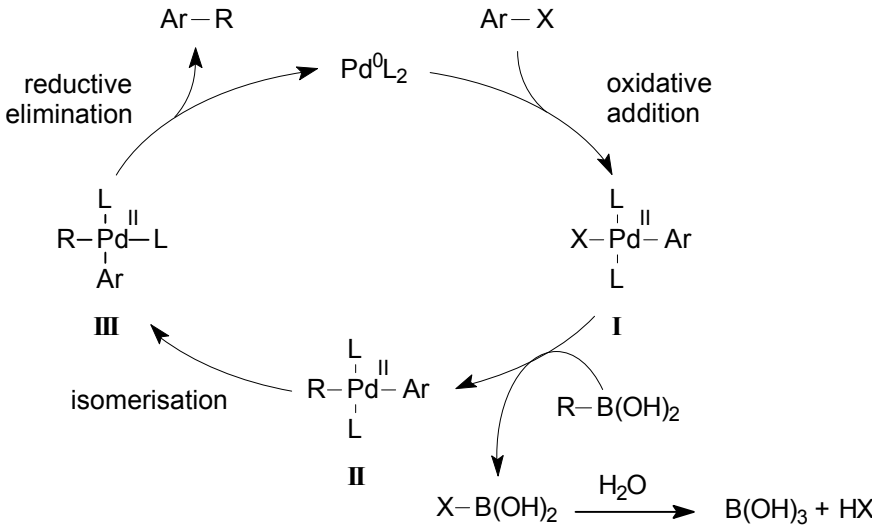

Scheme 4.9. The generally accepted mechanism for the Suzuki reaction.[28]

The substrates 3-bromopyridine (**14**) and 5-bromo-2-picoline (**11**) were selected as test reactions in order to find suitable conditions for the metal-catalysed cross coupling reactions on tetrabromo N4Py (**3**). These bromopyridines were employed in the palladium-catalysed Suzuki reaction with phenylboronic acid (**15**) and 3-amino-phenylboronic acid (**16**) in the presence of base (Scheme 4.10).[46] The boronic acid **16** was chosen to provide an amine functionality in the cross-coupled product that would allow the compound to be further derivatised by, for instance, an amide bond formation. When applied to the tetrabromide N4Py ligand **3**, this would provide an alternative means of coupling peptides to the N4Py scaffold.

The reaction of 3-bromopyridine (**14**) with **15** was initially catalysed by 5 mol% $Pd(PPh_3)_4$ in a refluxing mixture of acetonitrile and aqueous sodium carbonate to furnish the cross-coupled product **17**, after eighteen hours and subsequent purification, in 83% yield.[46e] Changing the solvent to benzene or toluene, or reducing the catalyst loading to 3 mol%, had no significant

effect.[54] In THF as the solvent the yield of the reaction was marginally increased to 87% when allowed to react overnight. Under identical conditions the corresponding Suzuki reaction of 3-bromopyridine (**14**) with **16** furnished the desired product **19** in 95% yield after purification.

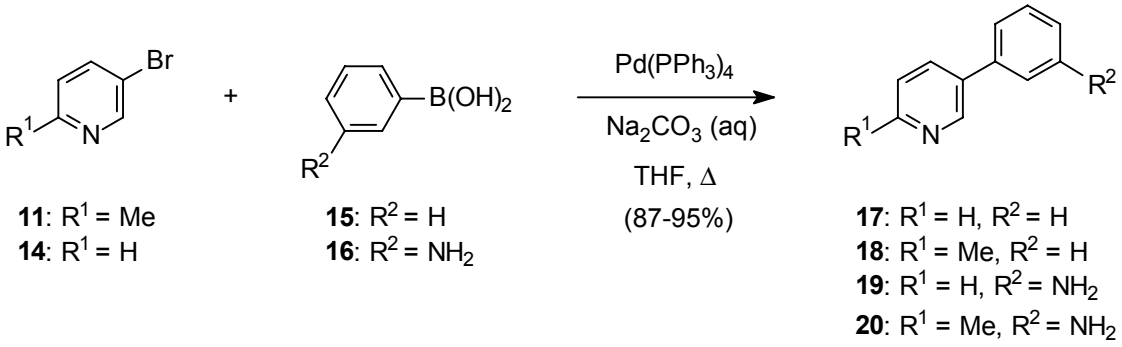

11: R^1 = Me
14: R^1 = H

15: R^2 = H
16: R^2 = NH_2

17: R^1 = H, R^2 = H
18: R^1 = Me, R^2 = H
19: R^1 = H, R^2 = NH_2
20: R^1 = Me, R^2 = NH_2

Scheme 4.10. The Suzuki reaction of bromopyridines **11** and **14**.

The tetrabromide N4Py ligand **3**, to which these cross couplings will ultimately be applied, is structurally quite different from 3-bromopyridine (**14**). In order to account for the alkyl substituents that constitute the core of ligand **3**, the efficiency of the Suzuki reaction was also examined using 5-bromo-2-picoline (**11**). Under conditions analogous to the preparation of **17**, the cross-coupled product **18** was isolated in an excellent yield of 95%. Similarly, the disubstituted pyridine derivative **20** was obtained in a 90% isolated yield from the reaction of **11** with **16**. Clearly, the substituents of the substrates employed have only a minor influence on the outcome of this Suzuki reaction, which in turn appears to be promising for their application to tetrabromo N4Py (**3**).

As an alternative procedure the boronic acid or ester moiety can in principle be introduced into the ligand system of **3** and subsequently employed in cross coupling reactions with various aryl halides or triflates. Procedures for an *in situ* palladium-catalysed halide displacement with a boronate ester prior to the Suzuki reaction have previously been reported.[40] This approach was tested on 2,5-dibromopyridine (**1**) and 3-bromopyridine (**14**) via their conversion into the boronate esters **21–23** after lithiation of the bromopyridines, followed by quenching the lithiated species with the corresponding boronate ester.[44,55–57] However, the subsequent $Pd(OAc)_2$-[40e] or $Pd(PPh_3)_4$-mediated reactions employing iodoanilines **24–26** were fruitless despite numerous attempts using refluxing mixtures of benzene and aqueous sodium carbonate or barium hydroxide.[54] The unsuccessful formation of the desired products **27–29** (Scheme 4.11) is presumably due to an ineffective formation of the intermediate boronates,[54] as related cross coupling reactions utilising **21** have been reported recently.[57]

The *in situ* hydroboration[45] of tetrahydropyranyl-protected allyl alcohol by 9-borabicyclo-[3.3.1]nonane (9-BBN) and the subsequent cross coupling with 3-bromopyridine mediated by $PdCl_2(PPh_3)_2$ was also attempted, but this reaction was not successful.[54] Presumably, the hydroboration of the alkene did not take place, which prevented the following Suzuki reaction. However, it can safely be assumed that under different reaction conditions this functionalisation of bromopyridines can be accomplished, as related procedures have been reported for the *in situ* hydroboration of terminal alkenyl compounds by 9-BBN, followed by the $Pd(PPh_3)_4$-catalysed Suzuki reaction of the resulting alkylborane with 3-bromopyridine.[58] Similarly, Reider

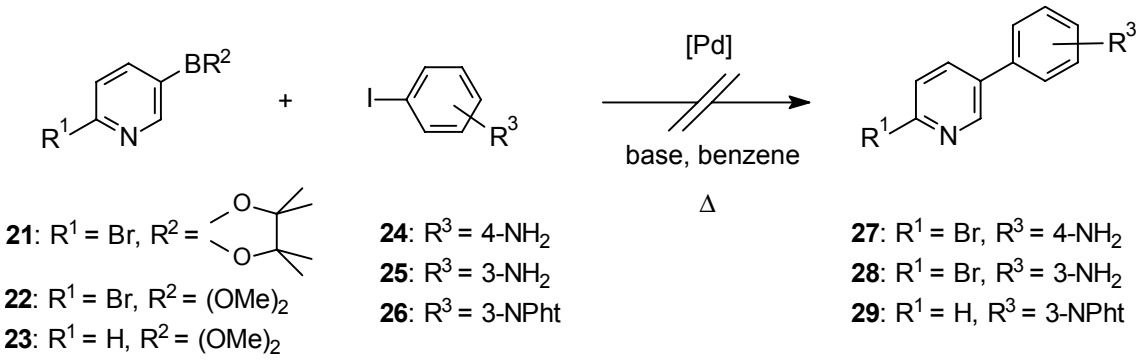

Scheme 4.11. Attempted synthesis of the 3-aryl pyridines **27–29** via the pyridinylboronic esters **21–23**.

and co-workers have successfully introduced two amine functionalities with a C3-spacer to 2,5-dibromopyridine by an efficient double Suzuki reaction via a 9-BBN-mediated hydroboration of a phthalimide-protected allyl amine.[59]

Other promising examples of successful Suzuki reactions have been described using organoboronic acids[6,60] or potassium alkenyltrifluoroborates[61] on bromopyridines, which could lead to other methods of preparing tetrasubstituted N4Py derivatives from tetrabromo N4Py (**3**).

4.4.2 The Stille reaction

The Stille reaction most often involves the palladium- or nickel-catalysed[62] cross coupling of an aryl, alkynyl, or vinyl tin reagent with an electrophile, commonly an aryl halide, although alkyl halides or triflates can also be employed.[26,29] This type of cross coupling reaction can be performed under neutral conditions and can be used as an alternative to the Suzuki reaction for the synthesis of biaryl compounds. Both cross coupling reactions are generally equally efficient.[29] However, the troublesome removal of the residual tin salts from the reaction product is the main disadvantage of the Stille reaction. Many authors have reported this complication and, consequently, several purification methods have been developed to work around this problem.[63]

The catalytic cycle is considered to be comparable to that of the Suzuki reaction (Scheme 4.9). However, in the Stille cross coupling reaction the rate determining step is often the transmetalation step instead of the oxidative addition, which is affected by the substituents of the substrates in the reaction.

The number of commercially available organostannanes is still limited and the reagents, therefore, generally need to be prepared prior to the Stille reaction. Their synthesis is usually achieved via a separate reaction step by quenching an organolithio species with an alkyltin chloride. Alternatively, these stannanes can sometimes be prepared separately by the palladium-catalysed cross coupling of a hexa-alkylditin and an aryl halide,[64] or *in situ* for inter-[65] and intramolecular reactions.[66] An intermolecular cross coupling of 2-bromopyridines[67] or 2-pyridinyl triflates[68] with functionalised aryl bromides has also been reported, in which a selective formation of the organostannane was catalysed *in situ* by $Pd(PPh_3)_4$ to furnish 2-arylpyridines in moderate to good yields.

In order to evaluate the Stille reaction as a potential means to functionalise tetrabromo N4Py (**3**), several test reactions were carried out on the 3-pyridinylstannanes **30** and **31** (Scheme 4.12). Bromopyridinylstannanes have often been utilised in the synthesis of heteroarylene building blocks[44,69] for polyheterocyclic molecules.[17,19,70] The organostannanes **30** and **31** were obtained from 2,5-dibromopyridine (**1**) and 3-bromopyridine (**14**) in 99% and 93% isolated yields, respectively, via the lithiation of the bromopyridines and the subsequent reaction with tributyltin chloride. Next, stannanes **30** and **31** were employed in a cross coupling reaction with 4-iodo-aniline (**24**) and the phthalimide-protected 3-iodo-aniline[71] (**26**). Unfortunately, 3-arylpyridine **27** could not be obtained from the reaction of stannane **30** with aryl iodide **24** when catalysed by 2 mol% $Pd(PPh_3)_4$, even after refluxing in THF for three days. In contrast, the use of the *N*-protected iodoaniline **26** under analogous conditions resulted in a full and clean conversion to the cross-coupled product **32**. Similarly, the 3-arylpyridine **29** was selectively formed from stannane **31**. Unfortunately, the tedious removal of the residual tin salts resulted in poor isolated yields of the products that were still contaminated with traces of tin residues.[54] Therefore, no yields are reported in Scheme 4.12. However, ^{1}H NMR indicated that the cross-coupled products **29** and **32** were indeed obtained, as the characteristic aromatic signals for 2,5-disubstituted pyridines were shifted compared to those of the starting material. In addition, mass analysis of these products confirmed their structural composition.

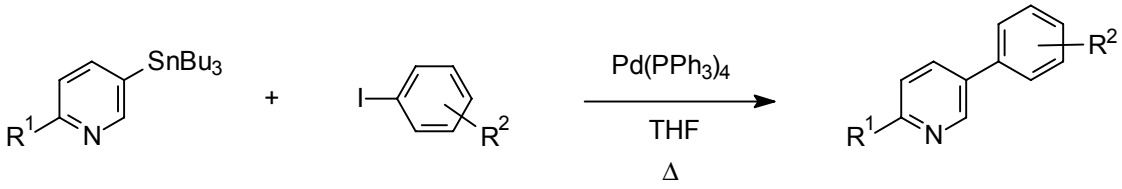

30: R^1 = Br
31: R^1 = H

24: R^2 = 4-NH_2
26: R^2 = 3-NPht

27: R^1 = Br, R^2 = 4-NH_2
29: R^1 = H, R^2 = 3-NPht
32: R^1 = Br, R^2 = 3-NPht

Scheme 4.12. The Stille reaction applied in the formation of 3-arylpyridines **27**, **29**, and **32** from the 3-pyridinylstannanes **30** and **31**.

The use of toluene as a solvent or $PdCl_2(PPh_3)_2$ as a catalyst in the presence of copper iodide provided no significant improvements to the efficiency of the reaction. Copper iodide is frequently used to activate the organostannane,[72] as well as other reagents in alternative cross coupling reactions like the Heck and Sonogashira reaction (*vide infra*).

For the application of the Stille reaction to tetrabromo N4Py (**3**) it would be beneficial if the cross-coupled products could be obtained directly from **3** via a metal-catalysed reaction with organostannanes. This would eliminate the necessity to convert the bromides in **3** into stannanes prior to the cross coupling reaction, either *in situ* or via a separate reaction step. Therefore, the palladium-catalysed reaction of 3-bromopyridine (**14**) with tributyl(phenyl)tin (**33**) was examined (Scheme 4.13). After three days in refluxing THF the product 3-phenylpyridine (**17**) was isolated, however the tin residues could not be removed completely from the product by column chromatography. Due to the encountered problem with this route, it was not explored any further.

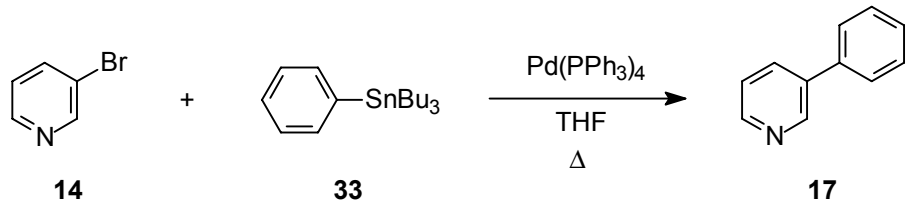

Scheme 4.13. Formation of 3-phenylpyridine (**17**) via the Stille cross coupling methodology.

4.4.3 The Sonogashira reaction

Metal-catalysed cross couplings of terminal acetylenes with aryl halides are referred to as Sonogashira reactions.[34,35] Transition metals (commonly copper iodide[35] or silver iodide[73]) as co-catalysts assist the activation of the acetylene C–H bond, which enables these reactions to proceed at room temperature and under mild conditions.[74] Nowadays, many variations of this methodology are used as a convenient way of preparing a range of aryl acetylenes and alkylenes, as well as allenyl acetylenes.[35]

Again, the catalytic cycle is related to the mechanism of the Suzuki reaction (Scheme 4.9). The main difference is the transmetalation step of the cycle, which now involves an *in situ* formation of an alkynylcopper(I) species.[35] The reactive palladium species is a Pd^0 complex, formed either from a palladium(0) catalyst like $Pd(PPh_3)_4$, or from a palladium(II) catalyst, which is then reduced *in situ* by the alkynylcopper(I) species present. The reaction medium is most often diethylamine or triethylamine, which serves both as a solvent and a base to trap the hydrogen iodide formed during the reaction.

The Sonogashira reaction with bromopyridines[6,18,75,76] was examined on **14** as a test substrate for the possible application of this cross coupling methodology to tetrabromo N4Py (**3**). By employing 1 mol% $PdCl_2(PPh_3)_2$ as the catalyst and 0.5 mol% copper iodide as a co-catalyst, **14** was converted into the pyridine derivatives **36** and **37** by the reaction with 3-butyn-1-ol (**34**) or its acetyl-protected analogue **35**, respectively.

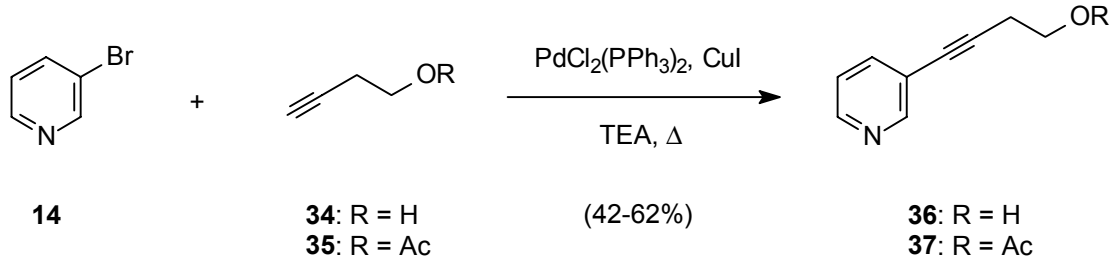

Scheme 4.14. The Sonogashira reaction of 3-bromopyridine (**14**) with the terminal acetylenes **34** and **35**.

Although diethylamine[77] as the solvent furnished the cross-coupled product **36**, superior isolated yields were obtained when triethylamine[78] (TEA) was used (62% vs. 42%). Despite a complete and clean conversion of the starting materials according to NMR analysis, the product could only be isolated in a moderate yield, presumably due to a loss of product during the purification

by column chromatography. The acylated propargylic alcohol **35** was employed under similar conditions in the hope of improving the purification step, but unfortunately product **37** could only be isolated in 48% yield. As an alternative procedure,[18] the cross coupling of **14** and **34** mediated by 5 mol% $Pd(PPh_3)_4$ was attempted in THF with 1.5 equivalent of TEA, but this unfortunately resulted in an inferior reaction, as **36** was obtained only in 22% yield after column chromatography.

4.4.4 Other metal-catalysed coupling reactions

The Heck reaction generally involves the palladium-catalysed arylation of olefins by aryl iodides to furnish various substituted olefins, dienes or other unsaturated compounds.[36,37] Nowadays, aryl chlorides[79] and aryl anhydrides[80] are also employed in this cross coupling reaction. The Heck reaction has also been described for bromopyridines.[81] Generally, palladium(II) catalysts like $Pd(OAc)_2$ or $PdCl_2(PPh_3)_2$ are used for this reaction, which are then reduced *in situ* to the active palladium(0) species by the phosphine ligands or base present.[37] However, palladium(0) complexes like $Pd(PPh_3)_4$ have also been employed successfully in the Heck reaction.[37]

Again, 3-bromopyridine (**14**) was used as a model compound for the Heck reaction on tetrabromo N4Py (**3**). In the cross coupling reaction with allyl alcohol (**38**) catalysed by $Pd(OAc)_2$, the aldehyde product **40** could not be obtained (Scheme 4.15). When triphenylphosphine was used as an additive, sodium bicarbonate as a base, and hexamethylphosphoramide (HMPA) as the solvent,[82] a complex product mixture was obtained after seventeen hours under reflux conditions in which **40** could not be detected by NMR or mass analysis. No conversion at all was observed when the solvent was changed to *N*-methylpyrrolidinone (NMP) with sodium acetate as a base and tetrabutylammonium bromide as the additive.[83]

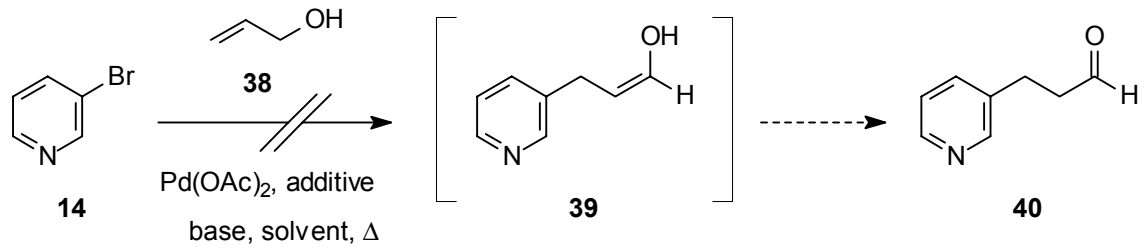

Scheme 4.15. Unsuccessful Heck reaction of 3-bromopyridine (**14**).

Under different conditions the reaction might prove to be fruitful as bromopyridines have been applied with some success in the Heck reaction.[81,83] The aldehyde **40** is the expected product of this reaction, formed via tautomerisation of the initially formed cross-coupled product **39**. The terminal functionality could thus facilitate further derivatisation of the N4Py ligand once applied to the tetrabromide N4Py derivative **3**.

New cross coupling methodologies are continuously being reported, and these contributions might in turn provide alternative means of functionalising tetrabromo N4Py (**3**). Other cross coupling methods that have been described so far and that might be applied to halopyridines or compounds obtained from these are, for instance, the Negishi[5] or the Kumada[84] cross coupling

reactions.[47] The Kumada coupling involves the palladium- or nickel-catalysed[85] cross coupling of a Grignard reagent and an aryl or alkenyl halide or triflate.[86–88] The Negishi reaction[89] between bromopyridines and a *n*-alkyl iodide is catalysed by $PdCl_2(PPh_3)_2$.[90] A transformation of the alkyl halide occurs *in situ* with a zinc-copper couple to produce the reactive alkylzinc iodide. This coupling reaction is more effective for 2-bromopyridine than for 3-bromopyridine.[90]

Jackson and co-workers have developed a related methodology to prepare various unnatural amino acids via palladium-catalysed cross coupling reactions on iodoalanine **41**.[91] The use of Rieke™ zinc has been reported to give the best results for the zincation step.[92] When applied to tetrabromo N4Py (**3**), this methodology could enable the direct introduction of amino acids into the N4Py ligand system. This zinc coupling methodology was thus applied to the direct cross coupling of bromopyridines **14** and **43** to iodoalanine **41** via **42** to furnish the pyridinylalanine derivatives **44** and **45** (Scheme 4.16).[54,92]

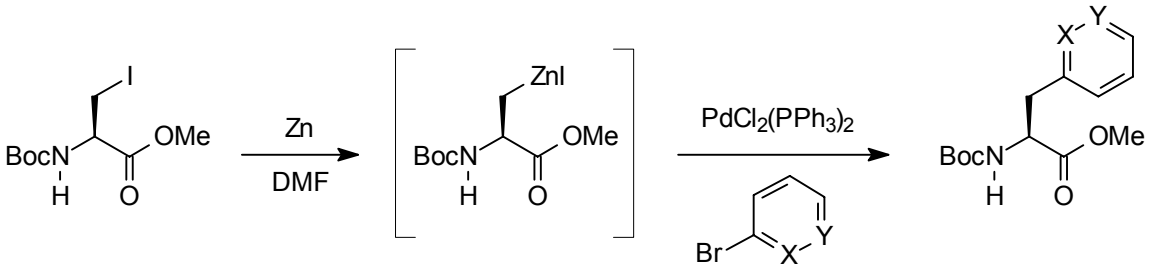

41 **42** **14**: X = CH, Y = N **43**: X = N, Y = CH **44**: X = CH, Y = N **45**: X = N, Y = CH

Scheme 4.16. The direct coupling of iodoalanine **41** to bromopyridines **14** and **43**.

Other cross coupling reactions on bromopyridines that could in principle be considered include the palladium-catalysed carbonylation of bromopyridines with carbon monoxide and phenylboronic acid to phenyl pyridinyl ketones.[42b] Also, the $Pd(PPh_3)_4$-mediated cyanation of bromopyridines has been described using tributyltin cyanide.[93] Alternatively, a reaction with $Zn(CN)_2$ in DMF catalysed by $Pd_2(dba)_3$ with 1,1'-bis(diphenylphosphino)ferrocene (dppf) as ligand was reported.[94] The latter procedure allowed the successful preparation of nitrile **47** during the development of a synthetic pathway of a tetrasubstituted N4Py ligand (Chapter 3). After refluxing for one night, the bromide **46** was almost fully converted into the nitrile **47**, which was isolated in 40% yield after column chromatography.

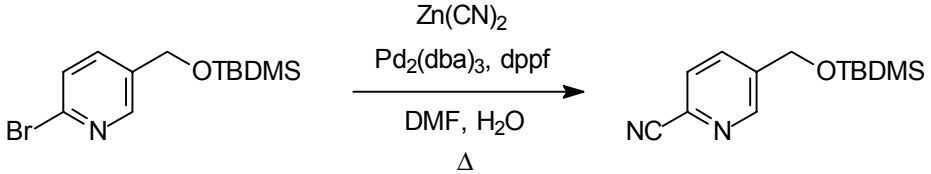

46 (40%) **47**

Scheme 4.17. The palladium-catalysed preparation of nitrile **47** from bromide **46**.

Pioneering work was undertaken by Knochel and colleagues[95] on the palladium- or iron-catalysed[96] functionalisation of halopyridines by cross coupling reactions that employ aryl-magnesium reagents and copper cyanide as a co-catalyst. These Grignard reagents are

generally obtained via a halide-magnesium exchange reaction utilising isopropylmagnesium bromide. Under these conditions reagents can be used that incorporate a variety of functional groups.[97] Related to this type of cross coupling is the metal-catalysed reaction of alkylmagnesium halides with bromopyridines.[18,98]

By using the metal-catalysed cross coupling reactions not only C–C bonds can be created, but also C–N bonds.[99] Various metal-phosphine complexes have been found to be capable of catalysing this C–N bond formation in aromatic heteroatom coupling reactions.[49,100] For instance, the palladium-[99,101,102] or nickel-catalysed[103] aminations of monohalopyridines, or a regioselective palladium(II)-catalysed amination of dichloropyridines[104] to secondary and tertiary amines, were achieved in good yields. Furthermore, intermolecular C–N bond formation between aryl bromides, iodides, and triflates and amides has been mediated by a palladium[105] or copper[106] catalyst, although the use of halopyridines has not as yet been reported by researchers.

4.5 Functionalisation of tetrabromo N4Py

From the test reactions performed on 3-bromopyridines described in the previous sections it is clear that bromopyridines are most susceptible to the Suzuki reactions. These cross coupling reactions provide the resulting arylpyridine products in excellent yields after purification. An additional advantage is that a wide range of organoboronic acids are commercially available, which might facilitate the preparation of various derivatives of the tetrabromide N4Py ligand **3**. Although the Stille reaction proved to be equally efficient in the model cross coupling reactions, the troublesome removal of the residual tin salts from the reaction product disfavoured its application in the functionalisation of **3**.

The reaction of tetrabromo N4Py (**3**) with four equivalents of phenylboronic acid (**15**) and 4 mol% $Pd(PPh_3)_4$ as the catalyst (equivalent to 1 mol% of palladium catalyst per bromide) in a refluxing mixture of toluene and aqueous sodium carbonate could not be driven to completion.[54] By the addition of more phenylboronic acid and catalyst, up to ten equivalents of **15** and 12 mol% $Pd(PPh_3)_4$, a complete conversion of the starting material to a single compound was obtained after a week under reflux conditions, but unfortunately not to the desired tetraphenyl N4Py derivative **48**. NMR analysis clearly indicated that the resonance signals, characteristic for N4Py molecules, were significantly shifted. Typically, the doubly benzylic proton of a N4Py ligand is observed at approximately 5.2 ppm and the other benzylic methylene protons of the N4Py core around 3.9 ppm. Both signals were absent in the NMR spectrum obtained for the crude product of this Suzuki reaction, and a new signal at 4.4 ppm was observed. This presumably can be attributed to a degradation product formed due to the prolonged reaction time. In addition, the protons at the 6-positions of the pyridine rings in tetrasubstituted N4Py ligands are always observed as a set of two singlets at 8.2 to 8.4 ppm, due to the dissymmetry between the upper and lower half of the molecule. The ^{1}H NMR spectrum of this degradation product, however, presented only one signal in this region.

Therefore, the reaction was repeated in toluene with ten equivalents phenylboronic acid (**15**) and 12 mol% $Pd(PPh_3)_4$, which afforded product **48** after one night at reflux and subsequent workup in 80% yield (Scheme 4.18). The ^{1}H NMR spectrum showed the characteristic signals that can be expected for tetrafunctionalised N4Py ligands as described

above. The molecular ion of **48** and its expected fragmentations were detected by mass spectroscopy and confirmed that indeed the tetrasubstituted cross-coupled was obtained. No detectable amounts of mono-, di- or trisubstituted products were present. These products from incomplete reactions, if present, should be detectable by NMR, as the electronic effect of the phenyl groups on the N4Py ligand is substantially different from that of the bromides. A trace of the previously observed side-product was also present. The identity of this compound has not yet been elucidated.

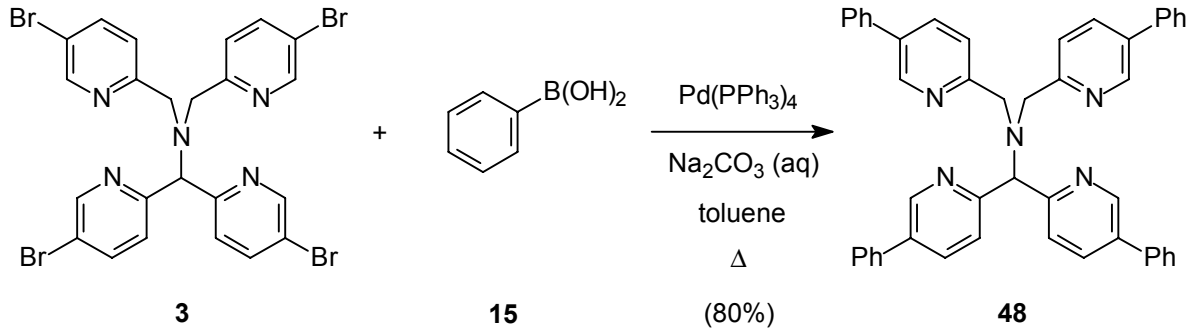

3 **15** (80%) **48**

Scheme 4.18. The successful tetrafunctionalisation of tetrabromo N4Py (**3**) by the Suzuki reaction with phenylboronic acid (**15**).

In the test reactions on several bromopyridines, it was shown that THF as the solvent generally gave rise to superior efficiencies over toluene in Suzuki cross coupling reactions. Therefore, the Suzuki reaction of **3** with phenylboronic acid (**15**) was also performed in THF. After one hour at reflux a full conversion of the starting material **3** was already observed. Unfortunately, this was not the desired product. Again, an unidentified product was observed by NMR analysis, indicating that in THF a species is formed that is presumably very reactive and results in the formation of the unwanted product. Even when samples were taken after a few minutes and analysed by NMR, only the unidentified compound could be observed without any trace of the desired product **48**.

In order to test the susceptibility of tetrabromo N4Py (**3**) towards halogen-metal exchange and subsequent quenching with electrophiles, **3** was treated at room temperature with 4.5 equivalents of isopropylmagnesium bromide as a solution in THF (Scheme 4.19). Mass analysis of a sample that was quenched with water, however, only showed the dibromide N4Py derivative **49a**. Addition of more isopropylmagnesium bromide did not result in a complete magnesium-bromide exchange, even after heating at reflux temperature. When a sample was quenched with D_2O, mass analysis revealed the incorporation of three deuterium atoms which suggested the formation of **49b**. Not only does this indicates that magnesium-bromide exchange occurs at two of the four sites, but also that the doubly benzylic position in **3** is deprotonated. The addition of DMF to the reaction mixture afforded the dialdehyde N4Py derivative **49c**, which has been characterised by NOESY NMR experiments. The doubly benzylic position apparently does not react with DMF, and is therefore reprotonated during workup. These findings indicate that the lower half of **3** is not susceptible towards a metal-halogen exchange, possibly due to the delocalisation of the negative charge over the two adjacent pyridine rings.

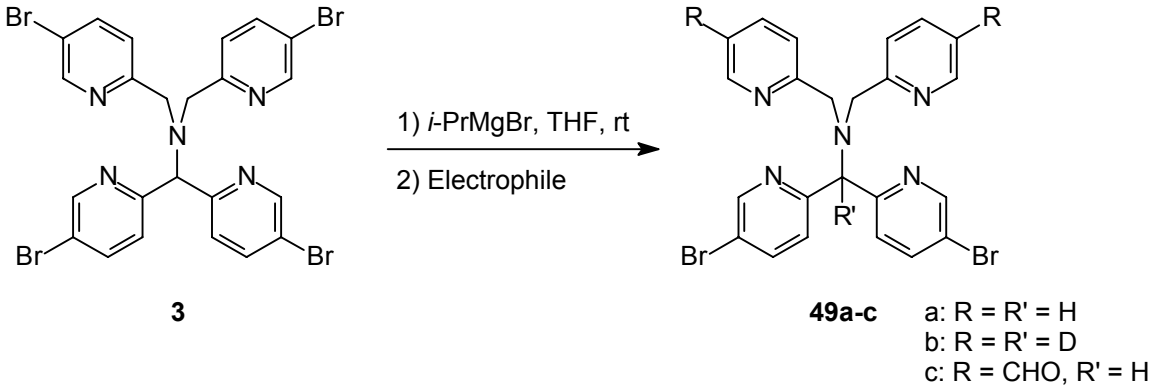

Scheme 4.19. Regioselective magnesium-bromide exchange of tetrabromo N4Py.

4.6 Discussion and conclusions

Within the fascinating field of cross coupling methodologies new contributions to metal-catalysed reactions are continuously being reported as replacements for long-established chemical procedures, or as simplifications of complicated bond formations and structure modifications. It is therefore likely that for reactions that have until now been accompanied by poor results, or even proven to be non-susceptible to their metal-mediated versions, a cross coupling variation will be invented. In light of the recent progressions in this field so far, it is only a question of time before the current procedures are superseded by even more refined versions.

From the investigated cross coupling reactions in this chapter it has become evident that the Suzuki reaction is the most effective and practical method for the modification of bromopyridines. Fortunately, this reaction applied to tetrabromo N4Py (**3**), which entails four palladium-mediated functionalisations on a single molecule, proceeded efficiently to furnish the cross-coupled product tetraphenyl N4Py (**48**) in an excellent yield of 80% with no detectable amounts of products from incomplete cross coupling reactions on **3**. These findings seem to indicate that other high yielding cross coupling reactions on a bromopyridine can also be applied to provide the corresponding tetrasubstituted N4Py derivatives.

The synthesis of the tetrabromide N4Py derivative **3** could be accomplished by taking advantage of the reported change in regioselectivity in the lithiation of 2,5-dibromopyridine by substituting a co-ordinating solvent by a non-co-ordinating solvent.[4] This enabled the construction of the N4Py core while preserving the remaining bromide on the pyridine ring for further functionalisation of the final ligand **3**. The developed synthetic pathway to tetrabromo N4Py (**3**) still requires further optimisation, for instance in the formation of bispyridinyl ketone **8**. The troublesome dialkylation of bispyridinyl methylamine **10** is a well-known problem in the preparation of many N4Py derivatives, which can sometimes lead to disappointing results.

4.7 Experimentals

General information

For general remarks on instrumentation, methods, and chemicals, see the Experimental Section in Chapter 3. The NMR spectra of compounds **44** and **45** were recorded on a Bruker 250 spectrometer (^{1}H NMR at 250 MHz, ^{13}C NMR at 62.8 MHz). 5-Bromo-2-picoline[21] and 2-methoxy-4,4,5,5-tetramethyl-1,2,3-dioxaborolane[107] were prepared according to literature procedures and all the spectroscopic data were in good agreement with the literature.

5-Bromo-2-pyridinecarbaldehyde[4] **(7)**

To a suspension of 2,5-dibromopyridine (9.47 g, 39.2 mmol) in dry toluene (500 mL) at –80°C was slowly added *n*-BuLi (29 mL, 46 mmol, 1.2 equiv) under a nitrogen atmosphere. After stirring the mixture at –80°C for 2 h neat DMF (3.9 mL, 50 mmol, 1.3 equiv) was added. The reaction mixture was allowed to warm to room temperature after an additional hour. Dilute HCl (1 M, 100 mL) was added and the mixture was stirred for 15 min. After separation the water layer was extracted with diethyl ether (2x50 mL). The organic layer was washed with brine (50 mL) and dried over Na_2SO_4. Concentration by rotary evaporation afforded **7** as a light brown solid (6.66 g, 91%).[108]

^{1}H NMR ($CDCl_3$, 300 MHz) δ 7.80 (d, J = 8.1 Hz, 1H), 7.98 (dd, J = 8.1, 2.2 Hz, 1H), 8.80 (d, J = 1.8 Hz, 1H), 9.99 (s, 1H). ^{13}C NMR ($CDCl_3$, 75.5 MHz) δ 122.4 (d), 125.9 (s), 139.6 (d), 150.9 (s), 151.3 (d), 192.0 (d). HRMS calcd for C_6H_4NOBr 184.948, found 184.947.

Bis(5-bromo-2-pyridinyl)methanone (8)

Method A: The same procedure as described for **7**, using 2,5-dibromopyridine (8.62 g, 35.6 mmol) and *n*-BuLi (27 mL, 43 mmol, 1.2 equiv). Quenching the reaction mixture with a solution of aldehyde **7** (6.64 g, 35 mmol) in dry toluene (175 mL) furnished after workup a residual brown oil that was taken up in CH_2Cl_2 (300 mL). Activated MnO_2 (12.8 g, 133 mmol, 3.8 equiv) was added in portions over 8 h to the suspension at reflux. The solvent was evaporated, the residue filtered through Celite and washed with ethyl acetate. After evaporation of the solvent **8** was precipitated from diethyl ether as a brown solid (3.07 g, 26%).[109]

Method B: The same procedure as described for **7**, employing 2,5-dibromopyridine (10.7 g, 44.3 mmol) in dry toluene (1 L) and *n*-BuLi (29 mL, 46 mmol, 1.05 equiv). After 2 h at –80°C the reaction was quenched with freshly distilled diethyl carbonate (2.7 mL, 22 mmol, 0.5 equiv). After further workup and extractions using ethyl acetate, removal of the solvent furnished a dark brown oil, which solidified on standing. By triturating the crude product with diethyl ether pure **8** was obtained as a light brown solid (2.77 g, 37%). Recrystallisation from diethyl ether afforded the analytically pure product.

mp 191.8–192.7°C. ^{1}H NMR ($CDCl_3$, 300 MHz) δ 7.98 (d, J = 8.2 Hz, 2H), 8.03 (dd, J = 8.2, 2.0 Hz, 2H), 8.77 (d, J = 2.0 Hz, 2H). ^{13}C NMR ($CDCl_3$, 50.3 MHz) δ 124.7 (s), 126.3 (d), 139.4 (d), 150.3 (d), 152.1 (s), 191.0 (s). HRMS calcd for $C_{11}H_6N_2OBr_2$ 339.885, found 339.885. Anal. calcd for $C_{11}H_6N_2OBr_2$: C 38.60; H 1.80; N 8.20; Br 46.70. Found: C 38.33; H 1.80; N 8.01; Br 47.04.

Bis(5-bromo-2-pyridinyl)methanone oxime (9)

A mixture of **8** (2.77 g, 8.10 mmol), hydroxylammonium chloride (3.0 g, 42 mmol, 5 equiv), and pyridine (3.4 mL, 42 mmol, 5 equiv) in ethanol (60 mL) was refluxed for 1.5 h and subsequently cooled to room temperature. The mixture was poured into ice water and stirred in an ice bath for 1 h. The solids were collected by filtration and washed with cold dilute ethanol (50%). After drying in air the product was obtained as a light brown solid (2.63 g, 91%). Recrystallisation from ethanol/water afforded analytically pure **9** as fine, lilac/grey needles.

mp 191.1–191.7°C. ^{1}H NMR ($CDCl_3$, 300 MHz) δ 7.63 (d, J = 8.4 Hz, 1H), 7.76 (d, J = 8.4 Hz, 1H), 7.92 (dd, J = 8.4, 1.8 Hz, 1H), 7.99 (dd, J = 8.4, 1.8 Hz, 1H), 8.65 (d, J = 1.8 Hz, 1H), 8.70 (d, J = 1.8 Hz, 1H). ^{1}H NMR (CD_3OD, 300 MHz) δ 7.56 (d, J = 8.4 Hz, 1H), 7.83

(d, J = 8.4 Hz, 1H), 8.01 (dd, J = 8.4, 2.2 Hz, 1H), 8.10 (dd, J = 8.4, 2.2 Hz, 1H), 8.50 (d, J = 2.2 Hz, 1H), 8.68 (d, J = 2.2 Hz, 1H). ^{13}C NMR ($CDCl_3$, 50.3 MHz) δ 119.8 (s), 120.3 (s), 122.8 (d), 127.0 (d), 138.7 (d), 139.4 (d), 149.5 (d), 150.0 (d), 150.6 (s), 153.0 (s), 153.9 (s). HRMS calcd for $C_{11}H_7N_3OBr_2$ 354.895, found 354.896. Anal. calcd for $C_{11}H_7N_3OBr_2$: C 37.00; H 2.00; N 11.80; Br 44.80. Found: C 36.58; H 2.06; N 11.41; Br 44.58.

Bis(5-bromo-2-pyridinyl)methylamine (10)

Zinc dust (1.1 g, 17 mmol, 3.4 equiv) was carefully added in small portions over 5 min to a suspension of **9** (1.79 g, 5.01 mmol) in acetic acid (30 mL) and water (15 mL). The mixture was stirred at room temperature for 30 min, filtered over Celite and washed with water. After evaporation of the solvent the residue was neutralised with concentrated ammonia (25 mL, 25% v/v) and extracted with CH_2Cl_2 (3x20 mL). The organic layer was washed with brine (15 mL), dried over Na_2SO_4, and concentrated *in vacuo* to furnish pure **10** as a brown viscous oil that solidified on standing (1.62 g, 94%).

^{1}H NMR ($CDCl_3$, 300 MHz) δ 2.38 (br. s, 2H), 5.24 (s, 1H), 7.29 (d, J = 8.4 Hz, 2H), 7.72 (dd, J = 8.4, 1.8 Hz, 2H), 8.55 (d, J = 1.8 Hz, 2H). ^{13}C NMR ($CDCl_3$, 75.5 MHz) δ 61.1 (d), 119.1 (q), 123.0 (d), 139.2 (d), 150.1 (d), 160.6 (q). HRMS calcd for $C_{11}H_9N_3Br_2$ 340.916, found 340.916.

5-Bromo-2-picoline *N*-oxide (12)[21b]

A mixture of 5-bromo-2-picoline (11.7 g, 68.0 mmol) and mCPBA (20.9 g, 97.0 mmol, 1.4 equiv) in CH_2Cl_2 (300 mL) was stirred at room temperature overnight. Saturated Na_2CO_3 (300 mL) was added and after stirring for 30 min the layers were separated. The water layer was extracted with CH_2Cl_2 (6x50 mL), and the combined organic layers were washed with brine (50 mL) and dried over Na_2SO_4. Evaporation of the solvent yielded **12** as a light yellow solid that was recrystallised from diethyl ether (12.5 g, 98%).

mp 119.3–120.4°C (lit.[110] 117–118°C). ^{1}H NMR ($CDCl_3$, 300 MHz) δ 2.43 (s, 3H), 7.11 (d, J = 8.4 Hz, 1H), 7.29 (dd, J = 8.4, 1.1 Hz, 1H), 8.38 (d, J = 1.1 Hz, 1H). ^{13}C NMR ($CDCl_3$, 75.5 MHz) δ 17.2 (q), 117.1 (s), 126.3 (d), 128.2 (d), 140.5 (d), 147.9 (s). HRMS calcd for C_6H_6BrNO 186.963, found 186.963.

5-Bromo-2-(chloromethyl)pyridine (13)

Protected from moisture TFAA (10 mL, 71 mmol, 5 equiv) was carefully and slowly added to **12** (2.63 g, 14.0 mmol). After the vigorous thermal reaction had ceased, the orange mixture was stirred at room temperature for 30 min, and then refluxed for 30 min. Saturated $NaHCO_3$ was carefully added after cooling to room temperature until pH 8 was reached. The resulting red solution was stirred at room temperature under nitrogen overnight. The mixture was extracted with CH_2Cl_2 (6x25 mL), and the combined organic layers were washed with brine (25 mL) and dried over Na_2SO_4. Evaporation of the solvent yielded **13** as a dark brown oil (2.15 g, 81%), which was used without any further purification.[21b]

^{1}H NMR ($CDCl_3$, 300 MHz) δ 3.41 (br. s, 1H), 4.72 (s, 2H), 7.20 (d, J = 8.3 Hz, 1H), 7.81 (dd, J = 8.3, 2.2 Hz, 1H), 8.60 (d, J = 2.2 Hz, 1H). ^{13}C NMR ($CDCl_3$, 75.5 MHz) δ 63.9 (t), 118.8 (s), 121.9 (d), 139.3 (d), 149.3 (d), 158.5 (s). HRMS calcd for C_6H_6NOBr 186.963, found 186.965.

Thionyl chloride (0.89 mL, 12 mmol, 1.5 equiv) was slowly added to a solution of crude 5-bromo-2-(hydroxymethyl)pyridine (1.51 g, 8.03 mmol) in CH_2Cl_2 (30 mL) at 0°C, protected from moisture. After being allowed to warm to room temperature the reaction mixture was stirred overnight. Saturated $NaHCO_3$ (20 mL) was added and the layers were separated. The water layer was extracted with CH_2Cl_2 (3x10 mL). The combined organic layers were washed with brine (10 mL) and dried over Na_2SO_4. Concentration by rotary evaporation furnished **13** as a dark brown oil (1.63 g, 97%) that was used without further purification. The product can be stored at –20°C under nitrogen for many months without any detectable signs of degradation.
^{1}H NMR ($CDCl_3$, 300 MHz) δ 4.61 (s, 2H), 7.37 (d, J = 8.4 Hz, 1H), 7.84 (dd, J = 8.4, 2.2 Hz, 1H), 8.62 (d, J = 2.2 Hz, 1H). ^{13}C NMR ($CDCl_3$, 75.5 MHz) δ 45.8 (t), 120.0 (s), 124.0 (d), 139.5 (d), 150.3 (d), 155.0 (s). HRMS calcd for C_6H_6NClBr 204.929, found 204.929.

_N_-[Bis(5-bromo-2-pyridinyl)methyl]-_N_,_N_-bis[(5-bromo-2-pyridinyl)methyl]amine (3)
A mixture of **10** (0.72 g, 2.1 mmol), **13** (1.8 g, 8.7 mmol, 4 equiv), DIEA (7.2 mL, 41 mmol, 20 equiv), and dry acetonitrile (1.5 mL) was heated at 80°C under a nitrogen atmosphere for 2 days. After evaporation of the solvent the residue was taken up in CH_2Cl_2 (10 mL), washed with water (3x5 mL), brine (10 mL), and dried over Na_2SO_4. Concentration by rotary evaporation afforded a dark brown, viscous oil that solidified on standing. After purification by flash chromatography over alumina using a gradient of hexane/ethyl acetate/TEA (40:9:1 to 30:9:1) and evaporation of the solvents, the residue was precipitated from diethyl ether to furnish **3** as a white solid (0.83 g, 58%). Recrystallisation from CH_2Cl_2/diethyl ether afforded pure **3** as white needles.
mp 151.6–152.2°C. ^{1}H NMR ($CDCl_3$, 300 MHz) δ 3.84 (s, 4H), 5.21 (s, 1H), 7.40 (d, J = 8.4 Hz, 1H), 7.55 (d, J = 8.4 Hz, 1H), 7.72 (dd, J = 8.4, 2.2 Hz, 1H), 7.78 (dd, J = 8.4, 2.2 Hz, 1H), 8.56 (d, J = 2.2 Hz, 1H), 8.59 (d, J = 2.2 Hz, 1H). ^{13}C NMR ($CDCl_3$, 75.5 MHz) δ 56.3 (t), 70.7 (d), 119.0 (s), 119.5 (s), 124.4 (d), 125.2 (d), 138.9 (d), 139.0 (d), 150.1 (d), 150.3 (d), 157.7 (s). MS CI $[M+H]^+$ calcd for $C_{23}H_{18}Br_4N_5$ m/z 679.8, found 679.9. Anal. calcd for $C_{23}H_{17}Br_4N_5$: C 40.44; H 2.51; N 10.25; Br 46.79. Found: C 39.54; H 2.39; N 9.96; Br 45.60.

3-Phenylpyridine (17)
Method A: A mixture of 3-bromopyridine (0.31 g, 2.0 mmol), phenylboronic acid (0.27 g, 2.2 mmol, 1.1 equiv), $Pd(PPh_3)_4$ (69.3 mg, 60 µmol, 3 mol%), aqueous Na_2CO_3 (2 M, 6 mL), and 4 droplets of ethylene glycol was heated to reflux in THF (12 mL) under a nitrogen atmosphere overnight. The layers were separated and the organic layer was washed with aqueous Na_2CO_3 (2 M, 3x5 mL), brine (10 mL), and dried over Na_2SO_4. Evaporation of the solvent afforded a yellow oil that was purified by flash column chromatography over silica using hexane/ethyl acetate/triethylamine (30:9:1) as the eluent to furnish **17** as a colourless oil (0.27 g, 87%). R_f = 0.33 (SiO_2, hexane/ethyl acetate = 3:1).
Method B: A mixture of tributyl(phenyl)stannane (**33**) (0.37 g, 1.0 mmol), 3-bromopyridine (**14**) (0.16 g, 1.0 mmol), and $Pd(PPh_3)_4$ (16 mg, 14 µmol, 1.4 mol%) in dry THF (10 mL) was heated to reflux under a nitrogen atmosphere for 3 days. Dilute HCl (30 mL, 2 M) was added to the reaction mixture and the phases separated after stirring for 15 min. The aqueous phase was washed with CH_2Cl_2 (3x25 mL) and neutralised with concentrated ammonia (25% v/v). The resulting suspension was extracted with CH_2Cl_2 (7x25 mL). The organic phase was washed with

brine (25 mL) and dried over Na_2SO_4. After evaporation of the solvent the crude product was purified by column chromatography over silica using hexane/ethyl acetate (3:1) to afford **17** as a colourless oil (50 mg, 32%).[111]
^{1}H NMR (300 MHz, $CDCl_3$) δ 7.35 (dd, J = 8.1, 4.6 Hz, 1H), 7.40 (dt, J = 7.0, 2.2 Hz, 1H), 7.47 (dd, J = 7.2, 7.0 Hz, 2H), 7.57 (dt, J = 7.2, 2.2 Hz, 2H), 7.86 (dt, J = 8.1, 1.7 Hz, 1H), 8.58 (d, J = 4.6 Hz, 1H), 8.84 (d, J = 1.7 Hz, 1H). ^{13}C NMR (75.5 MHz, $CDCl_3$) δ 123.4 (d), 127.0 (d), 127.9 (d), 128.9 (d), 134.1 (d), 136.4 (s), 137.6 (s), 148.1 (d), 148.3 (d). HRMS calcd for $C_{11}H_9N$ 155.074, found 155.073.

2-Methyl-5-phenylpyridine (18)
Following the procedure for **17**, compound **18** was obtained as a colourless oil (0.32 g, 95%) from 5-bromo-2-picoline (0.34 g, 2.0 mmol) after workup and flash column chromatography over silica using hexane/ethyl acetate/triethylamine (30:9:1) as the eluent. R_f = 0.44 (SiO_2, hexane/ethyl acetate = 3:1).
^{1}H NMR (300 MHz, $CDCl_3$) δ 2.56 (s, 3H), 7.15 (d, J = 8.1 Hz, 1H), 7.33 (t, J = 7.0 Hz, 1H), 7.41 (dd, J = 7.5, 7.0 Hz, 2H), 7.51 (d, J = 7.5 Hz, 2H), 7.71 (dd, J = 8.1, 2.4 Hz, 1H), 8.70 (d, J = 2.4 Hz, 1H). ^{13}C NMR (75.5 MHz, $CDCl_3$) δ 23.9 (q), 123.0 (d), 126.8 (d), 127.6 (d), 128.8 (d), 133.5 (s), 134.5 (d), 137.7 (s), 147.3 (d), 157.0 (s). HRMS calcd for $C_{12}H_{11}N$ 169.089, found 169.089.

3-(3-Pyridinyl)aniline (19)
Following the procedure for **17**, compound **19** was obtained as a colourless viscous oil (68 mg, 95%) from 3-bromopyridine (66 mg, 0.42 mmol) and **16** (78 mg, 0.42 mmol) after workup and flash column chromatography over alumina using hexane/ethyl acetate/triethylamine (9:30:1) as the eluent. R_f = 0.42 (SiO_2, hexane/ethyl acetate = 3:1).
^{1}H NMR (200 MHz, $CDCl_3$) δ 3.77 (br. s, 2H), 6.71 (ddd, J = 8.0, 2.1, 1.0 Hz, 1H), 6.86 (dd, J = 2.1, 1.7 Hz, 1H), 6.94 (ddd, J = 7.7, 1.7, 1.0 Hz, 1H), 7.24 (dd, J = 8.0, 7.7 Hz, 1H), 7.32 (ddd, J = 8.0, 4.7, 0.8 Hz, 1H), 7.82 (ddd, J = 8.0, 2.1, 1.6 Hz, 1H), 8.55 (dd, J = 4.7, 1.6 Hz, 1H), 8.80 (d, J = 2.1 Hz, 1H). ^{13}C NMR (50.3 MHz, $CDCl_3$) δ 114.9 (d), 116.1 (d), 119.1 (d), 124.8 (d), 131.3 (d), 135.6 (d), 138.3 (s), 140.2 (s), 148.5 (s), 149.6 (d), 149.7 (d). HRMS calcd for $C_{11}H_{10}N_2$ 170.084, found 170.084.

3-(6-Methyl-3-pyridinyl)aniline (20)
Following the procedure for **17**, compound **20** was obtained as a light yellow solid (0.14 g, 90%) from 5-bromo-2-picoline (0.14 g, 0.84 mmol) and **16** (0.78 mg, 0.42 mmol) after workup and flash column chromatography over silica using hexane/ethyl acetate/triethylamine (10:20:1) as the eluent. R_f = 0.42 (SiO_2, hexane/ethyl acetate = 3:1).
mp 105.2–106.8°C. ^{1}H NMR (300 MHz, $CDCl_3$) δ 2.57 (s, 3H), 3.77 (br. s, 2H), 6.68 (dd, J = 7.9, 2.0 Hz, 1H), 6.84 (t, J = 2.0 Hz, 1H), 6.92 (d, J = 7.6 Hz, 1H), 7,17 (d, J = 8.0 Hz, 1H), 7.22 (dd, J = 7.9, 7.6 Hz, 1H), 7.71 (dd, J = 8.0, 2.3 Hz, 1H), 8.67 (d, J = 2.3 Hz, 1H). ^{13}C NMR (75.5 MHz, $CDCl_3$) δ 24.1 (q), 113.4 (d), 114.5 (d), 117.3 (d), 123.0 (d), 129.9 (d), 133.8 (s), 134.6 (d), 139.1 (s), 147.0 (s), 147.5 (d), 157.1 (s). HRMS calcd for $C_{12}H_{12}N_2$ 184.100, found 184.099.

2-Bromo-5-(4,4,5,5-tetramethyl-1,3,2-dioxaborolan-2-yl)pyridine (21)

The same procedure as described for **7**, using 2,5-dibromopyridine (1.0 g, 4.2 mmol), *n*-BuLi (2.7 mL, 4.4 mmol, 1.04 equiv) in dry diethyl ether (50 mL), followed by quenching with 2-methoxy-4,4,5,5-tetramethyl-1,3,2-dioxaborolane[107] (0.72 g, 4.6 mmol, 1.1 equiv) afforded after a neutral workup the product as a light yellow solid (0.69 g, 57%).[112]

^{1}H NMR (300 MHz, $CDCl_3$) δ 1.35 (s, 12H), 7.49 (d, J = 8.1 Hz, 1H), 7.89 (dd, J = 8.1, 1.8 Hz, 1H), 8.69 (d, J = 1.8 Hz, 1H). MS EI $[M]^+$ calcd for $C_{11}H_{15}BBrNO_2$ *m/z* 283.0, found 283, 285; $[M–CH_3]^+$ 268, 270. MS CI $[M+H]^+$ calcd for $C_{11}H_{16}BBrNO_2$ *m/z* 284.0, found 284, 286; $[M+NH_4]^+$ 301, 303; $[M–Br]^+$ 206.

***N*-(3-Iodophenyl)phthalimide (26)**

A mixture of 3-iodoaniline (2.5 g, 11.4 mmol) and phthalic anhydride (1.69 g, 11.4 mmol) was heated to reflux in acetic acid (50 mL) for 3 h. After cooling to room temperature the suspension was filtered over Celite and washed with cold ethanol. The residue was taken up in CH_2Cl_2 and filtered. Evaporation of the solvent afforded the product as a white powder (3.8 g, 94%), which could be recrystallised from toluene (3.0 g, 76%).

mp 194.5–194.7°C. ^{1}H NMR (300 MHz, $CDCl_3$) δ 7.22 (t, J = 8.1 Hz, 1H), 7.43 (ddd, J = 8.1, 1.1, 0.7 Hz, 1H), 7.72 (ddd, J = 8.1, 1.5, 1.1 Hz, 1H), 7.79 (dd, J = 5.5, 2.9 Hz, 2H), 7.82 (dd, J = 1.5, 0.7 Hz, 1H), 7.94 (dd, J = 5.5, 2.9 Hz, 2H). ^{13}C NMR (50.3 MHz, $CDCl_3$) δ 93.7 (s), 123.9 (d), 125.8 (d), 130.4 (d), 131.5 (s), 133.4 (s), 134.6 (d), 135.2 (d), 137.0 (d), 167.1 (s). MS EI $[M]^+$ calcd for $C_{14}H_8INO_2$ *m/z* 349.0, found 349.

2-Bromo-5-(tributylstannyl)pyridine (30)

To a solution of 2,5-dibromopyridine (10.0 g, 41.4 mmol) in dry diethyl ether (500 mL) at –80°C under a nitrogen atmosphere was slowly added *n*-BuLi (27.0 mL, 43.2 mmol, 1.04 equiv). After 60 min at –80°C tributyltin chloride (12.3 mL, 45.2 mmol, 1.1 equiv) was added to the red solution. After 1 h at –80°C the reaction mixture was allowed to warm to room temperature. A saturated ammonium chloride solution (125 mL) was added and the layers were separated. The water layer was extracted with diethyl ether (3x100 mL). The combined organic layers were washed with brine (50 mL) and dried over Na_2SO_4. Concentration by rotary evaporation afforded a light yellow oil, which was purified by flash column chromatography over silica using hexane/ethyl acetate (30:1) as the eluent to furnish **30** as a colourless oil (18.3 g, 99%). R_f = 0.36 (SiO_2, hexane/ethyl acetate = 30:1).

^{1}H NMR (300 MHz, $CDCl_3$) δ 0.84–1.62 (m, 27 H), 7.40 (d, J = 7.7 Hz, 1H), 7.56 (dd, J = 7.7, 1.8 Hz, 1H), 8.30 (s, 1H). ^{13}C NMR (50.3 MHz, $CDCl_3$) δ 9.5 (t), 13.4 (q), 27.0 (t), 28.3 (t), 127.9 (d), 133.4 (s), 134.1 (s), 145.9 (d), 155.9 (d). MS EI $[M]^+$ calcd for $C_{17}H_{30}BrNSn$ *m/z* 447.0, found 447; $[M–C_4H_9]^+$ 390; $[M–2C_4H_9]^+$ 334; $[M–3C_4H_9]^+$ 278. MS CI $[M+H]^+$ calcd for $C_{17}H_{31}BrNSn$ *m/z* 448.0, found 448.[113]

3-(Tributylstannyl)pyridine (31)

The same procedure as described for **30**, using 3-bromopyridine (1.49 g, 9.4 mmol), *n*-BuLi (6.2 mL, 9.9 mmol, 1.04 equiv) in dry diethyl ether (100 mL), and quenched with tributyltin chloride (2.8 mL, 10.3 mmol, 1.1 equiv) to furnish a residual yellow oil after workup. Purification by flash column chromatography over silica using a gradient of hexane/ethyl acetate

(30:1 to 3:1) furnished **31** as a colourless oil (3.3 g, 93%). R_f = 0.29 (SiO_2, hexane/ethyl acetate = 30:1).
^{1}H NMR (300 MHz, $CDCl_3$) δ 0.75–1.68 (m, 27H), 7.20 (dd, J = 7.3, 4.6 Hz, 1H), 7.72 (ddd, J = 7.3, 1.8, 1.5 Hz, 1H), 8.49 (dd, J = 4.6, 1.5 Hz, 1H), 8.58 (s, 1H).

***N*-(3-(3-Pyridinyl)phenyl)phthalimide (29)**
Following the procedure for **17** (Method B), using a mixture of stannane **31** (0.50 g, 1.4 mmol), iodide **26** (0.47 g, 1.4 mmol), and $Pd(PPh_3)_4$ (31 mg, 27 µmol, 2 mol%) in dry THF (10 mL). Workup and purification afforded **29** as a light brown solid (20 mg, 5%).[111]
^{1}H NMR (300 MHz, $CDCl_3$) δ 7.36 (dd, J = 8.0, 4.7 Hz, 1H), 7.49 (m, 1H), 7.61 (m, 2H), 7.66 (s, 1H), 7.80 (dd, J = 5.5, 3.1 Hz, 2H), 7.89 (d, J = 8.0 Hz, 1H), 7.97 (dd, J = 5.5, 3.1 Hz, 2H), 8.60 (d, J = 4.7 Hz, 1H), 8.86 (s, 1H).

***N*-(3-(6-Bromo-3-pyridinyl)phenyl)phthalimide (32)**
The same procedure as described for **29**, using stannane **30** (0.67 g, 1.5 mmol). Workup and purification afforded **32** as a yellow solid (30 mg, 5%).[111]
^{1}H NMR (300 MHz, $CDCl_3$) δ 7.50–7.64 (m, 5H), 7.75 (dd, J = 8.4, 2.6 Hz, 1H), 7.81 (dd, J = 5.5, 3.3 Hz, 2H), 7.97 (dd, J = 5.5, 3.3 Hz, 2H), 8.60 (d, J = 2.6 Hz, 1H). MS CI $[M+H]^+$ calcd for $C_{19}H_{11}N_2BrO_2$ m/z 379.0, found 379, 381 (396, 398 $[M+NH_4]^+$, 301 $[M-Br]^+$, 156 $[M-Pht-Br]^+$).

Tributyl(phenyl)stannane (33)
The same procedure as described for **30**, using bromobenzene (0.50 mL, 4.8 mmol), *n*-BuLi (3.0 mL, 4.8 mmol) in dry THF (25 mL), and quenched with tributyltin chloride (1.4 mL, 5.3 mmol, 1.1 equiv) to furnish a residual colourless oil after workup. Purification by flash column chromatography over alumina using hexane/ethyl acetate (30:1) as the eluent furnished **33** as a colourless oil (1.3 g, 73%). R_f = 0.80 (SiO_2, hexane/ethyl acetate = 30:1).
^{1}H NMR (200 MHz, $CDCl_3$) δ 0.84–1.56 (m, 27H), 7.23–7.34 (m, 2H), 7.43–7.48 (m, 3H).
^{13}C NMR (50.3 MHz, $CDCl_3$) δ 9.4 (t), 13.6 (q), 27.3 (t), 29.0 (t), 127.8 (d), 136.4 (d), 141.5 (s).
MS EI $[M]^+$ calcd for $C_{18}H_{32}Sn$ m/z 368.2, found 367; $[M-C_4H_9]^+$ 311; $[M-2C_4H_9]^+$ 255; $[M-3C_4H_9]^+$ 197.[113]

4-(3-Pyridinyl)-3-butyn-1-ol (36)
A mixture of 3-bromopyridine (0.48 mL, 5.0 mmol), freshly distilled 3-butyn-1-ol (0.57 mL, 7.5 mmol, 1.5 equiv), $PdCl_2(PPh_3)_2$ (35 mg, 50 µmol, 1 mol%), and CuI (4.8 mg, 25 µmol, 0.5 mol%) in dry TEA was stirred at room temperature for 3 days under a nitrogen atmosphere. The solvent was evaporated *in vacuo* and the residue was partitioned between CH_2Cl_2 (10 mL) and water (10 mL). After separation of the layers the aqueous layer was extracted with CH_2Cl_2 (5x10 mL). The combined organic layers were washed with water (2x10 mL), brine (10 mL), and dried over Na_2SO_4. Evaporation of the solvent afforded an orange oil (0.99 g) that was purified by flash column chromatography over silica using hexane/ethyl acetate/triethylamine (20:20:1) as the eluent to furnish **36** as a colourless oil (0.45 g, 62%).
^{1}H NMR (300 MHz, $CDCl_3$) δ 2.58 (t, J = 6.5 Hz, 2H), 3.72 (t, J = 6.5 Hz, 2H), 4.73 (br. s, 1H), 7.08 (dd, J = 8.0, 4.8 Hz, 1H), 7.55 (d, J = 8.0 Hz, 1H), 8.32 (d, J = 4.8 Hz, 1H), 8.47

(d, J = 1.1 Hz). ^{13}C NMR (50.3 MHz, $CDCl_3$) δ 23.6 (t), 60.3 (t), 78.0 (s), 91.2 (s), 120.8 (s), 122.9 (d), 138.7 (d), 147.4 (d), 151.7 (d). HRMS calcd for C_9H_9NO 147.068, found 147.069.

4-(3-Pyridinyl)-3-butynyl acetate (37)

Following the procedure for **36**, compound **37** was obtained as a light yellow oil (0.44 g, 47%) from **14** (0.48 mL, 5.0 mmol) and **35** (0.72 g, 7.5 mmol, 1.5 equiv) after workup and flash column chromatography over alumina using hexane/ethyl acetate (9:1) as the eluent.
^{1}H NMR (300 MHz, $CDCl_3$) δ 2.07 (s, 3H), 2.74 (dd, J = 7.0, 6.6 Hz, 2H), 4.23 (dd, J = 7.0, 6.6 Hz, 2H), 7.19 (dd, J = 7.7, 4.9 Hz, 1H), 7.65 (d, J = 7.7 Hz, 1H), 8.47 (d, J = 4.9 Hz, 1H), 8.61 (s, 1H). ^{13}C NMR (75.5MHz, $CDCl_3$) δ 19.9 (q), 20.8 (t), 62.1 (t), 78.8 (s), 89.1 (s), 122.9 (s), 138.5 (d), 148.3 (d), 151.0 (d), 152.4 (d), 169.1 (s). MS CI $[M+H]^+$ calcd for $C_{11}H_{12}NO_2$ m/z 190.1, found 190.

3-Pyridinylalanine derivative 44

Zinc dust (0.13 g, 2.0 mmol, 2 equiv) was activated by heating under vacuum in the presence of iodine (15 mg, 60 µmol). After cooling under a nitrogen atmosphere, a solution of iodoalanine **41** (0.33 g, 1.0 mmol) in dry DMF (0.30 mL) was added at 0°C and stirred for 3 h. $PdCl_2(PPh_3)_2$ (38 mg, 54 µmol, 5.4 mol%) and 3-bromopyridine (0.21 g, 1.3 mmol, 1.3 equiv) were added and the mixture was stirred at 40°C for 4 h. Water (10 mL) and ethyl acetate (10 mL) were added and the layers were separated. After extracting the aqueous layer with ethyl acetate (3x10 mL), the combined organic layers were washed with water (3x10 mL) and dried over $MgSO_4$. Evaporation of the solvent afforded a yellow oil (0.45 g), which was purified by column chromatography over silica using a gradient of petroleum ether (40-60)/ethyl acetate (2:1 to 1:1) to afford pure **44** as a light yellow oil (0.08 g, 29%). R_f = 0.29 (SiO_2, hexane/ethyl acetate = 30:1).
^{1}H NMR (250 MHz, $CDCl_3$) δ 1.38 (s, 9H), 2.98 (dd, J = 14.0, 6.4 Hz, 1H), 3.12 (dd, J = 14.0, 5.5 Hz, 1H), 3.68 (s, 3H), 4.53 (ddd, J = 7.6, 6.4, 5.5 Hz, 1H), 5.74 (d, J = 7.6 Hz, 1H), 7.17 (dd, J = 7.9, 4.7 Hz, 1H), 7.44 (dt, J = 7.9, 1.4 Hz, 1H), 8.28 (s, 1H), 8.44 (dd, J = 4.7, 1.4 Hz, 1H). ^{13}C NMR (62.8 MHz, $CDCl_3$) δ 28.1 (q), 35.5 (t), 52.3 (q), 54.0 (d), 80.0 (s), 123.3 (d), 131.7 (s), 136. 7 (d), 148.3 (d), 150.4 (d), 154.8 (s), 171.7 (s).

2-Pyridinylalanine derivative 45

The same procedure as described for **44**, using 2-bromopyridine (0.21 g, 1.3 mmol, 1.3 equiv) to afford after workup and column chromatography pure **45** as a light yellow oil (0.11 g, 39%). R_f = 0.46 (SiO_2, hexane/ethyl acetate = 30:1).
^{1}H NMR (250 MHz, $CDCl_3$) δ 1.37 (s, 9H), 3.20 (dd, J = 14.6, 5.3 Hz, 1H), 3.28 (dd, J = 14.6, 5.5 Hz, 1H), 3.65 (s, 3H), 4.64 (ddd, J = 8.3, 5.5, 5.3 Hz, 1H), 5.87 (d, J = 8.3 Hz, 1H), 7.03 (m, 2H), 7.50 (dt, J = 7.6, 1.8 Hz, 1H), 8.40 (dd, J = 4.0, 1.8 Hz, 1H). ^{13}C NMR (62.8 MHz, $CDCl_3$) δ 28.20 (q), 39.20 (t), 52.15 (q), 52.90 (d), 79.61 (s), 121.72 (d), 123.61 (d), 136.45 (d), 149.10 (d), 155.42 (s), 157.06 (s), 172.35 (s).

2-Cyano-5-({[*tert*-butyl(dimethyl)silyl]oxy}methyl)pyridine (47)[114]

A mixture of bromide **41**[115] (3.0 g, 10 mmol), $Zn(CN)_2$ (0.70 g, 6.0 mmol), dppf (8.4 mg, 15 µmol, 0.15 mol%), and $Pd_2(dba)_3$ (5.9 mg, 6.4 µmol, 0.064 mol%) was heated in DMF (5 mL) and water (50 µL) under nitrogen at 110°C overnight. After the addition of water (10 mL) and

diethyl ether (25 mL) the layers were separated. The organic layer was washed with water (4x5 mL), brine (5 mL), and dried over Na_2SO_4. Evaporation of the solvent furnished a black residue that was purified by flash column chromatography over silica using a gradient of hexane/diethyl ether (5:1 to 3:1). The product was obtained as a light brown oil (0.98 g, 40%). R_f = 0.43 (SiO_2, hexane/diethyl ether = 3:1).
^{1}H NMR ($CDCl_3$, 300 MHz) δ 0.11 (s, 6H), 0.93 (s, 9H), 4.81 (s, 2H), 7.66 (d, J = 8.1 Hz, 1H), 7.80 (dd, J = 8.1, 1.1 Hz, 1H), 8.64 (s, 1H). ^{13}C NMR ($CDCl_3$, 75.5 MHz) δ –5.4 (q), 18.1 (s), 25.7 (q), 62.0 (t), 117.3 (s), 128.0 (d), 132.1 (s), 134.2 (d), 140.9 (s), 148.9 (d). HRMS calcd for $C_{13}H_{20}N_2OSi$ 248.134, found 248.135.

***N*-[Bis(5-phenyl-2-pyridinyl)methyl]-*N*,*N*-bis[(5-phenyl-2-pyridinyl)methyl]amine (48)**
A mixture of tetrabromo N4Py (**3**) (0.20 g, 0.30 mmol), phenylboronic acid (0.36 g, 3.0 mmol, 10 equiv), $Pd(PPh_3)_4$ (40 mg, 34 µmol, 12 mol%), aqueous Na_2CO_3 (2 M, 2 mL), and 4 droplets of ethylene glycol was heated at reflux in toluene (4 mL) under a nitrogen atmosphere overnight. The layers were separated and the aqueous phase was extracted with CH_2Cl_2 (3x10 mL). The combined organic layers were washed with aqueous Na_2CO_3 (2 M, 3x5 mL), brine (10 mL), and dried over Na_2SO_4. Evaporation of the solvent afforded the product as a dark yellow oil that solidified upon standing (0.16 g, 80%).
^{1}H NMR (300 MHz, $CDCl_3$) δ 4.10 (s, 4H), 5.50 (s, 2H), 7.30–7.90 (m, 28H), 8.72 (d, J = 2.2 Hz, 2H), 8.82 (s, 1H). ^{13}C NMR (50.3 MHz, $CDCl_3$) δ 57.3 (t), 72.4 (d), 115.6 (d), 119.0 (d), 123.0 (d), 123.8 (d), 126.8 (d), 126.9 (d), 127.8 (d), 128.2 (d), 128.4 (d), 128.8 (d), 131.8 (d), 132.0 (d),134.6 (d), 134.7 (s), 134.9 (s), 137.5 (d), 147.2 (d), 147.6 (d), 158.3 (s), 158.6 (s). MS CI $[M+H]^+$ calcd for $C_{47}H_{38}N_5$ *m/z* 672.3, found 672; Fragmentations *m/z* 352, 323, 170.[113]

6-({[bis(5-bromo-2-pyridinyl)methyl][(5-formyl-2-pyridinyl)methyl]amino}methyl)-nicotinaldehyde (49c)
To **3** was added isopropylmagnesium bromide (4.5 equiv, 2 M in THF) and the mixture was stirred at room temperature for 1 h. A sample was quenched with water and analysed by ESI-MS to reveal the mass of **49a**. More isopropylmagnesium bromide (4 equiv) was added and the reaction mixture was heated to reflux for 1 h. Dry DMF (15 equiv) was added. The mixture was washed with water, brine, and dried over Na_2SO_4. Evaporation of the solvent afforded a brown oil.
^{1}H NMR (300 MHz, $CDCl_3$) δ 4.03 (s, 4H), 5.27 (s, 1H), 7.52 (d, J = 8.2 Hz, 2H), 7.71 (d, J = 8.2 Hz, 2H), 7.76 (dd, J = 8.2, 1.8 Hz, 2H), 8.07 (dd, J = 8.2, 1.8 Hz, 2H), 8.58 (d, J = 1.8 Hz, 2H), 8.93 (d, J = 1.8 Hz, 2H), 10.04 (s, 2H). ^{13}C NMR (50.3 MHz, $CDCl_3$) δ 58.0 (t), 71.8 (d), 120.5 (s), 124.1 (d), 126.0 (d), 130.9 (s), 136.9 (d), 139.8 (d), 150.2 (d), 152.4 (d), 158.2 (s), 166.2 (s), 191.1 (d).

4.8 References and notes

1. For an explanation of the abbreviations used, see Appendix 1 (p. 149).
2. Parham, W. E.; Piccirilli, R. M. *J. Org. Chem.* **1977**, *42*, 257–260.
3. Kondo, Y.; Shilai, M.; Uchiyama, M.; Sakamoto, T. *J. Chem. Soc.*, *Perkin Trans. 1* **1996**, 1781–1782.

4. Wang, X.; Rabbat, P.; O'Shea, P.; Tillyer, R.; Grabowski, E. J. J.; Reider, P. J. *Tetrahedron Lett.* **2000**, *41*, 4335–4338.
5. Nshimyumukiza, P.; Cahard, D.; Rouden, J.; Lasne, M.-C.; Plaquevent, J.-C. *Tetrahedron Lett*. **2001**, *42*, 7787–7790
6. Bolm, C.; Ewald, M.; Felder, M.; Schlingloff, G. *Chem. Ber.* **1992**, *125*, 1169–1190.
7. (a) Tsukube, H.; Uenishi, J.; Higaki, H.; Kikkawa, K.; Tanaka, T.; Wakabayashi, S.; Oae, S. *J. Org. Chem.* **1993**, *58*, 4389–4397. (b) Cai, D.; Hughes, D. L.; Verhoeven, T. R. *Tetrahedron Lett.* **1996**, *37*, 2537–2540.
8. Paterson, M. A.; Mitchell, J. R. *J. Org. Chem.* **1997**, *62*, 8237–8239.
9. Lai, Y.-H. *Synthesis* **1981**, 585–604.
10. (a) Trécourt, F.; Breton, G.; Bonnet, V.; Mongin, F.; Marsais, F.; Quéguiner, G. *Tetrahedron Lett.* **1999**, *40*, 4339–4342. (b) Trécourt, F.; Breton, G.; Bonnet, V.; Mongin, F.; Marsais, F.; Quéguiner, G. *Tetrahedron* **2000**, *56*, 1349–1360.
11. (a) Abarbi, M.; Dehmel, F.; Knochel, P. *Tetrahedron Lett.* **1999**, *40*, 7449–7453. (b) Abarbri, M.; Thibonnet, J.; Bérillon, L.; Dehmel, F.; Rottländer, M.; Knochel, P. *J. Org. Chem*. **2000**, *65*, 4618–4634.
12. See the Experimental Section in Chapter 3 for the preparation of compounds **29** and **33**.
13. Iida, T.; Wada, T.; Tomimoto, K.; Mase, T. *Tetrahedron Lett.* **2001**, *42*, 4841–4844.
14. See Scheme 3.2 in Chapter 3, p. 47.
15. X. Wang, *personal communication* (See reference 4).
16. Alternatively, ethyl chloroformate can also be used to quench the reaction.
17. Lehmann, U.; Schlüter, A. D. *Eur. J. Org. Chem*. **2000**, 3483–3487.
18. Song, J. J.; Yee, N. K. *J. Org. Chem.* **2001**, *66*, 605–608.
19. Colasson, B. X.; Dietrich-Buchecker, C.; Sauvage, J.-P. *Synlett* **2002**, 271–272.
20. Roelfes, J. G., In *Models for Non-Heme Iron Containing Oxidation Enzymes*, Ph. D. thesis, Groningen, 2000.
21. (a) Abblard, J.; Decoret, C.; Cronenberger, L.; Pacheco, H. *Bull. Soc. Chim. Fr.* **1972**, 2466–2481. (b) Guthikonda, R. N.; Cama, L. D.; Quesada, M.; Woods, M. F.; Salzmann, T. N.; Christensen, B. G. *J. Med. Chem.* **1987**, *30*, 871–880.
22. Picolyl chloride **13** can be stored for many months under a nitrogen atmosphere in a freezer without any detectable signs of decomposition.
23. See Chapter 3.
24. J. G. Roelfes, *personal communication*.
25. Miyaura, N.; Suzuki, A. *J. Chem. Soc.*, *Chem Commun.* **1979**, 866–867.
26. Stille, J. K. *Angew. Chem. Int Ed. Engl.* **1986**, *25*, 508–524.
27. (a) Hassan, J.; Penalva, V.; Lavenot, L.; Gozzi, C.; Lemaire, M. *Tetrahedron* **1998**, *54*, 13793–13804. (b) Hassan, J.; Hathroubi, C.; Gozzi, C.; Lemaire, M. *Tetrahedron Lett*. **2000**, *41*, 8791–8794.
28. For Suzuki cross coupling reactions, see (a) Miyaura, N.; Suzuki, A. *Chem. Rev.* **1995**, *95*, 2457–2483. (b) Suzuki, A., In *Metal-catalyzed Cross-coupling Reactions*; Diederich, F.; Stang, P. J., Eds.; Wiley-VCH Verlag GmbH: Germany, 1998; pp. 49–97. (c) Suzuki, A. *J. Organometal. Chem.* **1999**, *576*, 147–168.

29. For Stille cross coupling reactions, see (a) Mitchell, T. N. *Synthesis* **1992**, 803–815. (b) Farina, V.; Krishnamurthy, V.; Scott, W. J., In *Organic Reactions*; Paquette, L. A. *et al*., Eds.; John Wiley & Sons, Inc.: USA, 1997; Vol. 50. (c) Mitchell, T. N., In *Metal-catalyzed Cross-coupling Reactions*; Diederich, F.; Stang, P. J., Eds.; Wiley-VCH Verlag GmbH: Germany, 1998; pp. 167–202.
30. Genet , J. P.; Savignac, M. *J. Organometal. Chem*. **1999**, *576*, 305–317.
31. (a) Zou, G.; Reddy, Y. K.; Falck, J. R. *Tetrahedron Lett.* **2001**, *42*, 7213–7215. (b) Molander, G. A.; Yun, C.-S. *Tetrahedron* **2002**, *58*, 1465–1470.
32. Chemler, S. R.; Trauner, D.; Danishefsky, S. J. *Angew. Chem. Int. Ed*. **2001**, *40*, 4544–4568.
33. Netherton, M. R.; Dai, C.; Neuschütz, K.; Fu, G. C. *J. Am. Chem. Soc*. **2001**, *123*, 10099–10100.
34. Sonogashira, K.; Tohda, Y.; Hagihara, N. *Tetrahedron Lett.* **1975**, 4467–4470.
35. For Sonogashira cross coupling reactions, see (a) M. Schlosser (Ed.), In *Organometallics in Synthesis*; John Wiley: Chichester, 1994. (b) Sonogashira, K., In *Metal-catalyzed Cross-coupling Reactions*; Diederich, F.; Stang, P. J., Eds.; Wiley-VCH Verlag GmbH: Germany, 1998; pp. 203–230.
36. Heck, R. F.; Nolley, J. P., Jr. *J. Org. Chem.* **1972**, *37*, 2320–2322.
37. (a) Bräse, S.; De Meijere, A., In *Metal-catalyzed Cross-coupling Reactions*; Diederich, F.; Stang, P. J., Eds.; Wiley-VCH Verlag GmbH: Germany, 1998; pp. 99–166. (b) Beletskaya, I. P.; Cheprakov, A. V. *Chem. Rev.* **2000**, *100*, 3009–3066. (c) Whitcombe, N. J.; Hii, K. K.; Gibson, S. E. *Tetrahedron* **2001**, *57*, 7449–7476.
38. See Söderberg, B. C. G. *Coord. Chem. Rev.* **2002**, *224*, 171–243 for an overview with 1621 references on transition metals in organic synthesis with highlights for the year 1999.
39. (a) Littke, A. F.; Fu, G. C. *Angew. Chem. Int. Ed.* **1998**, *37*, 3387–3388. (b) Wolfe, J. P.; Buchwald, S. L. *Angew. Chem. Int. Ed.* **1999**, *38*, 2413–2416. (c) Stürmer, R. *Angew. Chem. Int. Ed.* **1999**, *38*, 3307–3308. (d) Wolfe, J. P.; Singer, R. A.; Yang, B. H.; Buchwald, S. L. *J. Am. Chem. Soc.* **1999**, *121*, 9550–9561. (e) Zhang, C.; Huang, J.; Trudell, M. L.; Nolan, S. P. *J. Org. Chem*. **1999**, *64*, 3804–3805. (f) Zapf, A.; Ehrentraut, A.; Beller, M. *Angew. Chem. Int. Ed.* **2000**, *39*, 4153–4155. (g) Bedford, R. B.; Cazin, C. S. J. *Chem. Commun*. **2001**, 1540–1541.
40. (a) Ishiyama, T.; Murata, M.; Miyaura, N. *J. Org. Chem.* **1995**, *60*, 7508–7510. (b) Ishiyama, T.; Itoh, Y.; Kintano, T.; Miyaura, N. *Tetrahedron Lett.* **1997**, *38*, 3447–3450. (c) Murata, M.; Watanabe; S.; Masuda, Y. *J. Org. Chem.* **1997**, *62*, 6458–6459. (d) Murata, M.; Oyama, T.; Watanabe; S.; Masuda, Y. *J. Org. Chem.* **2000**, *65*, 164–168. (e) Baudoin, O.; Guénard, D.; Guéritte, F. *J. Org. Chem.* **2000**, *65*, 9268–9271. (f) Wong, K.-T.; Chien, Y.-Y.; Liao, Y.-L.; Lin, C.-C.; Chou, M.-Y.; Leung, M.-K. *J. Org. Chem.* **2000**, *65*, 1041–1044.
41. (a) Cho, J.-Y.; Tse, M. K.; Holmes, D.; Maleczka, R. E., Jr.; Smith III, M. R. *Science* **2002**, *295*, 305–308. (b) Ishiyama, T.; Takagi, J.; Ishida, K.; Miyaura, N.; Anastasi, N. R.; Hartwig, J. F. *J. Am. Chem. Soc.* **2002**, *124*, 390–391.
42. (a) Wu, G. G.; Wong, Y.; Poirier, M. *Org. Lett.* **1999**, *1*, 745–747. (b) Couve-Bonnaire, S.; Carpentier, J.-F.; Mortreux, A.; Castanet, Y. *Tetrahedron Lett*. **2001**, *42*, 3689–3691.

43. Tilley, J. W.; Zawoiksi, S. *J. Org. Chem.* **1988**, *53*, 386–390.
44. Lehmann, U.; Henze, O.; Schlüter, A. D. *Chem. Eur. J.* **1999**, *5*, 854–856.
45. Vice, S.; Bara, T.; Bauer, A.; Evans, C. A.; Ford, J.; Josien, H.; McCombie, S.; Miller, M.; Nazareno, D.; Palani, A.; Tagat, J. *J. Org. Chem*. **2001**, *66*, 2487–2492.
46. For bromopyridines in Suzuki reactions, see (a) Thompson, W. J.; Gaudino, J. *J. Org. Chem.* **1984**, *49*, 5237–5243. (b) Stavenuiter, J.; Hamzink, M.; Van der Hulst, R.; Zomer, G.; Westra, G.; Kriek, E. *Heterocycles* **1987**, *26*, 2711–2716. (c) Thompson, W. J.; Jones, J. H.; Lyke, P. A.; Thies, J. E. *J. Org. Chem.* **1988**, *53*, 2052–2055. (d) Aliprantis, A. O.; Canary, J. W. *J. Am. Chem. Soc.* **1994**, *116*, 6985–6986. (e) Gong, Y.; Pauls, H. W. *Synlett* **2000**, 829–831.
47. Li, J. J.; Gribble, G. W., In *Palladium in Heterocyclic Chemistry: A Guide for the Synthetic Chemist*, Pergamon: Oxford, UK, 2000; Vol. 20, pp. 183–232.
48. Feuerstein, M.; Laurenti, D.; Bougeant, C.; Doucet, H.; Santelli, M. *Chem. Commun.* **2001**, 325–326.
49. Witulski, B. *Synlett* **1999**, 1223–1226.
50. (a) Indolese, A. F. *Tetrahedron Lett.* **1997**, *38*, 3513–3516. (b) Saito, S.; Oh-tani, S.; Miyaura, N. *J. Org. Chem*. **1997**, *62*, 8024–8030.
51. Ishiyama, T.; Ishida, K. Miyaura, N. *Tetrahedron* **2001**, *57*, 9813–9816.
52. LeBlond, C. R.; Andrews, A. T.; Sun, Y.; Sowa, J. R., Jr. *Org. Lett*. **2001**, *3*, 1555–1557.
53. Lipshutz, B. H.; Sclafani, J. A.; Blomgren, P. A. *Tetrahedron* **2000**, *56*, 2139–2144.
54. Van den Berg, T. A., *Undergraduate report*, University of Groningen: The Netherlands, **2002**.
55. Fernando, S. R. L.; Maharoof, U. S. M.; Deshayes, K. D.; Kinstle, T. H.; Ogawa, M. Y. *J. Am. Chem. Soc*. **1996**, *118*, 5783–5790.
56. Conditions analogous to reference 40e.
57. Bouillon, A.; Lancelot, J.-C.; Collot, V.; Bovy, P. R.; Rault, S. *Tetrahedron* **2002**, *58*, 2885–2890.
58. (a) Bhagwat, S. S.; Gude, C.; Cohen, D. S.; Dotson, R.; Mathis, J.; Lee, W.; Furness, P. *J. Med. Chem.* **1993**, *36*, 205–210. (b) Alvarez, R.; Herrero, M.; López, S.; De Lera, A. R. *Tetrahedron* **1998**, *54*, 6793–6810. (c) Baldwin, J. E.; James, D. A.; Lee, V. *Tetrahedron Lett.* **2000**, *41*, 733–736.
59. Palucki, M.; Hughes, D. L.; Yasuda, N.; Yang, C.; Reider, P. J. *Tetrahedron Lett*. **2001**, *42*, 6811–6814.
60. Feuerstein, M.; Doucet, H.; Santelli, M. *Tetrahedron Lett*. **2001**, *42*, 5659–5662.
61. Molander, G. A.; Rivero, M. R. *Org. Lett*. **2002**, *4*, 107–109.
62. Shirakawa, E.; Yamasaki, K.; Hiyama, T. *Synthesis* **1998**, 1544–1549.
63. (a) Leibner, J. E.; Jacobus, J. *J. Org. Chem.* **1979**, *44*, 449–450. (b) Berge, J. M.; Roberts, S. M. *Synthesis* **1979**, 471–472. (c) Crich, D.; Sun, S. *J. Org. Chem.* **1996**, *61*, 7200–7201. (d) Renaud, P.; Lacôte, E.; Quaranta, L. *Tetrahedron Lett.* **1998**, *39*, 2123–2126. (e) Edelson, B., S.; Stoltz, B. M.; Corey, E. J. *Tetrahedron Lett.* **1999**, *40*, 6729–6730. (f) Salomon, C. J.; Danelon, G. O.; Mascaretti, O. A. *J. Org. Chem.* **2000**, *65*, 9220–9222.
64. Knight, S. D.; Overman, L. E.; Pairaudeau, G. *J. Am. Chem. Soc*. **1995**, *117*, 5776–5788.

65. (a) Azizian, H.; Eaborn, C.; Pidcock, A. *J. Organomet. Chem.* **1981**, *215*, 49–58. (b) Yokoyama, Y.; Ito, S.; Takahashi, Y.; Murakami, Y. *Tetrahedron Lett.* **1985**, *26*, 6457–6460. (c) Kelly, T. R.; Lang, F. *J. Org. Chem.* **1996**, *61*, 4623–4633. (d) Schwab, P. F. H.; Fleischer, F.; Michl, J. *J. Org. Chem*. **2002**, *67*, 443–449.
66. Kelly, T. R.; Li, Q.; Bhushan, V. *Tetrahedron Lett.* **1990**, *31*, 161–164.
67. Zhang, N.; Thomas, L.; Wu, B. *J. Org. Chem.* **2001**, *66*, 1500–1502.
68. Hitchcock, S. A.; Mayhugh, D. R.; Gregory, G. S. *Tetrahedron Lett*. **1995**, *36*, 9085–9088.
69. (a) Henze, O.; Lehmann, U.; Schlüter, A. D. *Synthesis* **1999**, 683–687. (b) Manickam, G.; Schlüter, A. D. *Synthesis* **2000**, 442–446.
70. (a) Hanan, G. S.; Schubert, U. S.; Volkmer, D.; Rivière, E.; Lehn, J.-M.; Kyritsakas, N.; Fischer, J. *Can. J. Chem.* **1997**, *75*, 169–182. (b) Romero-Salguero, F. J.; Lehn, J.-M. *Tetrahedron Lett.* **1999**, *40*, 859–862. (c) Schubert, U. S.; Eschbaumer, C.; Weidl, C. H. *Synlett* **1999**, 342–344. (d) Schubert, U. S.; Eschbaumer, C. *Org Lett*. **1999**, *1*, 1027–1029.
71. Procedure analogous to Vogel, A. I., In *Vogel's Textbook of Practical Organic Chemistry*; Furniss, B. S.; Hannaford, A. J.; Smith, P. W. G.; Tatchell, A. R., Eds.; Longman Group, Ltd.: UK, 1989; 5th edition, p. 1276.
72. (a) Liebeskind, L. S.; Fengl, R. W. *J. Org. Chem.* **1990**, *55*, 5359–5364. (b) Farina, V.; Kapadia, S.; Krishnan, B.; Wang, C.; Liebeskind, L. S. *J. Org. Chem.* **1994**, *59*, 5905–5911. (c) Ellingboe, J. W.; Antane, M.; Nguyen, T. T.; Collini, M. D.; Antane, S.; Bender, R.; Hartupee, D.; White, V.; McCallum, J.; Park, C. H.; Russo, A.; Osler, M. B.; Wojdan, A.; Dinish, J.; Ho, D. M.; Bagli, J. F. *J. Med. Chem.* **1994**, *37*, 542–550.
73. Bertrus, P; Pale, P. *Tetrahedron Lett.* **1996**, *37*, 2019–2022.
74. (a) Okuro, K.; Furuune, M.; Miura, M.; Nomura, M. *Tetrahedron Lett.* **1992**, *33*, 5363–5364. (b) Okuro, K.; Furuune, M.; Enna, M.; Miura, M.; Nomura, M. *J. Org. Chem.* **1993**, *58*, 4716–4721.
75. Snider, B. B.; Shi, B. *Tetrahedron Lett*. **2001**, *42*, 1639–1642.
76. For 2-chloro-5-iodopyridine as a substrate, see (a) Baxter, P. N. W. *J. Org. Chem*. **2000**, *65*, 1257–1272. (b) Baxter, P. N. W. *J. Org. Chem*. **2001**, *66*, 4170–4179.
77. Ames, D. E.; Bull, D.; Takundu, C. *Synthesis*, **1981**, 364–356.
78. Minn, K. *Synlett* **1991**, 115–116.
79. Littke, A. F.; Fu, G. C. *J. Org. Chem*. **1999**, *64*, 10–11.
80. Stephan, M. S.; Teunissen, A. J. J. M.; Verzijl, G. K. M.; De Vries, J. G. *Angew. Chem. Int. Ed*. **1998**, *37*, 662–664.
81. (a) Bumagin, N. A.; Bykov, V. V.; Sukhomlinova, L. I.; Tolstaya, T. P.; Beletskaya, I. P. *J. Organomet. Chem*. **1995**, *486*, 259–262. (b) Ford, N. F.; Browne, L. J.; Campbell, T.; Gemenden, C.; Goldstein, R.; Gude, C.; Wasley, J. W. F. *J. Med. Chem.* **2000**, *28*, 164–170. (c) Cannes, C.; Condon, S.; Durandetti, M.; Perichon, J.; Nedelec, J. Y. *J. Org. Chem*. **2000**, *65*, 4575–4583. (d) Feuerstein, M.; Doucet, H.; Santelli, M. *J. Org. Chem*. **2001**, *66*, 5923–5925.
82. Tamaru, Y.; Yamada, Y.; Yoshida, Z.-I. *J. Org. Chem.* **1978**, *43*, 3396–3398.
83. J. G. de Vries, *personal communication*.

84. Pino, P.; Piccolo, O.; Straub, B.; Consiglio, G.; Tran, D. C. *Helv. Chim. Acta* **1982**, *65*, 2102–2109.
85. For the use of nickel on charcoal for the cross coupling reaction of aryl chlorides, see (a) Lipshutz, B. H.; Tomioka, T.; Blomgren, P. A.; Sclafani, J. A. *Inorg. Chim. Acta* **1999**, *296*, 164–169. (b) Lipshutz, B. H.; Blomgren, P. A. *J. Am. Chem. Soc.* **1999**, *121*, 5819–5820.
86. (a) Tamao, K.; Sumitani, K.; Kumada, M. *J. Am. Chem. Soc.* **1972**, *94*, 4374–4376. (b) Tamao, K.; Kiso, Y. Sumitani, K.; Kumada, M. *J. Am. Chem. Soc.* **1972**, *94*, 9268–9269. (c) Tamao, K.; Zembayashi, M.; Kiso, Y.; Kumada, M. *J. Organometal. Chem.* **1973**, *55*, C91–C94. (d) Tamao, K.: Sumitani, K.; Kiso, Y.; Zembayashi, M.; Fujioka, A.; Kodama, S.; Nakajima, I.; Minato, A.; Kumada, M. *Bull. Chem. Soc. Jpn*. **1976**, *49*, 1958–1969. (e) Hayashi, T.; Konishi, M.; Kobori, Y.; Kumada, M. *J. Am. Chem. Soc.* **1984**, *106*, 158–163.
87. Corriu, R. J. P.; Masse, J. P. *J. Chem. Soc., Chem. Commun.* **1972**, 144.
88. For the application of aryl fluorides with arylmagnesium bromides, see Böhm, V. P. W.; Gstöttmayr, C. W. K.; Weskamp, T.; Herrmann, W. A. *Angew. Chem. Int. Ed*. **2001**, *40*, 3387–3389.
89. (a) Negishi, E.; Baba, S. *J. Chem. Soc., Chem. Commun.* **1976**, 596–597. (b) Negishi, E.; King, A. O.; Okukadu, N. *J. Org. Chem.* **1977**, *42*, 1821–1823. (c) King, A. O.; Okukadu, N.; Negishi, E. *J. Chem. Soc., Chem. Commun.* **1977**, 683–684. (d) King, A. O.; Negishi, E. *J. Org. Chem.* **1978**, *43*, 358–360.
90. Sakamoto, T.; Nishimura, S.; Kondo, Y.; Yamanaka, H. *Synthesis* **1988**, 485–486.
91. (a) Jackson, R. F. W.; James, K.; Wythes, M. J.; Wood, A. *J. Chem. Soc., Chem. Commun.* **1989**, 644–645. (b) Jackson, R. F. W.; Turner, D.; Block, M. H. *Synlett* **1996**, 862–864. (c) Dexter, C. S.; Jackson, R. F. W. *J. Chem. Soc., Chem. Commun.* **1998**, 75–76. (d) Dexter, C. S.; Jackson, R. F. W. *J. Org. Chem.* **1999**, *64*, 7579–7585. (e) Dexter, C. S.; Jackson, R. F. W.; Elliott, J. *Tetrahedron* **2000**, *56*, 4539–4540.
92. Walker, M. A.; Kaplita, K. P.; Chen, T.; King, H. D. *Synlett* **1997**, 169–170.
93. Uehling, D. E.; Nanthakumar, S. S.; Croom, D.; Emerson, D. L.; Leitner, P. P.; Luzzio, M. J.; McIntyre, G.; Morton, B.; Profeta, S.; Sisco, J.; Sternbach, D. D.; Tong, W. Q.; Vuong, A.; Besterman, J. M. *J. Med. Chem.* **1995**, *38*, 1106–1118.
94. Maligres, P. E.; Waters, M. S.; Fleitz, F.; Askin, D. *Tetrahedron Lett.* **1999**, *40*, 8193–8195.
95. (a) Rottländer, M.; Boymond, L.; Bérillon, L.; Leprêtre, A.; Varchi, G.; Avolio, S.; Laaziri, H.; Quéguiner, G.; Ricci, A.; Cahiez, G.; Knochel, P. *Chem. Eur. J.* **2000**, *6*, 767–770. (b) Boudier, A.; Bromm, L. O.; Lotz, M.; Knochel, P. *Angew. Chem. Int. Ed.* **2000**, *39*, 4414–4435.
96. Dohle, W.; Kopp, F.; Cahiez, G.; Knochel, P. *Synlett* **2001**, 1901–1904.
97. Bonnet, V.; Mongin, F.; Trécourt, F.; Quéguiner, G.; Knochel, P. *Tetrahedron Lett.* **2001**, *42*, 5717–5719.
98. Fürstner, A.; Leitner, A. *Angew. Chem. Int. Ed.* **2002**, *41*, 609–612.
99. (a) Hartwig, J. F. *Angew. Chem. Int. Ed.* **1998**, *37*, 2046–2067. (b) Wolfe, J. P.; Wagaw, S.; Marcoux, J.-F.; Buchwald, S. L. *Acc. Chem. Res.* **1998**, *31*, 805–818.

100. (a) Guram, A. S.; Rennels, R. A.; Buchwald, S. L. *Angew. Chem. Int. Ed. Engl.* **1995**, *34*, 1348–1350. (b) Louie, J.; Hartwig, J. F. *Tetrahedron Lett*. **1995**, *36*, 3609–3612. (c) Wagaw, S.; Buchwald, S. L. *J. Org. Chem*. **1996**, *61*, 7240–7241. (d) Frost, C. G.; Mendoça, P. *J. Chem. Soc., Perkin Trans. 1* **1998**, 2615–2623. (e) Yang, B. H.; Buchwald, S. L. *J. Organomet. Chem*. **1999**, *576*, 125–146. (f) Lipshutz, B. H.; Ueda, H. *Angew. Chem. Int. Ed.* **2000**, *39*, 4492–4494. (g) Kwong, F. Y.; Klapars, A.; Buchwald, S. L. *Org. Lett.* **2002**, *4*, 581–584.
101. Grasa, G. A.; Viciu, M. S.; Huang, J.; Nolan, S. P. *J. Org. Chem*. **2001**, *66*, 7729–7737.
102. Huang, X.; Buchwald, S. L. *Org. Lett.* **2001**, *3*, 3417–3419.
103. Brenner, E.; Schneider, R.; Fort, Y. *Tetrahedron* **1999**, *55*, 12829–12842.
104. Jonckers, T. H. M.; Maes, B. U. W.; Lemière, G. L. F.; Dommisse, R. *Tetrahedron* **2001**, *57*, 7027–7034.
105. Yin, J.; Buchwald, S. L. *Org. Lett.* **2000**, *2*, 1101–1104.
106. Klapars, A.; Antilla, J. C.; Huang, X.; Buchwald, S. L. *J. Am. Chem. Soc.* **2001**, *123*, 7727–7729.
107. Versleijen, J., In *Isocyanomethylboranes, isocyanomethylphosphonates and phosphoramidites for use in organic synthesis*, Ph. D. thesis, Groningen, 2001, p. 52.
108. The crude product consisted of approximately 82% **6** and about 18% of the regio-isomer **5**, as determined by ^{1}H NMR. The calculated yield of **6**, therefore, was 75%. The unstable aldehyde prevents purification and storage for a prolonged time (see reference 15).
109. The low yield was attributed to the impure aldehyde that was used, the instability of the aldehyde, the incomplete regioselectivity in the lithiation reaction, and the reaction of the aldehyde with the excess *n*-BuLi that was still present in the reaction mixture.
110. Blanz, E. J., Jr.; French, F. A.; DoAmaral, J. R.; French, D. A. *J. Med. Chem*. **1970**, *13*, 1124–1130.
111. The reported low yield is due to a loss of product by column chromoatography. Even after this purification step the product still contained tin salts. However, the Stille reaction proceeded cleanly as indicated by ^{1}H NMR analysis of the crude product.
112. See also reference 44 for an alternative procedure via the transesterification of the corresponding boronic acid with pinacol.
113. Exact mass (HRMS) was not possible.
114. Procedure analogous to reference 94.
115. See the Experimental Section in Chapter 3 for the preparation of compound **7**.

Chapter 5

Characterisation and application of tetrasubstituted N4Py iron complexes

5.1 Introduction

Several tetrasubstituted N4Py derivatives have been described in earlier chapters.[1] The synthesis of such pentadentate ligands was centred on the construction of a tetrafunctionalised N4Py derivative that would facilitate the covalent attachment of four peptide chains (Chapter 3). During the development of a synthetic pathway to this type of template, some N4Py derivatives were prepared enabling the spectroscopic features and the oxidation behaviour of their iron complexes to be examined. These experimental results will be presented and discussed in this chapter. Furthermore, the peroxidase activity of a N4PyFe-peptide complex will be described, as well as the stability of the sulphur linker that has been used to couple the peptides to the ligand.

5.2 Iron(II) complexes of tetrasubstituted N4Py ligands

The iron(II) complex **2a** of N4Py (**1a**) has previously been fully characterised and has shown to be a good functional mimic of the non-haem glycopeptide iron bleomycin (Fe–BLM).[2] A catalytic cycle was proposed for N4PyFe (summarised in Chapter 2),[2] which could also be applicable to Fe–BLM.

Several structural variations on **2a** have been carried out to ascertain the correlation between the composition of the iron(II) complex and its oxidation behaviour.[2b] These changes involved altering the oxidation state of the metal ion, the nature of axial ligand, and the N4Py ligand itself. Various mono- and disubstituted derivatives of **1a** and their iron complexes have been prepared and characterised as low-spin iron(II) complexes.[2] The complex **2a** will be referred to here only as a reference for the newly developed tetrasubstituted N4Py complexes **2b–f**.[2,3]

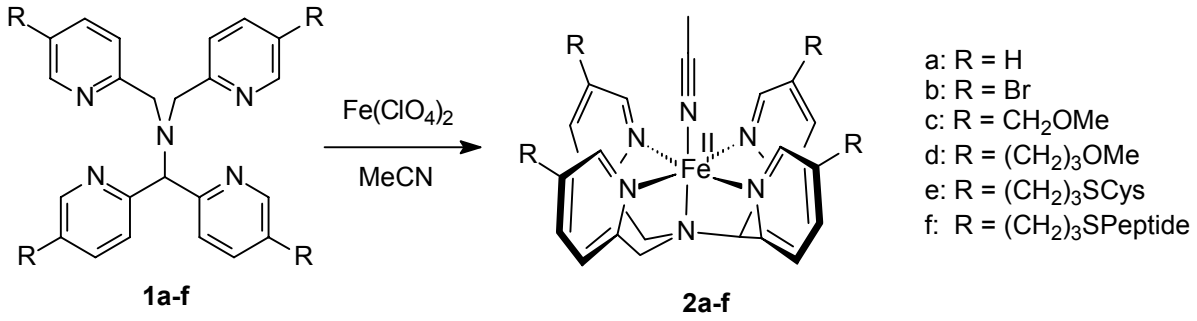

Scheme 5.1. The iron(II) complexes of N4Py (**1a**) and tetrasubstituted N4Py derivatives **1b–f** (peptide=Ac–CGLHELLKG–NH_2, coupled via the cysteine residue).[4]

Upon the addition of iron(II) perchlorate to the pentadentate ligands **1a–f** in acetonitrile the iron complexes **2a–f** were obtained (Scheme 5.1). The synthesis and characterisation of these tetrasubstituted N4Py derivatives **1b–f** have been described in earlier chapters. The corresponding iron complexes have not yet been discussed with the exception of **2e** and **2f**, which were described in Chapter 3.[5]

The ^{1}H NMR spectra of **2b–d** in CD_3CN revealed signals in the diamagnetic range of 0–10 ppm, which is distinctive for low-spin iron(II) complexes of N4Py ligands.[2] The UV-Vis absorption bands of **2b–f** (Table 5.2 p. 123, Figure 5.5 p. 122) also correlate well with those of the previously prepared iron(II) complexes of N4Py derivatives with maximum absorptions typically around 380 and 460 nm as expected.[2b,5] In addition, the electrospray ionisation mass analyses (ESI-MS) were in accordance with the postulated composition of the complexes **2b–d**.

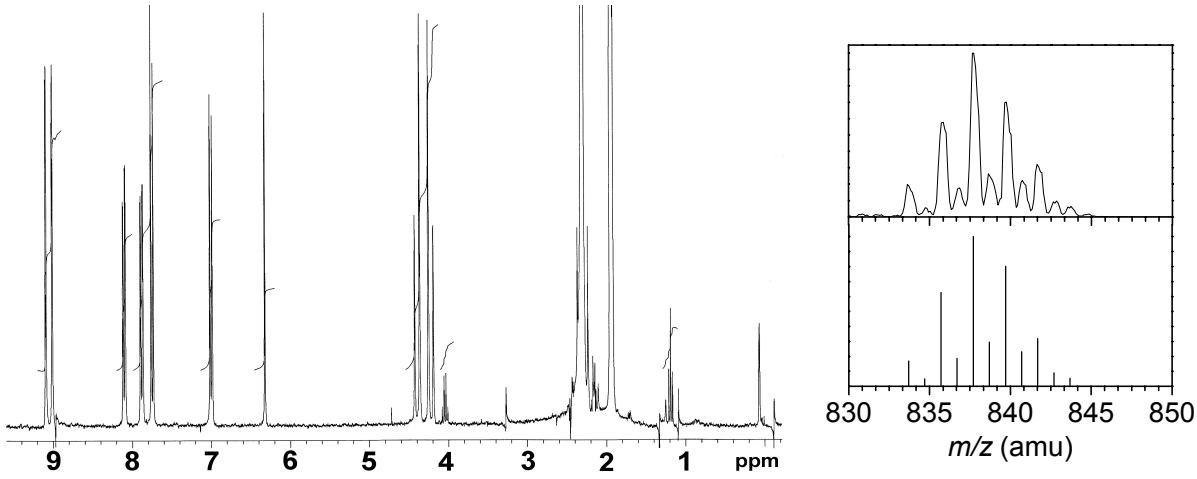

Figure 5.1. The ^{1}H NMR spectrum of **2b** in CD_3CN (left), and the observed and calculated isotope distribution patterns for [**2b**–$(ClO_4)^-$–(MeCN)]$^+$ (top and bottom right, respectively).

The solvent not only has an effect on the λ_{max} and the extinction coefficient (*vide infra*), but also on the stability of the iron(II) complexes of N4Py and its derivatives. In solvents such as acetone, methanol, or water the stability is limited to approximately one day, presumably due to the exchange of the axial ligand.[2b] Therefore, it is not surprising that these complexes are most stable in acetonitrile, for at least several weeks, as verified by UV-Vis spectroscopy.

The characteristic UV-Vis absorption bands for $[(N4Py4Br)Fe(MeCN)](ClO_4)_2$ (**2b**) in methanol were found to be extremely temperature-dependent. The individual absorption bands for **2b** around 380 and 460 nm could not be detected at 20°C, although these bands became more distinct as the temperature was lowered, which was accompanied by an increase in absorption (Figure 5.2). The extinction coefficient of **2b** at –10°C, however, is still significantly lower than that observed for **2a** under similar conditions (**2a**: λ_{max} 453 nm, ε 42 x 10^2 $M^{-1}cm^{-1}$; **2b**: λ_{max} 455 nm, ε 26 x 10^2 $M^{-1}cm^{-1}$).

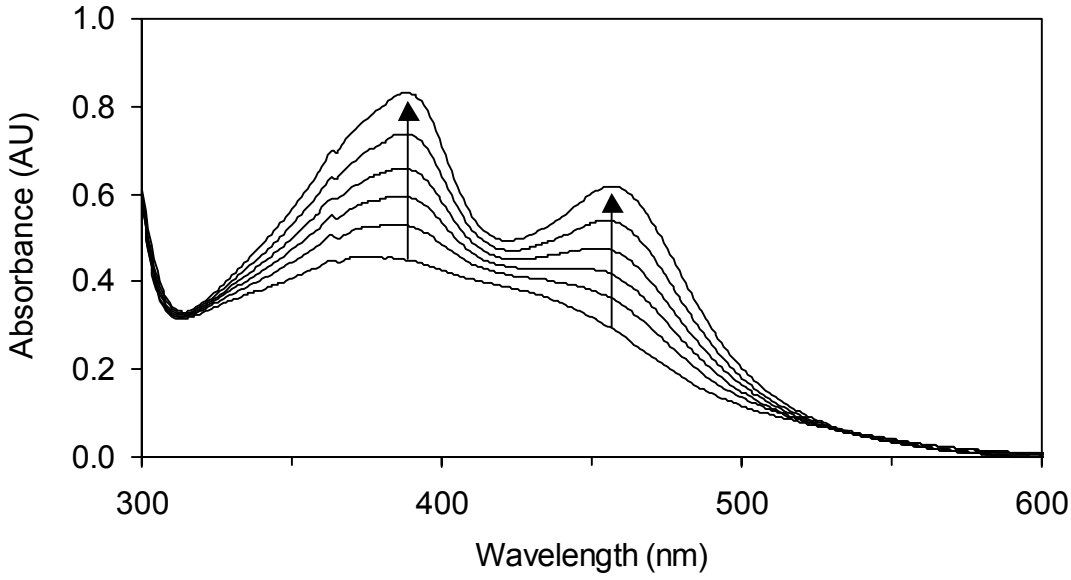

Figure 5.2. UV-Vis spectra of **2b**: increase in absorption in methanol as the temperature is lowered from 20°C to 5, 0, –5, –10, and –15°C, respectively.

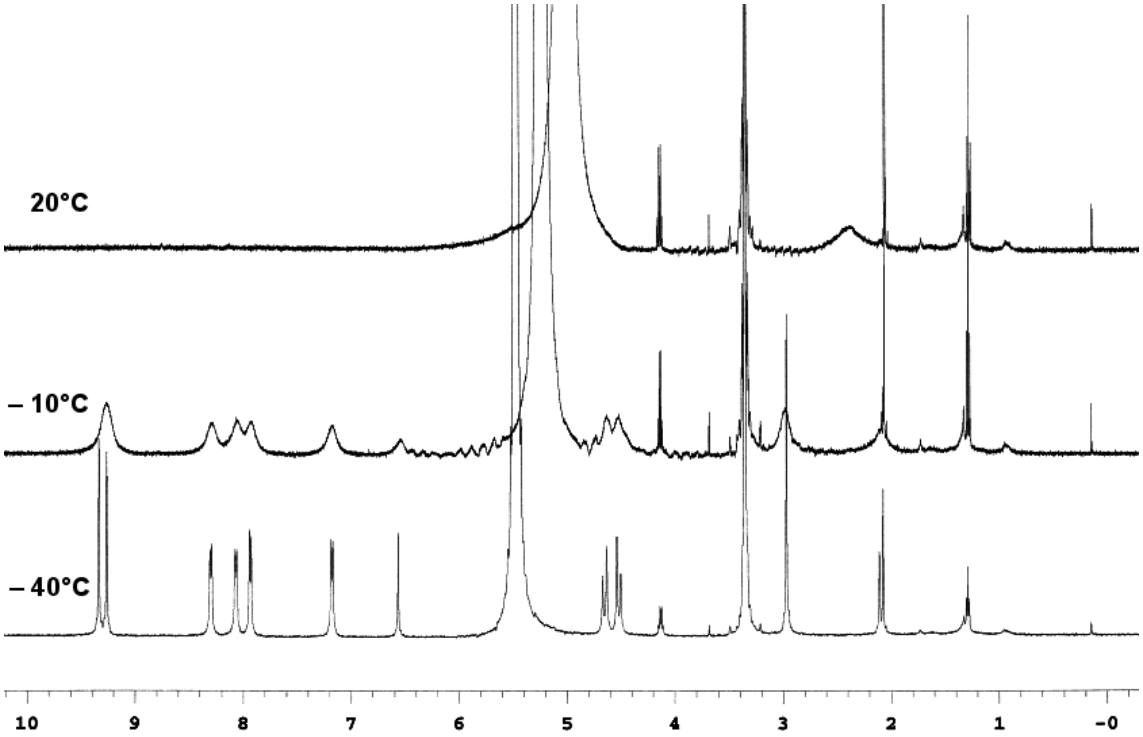

Figure 5.3. Temperature-dependent ^1H NMR spectra of **2b** in CD_3OD.

A plausible explanation for this temperature-dependent UV-Vis absorption of **2b** in methanol might be the initial formation of a high-spin $Fe^{III}OMe$ complex at room temperature. This species has previously also been described for **2a**,[2b] although it is not as readily formed as that of **2b**. As the temperature is then lowered, this species becomes a low-spin iron(II) complex. The spin transition was confirmed by temperature-dependent ^1H NMR analysis (Figure 5.3), which revealed a paramagnetic spectrum with very broad signals in the range of 0 to 100 ppm at 10°C and higher temperatures. At –10°C a diamagnetic spectrum was observed with well defined, although broadened signals from 0 to 10 ppm. The exact composition of this low-spin species and the process involved still need to be ascertained.

Crystals of the iron(II) complexes **2b** and **2c** suitable for X-ray analysis were obtained by the slow diffusion of ethyl acetate into their solutions in acetonitrile (Figure 5.4). Five co-ordination sites to the iron centre are occupied by the chelating ligand and a solvent derived acetonitrile molecule functions as an axial ligand. This mode of co-ordination to the metal ion is analogous to that observed for N4Py (**1a**).[3] As can be seen in Figure 5.4, the bromine atoms of **1b** and the side chains in **1c** are directed away from the iron centre in the complex. The same spatial arrangement can, therefore, also be predicted for other tetrasubstituted N4Py ligands with functional groups in the same positions as in **1b** and **1c**.

Although the iron-nitrogen bond lengths of **2b** and **2c** are comparable to those found for N4PyFe (**2a**), all of the bonds between the pyridine nitrogens and the iron centre ($Fe–N_{py}$) are shorter than was found for **2a** (Table 5.1). In contrast to **2a**, the bond lengths of the iron centre to the acetonitrile nitrogen ($Fe–N_{MeCN}$) in **2b** and **2c** are slightly elongated, whereas the bond lengths of the tertiary amine to the metal centre ($Fe–N_{amine}$) are comparable in all three complexes. Another difference is the distance of the iron centre above the mean plane that is constructed by the four equatorial pyridine nitrogen atoms ($Fe–N_{py–mean\ plane}$), which are identical in **2a** and **2b** but is shorter in **2c**. Electronic effects alone are, in our opinion, insufficient to explain these observations. Therefore, these minor differences in bond lengths in **2a**, **2b** and **2c** are most likely due to the differences in temperature during the X-ray analysis (See footnote in Table 5.1).

Table 5.1. Selected bond distances for **2b** and **2c**. The standard deviations are given in parentheses (**2a** is included for comparison).[a]

Bond (Å)		**2a**[3]	**2b**[6]	**2c**
$Fe–N_{amine}$	N1	1.961(3)	1.965(3)	1.958(3)
$Fe–N_{py}$	N2	1.976(3)	1.965(3)	1.957(3)
	N3	1.967(3)	1.956(3)	1.960(3)
	N4	1.968(3)	1.962(3)	1.960(3)
	N5	1.975(3)	1.970(3)	1.967(3)
$Fe–N_{MeCN}$	N6	1.915(3)	1.927(4)	1.928(3)
$Fe–N_{py–mean\ plane}$		0.2071(5)	0.207(1)	0.197(1)

a) X-ray diffraction of **2a** was performed at 130 K, **2b** at 90 K, and **2c** at 100 K.

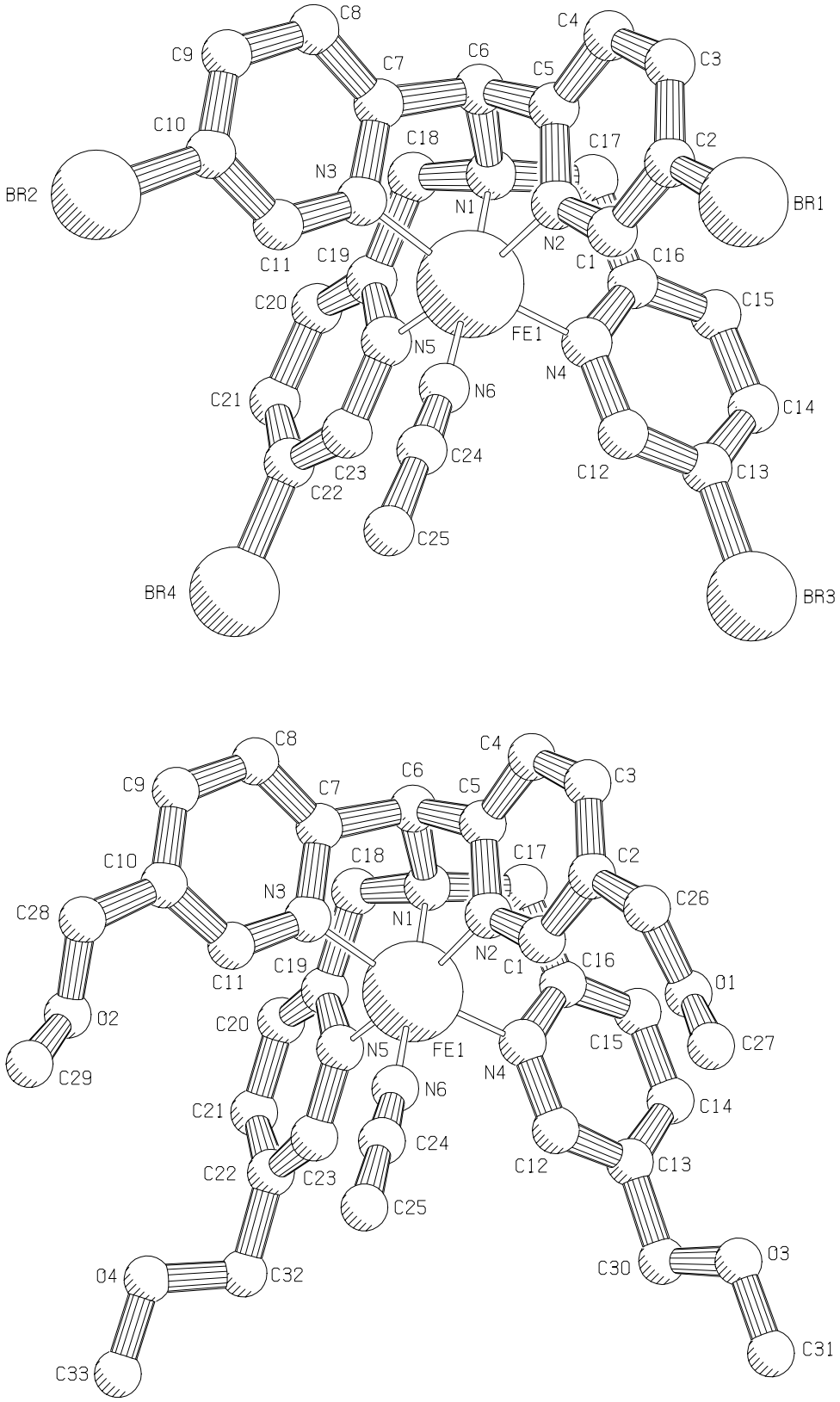

Figure 5.4. Pluto representation of **2b** (top) and **2c** (bottom). Hydrogen atoms and counterions are omitted for clarity.

5.3 Iron(III) hydroperoxo species

Upon the addition of excess hydrogen peroxide to **2a–f** the iron complexes are converted to the corresponding iron(III) hydroperoxo species **3a–f** (Scheme 5.2). The nature of this species was previously elucidated for N4PyFe (**2a**),[2] and the mechanism of its formation and further reaction is also considered to be applicable to other N4Py derivatives. In acetone the conversion to the hydroperoxide species ($Fe^{III}OOH$) is fast and complete, and can be monitored by UV-Vis spectroscopy (depicted in Figure 5.5 for **2a–d**). The complex **2e** can also be converted into its $Fe^{III}OOH$ species **3e**, although this was considerably less stable, was prepared as a model for peptide-bound N4PyFe complexes like **2f** to study the stability of the complex and its sulphur linker towards the applied oxidative conditions (*vide infra*).

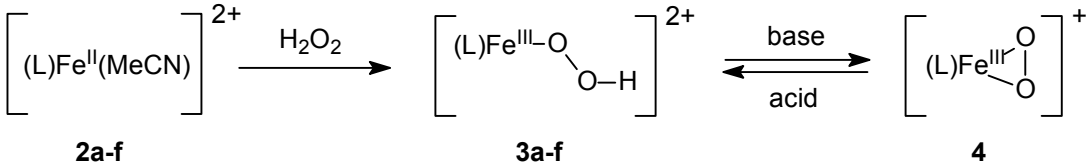

Scheme 5.2. Formation of the purple end-on $Fe^{III}OOH$ species **3a–f** from the corresponding iron(II) complexes **2a–f**, and the reversible conversion of **3a** to the blue $Fe^{III}O_2$ species **4**.

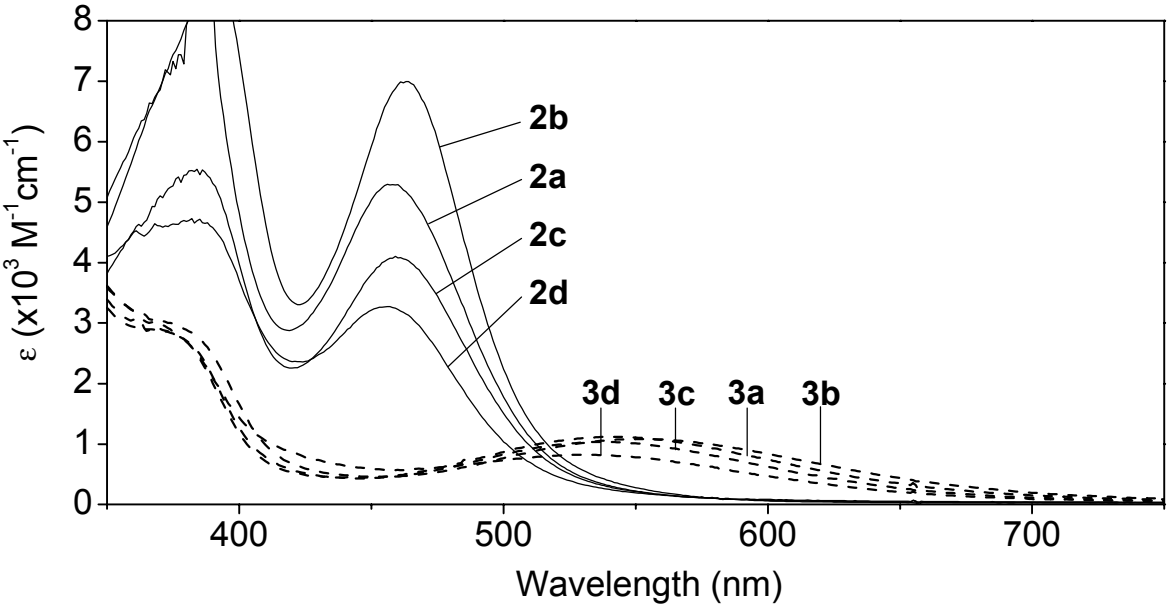

Figure 5.5. UV-Vis spectra of the iron(II) complexes **2a–d** (solid lines) and the corresponding $Fe^{III}OOH$ species **3a–d** (dashed lines) in acetone at 20°C.

The spectroscopic data for the iron(II) complexes **2a–d** and their iron(III) hydroperoxo species **3a–d** are summarised in Table 5.2 where acetone or acetonitrile was employed as the solvent. The purple intermediates **3b** and **3c** exhibit absorptions around 540 nm with extinction coefficients of 1000–1200 $M^{-1}cm^{-1}$, which are characteristic for low-spin end-on $Fe^{III}OOH$ species.[2,7] The lower extinction coefficients of **3d** and **3e** were attributed to the rapid decomposition of the intermediate, which is thought to occur during the conversion of the

iron(II) complex to the hydroperoxide species. The degradation of **3d** was also accompanied by a substantial amount of catalase activity, which involves the decomposition of hydrogen peroxide to dioxygen and water.

Similar to the complexes **2a–d**, the characteristics and the stability of the $Fe^{III}OOH$ intermediate was also found to be solvent-dependent. The general trend comprises of a small red shift for the iron(II) complexes on the exchange of acetonitrile as the solvent for acetone, which becomes more distinct for the corresponding $Fe^{III}OOH$ species. In addition, the complexes **2a–d** generally exhibit a higher extinction coefficient in acetonitrile, in contrast to their corresponding $Fe^{III}OOH$ species **3a–d**. This is considered to be caused by the unfavourable exchange of the axial ligand in acetonitrile, which results in a slow and incomplete formation of the peroxide species **3a–d**, and consequently leads to a lower absorption intensity for these intermediates.[2]

Table 5.2. Spectroscopic data of the Fe^{II} and $Fe^{III}OOH$ complexes of N4Py and its derivatives in acetone at room temperature.[a]

		$[(L)Fe^{II}(MeCN)](ClO_4)_2$		$[(L)Fe^{III}OOH](ClO_4)_2$	
Entry	Ligand (L)	λ_{max} (nm)	ε (x 10^2 $M^{-1}cm^{-1}$)	λ_{max} (nm)	ε (x 10^2 $M^{-1}cm^{-1}$)
1	**1a**	457 (455)	53 (48)	539 (520)	11 (7.2)
2	**1b**	464 (460)	70 (88)	553 (544)	11 (8.9)
3	**1c**	461 (457)	41 (59)	538 (522)	10 (7.8)
4	**1d**	457 (454)	33 (46)	531 (517)	8.2 (6.4)
5	**1e**[b]	456 (n.d.)	37 (n.d.)	525 (n.d.)	3.4 (n.d.)

a) The results in parentheses refer to acetonitrile as solvent. n.d. = not determined.
b) At 0°C, $\lambda_{max,\mathbf{2e}}$ 457 nm, ε 26 x 10^2 $M^{-1}cm^{-1}$; $\lambda_{max,\mathbf{3e}}$ 531 nm, ε 3.7 x 10^2 $M^{-1}cm^{-1}$.

It is known that a more electron-withdrawing ligand will be a weaker σ bond donor and a stronger π acceptor.[7] Consequently, the electron density on the metal centre will be decreased, thus resulting in a higher redox potential of the corresponding complex.[2b,7] The decrease in the energy of the ligand-to-metal charge transfer band for the $Fe^{III}OOH$ species will be accompanied by an increase in the λ_{max}.[2b,7] Substituents at the 5-position of the pyridine rings in disubstituted N4Py ligands were previously found to have only a minor electronic effect on the metal ion.[2b] However, the redox potential of the tetrabromide N4PyFe derivative **2b** was found to be substantially higher than that of N4PyFe **2a** ($E_{½}$ = 1010 mV vs. SCE)[2] and a dibromo N4PyFe derivative[8] ($E_{½}$ = 1100 mV vs. SCE).[2b] The cyclic voltammetry measurements for **2b** displayed a reversible oxidation wave with a redox potential for the Fe^{II}/Fe^{III} couple of 1198 mV vs. SCE and an observed peak-to-peak separation of 105 mV (Figure 5.6). Forward and reverse differential pulse voltammetry at a scan rate of 10 mVs^{-1} confirmed this process to be reversible with a redox potential for the Fe^{II}/Fe^{III} couple of 1196 mV vs. SCE.

The general trend infers that the introduction of a greater number of electron-withdrawing groups into the N4Py ligand results in an increase in the redox potential of the corresponding

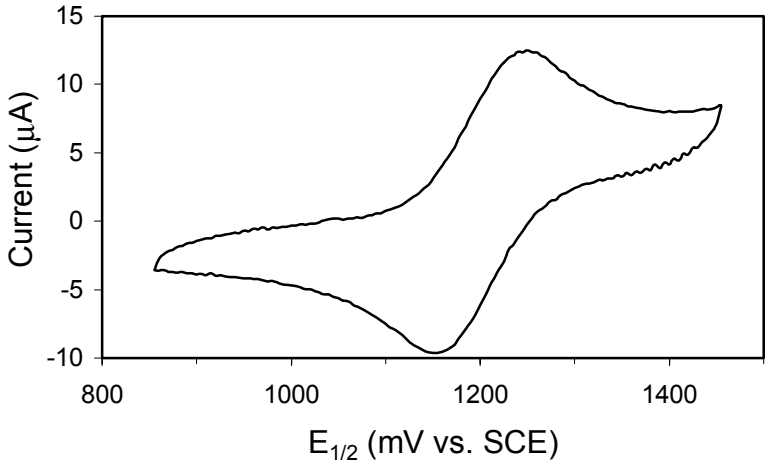

Figure 5.6. Cyclic voltammogram of **2b** in acetonitrile at 22°C (scan rate 100 mVs $^{-1}$).

iron(II) complex. This in turn gives rise to the observed relatively large red shift for the $Fe^{III}OOH$ species **3b** (Table 5.2, entries 1 and 2). The electronic effect of the methoxymethyl groups or the alkyl spacers in **3c** and **3d** influence the absorption maxima only to a minor extent. Unfortunately, as the redox potentials for **2c** and **2d** have not yet been determined, conclusive evidence cannot be provided for the relationship between the redox potential of N4PyFe complexes and the absorption maximum of their iron(III) hydroperoxo species.

The $Fe^{III}OOH$ species of **2e** could not be detected by a stepwise titration of the iron(II) complex with hydrogen peroxide in acetone at room temperature. However, when a single aliquot of excess hydrogen peroxide was added to **2e** the intermediate **3e** could be observed for a limited period. Its lifetime was significantly extended to approximately fifteen minutes by reducing the temperature of the solution to 0°C. The pH appeared to have only a minor effect on the extinction coefficient of **2e** (λ_{max} 452 nm, $\varepsilon_{pH\ 4}$ 35 x 10^2 $M^{-1}cm^{-1}$, $\varepsilon_{pH\ 7}$ 38 x 10^2 $M^{-1}cm^{-1}$, $\varepsilon_{pH\ 10}$ 33 x 10^2 $M^{-1}cm^{-1}$) at room temperature. The intermediate **3e** could not be detected even under these conditions. A fine light yellow solid was always observed in the cuvette subsequent to these UV-Vis experiments. Unfortunately, the identity of this material could not be established by mass analysis. Nevertheless, it was hypothesised that this residue could be the product from the oxidative degradation of the ligand. Similar observations were made when employing the dipeptide-bound N4PyFe complex described in Chapter 2.[9]

In an attempt to oxidise 1,2,4,5-tetramethoxybenzene (Scheme 5.5C, p. 130) by **2e** the oxidation reaction was monitored by ESI-MS at room temperature. It was verified that a rapid decomposition of the catalyst occurred in the absence of any detectable oxidation of the substrate (Figure 5.7). Although the intensities of the peaks cannot be quantified, it is clear that the disappearance of **2e** (*m/2z* 646.0 amu for $[M-2(ClO_4)^- - (MeCN)]^{2+}$) is accompanied by the formation of a new, related species, possibly from the oxidation of the sulphur atoms in ligand **1e**.

One suggestion for the assignment of the peak at 654.6 amu is the introduction of one oxygen atom in the doubly-charged species from **2e**. The mass of 670.4 amu could originate from the complex **2e** after the oxidation of three sulphur atoms to the corresponding sulphoxides. If so, it still remains a mystery as to why no further oxidation of the sulphur linkers was observed. The visual observations during the UV-Vis experiments, however, did confirm that the catalyst had decomposed under the employed oxidative conditions (*vide supra*). The

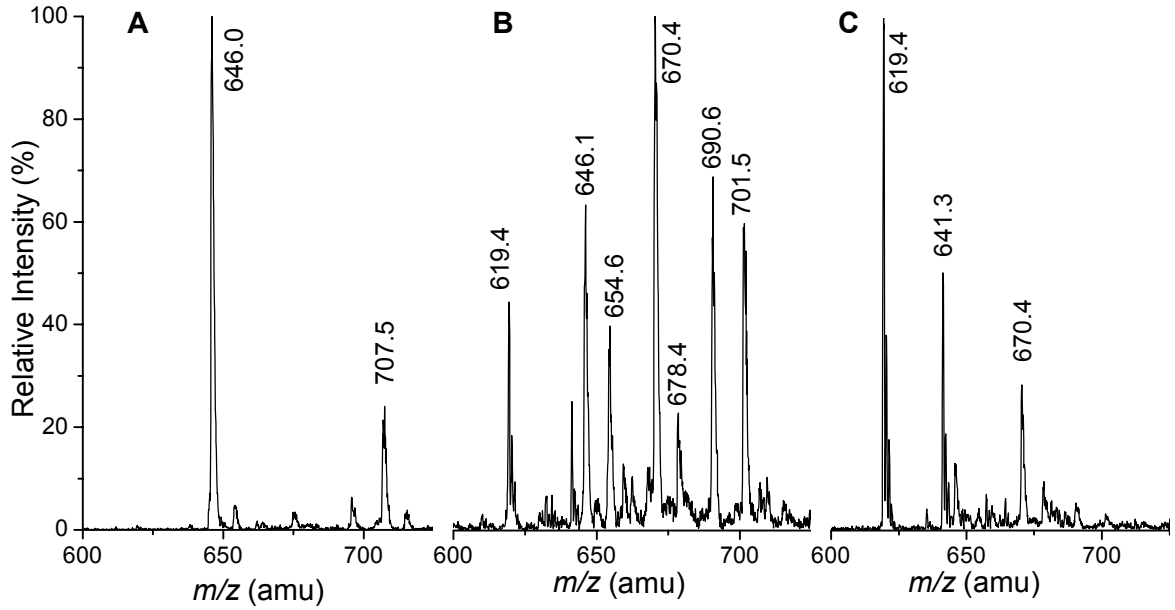

Figure 5.7. ESI-MS analysis for the oxidation of 1,2,4,5-tetramethoxybenzene by **2e** (*m/2z* 646.0 amu) at room temperature by hydrogen peroxide at t = 0 (A), t = 1 min (B), and t = 20 min (C).

masses at *m/z* 619.4 and 641.3 were assigned to singly-charged species, although their exact identity still remains unknown, as is the structure of the doubly-charged species at *m/z* 690.6 and 701.5. These observed masses, however, also cannot be assigned to the corresponding $Fe^{III}OOH$ intermediate.

The iron(III) hydroperoxo species **3a** (λ_{max} 548 nm, ε 12 x 10^2 $M^{-1}cm^{-1}$) can be deprotonated reversibly to the conjugate base **4** (λ_{max} 690 nm, ε 440 $M^{-1}cm^{-1}$) in methanol at –10°C (Scheme 5.2). UV-Vis, EPR, and resonance Raman spectroscopy as well as ESI-MS analysis established the nature of this high-spin $Fe^{III}-\eta^2-O_2$ species **4**.[10] It can be assumed that this interconversion will also be applicable to the iron(II) complexes of N4Py derivatives in general.

Although the purple intermediate **3b** can be generated readily in acetone and acetonitrile at 20°C, in methanol this conversion is by no means complete (λ_{max} 557 nm, ε 3.5 x 10^2 $M^{-1}cm^{-1}$). Surprisingly, no significant formation of **3b** was observed at –10°C in methanol. Instead a new small absorption at 509 nm was detected (Figure 5.8). Presumably, the axial methoxy ligand in the $Fe^{III}OMe$ species that is formed *in situ* is bound too strongly to the metal ion, and thus prevents a facile conversion to the purple intermediate **3b**. The addition of base resulted in the immediate disappearance of the absorption bands for the observed intermediate, but did not lead to the formation of a $Fe^{III}-\eta^2-O_2$ species as found for **3a**. This was surprising as it was assumed that the electron-withdrawing bromides in the $Fe^{III}OOH$ species **3b** would promote its deprotonation. However, if the $Fe^{III}OOH$ species is not formed due to the strongly bound methoxy ligand, then this would explain the absence of the corresponding blue species.

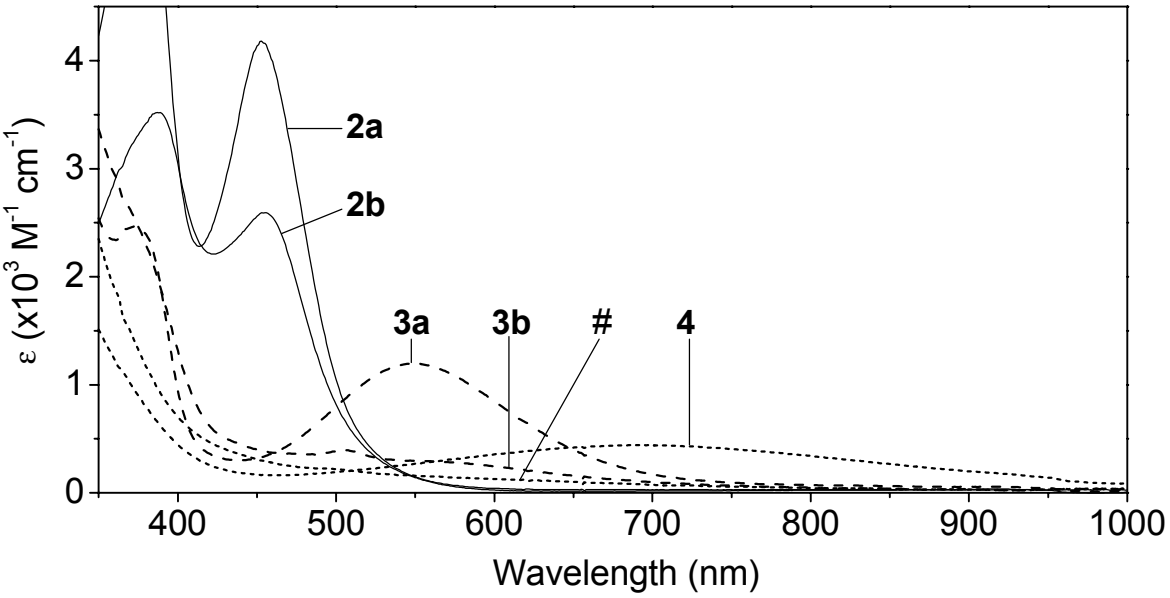

Figure 5.8. UV-Vis spectra of **2a** and **2b** in methanol at −10°C (thin solid lines), after the addition of 5 equiv H_2O_2 (dashed lines), and 5 equiv NH_4OH (dotted lines) (# = **3b** + 5 equiv NH_4OH).

5.4 Oxidation of organic substrates

As previously observed for **2a**, its $Fe^{III}OOH$ species is capable of oxidising a variety of organic substrates such as benzene, styrene, benzyl alcohol, cyclohexene and cyclohexane.[11] The proposed mechanism for the oxidation of alkanes was discussed and summarised in Chapter 2.[2b,11b]

$$\underset{\textbf{3a}}{[(N4Py)Fe^{III}O{-}OH]^{2+}} \xrightarrow[\text{cleavage}]{\text{homolytic}} [(N4Py)Fe^{IV}{=}O]^{2+} + {\bullet}OH$$

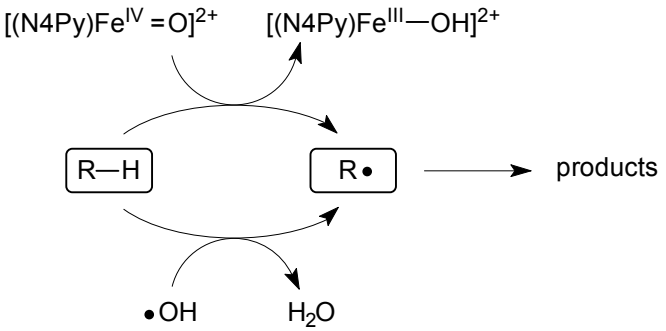

Scheme 5.3. Proposed mechanism for substrate (R−H) oxidation by **3a**.[2b]

The influence of the substituents in the ligands **1b–d** towards the oxidation behaviour of the corresponding iron(II) complexes **2b–d** was examined using the substrates cyclohexene (**5**) and cyclohexane (**9**) (Scheme 5.4). These substrates were selected due to their high turnover (expressed in TON, mol product per mol catalyst) in oxidation reactions catalysed by **2a** and thereby provided a suitable basis on which to assess the catalytic activity of **2b–d**.

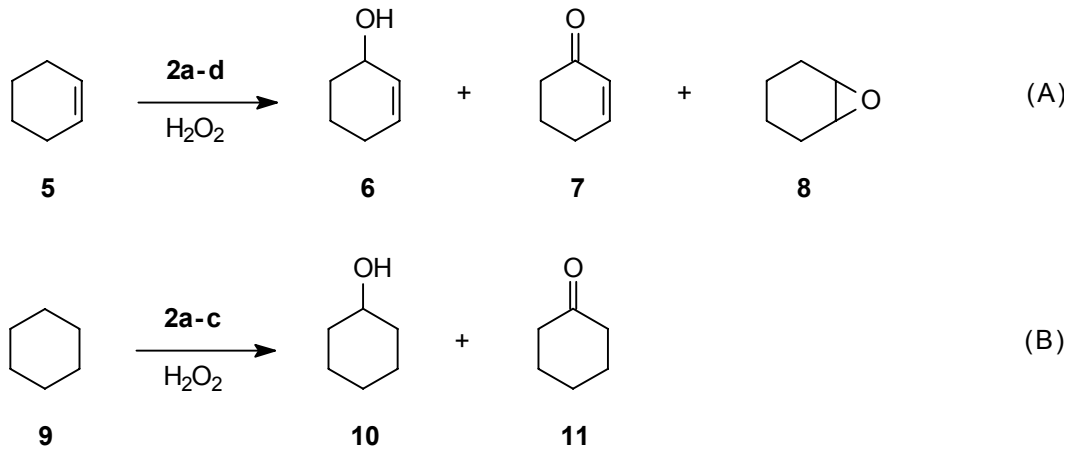

Scheme 5.4. The anticipated products for the oxidation of cyclohexene (A) and cyclohexane (B).

The catalytic oxidation reactions were carried out in acetone or acetonitrile at 20°C under a nitrogen atmosphere in the presence of an excess of substrate (substrate/H_2O_2/catalyst = 1000:100:1). The catalysts **2a–d** were used as a stock solution in acetonitrile. The oxidation was initiated by the addition of a single aliquot of hydrogen peroxide. Within the examined time-span a blank reaction by hydrogen peroxide could not be detected, even in the presence of an equal catalytic quantity of iron perchlorate. Therefore, the observed oxidation of the substrates was solely attributed to the catalytic activity of **2a–d**. The conversions of **5** and **9** over time employing acetone as the solvent are shown in Figure 5.9 and Figure 5.10, respectively. Table 5.3 summarises the TONs of the catalysts when subjected to a reaction time of one hour.

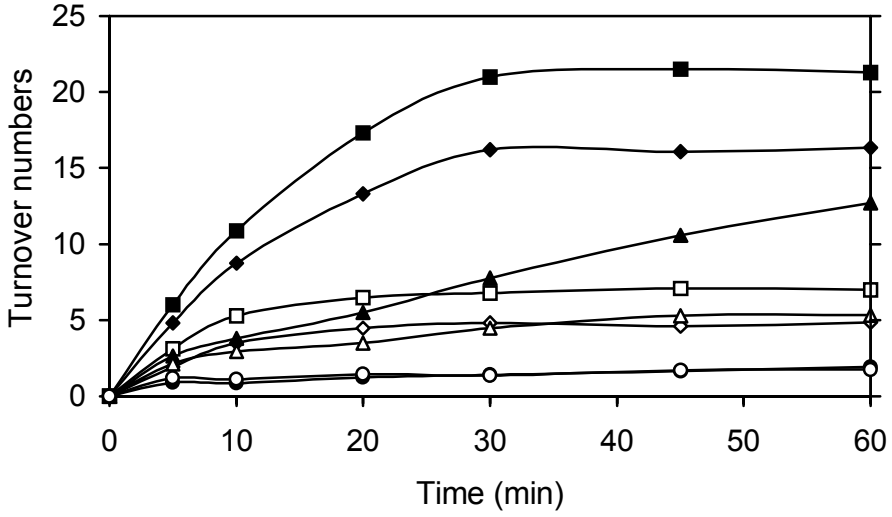

Figure 5.9. Catalytic oxidation of cyclohexene to cyclohexenol (solid) and cyclohexenone (open) by hydrogen peroxide in acetone at 20°C (**2a**: –■–,–□–; **2b**: –◆–,–◇–; **2c**: –▲–,–△– ; **2d**: –○–,–●–).

The iron(II) complex **2a** is clearly the most active catalyst of all the complexes **2a–d** for the oxidation of cyclohexene. The final TON of 21.3 for **2a** (Table 5.3, entry 1) was comparable to the previously reported TON of 23.1.[11b] Although the purple colour of the $Fe^{III}OOH$

intermediates **3a–c** disappeared after approximately 15 minutes, the oxidation reaction ceased after a further 15 minutes for **2a** and **2b**, as can be seen in Figure 5.9 and Figure 5.10. This observation was not attributed to a complete deactivation of the catalyst, as the addition of further hydrogen peroxide caused the reaction to recommence. The same was also applicable to **2b**, which, although less active than **2a**, displayed a similar oxidation behaviour over time.

Within the timeframe of one hour the reactivity of the catalyst **2c** towards cyclohexene was not only lower than that of **2a** or **2b**, it was also almost linear as opposed to the exponential curves as observed for **2a** and **2b**. In addition, the dissipation of the curves for **2c** in Figure 5.9 indicates an increased product selectivity over time. The catalyst **2d** seemed to be deactivated almost immediately and consequently did not yield more than two turnovers (Table 5.3). In all the above cases, the oxidation product cyclohexene oxide (**8**) was only formed in minute quantities, if at all.

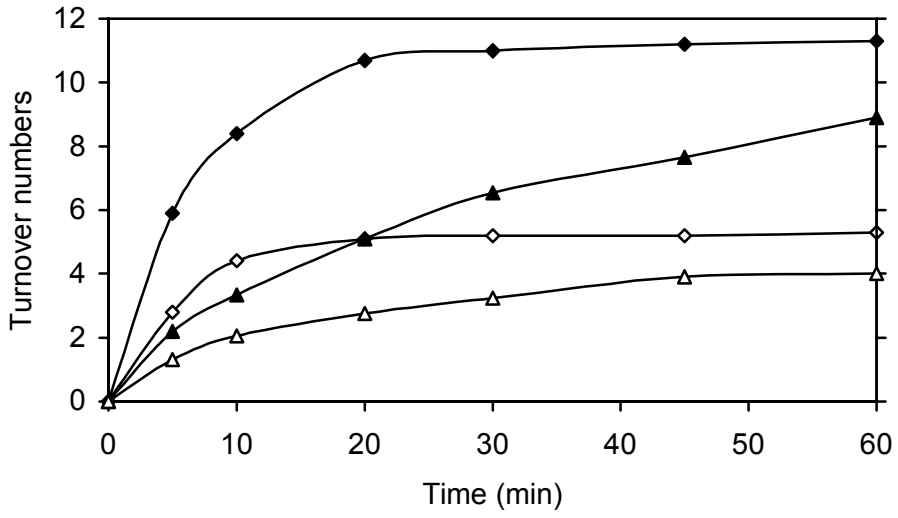

Figure 5.10. Catalytic oxidation of cyclohexane to cyclohexanol (solid) and cyclohexanone (open) by hydrogen peroxide in acetone at 20°C (**2b**: –◆–,–◇–; **2c**: –▲–,–△–).

In the oxidation of cyclohexane the behaviour of the catalysts **2b** and **2c** was comparable to that shown in Figure 5.9. As before, the iron(II) complex **2b** was found to be less reactive than **2a** (Table 5.3, entry 2) and the conversion ceased after approximately thirty minutes. In addition to this, the activity of **2c** proceeded beyond the allocated reaction time of one hour, which was accompanied by an increased selectivity over time. Due to the previously observed deactivation of the catalyst **2d**, this iron(II) complex was not examined for the oxidation of cyclohexane.

In order to determine the maximum number of turnovers for each catalyst, an excess of hydrogen peroxide was slowly administered to the reaction mixture over one hour. The results in Table 5.3 (in brackets) not only illustrated that a higher turnover can be obtained, but also that the selectivity of the reaction is inverted when cyclohexene is employed as the substrate. This selectivity is best expressed as the ratio of alcohol over ketone product (A/K). The ratios in Table 5.4 indicate that this selectivity is virtually unaffected using the substrate cyclohexane, which suggests that the mechanism involved is also unaffected. In general, an A/K ratio of one

Table 5.3. Turnover numbers of the iron(II) complexes of N4Py and its derivatives for the catalytic oxidation reactions in acetone after one hour at room temperature.[a]

Entry	Substrates	Products	**2a**	**2b**[b]	**2c**	**2d**
1	cyclohexene	**6**	21 (24)	16 (17)	13 (14)	2 (2)
		7	7 (5)	5 (27)	5 (31)	2 (4)
		8	– (13)	0.1 (3)	2 (8)	1 (2)
2	cyclohexane	**10**	17[c]	11 (16)	9 (16)	n.d.
		11	7[c]	5 (9)	4 (6)	n.d.

a) Results in parentheses refer to a slow addition of 2000 equiv H_2O_2 over one hour.
b) TONs in acetonitrile as the solvent: **6**: 8, **7**: 5, **8**: –.
(Compared to N4PyFe:[c] **6**: 28, **7**: 7, **8**: 1)
c) Taken from the Ph. D. thesis of Gerard Roelfes.[2,11b]

will be obtained if free radical intermediates are involved in the reaction,[12] which can react, for instance, with dioxygen to propagate a radical chain auto-oxidation process. This ratio is only observed for the oxidation of cyclohexene by **2d**. In light of the calculated A/K ratio and the catalase activity during the UV-Vis experiments (*vide supra*), the decomposition of **2d** is attributed to the formation of free radicals during the oxidation reaction.

Table 5.4. The ratios of alcohol (A) over ketone (K) product formation in acetone at 20°C.[a]

Entry	Catalyst	A/K (cyclohexene)	A/K (cyclohexane)
1	**2a**	3.0 (0.4)	2.6 (n.d.)[b]
2	**2b**	3.4 (0.6)	2.1 (1.7)
3	**2c**	2.4 (0.5)	2.2 (2.6)
4	**2d**	1.1 (0.5)	n.d.

a) Results in parentheses refer to a slow addition of 2000 equiv H_2O_2 over 1 h.
b) Taken from the Ph. D. thesis by Gerard Roelfes.[2]

The $Fe^{III}OOH$ intermediate in the presence of hydrogen peroxide is capable of oxidising alcohols like cyclohexanol to the corresponding ketone.[11b] However, the observed A/K < 1 for cyclohexene upon the slow addition of excess hydrogen peroxide is not due to the *in situ* oxidation of the alcohol to the ketone, as the A/K ratios were found to be relatively constant for **2b** and **2c** during and after the addition of hydrogen peroxide. It was previously established that slow addition of 100 equivalents of hydrogen peroxide leads to an increase in the A/K ratio.[11b] Presumably, the addition of 2000 instead of 100 equivalents of hydrogen peroxide with respect to the catalyst has affected the rate-determining step of the reaction, or altered the mechanism. However, at the present time no conclusive evidence can be provided to either support or disprove this conjecture. A full kinetic study will have to be undertaken to provide such

evidence. The higher hydrogen peroxide concentration can also give rise to more decomposition by catalase. The produced dioxygen in turn can react with free radicals present to propagate the radical chain process,[12] but this would result in A/K ratios of one as opposed to the observed values of less than one.

5.5 Assays for screening peroxidase activity

Peroxidases catalyse the oxidation of a wide range of substrates using hydrogen peroxide as the terminal oxidant.[13] Their huge structures, however, make it difficult to study or determine the factors that govern their function and behaviour. Therefore, microperoxidases (right) are commonly used as models for these haemoproteins.[14,15,16] These small haem-peptide fragments can be obtained by the proteolytic digestion of cytochromes *c*, and contain a small peptide fragment that is covalently linked to the haem via two cysteine residues.

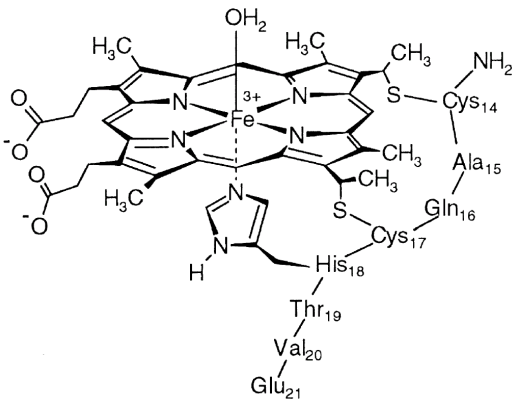

Substrates that are used to investigate the peroxidase activity of newly developed peroxidases or their mimics are usually probes that enable their conversion to be monitored by UV-Vis spectroscopy.[17] A typical reaction to test for peroxidase activity involves the oxidation of *o*-methoxyphenol (**12**) to compound **13**,[18] which is sometimes referred to as tetraguaiacol (Scheme 5.5A).[14b,19,20] When subjected to the oxidising conditions the substrate 2,2'-azinobis-(3-ethyl-benzothiazoline-6-sulphonic acid) (ABTS, Scheme 5.5B) is converted into a radical cation (*vide infra*).[15,21] Even though these probes can be readily applied as assays for peroxidase activity, they do not enable the selectivity of the catalyst to be monitored. The probe tetramethoxybenzene[22] (**14**) creates an opportunity to determine the product selectivity of the

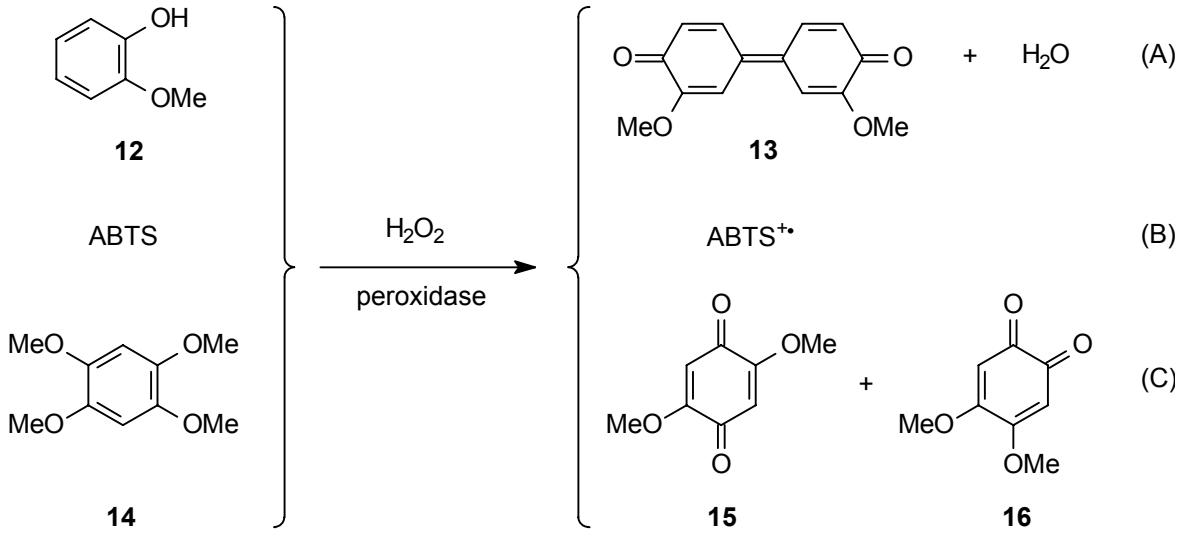

Scheme 5.5. Assays for screening peroxidase activity.

peroxidation reaction that is catalysed by the (artificial) enzyme or mimic (Scheme 5.5C).[23] A drawback for this assay, however, is that it necessitates the need for a standardised HPLC method to quantify the product distribution.

5.6 Oxidation of ABTS by non-haem catalysts

The peroxidase activity and the pH-dependency of N4PyFe (**2a**) and the peptide complex **2f** were determined by monitoring spectrophotometrically the formation of the emerald green $ABTS^{+\bullet}$ radical cation over time at 660 nm (ε 1.47 x 10^4 $M^{-1}cm^{-1}$).[16b] This probe had also been used to establish the peroxidase activity of the dipeptide-bound N4PyFe catalyst presented in Chapter 2.[24]

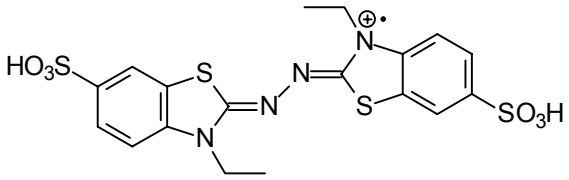

Figure 5.11. The ABTS radical cation.

It has been established that the rate limiting step for microperoxidases and other peroxidase enzymes is the formation of the reactive intermediate.[14a,15b,16,19d] This process obeys pseudo-first-order kinetics at low concentrations. Under the same conditions these kinetics could also apply to the peroxidation of ABTS using the non-haem catalysts **2a** or **2f**. However, a full kinetic study has not yet been undertaken to establish the kinetics for this reaction. The following discussion is purely speculative with regards to the observed formation of $ABTS^{+\bullet}$ and the factors that could influence the peroxidation reaction.

By employing an ABTS/H_2O_2/catalyst ratio of 500:1000:1 the concentration of the substrate and the oxidant can be considered to have little or no effect on the rate of the reaction. The reactions were initiated by the addition of hydrogen peroxide to a thermostatically controlled and buffered (AcOH/NaOAc) solution of the substrate and the catalyst. The previously established optimal pH range of 3.0 to 4.5 was employed to study the catalytic activity of **2a** during the peroxidation of ABTS.[24]

The highest initial rate for the peroxidation by **2a** was observed at pH 3.5 (Figure 5.12A). The observed curvatures in the formation of $ABTS^{+\bullet}$ (Figure 5.12) were attributed to the deactivation of the catalyst. Similar oxidative degradation of the catalyst is also common for microperoxidases and haem oxygenases.[14a,15b,16,25] The catalyst is completely deactivated within approximately 100–400 seconds, depending on the applied pH. The continued formation of $ABTS^{+\bullet}$ originates from the non-catalysed peroxidation of ABTS by hydrogen peroxide. This is the main disadvantage of using ABTS as a probe for peroxidation activity. As a result, the experimental data for the peroxidation of ABTS catalysed by iron perchlorate, N4PyFe (**2a**), and the peptide-bound complex **2f** has to be corrected for this background reaction, which accentuates the deactivation of the catalyst over time (Figure 5.12B).

When compared to N4PyFe, the N4PyFe-peptide complex **2f** displayed a substantially lower activity for the peroxidation of ABTS under identical conditions (Figure 5.12B). This result

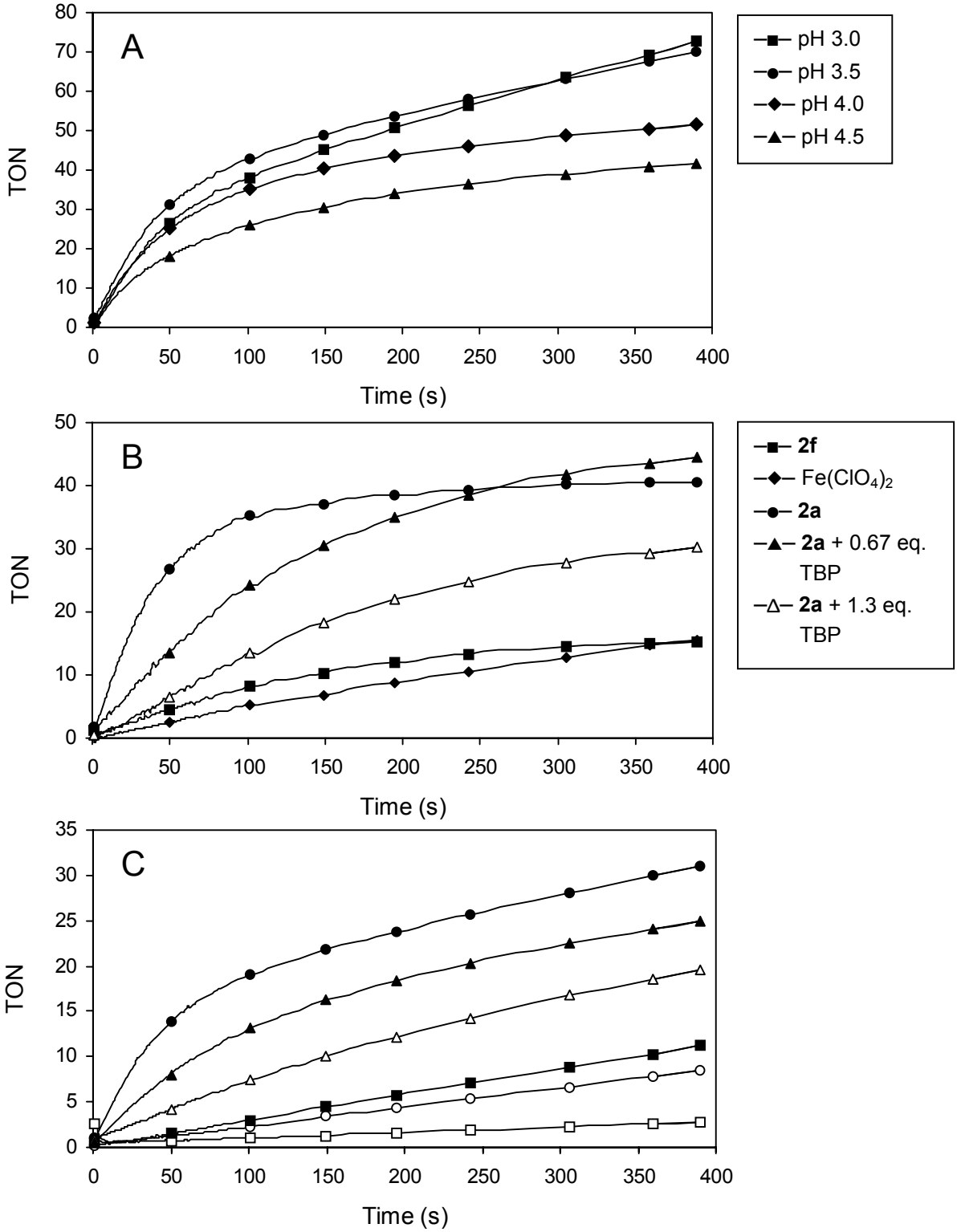

Figure 5.12. Formation of the $ABTS^{+\bullet}$ radical cation over time at 20°C, expressed in turnover numbers (TON). (A) pH-dependency of **2a**; (B) background corrected oxidation of ABTS by **2a**, **2f**, and iron(II) perchlorate at pH 3.5, and by **2a** in the presence of the radical scavenger 2,4,6-tri-*tert*-butylphenol (TBP); (C) effect of TEMPO on the catalytic activity of **2a** at pH 3.5 (–○– background reaction by H_2O_2; –●– H_2O_2 and **2a**; –□– TEMPO; –■– TEMPO and H_2O_2; –▲– H_2O_2 and **2a** in the presence of 0.3 equiv TEMPO with respect to H_2O_2; –Δ– H_2O_2 and **2a** in the presence of 1 equiv TEMPO with respect to H_2O_2).

is attributed to the steric interactions between the peptide chains of the catalyst and the ABTS substrate. However, these peptides appear to prolong the lifetime of the catalyst from approximately 150 to almost 400 seconds. It was already established that a reduction in temperature extends the lifetime of the $Fe^{III}OOH$ intermediate **3f** (*vide supra*). Therefore, by lowering the temperature and changing the solvent to acetone for example, the oxidative decomposition of the complex by the hydroxyl radicals might be reduced. The use of another, smaller substrate molecule like 1,2,4,5-tetramethoxybenzene (**14**) might also improve the catalytic turnover by reducing the steric interactions.

The turnover towards the end of the reaction period is also far too low to support the reduced reaction rate of $ABTS^{+\bullet}$ formation due to a complete consumption of hydrogen peroxide. This observation was further validated upon the addition of more hydrogen peroxide, which did not appear to affect the reaction. The addition of a new batch of catalyst **2a**, however, was able to induce a small and brief increase in the reaction rate. An initial increase in the catalyst loading also led to an enhanced reaction rate.

It has been suggested that hydroxyl radicals are involved in the catalytic oxidation of alkanes by N4PyFe (**2a**).[2b] The oxidation of ABTS to $ABTS^{+\bullet}$ can also be accomplished efficiently by hydroxyl radicals only.[26] Furthermore, these strongly oxidising species, as well as hydrogen peroxide itself, could be the source of the catalyst's degradation.

If the rate-determining step of the peroxidation by **2a** involves the formation of the $Fe^{III}OOH$ intermediate, then the addition of a hydroxyl radical scavenger should not have any effect on the initial reaction rate but only on the lifetime of the catalyst. However, the addition of tri-*tert*-butylphenol, an efficient radical scavenger,[16b] not only gave rise to an increased lifetime of the catalyst, but also to a reduction in the reaction rate (Figure 5.12B). These observations imply that the rate determining step does not in fact involve the formation of the transient $Fe^{III}OOH$ intermediate, but rather the reaction of the reactive species with the substrate ABTS. Trapping these hydroxyl radicals and/or the proposed one-electron oxidation species $[(N4Py)Fe^{IV}(O)]^{2+}$ (Scheme 5.3) with the scavenger will consequently result in the observed drop in the reaction rate. In addition, these findings strongly support the suggestion that hydroxyl radicals are involved in the catalytic cycle of **2a**.[2b,11b]

A drop in the rate of $ABTS^{+\bullet}$ formation was also observed when the free radical 2,2,6,6-tetramethylpiperidin-1-oxyl (**17**, TEMPO) was used for the reaction catalysed by **2a** (Figure 5.12C). The addition of 2,2,6,6-tetramethylpiperidine (TEMP) had a similar, but less pronounced, negative effect on the reaction rate (not shown). However, the use of either of these reagents did not lead to an extended lifetime for the catalyst. The effect of TEMPO and TEMP was dependent upon the amount that was added to the reaction mixture. Although ABTS has also been applied as a scavenger of free radicals like hydroxyl and bromine radicals, as well as ferryl porphyrins,[27] TEMPO itself was not able to oxidise efficiently ABTS to the $ABTS^{+\bullet}$ radical cation (Figure 5.12C). In fact, the reaction of TEMPO with ABTS was substantially slower than that observed for hydrogen peroxide, even in the presence of **2a** (not shown). The combination of hydrogen peroxide and TEMPO resulted only in a minor increase in the rate of the background reaction (Figure 5.12C).

From these observations it can be concluded that TEMPO reacts with the $Fe^{III}OOH$ intermediate and interferes with the homolytic O–O bond dissociation. Consequently, the formation of the hydroxyl radicals and the one-electron $[(N4Py)Fe^{IV}(O)]^{2+}$ species is hampered

(Scheme 5.3). The mechanism involved could be related to the suggested mechanism for the oxidation of alcohols using TEMPO.[28] The oxoammonium salt **18**, formed by a disproportionation of TEMPO (**17**), can react with the $Fe^{III}OOH$ species **3a**, as shown in Scheme 5.6. The equilibrium between **18** and **20** subsequently can result in the slow release of **3a**, and therefore in a slower formation of the hydroxyl radicals and $[(N4Py)Fe^{IV}(O)]^{2+}$, which leads to the reduced rate of the ABTS peroxidation and the catalyst degradation. Although highly speculative, this conjecture can account for the observations shown in Figure 5.12.

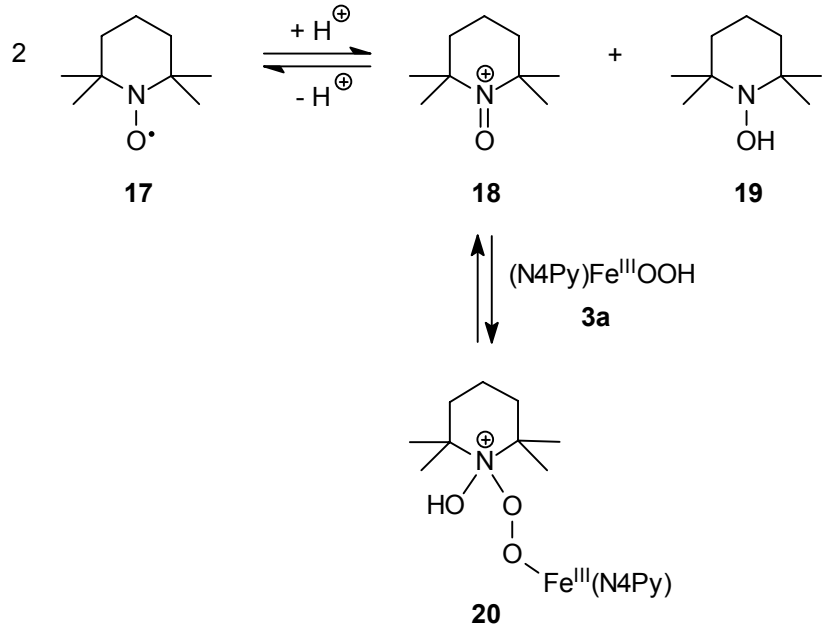

Scheme 5.6. Proposed mechanism for trapping the $Fe^{III}OOH$ intermediate by TEMPO.

UV-Vis experiments in acetone at room temperature independently established that the addition of TEMPO and TEMP to the purple $Fe^{III}OOH$ intermediate resulted in the immediate disappearance of its absorption band. If TEMPO was added before the addition of hydrogen peroxide, the formation of $Fe^{III}OOH$ was substantially slower and incomplete. The interaction between TEMP and $Fe^{III}OOH$ might be due to a simple acid/base reaction. Under these conditions the anticipated blue $[(N4Py)Fe^{III}-\eta^2-(OO)]^+$ species **4** was indeed detected by means of a very low and broad absorption band (λ_{max} 705 nm). The low stability was attributed to the employed solvent and temperature.

5.7 Discussion and conclusions

The introduction of four substituents at the 5-position of the pyridine rings in the N4Py ligand was found to influence the characteristic absorption maxima and the extinction coefficients of the corresponding iron(II) complexes only to minor extent. These results, therefore, infer that the proposed mechanism for the $Fe^{III}OOH$ formation from N4PyFe (**2a**) also applies to a broader range of N4Py derivatives. However, the exact nature of the substituent determines the stability and reactivity of the $Fe^{III}OOH$ intermediate, either by altering the redox potential of the iron complex, as in the case of **2b**, or by (presumably) the intramolecular oxidative degradation of the catalyst, as observed for **2d**.

The tetrasubstituted N4PyFe derivatives **2b** and **2c** proved to be active catalysts for the oxidation of cyclohexene and cyclohexane. Although reduced, the longer lasting reactivity of **2c** indicates that by tuning the substituents on the N4Py ligand the lifetime of the catalyst can also be prolonged.

The peroxidase activity of N4PyFe (**2a**) was found to be strongly pH-dependent, which might be due to a pH-controlled destruction of the catalyst, as a higher activity leads to a more rapid degradation of the catalyst. The synthesised N4PyFe-peptide complex **2f** also displayed peroxidase activity as demonstrated by the oxidation of chromogen ABTS. Although the observed activity is substantially lower than that of **2a**, a significantly higher activity compared to the background reaction by hydrogen peroxide was observed. Furthermore, the lifetime of catalyst **2f** was longer than that of **2a**. Mass spectrometry analysis during the oxidation of 1,2,4,5-tetramethoxybenzene by the tetracysteine derived N4PyFe complex **2e** indicated that oxygen atoms were introduced into the ligand system. Under the applied conditions oxidation of the substrate could not be detected. Nevertheless, before **2e** can be ruled out as an active oxidation catalyst, it is suggested that optimised reaction conditions are first established.

5.8 Experimentals

General information

For general information about chemicals and instrumentation, see Chapter 3. N4PyFe (**2a**) was prepared as described previously.[2a,3,11a] For the preparation and analysis of ligand **2b**, see Chapter 4. For the preparation and analysis of ligands **1c–f** and iron(II) complexes **2e** and **2f**, see Chapter 3. GC analyses were performed on an Agilent 6890 Series GC System, equipped with a HP-1 methyl siloxane capillary column (30.0 m x 250 μm x 0.25 μm). The injection port and FID detector were set at 300°C. The temperature profile for the cyclohexene oxidation started at 50°C for 3 min, then was raised to 70°C at 3°C/min and maintained at that temperature for 8 min, followed by a temperature increase of 10°C/min to 100°C, and then to 250°C at 30°C/min. For the cyclohexane oxidation the initial temperature was set to 40°C for 15 min, followed by 10°C/min to 180°C and maintained at that temperature for 3 min. Calibration curves for the oxidation products shown in Scheme 5.4 have been determined using bromobenzene as internal standard.

[(N4Py4Br)Fe(MeCN)](ClO$_4$)$_2$ (2b)

To a suspension of N4Py4Br (93 mg, 0.14 mmol) in methanol (3 mL) was added Fe(ClO$_4$)$_2$·6 H$_2$O (56 mg, 0.15 mmol, 1.1 equiv) in acetonitrile (1.5 mL). The resulting clear dark red/brown solution was stirred at room temperature for 15 min. Slow diffusion of ethyl acetate into this solution furnished **2b** as red crystals (115 mg, 87%).

^{1}H NMR (CD$_3$CN, 300 MHz) δ 4.31 (dd, J_{AB} = 51.8, 18.5 Hz, 4H), 6.32 (s, 1H), 7.00 (d, J = 8.4 Hz, 2H), 7.75 (d, J = 8.4 Hz, 2H), 7.88 (dd, J = 8.4, 1.8 Hz, 2H), 8.10 (dd, J = 8.4, 1.8 Hz, 2H), 9.01 (d, J = 1.8 Hz, 2H), 9.10 (d, J = 1.8 Hz, 2H). ESI-MS [M−(ClO$_4$)$^-$−(MeCN)]$^+$ calcd for $C_{23}H_{17}Br_4ClFeN_5O_4$ *m/z* 833.7, found 833.6. [M−2(ClO$_4$)$^-$−(MeCN)]$^{2+}$ calcd for $C_{23}H_{17}Br_4FeN_5$ *m/z* 367.4, found 367.8. Anal. calcd for $C_{25}H_{20}Br_4Cl_2FeN_6O_8$ C 30.68; H 2.07; N 8.59. Found: C 30.48; H 2.27; N 8.36.

[(N4Py(CH$_2$OMe)$_4$)Fe(MeCN)](ClO$_4$)$_2$ (2c)

To a solution of **1c** (32 mg, 0.059 mmol) in acetonitrile (1.5 mL) was added Fe(ClO$_4$)$_2$·H$_2$O (17 mg, 0.066 mmol, 1.1 equiv). The deep red solution was placed in a sealed container and ethyl acetate was allowed to diffuse slowly into the solution. A dark red oil was formed after a week. The solution was removed and the oil dissolved in acetonitrile. A fine red powder was formed, which was isolated and redissolved in acetonitrile. Slow diffusion of ethyl acetate provided **2c** as red crystals after two weeks (9 mg, 18%).

^{1}H NMR (CDCl$_3$, 300 MHz) δ 3.29 (s, 6H), 3.34 (s, 6H), 4.32 (dd, J_{AB} = 27.9, 8.1 Hz, 4H), 4.38 (s, 4H), 4.47 (s, 4H), 6.31 (s, 1H), 7.04 (d, J = 8.1 Hz, 2H), 7.63 (d, J = 7.7 Hz, 2H), 7.85 (m, 4H), 8.82 (s, 2H), 8.92 (s, 2H). ESI-MS [M−(ClO$_4$)$^-$−(MeCN)]$^+$ calcd for C$_{31}$H$_{38}$ClFeN$_5$O$_8$ *m/z* 698.2, found 698.0. [M − 2(ClO$_4$)$^-$]$^{2+}$ calcd for C$_{33}$H$_{40}$FeN$_6$O$_4$ *m/z* 320.1, found 320.3. [M−2(ClO$_4$)$^-$−(MeCN)]$^{2+}$ calcd for C$_{31}$H$_{37}$FeN$_5$O$_4$ *m/z* 299.6, found 300.0.

[(N4Py(CH$_2$CH$_2$CH$_2$OMe)$_4$)Fe(MeCN)](ClO$_4$)$_2$ (2d)

To a solution of **1d** (35 mg, 0.054 mmol) in acetonitrile (1.5 mL) was added Fe(ClO$_4$)$_2$·6 H$_2$O (22 mg, 0.060 mmol, 1.1 equiv). The deep red solution was placed in a sealed container and ethyl acetate was allowed to slowly diffuse into the solution. A dark red oil was formed after a week. Repeated attempts failed to yield crystals and **2d** was obtained as a dark red/brown oil (41 mg, 84%).

^{1}H NMR (CDCl$_3$, 300 MHz) δ 1.85 (m, 8H), 2.80 (m, 8H), 3.25 (s, 6H), 3.32–3.48 (m, 8H), 3.39 (s, 6H), 4.36 (dd, J_{AB} = 31.7, 18.1 Hz, 4H), 6.32 (s, 1H), 7.07 (d, J = 8.1 Hz, 2H), 7.61 (d, J = 7.7 Hz, 2H), 7.86 (s, 4H), 8.83 (s, 2H), 8.94 (s, 2H). ESI-MS [M − (ClO$_4$)$^-$ − (MeCN)]$^+$ calcd for C$_{39}$H$_{53}$ClFeN$_5$O$_8$ *m/z* 810.3, found 810.3. [M−2(ClO$_4$)$^-$]$^{2+}$ calcd for C$_{41}$H$_{56}$FeN$_6$O$_4$ *m/z* 376.2, found 376.4. [M−2(ClO$_4$)$^-$−(MeCN)]$^{2+}$ calcd for C$_{39}$H$_{53}$FeN$_5$O$_4$ *m/z* 355.7, found 355.9.

Cyclic voltammetry of 2b

The cyclic voltammetry measurements were performed by dr. Scott Killeen at Unilever Research, Vlaardingen, The Netherlands, on a three-electrode electrochemical cell interfaced to a Princeton Applied Research potentiostat (Model 273A). The electrodes used (Working: 5 mm diameter glassy carbon, Counter: Pt wire, Reference: Ag/AgCl (3 M KCl)) were freshly cleaned by standard techniques prior to each measurement. The supporting electrolyte was 0.1 M tetrabutylammonium perchlorate (puriss, Fluka) in acetonitrile (analytical grade, Mallinckrodt Baker BV). The sample for analysis was prepared by dissolving **2b** (3 mg) in the electrolyte (10 mL). All measurements were carried out at 22°C and degassed with argon prior to measurement. For CV experiments the scan rate was 100 mV s^{-1} with an increment of 5 mV. The differential pulse voltammetry experiments were conducted at a scan rate of 10mVs^{-1} with an increment of 2 mV.

X-ray crystallography[29]

The selected crystal was mounted on a glass fibre and aligned on a *Bruker*[30] *SMART APEX CCD* diffractometer (Platform with full three-circle goniometer) equipped with a 4K *CCD* detector and a *Bruker KRYOFLEX* low-temperature device. Intensity measurements were performed using graphite monochromatic Mo–K$\overline{\alpha}$ radiation from a sealed ceramic diffraction

tube (50 kV/40 mA). All calculations for refinement and graphics were performed on a Pentium III (Debian-Linux) computer at the University of Groningen with the program packages *SHELXL*[31] (least-square refinements), a locally modified version of the program *PLUTO*[32] (preparation of illustrations) and the *PLATON*[33] package (checking the final results for missed symmetry with the *MISSYM* option, solvent accessible voids with the *SOLV* option, and calculation of geometric data).

Structure analysis of 2b. Crystallisation from acetonitrile/ethyl acetate initially afforded **2b** as red square platelets, with a monoclinic unit cell with a $P2_1/n$ space group, as well as a disordered and fractional occupation with the solvent molecules. Recrystallisation furnished red octahedral-shaped crystals. Dimensions of the crystal used for analysis: 0.40 x 0.32 x 0.22 mm.

The final unit cell was elucidated from the *xyz* centroids of 7444 reflections after refinement and integration using the programs *SMART* and *SAINT*. In total 1800 frames were collected with an exposure time of 10 s per frame. Intensity data was corrected for Lorentz and polarisation effects, as well as for decay and absorption: a semi-empirical absorption correction was applied, based on the intensities of symmetry-related reflections measured at different angular settings (*SADABS*),[34] and reduced to F_o^2. The program suite *SHELXTL* was used for space group determination (*XPREP*).[31] The structure was solved by automated Patterson methods using the program *DIRDIF*.[35] The positional and (an)isotropic displacement parameters for the non-hydrogen atoms were refined on F^2 using full-matrix least-squares procedures.

The asymmetric unit cell contains eleven moieties: two iron complexes (cations) and four perchlorate anions, one ethyl acetate and four acetonitrile solvent molecules with no atom setting at a special position. The triclinic unit cell contains twenty-two discrete units separated by normal van der Waals distances.

Crystal data. $([C_{25}H_{20}Br_4FeN_6]^{2+})_2.(ClO_4^-)_4.C_4H_8O_2.(C_2H_3N)_4$; M = 2209.9 gmol^{-1}; triclinic; space group $P\bar{1}$ with a = 16.8760(8), b = 16.9697(8), c = 17.1403(8) Å; α = 64.758(1)°, β = 63.885(1)°, γ = 77.286(1)°; V = 3983.5(3) Å^3; Z = 2; D_x = 1.842 gcm^{-3}; λ = 0.71073 Å; μ = 45.86 cm^{-1}; F(000) = 2176; T = 90 K; *GooF* = 1.030; $wR(F^2)$ = 0.1105 for 20152 reflections and 974 parameters; $R(F)$ = 0.0423 for 15627 reflections obeying the $F_o \geq 4.0\ \sigma(F_o)$ criterion of observability.

Structure analysis of 2c. Red coloured triangular/block-shaped crystals were obtained after a troublesome crystallisation from acetonitrile by slow diffusion of ethyl acetate. Most of the crystals were joined together, which hampered the X-ray structure determination, however a small suitable specimen was found. Dimensions of the crystal used for analysis: 0.10 x 0.10 x 0.10 mm.

The final unit cell was obtained from the *xyz* centroids of 6038 reflections after refinement and integration using the programs *SMART* and *SAINT*. A total of 1800 frames were collected with an exposure time of 30 s per frame. Intensity data was corrected for Lorentz and polarisation effects, scale variation, and for decay and absorption. A multi-scan absorption correction was applied, based on the intensities of symmetry-related reflections measured at different angular settings (*SADABS*),[34] and reduced to F_o^2. The program suite *SHELXTL* was used for space group determination (*XPREP*).[31] The *E*-statistics of the triclinic unit cell were indicative of a centrosymmetric space group. The structure was solved by direct methods using

SIR-97.[36] The positional and anisotropic displacement parameters for the non-hydrogen atoms were refined. Refinement was complicated by a disorder problem: from the solution it was clear that one of the two perchlorate anions was highly disordered. The electron density of the atoms appeared to be diffuse, indicating transformational disorder. A disorder model with bond restraints and two different orientations were also introduced into the subsequent refinement. The site-occupation factor of the major fraction of the disordered perchlorate anions was refined to a value of 0.519(5).

The asymmetric unit consists of four moieties: a cationic iron complex, two perchlorate anions, one of which is highly disordered, and one acetonitrile solvent molecule. Reduced cell calculations did not indicate any higher metric lattice symmetry and examination of the final atomic co-ordinates of the structure did not yield any additional metric symmetry elements.
Crystal data. $[C_{33}H_{40}FeN_6O_4]^{2+}.(ClO_4^-)_2.C_2H_3N$; M_r = 880.52 gmol^{-1}; triclinic; space group *P*−1 with *a* = 10.2381(6), *b* = 13.1842(7), *c* = 16.4591(9) Å; α = 67.046(1)°, β = 77.949(1)°, γ = 75.701(1)°; *V* = 1966.57(19) Å^3; *Z* = 2; D_x = 1.487 gcm^{-3}; λ = 0.71073 Å; μ = 5.90 cm^{-1}; *F*(000) = 916; T = 100 K; *GooF* = 1.028; *wR*(F^2) = 0.1485 for 8855 reflections and 567 parameters, 8 restraints; *R*(*F*) = 0.0584 for 6275 reflections obeying the $F_o \geq 4.0\ \sigma(F_o)$ criterion of observability.

Catalytic oxidation of cyclohexene and cyclohexane

A 3.50 mM stock solution of the catalyst was prepared in acetonitrile. For the experiment a 1.0 mL aliquot was transferred into the reaction flask and the solvent evaporated *in vacuo*. A stock solution of the substrate (43.75 mmol) and bromobenzene (4.37 mmol) as an internal standard was prepared in the appropriate solvent (50.00 mL). A 4.0 mL aliquot of stock solution was added to the catalyst under a nitrogen atmosphere. Samples were taken at designated intervals, filtered over a small amount of silica gel, washed with diethyl ether/methanol (9:1, 1 mL), and analysed by gas chromatography. Duplicate experiments were performed to calculate the average number of turnovers (margin of error ~1 turnover).
Procedure A: The oxidation was initiated by injection of H_2O_2 (35 µL, 10 M, 30% in water) to the reaction mixture (catalyst/H_2O_2/substrate = 1:100:1000) at 20°C. Samples (200 µL) were taken at intervals of 5, 10, 20, 30, 45, and 60 min.
Procedure B: The H_2O_2 (0.75 mL, 10 M, 30% in water) was administered to the reaction mixture (catalyst/H_2O_2/substrate = 1:2000:1000) by a syringe pump over 1 h at 20°C. Samples (200 µL) were taken at intervals of 30, 60, and 90 min.

ABTS oxidation

All ABTS oxidation experiments were performed in 0.1 M acetate buffers at pH 3.0, 3.5, 4.0, and 4.5 using a magnetically stirred, thermostatically controlled quartz cuvette at 20°C. The increase in absorption due to the $ABTS^{+\bullet}$ radical cation formation was monitored by a UV-Vis spectrophotometer at 660 nm (ε 1.47 x 10^4 M^{-1}cm^{-1})[15b] at intervals of 1 s for 400 s with an incremental cycle time of 10% after an initial time of 60 s. The experimental conditions were identical to those described previously by Dr. C. T. Choma.[24]

5.9 References and notes

1. For an explanation of the abbreviations used, see Appendix 1 (p. 149).
2. (a) Roelfes, G.; Lubben, M.; Chen, K.; Ho, R. Y. N.; Meetsma, A.; Genseberger, S.; Hermant, R. M.; Hage, R.; Mandal, S. K.; Young, V. G., Jr.; Zang, Y.; Kooijman, H.; Spek, A. L.; Que, L., Jr.; Feringa, B. L. *Inorg. Chem.* **1999**, *38*, 1929–1936. (b) Roelfes, J. G., In *Models for Non-Heme Iron Containing Oxidation Enzymes*, Ph. D. thesis, Groningen, 2000.
3. (a) Lubben, M., In *Model Systems for Iron and Copper Containing Oxygenases*, Ph. D. thesis, Groningen, 1994; pp. 43–71. (b) Lubben, M.; Meetsma, A.; Wilkinson, E. C.; Que, L., Jr.; Feringa, B. L. *Angew. Chem. Int. Ed. Engl.* **1995**, *34*, 1512–1514.
4. See Appendix 2 (p. 151) for the structures and one-letter abbreviations of the amino acids.
5. See Chapter 3 for the characterisation of **2e** and **2f**.
6. Selected bond distances originate from residue 2 in the unit cell of **2b**. For residue 1 the bond lengths are: Fe–N1, 1.966(3); Fe–N2, 1.967(4); Fe–N3, 1.957(3); Fe–N4, 1.952(3); Fe–N5, 1.970(4); Fe–N6, 1.929(4); Fe–$N_{py-mean\ plane}$, 0.200(1).
7. Solomon, E. I.; Brunold, T. C.; Davis, M. I.; Kemsley, J. N.; Lee, S.-K.; Lehnert, N.; Neese, F.; Skulan, A. J.; Yang, Y.-S.; Zhou, J. *Chem. Rev.* **2000**, *100*, 235–349.
8. The iron(II) complex of the N4Py derivative **6b** in Chapter 2 (p. 34).
9. C. T. Choma, *personal communication*.
10. Ho, R. Y. N.; Roelfes, G.; Hermant, R.; Hage, R.; Feringa, B. L.; Que, L., Jr. *Chem. Commun.* **1999**, 2161–2162.
11. (a) Roelfes, G.; Lubben, M.; Leppard, S. W.; Schudde, E. P.; Hermant, R. M.; Hage, R.; Wilkinson, E. C.; Que, L., Jr.; Feringa, B. L. *J. Mol. Catal. A: Chem.* **1997**, *117*, 223–227. (b) Roelfes, G.; Lubben, M.; Hage, R.; Que, L., Jr.; Feringa, B. L. *Chem. Eur. J.* **2000**, *6*, 2152–2159.
12. Arends, I. W. C. E.; Ingold, K. U.; Wayner, D. D. M. *J. Am. Chem. Soc.* **1995**, *117*, 4710–4711.
13. (a) Everse, J., Everse, K. E., Grisham, M. B., In *Peroxidases in Chemistry and Biology*; CRC Press: Boca Raton, USA, 1991; Vol. 2, pp. 1–24. (b) Ball, D. P., In *Essays in Biochemistry*, *Metalloproteins*; Portland Press: UK, 1999; Vol. 34, pp. 51–69.
14. (a) Cunningham, I. D.; Bachelor, J. L.; Pratt, J. M. *J. Chem. Soc.*, *Perkin Trans. 2* **1991**, 1839–1843. (b) Chuang, W.-J.; Chang, Y.-D.; Jeng, W.-Y. *J. Inorg. Biochem.* **1999**, *75*, 93–97.
15. (a) Casella, L.; Poli, S.; Gullotti, M.; Selvaggini, C.; Beringhelli, T.; Marchesini, A. *Biochemistry* **1994**, *33*, 6377–6386. (b) Casella, L.; De Gioia, L.; Silvestri, G. F.; Monzani, E.; Redaelli, C.; Roncone, R.; Santagostini, L. *J. Inorg. Biochem.* **2000**, *79*, 31–40.
16. (a) Adams, P. A.; Goold, R. D. *J. Chem. Soc.*, *Chem. Commun.* **1990**, 97–98. (b) Adams, P. A. *J. Chem. Soc.*, *Perkin Trans. 2* **1990**, 1407–1414.
17. (a) Maehly, A. C.; Chance, B., In *Methods in Biochemical Analysis*; Glick, D., Ed.; 1954; Vol. 1, pp. 385–387. (b) Chance, B.; Maehly, A. C., In *Methods in Enzymology*; Colowick, S. P.; Kaplan, N. O., Eds.; Academic Press: New York, USA, 1964; pp. 770–773.
18. Iffland, A.; Tafelmeyer, P.; Gendreizig, S.; Johnsson, K. *Chimia* **2001**, *55*, 291–294.

19. (a) Fujita, A.; Senzu, H.; Kunitake, T.; Hamachi, I. *Chem. Lett.* **1994**, 1219–1222. (b) Doerge, D. R.; Divi, R. L.; Churchwell, M. I. *Anal. Biochem.* **1997**, *250*, 10–17. (c) Ochoe de Aspuru, E.; Zatón, A. M. L. *Spectrochim. Acta A* **1999**, *55*, 2343–2346. (d) Sakamoto, S.; Obataya, I.; Ueno, A.; Mihara, H. *J. Chem. Soc.*, *Perkin Trans. 2* **1999**, 2059–2069. (e) Obataya, I.; Kotaki, T.; Sakamoto, S.; Ueno, A.; Mihara, H. *Bioorg. Med. Chem. Lett.* **2000**, *10*, 2719–2722.
20. Other structures have also been suggested for tetraguaiacol. See references 17a and 19b.
21. (a) Childs, R. E.; Bradsley, W. G. *Biochem. J.* **1975**, *145*, 93–103. (b) Moffet, D. A.; Certain, L. K.; Smith, A. J.; Kessel, A. J.; Beckwith, K. A.; Hecht, M. H. *J. Am. Chem. Soc.* **2000**, *122*, 7612–7613.
22. Poigny, S.; Guyot, M.; Samadi, M. *Tetrahedron* **1998**, *54*, 14791–14802.
23. (a) Kersten, P. J.; Tien, M.; Kalyanaraman, B.; Kirk, T. K. *J. Biol. Chem.* **1985**, *260*, 2609–2612. (b) Kersten, P. J.; Kalyanaraman, B.; Hammel, K. E.; Reinhammar, B.; Kirk, T. K. *Biochem. J.* **1990**, *268*, 475–480. (c) Schoemaker, H. E. *Recl. Trav. Chim. Pays-Bas* **1990**, *109*, 255–272. (d) Popp, J. L.; Kirk, T. K. *Arch. Biochem. Biophys.* **1991**, *288*, 145–148.
24. Choma, C. T.; Schudde, E. P.; Kellogg, R. M.; Robillard, G. T.; Feringa, B. L. *J. Chem. Soc.*, *Perkin Trans. 1* **1998**, 769–773.
25. Florence, T. M. *J. Inorg. Biochem.* **1985**, *23*, 131–141.
26. Wolfenden, B. S.; Willson, R. L. *J. Chem. Soc.*, *Perkin Trans. 2* **1982**, 805–812.
27. Rush, J. D.; Koppenol, W. H. *J. Am. Chem. Soc.* **1988**, *110*, 4957–63.
28. De Nooy, A. E. J.; Besemer, A. C.; Van Bekkum, H. *Synthesis* **1996**, 1153–1174.
29. Data collection, structure analysis and refinement was carried out by A. Meetsma, Crystal Structure Center, Chemical Physics, Materials Science Center, University of Groningen: The Netherlands.
30. *SMART*, *SAINT*, *SADABS*, *XPREP* and *SHELXTL/NT*, Smart Apex *Software Reference Manuals*, Bruker AXS, Inc.: Madison, Wisconsin, USA, 2000.
31. Sheldrick, G. M., *SHELXL-97*, *Program for the Refinement of Crystal Structures*, University of Göttingen: Germany, 1997.
32. Meetsma, A., *PLUTO. Molecular Graphics Program*, University of Groningen: The Netherlands, 2001.
33. Spek, A. L., *PLATON. Program for the Automated Analysis of Molecular Geometry* (*A Multipurpose Crystallographic Tool*), University of Utrecht: The Netherlands, February 2002.
34. Sheldrick, G. M., *SADABS* (Version 2), *Empirical Absorption Correction Program*, University of Göttingen: Germany, 2000.
35. Beurskens, P. T.; Beurskens, G.; De Gelder, R.; García-Granda, S.; Gould, R. O.; Israël, R.; Smits, J. M. M., *The DIRDIF-99 program system*, Crystallography Laboratory, University of Nijmegen: The Netherlands, 1999.
36. Altomare, A.; Burla, M. C.; Camalli, M.; Cascarano, G. L.; Giacovazzo, C.; Guagliardi, A.; Moliterni, A. G. G.; Polidori, G.; Spagna, R. *J. Appl. Cryst.* **1999**, *32*, 115–119.

Chapter 6

Conclusions and future prospects

6.1 Introduction

Over the past decades numerous structure-stability and structure-function studies have been performed on native proteins and designed peptide structures. Today, this knowledge is applied to the construction of proteins with enhanced or modified enzymatic activities,[1] as well as relatively small peptide-based catalysts or architectures.[2] The examples illustrated and discussed in Chapter 1 of *de novo* designed four-helix bundle motifs clearly demonstrate that considerable progress has been made towards the design and synthesis of artificial proteins and enzyme mimics in recent years.[3]

Several of the reported four-helix bundles have successfully been provided with a catalytic function, often via the introduction of a prosthetic group like a haem or porphyrin moiety,[2c] or by a specific spatial arrangement of certain α-amino acids.[4] Although the catalytic activity of the designed structures is often inferior to that of the natural systems, the results appear to be quite promising to anticipate native-like behaviour of these synthetic enzymes analogues in the near future. Examples of artificial non-haem oxidising enzymes based on the four-helix bundle motif have yet to be reported to the best of our knowledge.

6.2 From natural enzyme to enzyme mimic

The iron(II) complex of the pentadentate ligand N4Py,[5,6] which was developed within our research group, was previously found to be an active catalyst for the oxidation of various organic substrates.[7] Mechanistic studies have led to a proposed catalytic cycle for the oxidation of alkanes by N4PyFe.[8] The characterised reaction intermediates have proved that this non-haem oxidation catalyst can also function as an effective model for the natural glycopeptide iron bleomycin.

The research presented in this thesis explored and developed synthetic procedures by which four functionalities could be introduced into the N4Py scaffold and thereafter enabled the coupling of four peptide chains. Previously in our group, Choma *et al*. successfully established

the preparation of a dipeptide-bound N4PyFe catalyst, which also displayed peroxidase activity.[9] The peptides were coupled via a cysteine residue to two chloromethylene substituents at the periphery of the N4Py ligand. This methodology, however, could not be applied to the construction of the corresponding tetrapeptide derivative, as the required N4Py template **4** (R = Cl) was found to be intrinsically unstable.

The four pyridine rings that are tethered to the central nitrogen atom in the N4Py ligand were subsequently functionalised to facilitate the covalent attachment of four peptide chains via a C3-spacer (Scheme 6.1). The resulting peptide-bound iron complexes were then obtained via the nucleophilic substitution of a cysteine thiolate in the peptide sequence, and subsequent inclusion of an iron(II) metal ion. Purification by reversed-phase HPLC furnished the target structure as a single product, which was validated by MALDI spectrometry.

This methodology could eventually enable the introduction of the N4PyFe complex into a four-helix bundle to examine the effect of the peptide environment on the catalytic activity of the iron complex. Conversely, the N4PyFe complex could also provide these peptide bundles with a catalytic function.

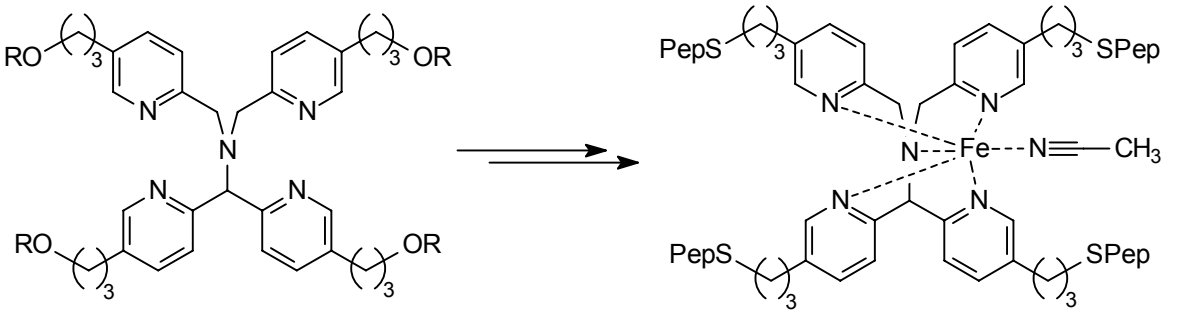

1 (R = OTBDMS)

2a (Pep = Ac-CGLHELLKG-NH_2)

2b (Pep = Ac-CGGGGDYKDDDDK-NH_2)

Scheme 6.1. The N4PyFe-peptide complexes **2a** and **2b**, prepared from the tetrafunctionalised N4Py derivative **1**.[10]

The peroxidase activity of the peptide-bound N4PyFe catalyst **2a** was examined for the oxidation of the chromogen ABTS (Chapter 5). Although the catalytic activity observed was substantially lower than that of N4PyFe, the lifetime of **2a** appeared to be extended compared to that of N4PyFe. These findings are still only considered to be a preliminary conclusion, as the results were obtained using a single substrate and peptide complex combination. By examining the stability of the related tetracysteine N4PyFe catalyst towards oxidation at room temperature, a rapid decomposition of the catalyst was observed, presumably initiated by the oxidation of the sulphide linker.

6.3 Alternatives for peptide coupling

Although peptides have been successfully coupled to the N4Py scaffold via a C3-spacer, modelling studies using different peptide sequences have revealed that the resulting four-helix bundle structure will be more compact employing a C1-spaced N4PyFe catalyst.[11] This necessitates the development of an alternative means of attaching peptides to the C1-spaced

N4Py ligand **3**, as the tetrachloro N4Py derivative **4** (R = Cl) was found to be far too unstable for this application. Some of the model reactions carried out to elucidate the origin of this instability could provide better solutions to overcome this problem.

The terminal hydroxyl functionalities in **3** can be deprotonated by sodium hydride in DMF and in principle allowed to react with *N*-bromoacylated peptides (Table 6.1, entry 1). Alternatively, the hydroxyl groups can be oxidised to aldehydes or carboxylic groups, and subsequently coupled to peptides via the *N*-termini or lysine residues in the sequence to form imine or amide bonds, respectively (Table 6.1, entries 4 and 5). However, attempts to form an amide bond between an amine and a carboxy derivatised N4Py ligand have so far been unsuccessful.[12] In Scheme 3.12 a procedure was described in which the benzylic hydroxyl group

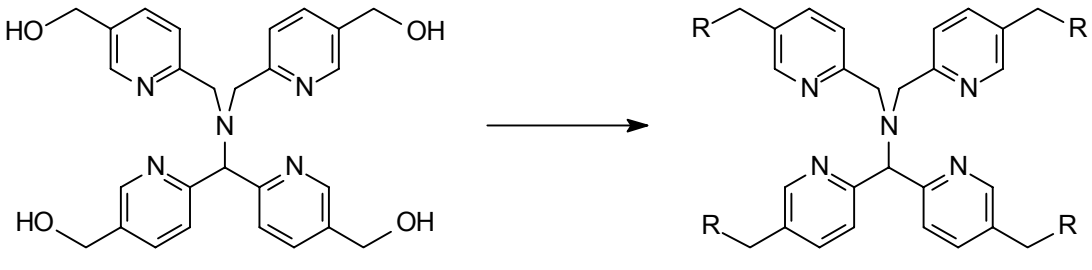

3 **4**

Table 6.1. A number of methods for peptide coupling after transforming the hydroxyl functionalities in **3**.

Entry	R	Peptide terminus	Linkage	Ref.
1	OH	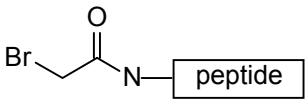	ether	13
2	SH	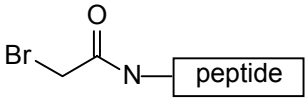	sulphide	14,15
3	SH	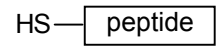	disulphide	16
4	CHO	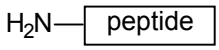	imine[a]	17
5	CO_2H	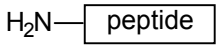	amide	18
6	NH_2	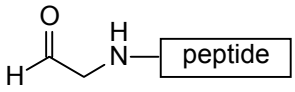	imine[a]	19
7	NH_2	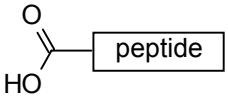	amide	18

a) Subsequent reduction of the imine provides a much more stable amine linkage.

of 3-(hydroxymethyl)pyridine was converted into a thiol under acidic conditions. As it was previously established that the tetrachloromethylene N4Py derivative **4** (R = Cl) was only stable as its hydrochloride salt, this procedure could facilitate the preparation of the corresponding tetrasulphide N4Py derivative **4** (R = SH). This can subsequently be allowed to react with *N*-bromoacylated peptides or a cysteine residue to form a thioether or a disulphide linkage, respectively (Table 6.1, entries 2 and 3). The tetrafunctionalised N4Py derivative with amine groups at the periphery (**4**, R = NH_2) might be obtained from **3** via the introduction of an appropriate linker that contains a (protected) amine functionality. However, as the corresponding model reactions, described in Chapter 3, were unsuccessful, this does not prove to be a viable option. As an alternative, the tetrabromide N4Py derivative **5** could enable these compounds to be prepared via metal-catalysed cross coupling reactions (Scheme 4.2), as presented in Chapter 4. These amine groups can subsequently be allowed to react with a carboxyl group in the peptide chain to form an amide bond (Table 6.1, entry 7). Alternatively, these amine functionalities can be used to couple peptides via an imine bond, which can then be reduced to afford a more stable amine bond (Table 6.1, entry 6).

By employing selectively removable protecting groups for lysine and cysteine (Table 6.2), the presence of more than one of these residues in a peptide chain can still enable a site-specific introduction of an appropriately functionalised N4PyFe catalyst. However, the stability of the peptide-bound N4Py ligand towards the applied deprotection conditions after coupling the peptides has yet to be ascertained.

Table 6.2. Some examples of selectively removable protecting groups for lysine and cysteine.

Entry	Residue	Protecting group[5]	Deprotection method	Ref.
1	Lysine	Alloc	$PdCl_2(PPh_3)_2$/Bu_3SnH/AcOH	14,20
2	Lysine	Boc	TFA	21
3	Lysine	Z	TMSOTf/TFA	21
4	Lysine	Dde	H_2NNH_2	20,22
5	Cysteine	Trt	TFA/DTT	14,22
6	Cysteine	Acm	$Hg(OAc)_2$, pH 4	14,22
7	Cysteine	*tert*-butyl	DTT	22
8	Cysteine	Acm	AgOTf/TFA	23

6.4 Tetrabromo N4Py as a versatile building block

The developed convergent synthetic route to the N4PyFe-peptide catalysts involves numerous reaction steps. The encountered dead-end after the lengthy synthetic pathway to the C1-spaced N4Py derivative **4** (R = Cl) was quite unfortunate. In the development of a total synthesis to complex natural compounds these unwanted terminations are often also encountered.[24] These natural compounds are generally far more complex, which might "justify" these dead-ends, although this does not imply that these can be identified earlier for more concise synthetic routes.

By modification of the synthetic route the corresponding C3-spaced derivative could be obtained. In order to avoid an iterative ligand construction of N4Py derivatives from their initial building blocks, N4Py4Br (**5**) was developed. This ligand can in principle enable a divergent synthesis of various N4Py ligand structures using cross coupling methodologies (Scheme 4.2). After the construction of the N4Py scaffold this ligand was functionalised by subsequent reactions at the bromide sites in the molecule, and thereby functioned as a building block. This procedure has already been successfully applied to the preparation of tetraphenyl N4Py (**6a**, R' = H) via the Suzuki reaction of **5** with phenylboronic acid. The examined test reactions on bromopyridines have indicated that other types of cross coupling reactions and reagents could also prove to be potential candidates for synthesising a wide range of N4Py derivatives.

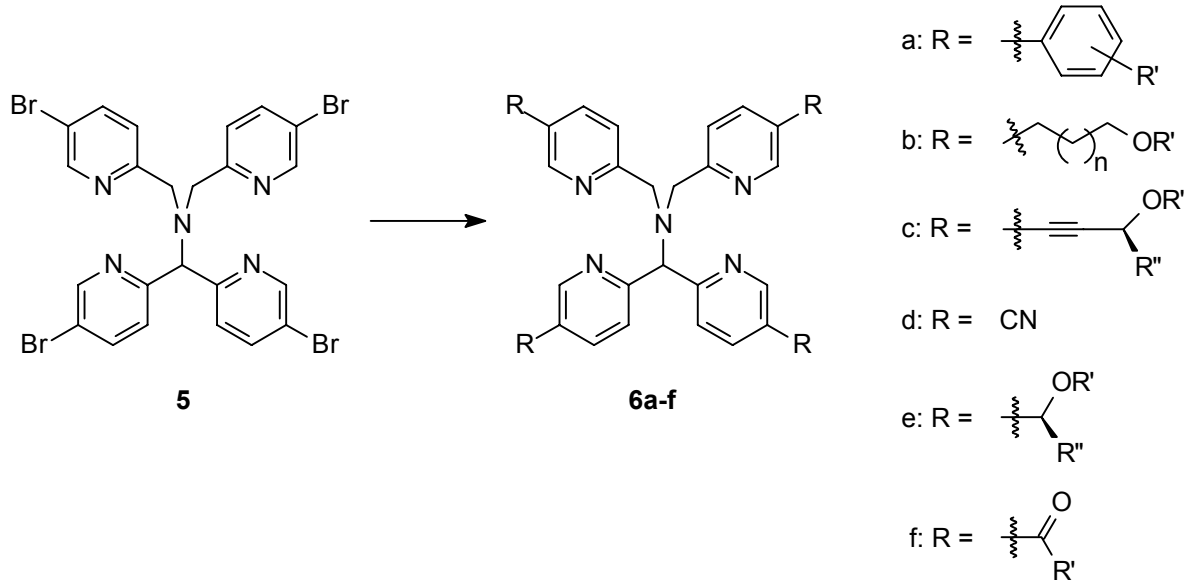

Scheme 6.2. A selection of potential N4Py ligands that can be envisaged from N4Py4Br (**5**) by, for instance, cross coupling (**6a–d**) or lithiation reactions (**6e–f**).

The iron complexes of the N4Py derivatives obtained from **5** could have interesting catalytic properties in oxidation reactions and also could enable the redox potential of the iron centre to be tuned to our advantage.[25] Furthermore, the introduction of appropriate tethers at the periphery of the N4Py ligand might also improve the stability of the catalyst. In Chapter 5 it was already demonstrated that the oxidation behaviour of tetrafunctionalised N4PyFe complexes is substantially different from the iron(II) complex of N4Py. In addition to this, the redox potential of $[(N4Py4Br)Fe(MeCN)](ClO_4)_2$ was found to be almost 200 mV higher than that of N4PyFe (1196 mV vs. 1010 mV).

6.5 Conclusions

The challenge presented in the original research proposal, which outlined the construction of an artificial peroxidase, has so far not entirely been met. The work described in this thesis presents an overview of the synthetic difficulties encountered during the preparation of a N4Py ligand with four covalently bound peptide chains. Unfortunately, due to the considerable amount of time that was invested in the development of a synthetic pathway to peptide-bound N4PyFe

catalysts and the accompanied complications during the HPLC purifications, the introduction of the N4PyFe catalyst inside a four-helix bundle has as yet not been accomplished. A peptide coupling with a sequence that was designed to fold into a four-helix bundle, although attempted,[26] proved to be unsuccessful.

In order to obtain an artificial enzyme, four peptide sequences will need to be attached to the ligand that will not only fold into a four-helix bundle, but eventually also discriminate between different substrate molecules (specificity) and/or possible reaction products (selectivity). This necessitates a design that will implement a certain synergy between the chemistry of the N4PyFe catalyst and the ability of the peptides surrounding it to provide a selective binding site that may discriminate between different substrates.

Further optimisation of the reaction conditions using model peptide-bound N4PyFe catalysts, for instance by substrate screening and investigating the pH- and temperature-dependence, could provide a better insight into the feasibility of employing the N4PyFe catalyst as a catalytic centre within a designed four-helix bundle. The peptide sequences introduced into the peptide-bound N4PyFe catalyst **2a** so far were not designed to fold into a four-helix bundle, and thus lacked a well-defined structure that could affect or control the oxidation process. Depending on which sequences are selected for the peptide coupling, the catalyst can be positioned either in the core of the bundle or as a tethering moiety. If the catalyst is to be located in the core, a cavity will have to be created to host the N4PyFe complex without disrupting the stability of the four-helix bundle. Such a cavity will not have to be incorporated into the design if the peptides are linked to the catalyst via their termini. However, such a design will not enable an optimal interaction of these peptides with the catalyst to modulate its activity.

The oxidation experiments in Chapter 5 have revealed that the sulphide linkage in the N4PyFe-peptide catalyst is prone to oxidation under the applied conditions. The bare N4PyFe catalyst, however, is also deactivated by oxidative degradation. If the results from the oxidation experiments of the examined tetracysteine N4PyFe derivative are ignored, then the N4Py ligand can be considered to be no more than a potential template for the construction of four-helix bundles with a non-haem iron-catalyst in the hydrophobic core. However, for the peptide complex to function properly as an artificial peroxidase a more stable linker, for instance an ether or amide bond, will be required. Preliminary results have already indicated that a disulphide linkage between a pyridine thiol and a cysteine residue in a peptide sequence can be readily obtained.[11] Furthermore, this disulphide linkage was found to be stable towards oxidation in the presence of hydrogen peroxide and N4PyFe.[11]

During the catalytic cycle of N4PyFe hydroxyl radicals are formed. The stability of the peptide chains towards these hydroxyl radicals could be quite low, although peptides have been reported to increase the stability of microperoxidases towards oxidative degradation.[27] However, it is important to remember that the catalytic cycle of $N4PyFe^{III}OOH$ most likely also involves a non-radical pathway via a more selective, iron centred oxidising intermediate, presumably $[(N4Py)Fe^{IV}O]^{2+}$.[8d] Therefore, suppressing the radical pathway will not only extend the lifetime of the catalyst by reducing, or even preventing, its oxidative degradation, but possibly also enhancing its selectivity during the oxidation reaction.

Although the only attempted Suzuki reaction on N4Py4Br (**5**) involved the synthesis of **6a** (R' = H), the outcome of this reaction and that of the performed model reactions in Chapter 4 seem to be encouraging for other related substrates. The exploration of the potential cross

coupling reactions and conditions has opened up a promising new domain to more readily accessible N4Py derivatives, whose preparation could unfortunately not be attempted due to a lack of time.

6.6 References and notes

1. (a) Penning, T. M.; Jez, J. M. *Chem. Rev*. **2001**, *101*, 3027–3046. (b) Lu,Y.; Berry, S. M.; Pfister, T. D. *Chem. Rev*. **2001**, *101*, 3047–3080. (c) Qi, D.; Tann, C.-M.; Haring, D.; Distefano, M. D. *Chem. Rev.* **2001**, *101*, 3081–3111.
2. (a) DeGrado, W. F.; Summa, C. M.; Pavone, V.; Nastri, F.; Lombardi, A. *Annu. Rev. Biochem.* **1999**, *68*, 779–819. (b) Baltzer, L.; Nilsson, H.; Nilsson, J. *Chem. Rev.* **2001**, *101*, 3153–3163. (c) Lombardi, A.; Nastri, F.; Pavone, V. *Chem. Rev.* **2001**, *101*, 3165–3189. (d) Moffet, D. A.; Hecht, M. H. *Chem. Rev.* **2001**, *101*, 3191–3203.
3. (a) Jaeger, K.-E.; Reetz, M. T. *Curr. Opin. Chem. Biol*. **2000**, *4*, 68–73. (b) Brakmann, S. *CHEMBIOCHEM* **2001**, *2*, 865–871. (c) Baltzer, L.; Nilsson, J. *Curr. Opin. Biotechnol*. **2001**, *12*, 355–360. (d) Bornscheuer, U. T.; Pohl, M. *Curr. Opin. Chem. Biol*. **2001**, *5*, 137–143. (e) Xing, G.; DeRose, V. J. *Curr. Opin. Chem. Biol.* **2001**, *5*, 196–200. (f) Woolfson, D. N. *Curr. Opin. Struct. Biol*. **2001**, *11*, 464–471. (g) Kennedy, M. L.; Gibney, B. R. *Curr. Opin. Struct. Biol*. **2001**, *11*, 485–490. (h) Gilardi, G.; Fantuzzi, A.; Sadeghi, S. J. *Curr. Opin. Struct. Biol*. **2001**, *11*, 491–499.
4. Baltzer, L.; Broo, K. S. *Biopolymers (Peptide Sci.)* **1998**, *47*, 31–40.
5. For an explanation of the abbreviations used, see Appendix 1(p. 149).
6. (a) Lubben, M., In *Model Systems for Iron and Copper Containing Oxygenases*, Ph. D. thesis, Groningen, 1994, pp. 43–71. (b) Lubben, M.; Meetsma, A.; Wilkinson, E. C.; Que, L., Jr.; Feringa, B. L. *Angew. Chem. Int. Ed. Engl.* **1995**, *34*, 1512–1514.
7. (a) Roelfes, G.; Lubben, M.; Leppard, S. W.; Schudde, E. P.; Hermant, R. M.; Hage, R.; Wilkinson, E. C.; Que, L., Jr.; Feringa, B. L. *J. Mol. Catal. A: Chem.* **1997**, *117*, 223–227. (b) Roelfes, G.; Lubben, M.; Hage, R.; Que, L., Jr.; Feringa, B.L. *Chem. Eur. J.* **2000**, *6*, 2152–2159.
8. (a) Roelfes, G.; Lubben, M.; Chen, K.; Ho, R. Y. N.; Meetsma, A.; Genseberger, S.; Hermant, R. M.; Hage, R.; Mandal, S. K.; Young, V. G., Jr.; Zang, Y.; Kooijman, H.; Spek, A. L.; Que, L., Jr.; Feringa, B. L. *Inorg. Chem.* **1999**, *38*, 1929–1936. (b) Ho, R. Y. N.; Roelfes, G.; Hermant, R.; Hage, R.; Feringa, B. L.; Que, L., Jr. *Chem. Commun.* **1999**, 2161–2162. (c) Ho, R. Y. N.; Roelfes, G.; Feringa, B. L.; Que, L., Jr. *J. Am. Chem. Soc.* **1999**, *121*, 264–265. (d) Roelfes, J. G., In *Models for Non-Haem Iron Containing Oxidation Enzymes*, Ph. D. thesis, Groningen, 2000.
9. Choma, C. T.; Schudde, E. P.; Kellogg, R. M.; Robillard, G. T.; Feringa, B. L. *J. Chem. Soc.*, *Perkin Trans. 1* **1998**, 769–773.
10. See Appendix 2 (p. 151) for the structure and one-letter abbreviations of the amino acids.
11. C. T. Choma, *personal communications*.
12. M. Klopstra, *forthcoming Ph. D. thesis*.
13. For phenolic alcohol groups, see Gibb, B. C.; Mezo, A. R.; Causton, A. S.; Fraser, J. R.; Tsai, F. C. S.; Sherman, J. C. *Tetrahedron* **1995**, *51*, 8719–8732.

14. Rau, H. K.; Haehnel, W. *J. Am. Chem. Soc.* **1998**, *120*, 468–476.
15. Mezo, A. R.; Sherman, J. C. *J. Am. Chem. Soc.* **1999**, *121*, 8983–8994.
16. Causton, A. S.; Sherman, J. C. *Bioorg. Med. Chem.* **1999**, *7*, 23–27.
17. Tahmassebi, D. C.; Sasaki, T. *J. Org. Chem.* **1998**, *63*, 728–731.
18. (a) Sasaki, T.; Kaiser, E. T. *Biopolymers* **1990**, *29*, 79–88. (b) Arai, T.; Kobata, K.; Mihara, H.; Fujimoto, T.; Nishino, N. *Bull. Chem. Soc. Jpn.* **1995**, *68*, 1989–1998.
19. Brask, J.; Jensen, K. J. *Bioorg. Med. Chem. Lett*. **2001**, *11*, 697–700.
20. Peluso, S.; Dumy, P.; Nkubana, C.; Yokokawa, Y.; Mutter, M. *J. Org. Chem.* **1999**, *64,* 7114–7120.
21. Hossain, M. A.; Matsumura, S.; Kanai, T.; Hamasaki, K.; Mihara, H.; Ueno, A. *J. Chem. Soc*., *Perkin Trans*. 2 **2000**, 1527–1533.
22. Schnepf, R.; Hörth, P.; Bill, E.; Wieghardt, K.; Hildebrandt, P.; Haehnel, W. *J. Am. Chem. Soc.* **2001**, *123*, 2186–2195.
23. Futaki, S.; Aoki, M.; Fukada, M.; Kondo, F.; Niwa, M.; Kitagawa, K.; Nakaya, Y. *Tetrahedron Lett.* **1997**, *38*, 7071–7074.
24. Sierra, M. A.; de la Torre, M. C. *Angew. Chem. Int. Ed*. **2000**, *39*, 1538–1559.
25. See Chapter 5 and reference 8d pp. 65–71 for the electronic effect of the ligand on the redox potential of the corresponding iron complex.
26. The selected sequence Ac–CEELLKKLEELLKKG–NH_2 was adapted from reference 15 after modelling studies by dr. C. T. Choma, using the Insight II software package, had indicated that a four-helix bundle could still be obtained when a cysteine residue is introduced into the original sequence.
27. Spee, J. H.; Boersma, M. G.; Veeger, C.; Samyn, B.; Van Beeumen, J.; Warmerdam, G.; Canters, G. W.; Van Dongen, W. M. A. M.; Rietjens, I. M. C. M. *Eur. J. Biochem.* **1996**, *241*, 215–220.

Appendix 1: Abbreviations

ABTS	2,2'-azinobis-(3-ethyl-benzothiazoline-6-sulphonic acid)
Acm	acetamidomethyl
Alloc	allyloxycarbonyl
9-BBN	9-borabicyclo[3.3.1]nonane
BLM	bleomycin
Boc	*tert*-butoxycarbonyl
dba	dibenzylideneacetone
Dde	2-(4,4-dimethyl-2,6-dioxocyclohexylidene)ethyl
DIEA	*N*,*N*-diisopropylethylamine
DMF	*N*,*N*-dimethylformamide
dppe	1,2-bis(diphenylphosphino)ethane
dppf	1,1'-bis(diphenylphosphino)ferrocene
DTT	dithiothreitol
EPR	electron paramagnetic resonance
ESI-MS	electrospray ionisation mass spectrometry
Fmoc	9-fluorenylmethoxycarbonyl
HMPA	hexamethylphosphoramide
mCPBA	*meta*-chloroperoxybenzoic acid
N3Py	*N*-[di(2-pyridinyl)methyl]-*N*-(2-pyridinylmethyl)amine
N4Py	*N*-[di(2-pyridinyl)methyl]-*N*,*N*-bis(2-pyridinylmethyl)amine
N4PyFe	$[(N4Py)Fe(MeCN)](ClO_4)_2$
NMR	nuclear magnetic resonance
Pht	phthalimide
Py5	2,6-bis{methoxy[di(2-pyridinyl)]methyl}pyridine
SCE	saturated calomel electrode
TBDMS	*tert*-butyldimethylsilyl
TEA	triethylamine
TEMP	2,2,6,6-tetramethylpiperidine
TEMPO	2,2,6,6-tetramethylpiperidin-1-oxyl
Tf	trifluoromethanesulphonyl or triflate
TFA	trifluoroacetic acid
TFAA	trifluoroacetic acid anhydride
THF	tetrahydrofuran
TMEDA	*N*,*N*,*N*',*N*'-tetramethylethylenediamine
TMS	trimethylsilyl
TON	turnover number
TPA	tris(2-pyridinylmethyl)amine
Trt	triphenylmethyl or trityl
Ts	*p*-toluenesulphonyl (tosyl)
Z	benzyloxycarbonyl

Appendix 2: α-amino acids; structures and abbreviations

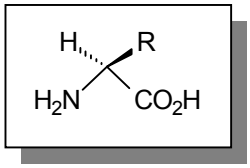

Name, three and one letter abbreviations			Side chain (R)
Alanine	Ala	A	
Arginine	Arg	R	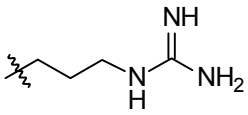
Asparagine	Asn	N	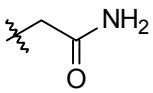
Aspartic acid	Asp	D	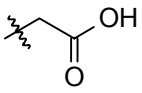
Cysteine	Cys	C	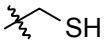
Glutamic acid	Glu	E	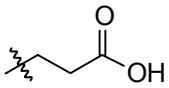
Glutamine	Gln	Q	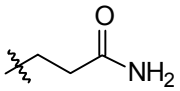
Glycine	Gly	G	H
Histidine	His	H	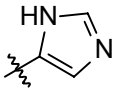
Isoleucine	Ile	I	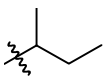

Name, three and one letter abbreviations			Side chain (R)
Leucine	Leu	L	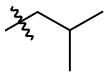
Lysine	Lys	K	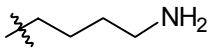
Methionine	Met	M	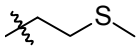
Phenylalanine	Phe	F	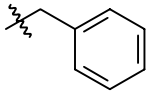
Proline	Pro	P	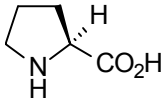
Serine	Ser	S	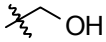
Threonine	Thr	T	
Tryptophan	Trp	W	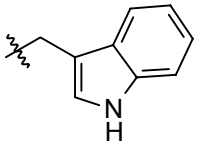
Tyrosine	Tyr	Y	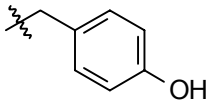
Valine	Val	V	

Samenvatting

Van natuurlijk enzym naar functionele modellen

Enzymen zijn zeer complexe en, op moleculaire schaal, meestal zeer grote structuren die betrokken zijn bij veel chemische processen in levende organismen. De rol die zij kunnen vervullen is niet alleen het bewerkstelligen van het transporteren of opslaan van stoffen in het lichaam, maar ook die van biokatalysator in stofwisselingsreacties. Als katalysator maakt het enzym het mogelijk om de activeringsenergie van een reactie te verlagen, waardoor substraatmoleculen sneller omgezet kunnen worden tot specifieke producten bij lage (lichaams)temperaturen. Deze enzymen, ook wel proteïnen of eiwitten genoemd, zijn natuurlijke polymeren, die opgebouwd zijn uit een specifieke selectie aminozuren in een door de evolutie bepaalde volgorde. Deze aminozuurvolgorde bepaalt vervolgens de manier waarop de peptidenketen zich tot een karakteristieke driedimensionale structuur opvouwt en welke functie de proteïne vervult. Die functie gaat verloren bij het verstoren of ontvouwen (denatureren) van de compacte 3D structuur. Echter, de proteïnen zijn in staat om hun natuurlijke toestand weer terug te vinden via een complex opvouwmechanisme, waarvan de 'bouwtekening' verborgen zit in de specifieke selectie van de betrokken aminozuren. Andersom kan een analoge 3D structuur van enzymen tot stand komen, terwijl de aminozuursamenstelling verschillend is.

De samenstelling en functie die enzymen nu hebben, is het gevolg van het evolutieproces tijdens de afgelopen miljarden jaren. In een hoog tempo echter wordt er de laatste decennia door vele onderzoekers gewerkt aan het ontrafelen van de exacte samenstelling van de vele enzymen en hun werkingsmechanisme. Bovendien wordt veel tijd en moeite gestopt in het vinden van de 'gebruiksaanwijzing' die kan vertellen welke selectie en volgorde van aminozuren nodig is om een gewenste enzymstructuur te verkrijgen. Op dit deelgebied van het biochemische onderzoek speelt zich onder andere het zogenaamde "*de novo* proteïne design" af. De afgelopen twee decennia is er al veel kennis verzameld over de gecompliceerde vouwprocessen die zich afspelen in het traject van peptidenketen tot driedimensionale structuur. Men is er nu zelfs in geslaagd om kleine, compacte peptidenstructuren te maken die een enzymfunctie kunnen nabootsen.

In hoofdstuk 1 is een overzicht gegeven van een groot aantal peptidenstructuren die gebaseerd zijn op het zogenaamde vier-helix bundel motief. Dit is een compacte organisatiestructuur, waarin vier α-helices geassocieerd kunnen zijn als vier individuele peptidenketens met elk een α-helix vorm (Figuur 1), als een dimeer van twee aan elkaar gekoppelde α-helices, of als een enkele keten met daarin vier α-helix domeinen, die zich kan opvouwen tot een vier-helix bundel. Om de stabiliteit van deze structuren te vergroten, of om

eventueel de helix bundel een functie te geven, worden deze peptidenketens ook wel aan een 'template' molecuul gebonden (Figuur 1).

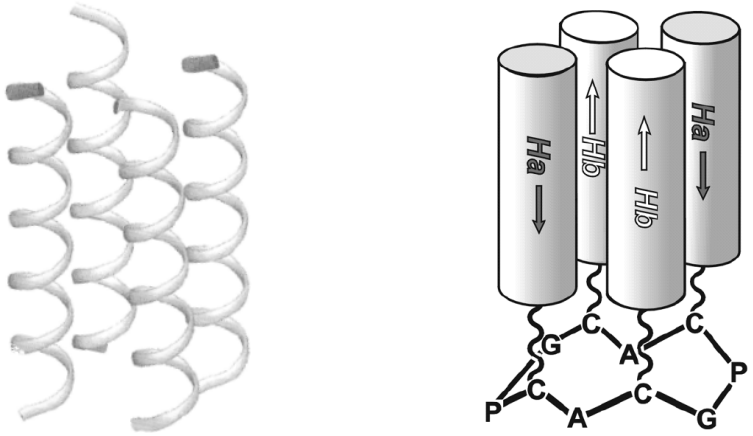

Figuur 1. Een vier-helix bundel als tetrameer van vier individuele α-helices (links) of verbonden aan een cyclische peptide als 'template' (rechts).

De drijvende kracht achter de associatie van de peptidenketens tot een vier-helix bundel is een soort schizofrenie in de individuele α-helices; één zijde bestaat uit waterminnende (hydrofiel) aminozuren, terwijl de andere zijde uit watermijdende (hydrofoob) aminozuren bestaat. In water zullen daarom de helices zich groeperen, waarbij de hydrofobe zijden zich naar elkaar zullen richten om het contact met de watermoleculen te minimaliseren.

Aan de hand van deze relatief eenvoudige peptidenstructuren hebben proteïne designers enkele processen kunnen bestuderen die betrokken zijn bij het vormen van de 3D structuur van een enzym, uitgaande van de primaire structuur van de eiwitketen. Hun toegeëigende kennis is vervolgens vaak met succes toegepast in het ontwerpen van een grote verscheidenheid aan vier-helix bundels, met of zonder katalytische functie. Echter, de activiteit van het kunstmatige enzym is meestal onderschikt aan die van de natuurlijke proteïne. Door de reeds gemaakte vorderingen in dit nog relatief prille onderzoeksgebied kunnen verbeteringen tot meer natuurlijke enzymen in de nabije toekomst verwacht worden.

Een niet-eitwitcomponent (een co-factor of prosthetische groep, zoals een heem molecule) is meestal vereist voor de werking van het enzym. Deze bevindt zich dan veelal in het actieve centrum waar de katalyse zich afspeelt. Het streven van sommige onderzoeksgroepen is dan ook om kleine moleculen of metaalcomplexen te ontwerpen die dezelfde hoge activiteit en selectiviteit hebben als de natuurlijke macromoleculen, met zo mogelijk zelfs een andere substraat voorkeur. In deze enzymmodellen is vaak, maar lang niet altijd, de ruimtelijke ordening van functionele groepen rond het katalytisch centrum in het eiwit gekopieerd. Echter, de efficiëntie van de natuurlijke biokatalysatoren blijkt zeer moeilijk bewerkstelligd te kunnen worden.

Verder bieden deze enzymmodellen de mogelijkheid om nog onbekende reactie-mechanismen van proteïnen te ontrafelen. Dat betekent overigens niet, dat een vereenvoudigd enzymmodel vanzelfsprekend tot een gemakkelijke benadering leidt en een snelle ontrafeling van het reactiemechanisme van een enzym geeft. Hiervoor moet ten eerste vastgesteld worden, dat het model een goed werkend en correct model is voor het enzym in kwestie. Het chemische

gedrag en de analytische data moet daarvoor overeenkomen met dat van het enzym. Verder moet het mechanisme van dit model natuurlijk nog opgehelderd worden, wil het inzicht kunnen verschaffen in de werking van het natuurlijke proteïne.

Van functionerend model naar kunstmatig enzym

In de onderzoeksgroep van prof. dr. B. L. Feringa is een katalysator ontwikkeld op basis van een niet-heem molecule, genaamd N4Py, waarvan het ijzercomplex N4PyFe als model fungeert voor ijzer-bleomycine (Figuur 2). Dit natuurlijke glycopeptide wordt als antibioticum toegepast in anti-tumor behandelingen. Het verbruikt hiervoor moleculair zuurstof om DNA te 'knippen' op specifieke posities in de DNA-keten. Daarnaast is deze geactiveerde vorm van bleomycine ook in staat om verschillende organische verbindingen te oxideren. De werkelijke samenstelling van geactiveerd bleomycine en het mechanisme van de oxidatieve werking zijn nog niet geheel opgehelderd. Wanneer dit wel achterhaald zou kunnen worden, zou het bijvoorbeeld mogelijk worden om varianten van bleomycine te maken, die effectiever werken of ook voor andere medicinale toepassingen gebruikt zouden kunnen worden.

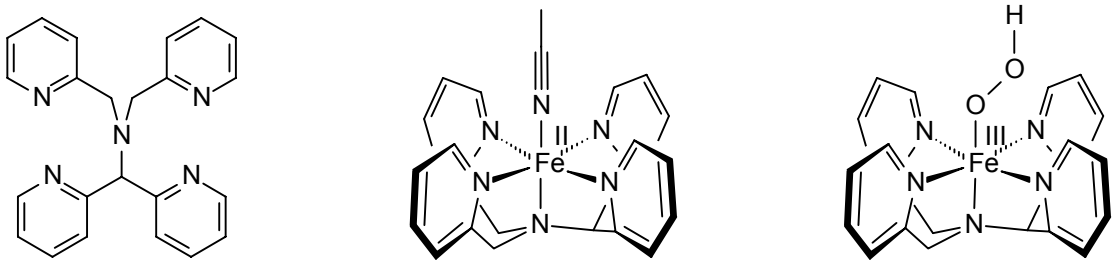

Figuur 2. Het N4Py ligand, het overeenkomstige niet-heem ijzercomplex N4PyFe en het reactieve intermediair N4PyFeOOH.

In het recente verleden zijn belangrijke vorderingen gemaakt in het ontrafelen van het oxidatiemechanisme van N4PyFe, en mede daardoor dat van ijzer-bleomycine. In hoofdstuk 2 is een beknopt overzicht gegeven van het resultaten die behaald zijn in onze onderzoeksgroep tijdens het promotieonderzoek van Gerard Roelfes. Net als ijzer-bleomycine bleek het reactieve intermediair N4PyFeOOH, gevormd door de reactie van N4PyFe met waterstofperoxide, niet alleen in staat te zijn om verscheidene organische verbindingen te kunnen oxideren, maar ook DNA te kunnen 'knippen'. Hoewel enkele belangrijke intermediairen in de katalytische cyclus van N4PyFe geïdentificeerd en gekarakteriseerd zijn, blijven enkele vragen nog onbeantwoord.

Het doel van dit onderzoek was om het N4Py ligand dusdanig aan te passen, dat er vier peptidenketens aan gekoppeld kunnen worden. Hierdoor zou het uiteindelijk mogelijk worden om N4Py toe te passen als een functionele 'template' in de vorming van een vier-helix bundel (Figuur 3). Een functie kan zo verkregen worden in de peptidenbundel, doordat het overeenkomstige ijzercomplex in staat is substraatmoleculen te oxideren. Door het samenspel van de katalytische werking van het N4PyFe-complex en zijn peptidenomgeving te optimaliseren, wordt het wellicht mogelijk om een kunstmatige peroxidase te ontwerpen.

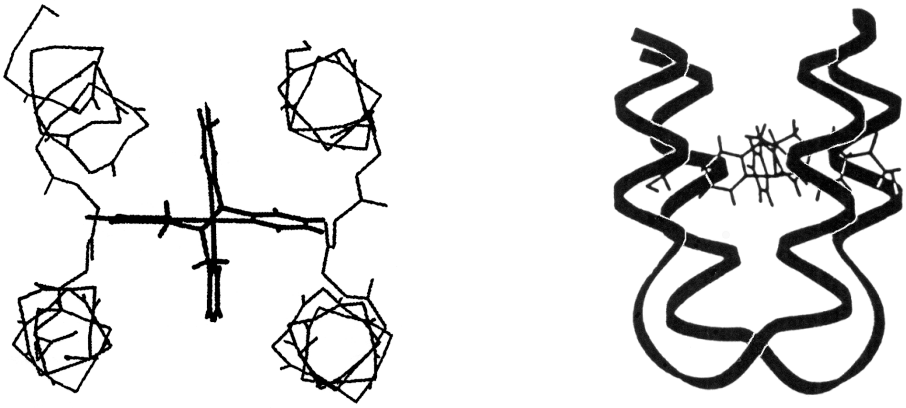

Figuur 3. De kristalstructuur van N4PyFe supergepositioneerd over dat van een dimere vier-helix bundel (links: bovenaanzicht, rechts: zijaanzicht).

In onze onderzoeksgroep zijn we er eerder in geslaagd om twee chloromethyleen groepen in het N4Py ligand aan te brengen. Hierdoor konden twee peptiden via een cysteine aminozuur in de sequentie aan het ligand gekoppeld worden door middel van een nucleofiele substitutie reactie. Het overeenkomstige ijzer(II)complex vertoonde peroxidase activiteit, en gaf daarmee aan, dat het mogelijk moet zijn om het N4PyFe-complex in een vier-helix bundel in te bouwen met behoud van een oxidatieve werking. De kracht van het gebruik van cysteine om peptiden aan het ligand te koppelen is, dat het thiolaat anion een goede nucleofiel is. Bovendien maakt deze strategie het mogelijk om het N4PyFe-complex overal in de vier-helix bundel te plaatsen, afhankelijk van de positie van de cysteine in de peptidensequentie.

In hoofdstuk 3 wordt een syntheseroute besproken, die het in principe mogelijk maakt om een groot aantal N4Py derivaten met vier functionele groepen te synthetiseren (**4**). Hierbij worden eerst de benodigde zijketens in 2,5-dibroompyridine (**1**) geïntroduceerd, waarna het ligand zelf opgebouwd wordt (Schema 1). Door deze convergente syntheseroute zijn we er uiteindelijk in geslaagd om vier peptidenketens via deze zijketens aan het N4Py ligand te koppelen. Als eerste werden één-koolstof (C1) zijketens geïntroduceerd, zoals die in het eerder gesynthetiseerde dipeptide-N4PyFe-complex waren gebruikt. Echter, het overeenkomstige tetragesubstitueerde N4Py ligand bleek niet stabiel genoeg te zijn om verder te kunnen functionaliseren. Na vele testreacties om de oorzaak van deze instabiliteit te achterhalen, is besloten om een langere (C3) zijketen te gebruiken. Het hiermee verkregen N4Py derivaat bleek gelukkig wel stabiel genoeg om vier peptidenketens aan te koppelen.

Het nadeel van deze convergente syntheseroute is, dat voor elke gewenste verandering in de zijketens de gehele synthese opnieuw doorlopen moet worden. Dit omvat ongeveer dertien reactiestappen, afhankelijk van de geïntroduceerde zijketens. Daar komt nog bij, dat succes met de uiteindelijk verkregen verbinding niet gegarandeerd kan worden, wat kan leiden tot de noodzaak van het synthetiseren van een andere derivaat. Het zou daarom gunstiger zijn om eerst een N4Py ligand te maken, die het vervolgens mogelijk maakt om vrijwel elke gewenste zijketen te kunnen introduceren, direct of na enkele functionaliseringsreacties. Deze divergente synthese wordt besproken in hoofdstuk 4, waarbij het N4Py derivaat **3** (Schema 1) gefunctionaliseerd kan worden door middel van metaal-gekatalyseerde cross koppelingreacties. De uitgevoerde testreacties op broompyridine verbindingen waren vaak zeer succesvol en vertegenwoordigen daarmee enkele veelbelovende functionaliseringsreacties om op **3** toe te

passen. Eén cross koppelingreactie, die al met succes is uitgevoerd, is de Suzuki reactie tussen **3** en fenylboorzuur, waardoor een tetrafenyl N4Py derivaat werd verkregen.

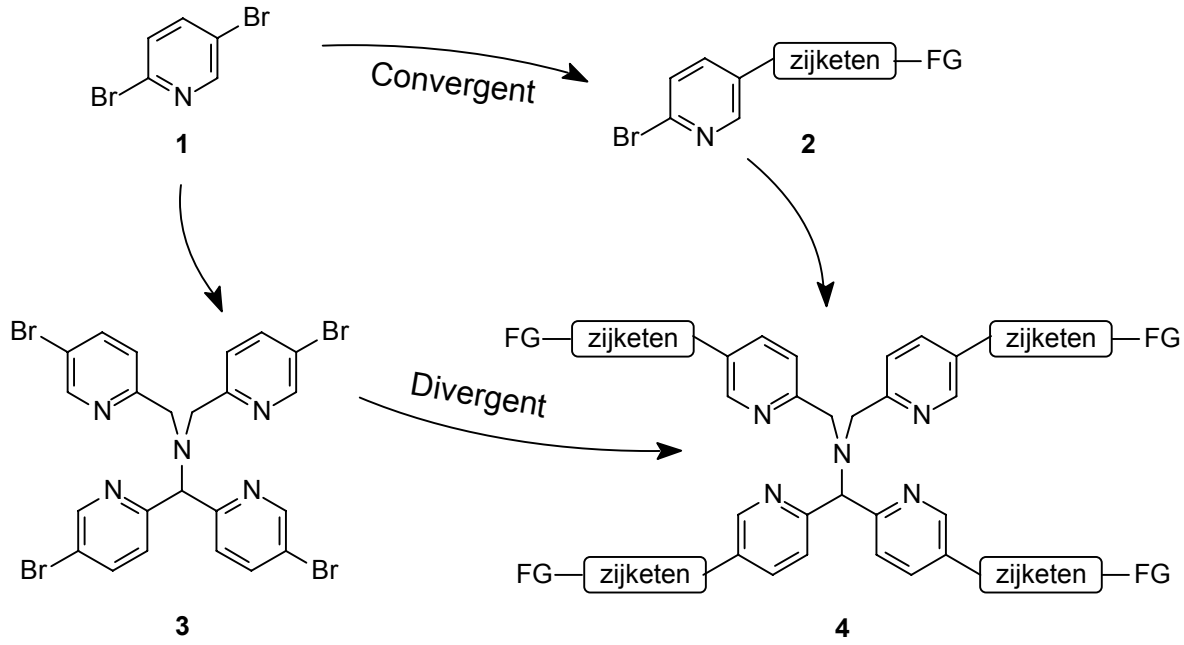

Schema 1. Convergente versus divergente synthese van tetragesubstitueerde N4Py liganden (FG = functionele groep).

De laatste decennia is ontzettend veel onderzoek verricht aan deze cross koppelingreacties, waardoor het vaak mogelijk is geworden om vele lang bekende of moeilijke syntheses te vervangen door een metaal-gekatalyseerde reactie onder redelijk milde omstandigheden. Door het snel stijgende aantal publicaties in dit onderzoeksgebied met daarnaast een toenemend aantal commercieel verkrijgbare reagentia voor deze cross koppelingreacties zou het mogelijk kunnen worden om een groot aantal N4Py derivaten te verkrijgen. De overeenkomstige ijzer(II)complexen zullen waarschijnlijk een verschillend gedrag gaan vertonen als katalysator in oxidatiereacties, waardoor het misschien mogelijk wordt om de N4PyFe-katalysator af te stellen op de gewenste eigenschappen.

Enkele tetragesubstitueerde N4Py liganden die in hoofdstuk 3 en 4 zijn besproken, zijn onderzocht op hun katalytische activiteit in de oxidatie van cyclohexeen en cyclohexaan (hoofdstuk 5). Hierbij werd duidelijk, dat er grote onderlinge verschillen ontstaan door de aangebrachte zijketens, niet alleen in de verhouding van de uiteindelijk verkregen producten, maar ook in het gedrag van de katalysatoren als die in de tijd gevolgd wordt. Verder worden in dit hoofdstuk de spectroscopische data van deze ijzercomplexen besproken en vergeleken. Bovendien worden de kristalstructuren van twee tetragesubstitueerde N4PyFe-complexen gepresenteerd.

Eén van de gesynthetiseerde N4Py-peptide-ijzercomplexen is onderzocht naar de katalytische activiteit die het vertoont in de peroxidatie van ABTS, een substraat waarvan de omzetting spectrofotometrisch gevolgd kan worden. De besproken resultaten in hoofdstuk 5 geven aan, dat dit peptidencomplex wel degelijk peroxidase activiteit vertoont, echter met een veel lagere katalytische 'turnover' dan N4PyFe zelf. Frappant genoeg lijkt het peptidencomplex

wel een langere levensduur te hebben dan N4PyFe, die beide onder de oxidatieve omstandigheden gedegradeerd worden. Massaspectrometrie-analyse tijdens oxidatie reacties met een tetracysteine N4PyFe-derivaat hebben aangetoond, dat zeer waarschijnlijk de sulfidebinding tussen het ligand en de peptidenketen geoxideerd wordt, wat dan vervolgens zal leiden tot de waargenomen degradatie. Het is verder duidelijk geworden, dat de temperatuur en de pH een duidelijk effect hebben op de activiteit en de levensduur van de N4PyFe-katalysator, en daarmee ook op de overeenkomstige N4PyFe-peptide-complexen.

Tot slot kan gesteld worden, dat er nog veel onderzoek gedaan moet worden naar het ontwerpen van een stabiele vier-helix bundel die het mogelijk moet maken om de N4PyFe-katalysator te kunnen huisvesten. Wel heeft dit onderzoek geleid tot twee verschillende syntheseroutes, die het mogelijk maken om de benodigde, en andere, N4Py derivaten te bereiden. Hoewel enkele synthesestrategieën voor de peptidenkoppeling aan het N4Py ligand zijn geprobeerd, met en zonder succes, zijn er nog vele andere mogelijkheden over die onderzocht kunnen worden. Hiervoor is echter niet alleen behoorlijk wat materiaal nodig, maar met de betrokken pyridinechemie vaak ook veel geduld en doorzettingsvermogen.